Docket No.: 00131-00350-US
(PATENT)

IN THE UNITED STATES PATENT AND TRADEMARK OFFICE

In re Patent Application of:
Ann S. Robinson et al.

Application No.: 10/673000

Confirmation No.: 9773

Filed: September 26, 2003

Art Unit: 1639

For: USE OF HYDROSTATIC PRESSURE TO INHIBIT AND REVERSE PROTEIN AGGREGATION AND FACILITATE PROTEIN REFOLDING

Examiner: M. C. T. Tran

DECLARATION UNDER 37 C.F.R. § 1.131

MS Amendment
Commissioner for Patents
P.O. Box 1450
Alexandria, VA 22313-1450

Dear Sir:

1. I, Anne Skaja Robinson, Clifford R. Robinson, Debora Foguel, and Jerson Lima Silva declare as follows:

2. I am the inventor named on the above-referenced patent application.

3. On a date prior to July 9, 1998, the earliest possible effective filing date of U.S. Patent No. 6,489,450 B2 (Randolph *et al.*), which was cited by the examiner, the invention of this application was reduced to practice by work performed in Brazil and the United States.

4. To establish reduction to practice of the invention of this application, the following attached documents are submitted as evidence:

Exhibit A : Copy of a draft article authored by D. Foguel, C.R. Robinson, P.C. de Sousa, J.L. Silva, and A.S. Robinson, and titled "Hydrostatic Pressure Rescues Native Protein from Aggregates."

Exhibit B : Copy of a letter dated June 24, 1998 from Alan Haley addressed to Professor Anna Robinson.

Exhibit C : D. Foguel, C.R. Robinson, P.C. de Sousa, J.L. Silva, and A.S. Robinson, "Hydrostatic Pressure Rescues Native Protein from Aggregates", Biotechnology and Bioengineering, 63:552-558 (1999)

Exhibit D : Copy of the original chromatogram of the high-performance liquid chromatography (HPLC) elution profile of native tailspike trimer, with dates redacted.

Exhibit E : Copy of the original chromatogram of the HPLC elution profile of denatured tailspike monomer, with dates redacted.

Exhibit F : Copy of the original chromatogram of the HPLC elution profile of a sample of denatured native tailspike taken after five minutes of refolding under aggregation conditions, with dates redacted.

Exhibit G : Copy of the original chromatogram of the HPLC elution profile of a sample of denatured native tailspike taken after thirty minutes of refolding under aggregation conditions, with dates redacted.

Exhibit H : Copy of the original chromatogram of the HPLC elution profile of a sample of denatured native tailspike taken after two hours of refolding under aggregation conditions, with dates redacted.

Exhibit I : Copy of the original chromatogram of the HPLC elution profile of a sample of denatured native tailspike taken after around 5 hours of refolding under ambient conditions, with dates redacted.

Exhibit J : Copy of the original chromatogram of the HPLC elution profile of a sample of denatured native tailspike subjected to around 3.5 hours of refolding under ambient conditions and then a pressure of 35,000 psi (2.4 kbar) for 90 minutes, with dates redacted.

Exhibit K : Copy of notebook page disclosing the data from a "tailing" assay performed on a sample of denatured native tailspike which was permitted to aggregate and then subjected to hydrostatic pressure treatment, with dates redacted.

Exhibit L : Copy of notebook page disclosing the data from a "tailing" assay performed on native tailspike, with dates redacted.

5. The draft article (**Exhibit A**) is evidence of the work that we did prior to July 9, 1998.

6. As described in the section titled *"Aggregation Reactions can be monitored by HPLC"* of the draft article (**Exhibit A**, pp. 6-7), we developed an HPLC assay using size exclusion HPLC which could be used to rapidly identify and quantitate aggregation intermediates.

7. As indicated in the paragraph spanning pages 6 and 7 of the draft article (**Exhibit A**), we determined by HPLC that the native trimeric tailspike protein eluted as a uniform peak around 6.7 minutes, and monomer eluted at 7.6 minutes. **Exhibit D** (trimer) and **Exhibit E** (monomer) are copies of the chromatograms from our initial work demonstrating that trimers and monomers elute at these particular timepoints.

8. As described in the first full paragraph on page 7 of the draft article (**Exhibit A**), to demonstrate that HPLC can be used as a probe for aggregation intermediates, tailspike was denatured, then rapidly diluted into refolding buffer. After the onset of aggregation, aliquots were removed at 5, 30 and 120 minutes and injected in the HPLC. The elution profiles at these three timepoints are shown in Figure 2B of the draft article (**Exhibit A, p. 20**). **Exhibit F** (5 minutes), **Exhibit G** (30 minutes) and **Exhibit H** (120 minutes) are copies of the original chromatograms from our work from which the data shown in Figure 2B is derived.

9. As described in the section titled "*Hydrostatic pressure inhibits and reverses tailspike aggregation*" (p. 8) and the description of Figure 3 (p. 16) of the draft article (**Exhibit A**), to test the effect of hydrostatic pressure upon aggregation, samples of native tailspike were denatured, then transferred to refolding buffer under conditions which favored aggregation. An identical set of samples were denatured, transferred to refolding buffer under aggregation conditions, and after more than 3 hours of aggregation at atmospheric conditions, then subjected to 35,000 psi (2.4 kbar) for 90 min. We then conducted an HPLC analysis of both the pressure-treated and non-pressure-treated samples. The elution profiles of the pressure-treated and non-pressure-treated samples are shown in Figure 3A of the draft article (**Exhibit A, p. 22**). **Exhibit I** (non-pressure treated) and **Exhibit J** (pressure-treated) are copies of the original chromatograms from our work from which the data shown in Figure 3A is derived.

10. Treatment with elevated hydrostatic pressure markedly increased the yield of native trimer, while substantially decreasing the extent of aggregation. Figure 3B of the draft article (**Exhibit A, p. 23**) shows the distribution of tailspike monomers, trimers, and aggregates for

4

pressure-treated tailspike samples and for the ambient aggregated tailspike sample and the results discussed in the second paragraph on page 8 of the draft article. As reflected in Figure 3B, we determined that the application of hydrostatic pressure decreased the percentage of aggregates and increased the percentage of trimers.

11. To assess whether tailspike trimers produced by pressure-treating aggregates recovered wild-type function, we subjected tailspike trimers to a "tailing" assay as described in the paragraph spanning pages 5-6, and in the section titled *"Tailspike trimers from pressure treatment have native-like structure and activity"* (pp. 8-9) of the draft article (**Exhibit A**). Samples of native tailspike and pressure-treated aggregates were diluted and incubated with tail-free heads as described. As described in the draft article, tailspike trimers produced by pressure treatment of aggregates were essentially fully active, and formed viral plaques efficiently. **Exhibit K** (pressure treated) and **Exhibit L** (native) are copies of the original notebook pages recording the data obtained from the tailing assays.

12. As noted in the last sentence of the first full paragraph on page 9 of the draft article (**Exhibit A**), these results confirmed that refolding under pressure produced tailspike trimers with essentially native structural and functional characteristics.

13. As reflected in the first paragraph of the section titled "Implications" of the draft article (**Exhibit A**, p. 9), we concluded from the above described work that application of hydrostatic pressure can be used to prevent aggregation during refolding and to reverse aggregation which has already taken place. After pressure is released, dissociated aggregates refold to form biologically active protein with native characteristics.

14. We submitted the draft article (**Exhibit A**) for publication to the journal *Biotechnology and Bioengineering* prior to July 9, 1998. As evidence of this we note the following two facts:

(1) the published article indicates a receipt date of "10 June, 1998" (**Exhibit C**, p. 552, first line above the abstract); and (2) a letter from Alan Haley, an editorial assistant for *Biotechnology and Bioengineering*, confirming receipt of the draft article in a letter dated "June 24, 1998" (**Exhibit B**).

15. The above facts establish that our work was done in Brazil and the United States prior to July 9, 1998.
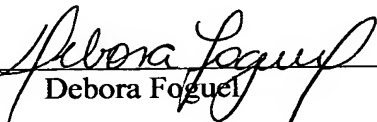
16. I hereby declare that all statements made herein of my own knowledge are true and that all statements made on information and belief are believed to be true; and further that these statements were made with the knowledge that willful false statements and the like so made are punishable by fine or imprisonment, or both, under Section 1001 of Title 18 of the United States Code and that such willful false statements may jeopardize the validity of the above-identified application or any patent issues thereon.

_____
Anne Skaja Robinson

Date 9/22/06

_____
Clifford R. Robinson

Date 9/22/06

_____
Debora Foguel

Date September 18, 2006

_____
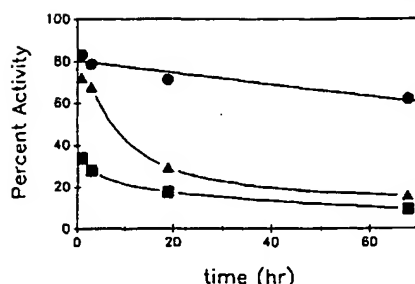Jerson Lima Silva

Date SEPTEMBER 18, 2006

FIG. 6. **Kinetics of unfolding of rhodanese at several urea concentrations.** Rhodanese samples were incubated at 10 °C in either 3 M (●), 4 M (▲), or 5 M (■) urea at 3.6 μg/ml rhodanese. Enzyme activity measurements were carried out at the indicated times and plotted as a percentage of the enzyme activity present prior to incubation.

hours for completion. The unfolding process at 10 °C is not complete at either 3 or 4 M urea, even after 68 h. Due to competing reactions that inactivate rhodanese, it is not practical at 10 °C to reach the equilibrium state by long incubation of dilute protein samples. However, it seems clear that the slow kinetics of unfolding at 10 °C can explain the noncoincidence between the observed unfolding and refolding transition curves.

DISCUSSION

A thermodynamically reversible unfolding process for rhodanese, unfolded in urea or guanidinium chloride, has only previously been observed in the presence of BME, thiosulfate, and a detergent such as lauryl maltoside (3, 4). The requirements for BME and thiosulfate are due to the sensitivity of rhodanese's sulfhydryl groups (3). Oxidation of these groups changes the conformation of rhodanese, resulting in exposure of hydrophobic surfaces (21, 22). These studies showed that reversibility of rhodanese folding can be achieved when aggregation is minimized and oxidative inactivation is prevented.

Previous studies detected some regain of rhodanese activity after dilution of denaturants (8), but they could not distinguish between inactivation/reactivation, which may follow different paths, and reversibility, in which the same path is followed for folding and unfolding. Thus, it was not possible to construct transition profiles showing the extent to which unfolding was "thermodynamically" reversible for rhodanese unfolded without accessory substances.

Reversibility was shown when aggregation was minimized by the use of the detergent lauryl maltoside, supporting the view that hydrophobic interactions play an important role in refolding. In the absence of detergents, we have recently observed that rhodanese efficiently reactivates when the chaperonin proteins, cpn60 and cpn10 from *Escherichia coli*, are present during refolding (14). The combination of thiosulfate and BME was also required to prevent oxidative inactivation in this case. The replacement of detergent with the chaperonins suggested that these proteins were responsible for the suppression of unwanted hydrophobic interactions, in agreement with their proposed role in the *in vivo* folding process (23–26). It was also demonstrated that cpn60 contains hydrophobic surfaces (14). These may stabilize folding intermediates through hydrophobic interactions and, therefore, prevent "incorrect" interactions that can lead to aggregated states.

In the present study, we have demonstrated that significant recovery of activity of urea-unfolded rhodanese can be obtained in the absence of either detergents or chaperonins,

when intermolecular interactions that lead to aggregation are suppressed (3). Successful, nonassisted refolding involved lowering the concentration of the protein, lowering the temperature, and optimizing the concentration of urea during refolding. The requirement for urea implies that the best yield of refolding would be achieved by an intermediate dilution of the perturbant before its final removal.

In this nonassisted process, no significant recovery was obtained when unfolded rhodanese was diluted into buffer at protein concentrations exceeding 10 μg/ml. This is in contrast with the detergent-assisted refolding of rhodanese where complete recovery was observed at a protein concentration of 50 μg/ml (3). These results are consistent with previous reports showing a concentration dependence of the ability to reactivate a fraction of unfolded rhodanese, as well as of the stability of native enzyme (8, 27). Both reactivation and stability display optima at low protein concentrations. These optima were interpreted as resulting from a balance of two effects; high protein concentrations encourage aggregation, whereas low protein concentrations increase susceptibility both to surface adsorption and to limiting amounts of adventitious reactants, such as reactive oxygen species (27). Similarly, in the present study, we find that even under reducing conditions, a strong protein concentration dependence is observed for the reversible unfolding of rhodanese. The results indicate that there is an optimum concentration of the enzyme at which maximum recoveries can be obtained.

Nonassisted refolding is strongly temperature-dependent. Previous results on the temperature dependence of aggregation of rhodanese at high protein concentration suggested that hydrophobic interactions were involved in the competition between the refolding and aggregation (3, 28). This was supported by the observation that the aggregation rate is reduced at lower temperatures (3), where the hydrophobic effect is weakened. Our results indicate that almost complete recovery of activity can be achieved when a combination of low protein concentration, low temperature, and conditions that help to prevent oxidation are used for refolding rhodanese.

The present results are in accord with a model that was proposed to account for the role of detergents and chaperonins in rhodanese folding.

$$N \rightleftharpoons I_1 \rightleftharpoons I_2 \rightleftharpoons D$$
$$\text{fast} \ (nI_2) \Big\Updownarrow \text{slow}$$
$$I_{aggregate}$$
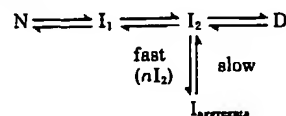
The major feature of this model is that aggregation kinetically competes with reactivation. Native rhodanese (N) passes through metastable intermediate(s) (I_1, I_2) in the course of unfolding/refolding. Activity is lost at an early stage, accompanied by relatively small structural changes, i.e. $N \rightarrow I_1$. Higher urea concentrations are required to fully unfold the enzyme, i.e. $I_2 \rightarrow D$. Further, the observations in Fig. 5A indicate that $I_1 \rightarrow N$ is rate limiting, which is consistent with previous suggestions (4).

A major side reaction that competes with the refolding process is aggregation. Noncovalent aggregation has been previously reported as a side reaction in the reconstitution of unfolded oligomeric enzymes, e.g. lactic dehydrogenase (29, 30). For rhodanese, aggregation can become effectively irreversible. Aggregation is protein concentration-dependent and has been suggested to involve intermediates that are still compact and have extensive, exposed hydrophobic surfaces represented here, collectively, as I_2. In the model, above, the step leading from I_2 to the aggregate (denoted as involving n

molecules of I_2, *i.e. n*I_2) is concentration-dependent, and the high order of this reaction can make it appear to be cooperative (31). Aggregation could also involve the unfolded species, D. However, partially folded species that rapidly form on dilution of unfolded rhodanese (4, 20) are prime candidates, since they possess organized hydrophobic surfaces. As with most aggregation reactions, the dissolution of large aggregates is expected to be slow and, therefore, appear to be irreversible. In contrast, the rate of aggregation can be controlled to a great extent by decreasing the concentration of rhodanese, as well as the temperature of the refolding reaction.

Ideally, aggregation could be avoided completely by using extremely low protein concentrations and temperatures. However, as the protein concentration is decreased, detrimental processes other than aggregation are seen, and the overall efficiency of reactivation decreases. These processes may include surface effects as well as oxidative reactions, driven by limiting quantities of reactants. For temperature, although recoveries may continue to increase as the temperature is lowered, slow kinetics make the refolding process less practical.

Rhodanese folding appears to conform to the "thermodynamic hypothesis" in that the native structure is thermodynamically most stable. However, practical folding to the native structure requires that the folding pathway be controlled so as to avoid kinetically trapping metastable conformers. Thus, biological protein-folding mechanisms may be designed to provide kinetic control.

REFERENCES

1. Westley, J. (1973) *Adv. Enzymol. Relat. Areas Mol. Biol.* **39**, 327–368
2. Ogata, K., Dai, X., and Volini, M. (1989) *J. Biol. Chem.* **264**, 2718–2725
3. Tandon, S., and Horowitz, P. M. (1989) *J. Biol. Chem.* **264**, 9859–9866
4. Tandon, S., and Horowitz, P. M. (1990) *J. Biol. Chem.* **265**, 5967–5970
5. Ploegman, J. H., Drent, G. H., Kalk, K. H., Hol, W. G. J., Heinrikson, R. L., Keim, P., Weng, L., and Russell, J. (1978) *Nature* **273**, 1245–1249
6. Hol, W. G. J., Lijk, L. J., and Kalk, K. H. (1983) *Fundam. Appl. Toxicol.* **3**, 370–376
7. Miller, D. M., Delgado, R., Chirgwin, J. M., Hardies, S. C., and Horowitz, P. M. (1991) *J. Biol. Chem.* **266**, 4686–4691
8. Horowitz, P. M., and Simon, D. (1986) *J. Biol. Chem.* **261**, 13887–13891
9. Mitraki, A., and King, J. (1989) *Bio/Technology* **7**, 690–696
10. Jaenicke, R. (1987) *Prog. Biophys. Mol. Biol.* **49**, 117–237
11. Fischer, G., and Schmid, F. X. (1990) *Biochemistry* **29**, 2205–2212
12. Tandon, S., and Horowitz, P. (1986) *J. Biol. Chem.* **261**, 15615–15618
13. Tandon, S., and Horowitz, P. M. (1987) *J. Biol. Chem.* **262**, 4486–4491
14. Mendoza, J. A., Rogers, E., Lorimer, G. H., and Horowitz, P. M. (1991) *J. Biol. Chem.* **266**, 13044–13049
15. Viitanen, P. V., Lubben, T. H., Reed, J., Goloubinoff, P., O'Keefe, D. P., and Lorimer, G. H. (1990) *Biochemistry* **29**, 5665–5671
16. Goloubinoff, P., Christeller, J. T., Gatenby, A. A., and Lorimer, G. H. (1989) *Nature* **342**, 884–889
17. Goloubinoff, P., Gatenby, A. A., and Lorimer, G. H. (1989) *Nature* **337**, 44–47
18. Horowitz, P. (1978) *Anal. Biochem.* **86**, 751–753
19. Sörbo, B. H. (1953) *Acta Chem. Scand.* **7**, 1129–1136
20. Horowitz, P. M., and Criscimagna, N. L. (1990) *J. Biol. Chem.* **265**, 2576–2583
21. Horowitz, P. M., and Bowman, S. (1987) *J. Biol. Chem.* **262**, 8728–8733
22. Horowitz, P. M., and Criscimagna, N. L. (1988) *J. Biol. Chem.* **263**, 10278–10283
23. Ostermann, J., Horwich, A. L., Neupert, W., and Hartl, F.-U. (1989) *Nature* **341**, 125–130
24. Rothman, J. E. (1989) *Cell* **59**, 591–601
25. Ellis, R. J. (1990) *Semin. Cell Biol.* **1**, 1–9
26. Georgopoulos, C., and Ang, D. (1990) *Semin. Cell Biol.* **1**, 19–25
27. Aird, B. A., and Horowitz, P. M. (1988) *Biochim. Biophys. Acta* **956**, 30–38
28. Horowitz, P., and Bowman, S. (1987) *J. Biol. Chem.* **262**, 5587–5591
29. Zettlmeissl, G., Rudolph, R., and Jaenicke, R. (1979) *Biochemistry* **18**, 5567–5571
30. Rudolph, R., Zettlmeissl, G., and Jaenicke, R. (1979) *Biochemistry* **18**, 5572–5575
31. Horowitz, P. M., and Bowman, S. (1987) *J. Biol. Chem.* **262**, 8728–8733

NCBI

Pub**Med**
www.pubmed.gov

A service of the National Library of
and the National Institutes

[Sign In] [Reg

| All Databases | PubMed | Nucleotide | Protein | Genome | Structure | OMIM | PMC | Journals | B |

Search PubMed for Kiefhaber T AND 825   Go   Clear   Save St

Limits   Preview/Index   History   Clipboard   Details

Display Abstract   Show 20   Sort by   Send to

All: 1   Review: 1   ☒

About Entrez

Text Version

Entrez PubMed
Overview
Help | FAQ
Tutorials
New/Noteworthy
E-Utilities

PubMed Services
Journals Database
MeSH Database
Single Citation Matcher
Batch Citation Matcher
Clinical Queries
Special Queries
LinkOut
My NCBI

Related Resources
Order Documents
NLM Mobile
NLM Catalog
NLM Gateway
TOXNET
Consumer Health
Clinical Alerts
ClinicalTrials.gov
PubMed Central

1: Biotechnology (N.Y.). 1991 Sep;9(9):825-9.   Related Articles, Links

Protein aggregation in vitro and in vivo: a quantitative model of the kinetic competition between folding and aggregation.

Kiefhaber T, Rudolph R, Kohler HH, Buchner J.

Universitat Bayreuth, Laboratorium fur Biochemie, FRG.

Protein aggregation is frequently observed as a major side-reaction of protein folding. We present quantitative models explaining the formation of aggregates during protein folding in vitro and in vivo on the basis of a kinetic competition between correct folding and aggregation reactions. Both models are in good agreement with experimental data. The model implies that, in vitro, the yield of native protein obtained upon refolding is determined by the rates of the competing first order folding and second order aggregation reactions. Therefore, a high protein concentrations aggregation dominates over folding and leads to the formation of insoluble protein. For in vivo protein synthesis, the model shows that the yield of native protein is only dependent on the rate of folding, on the rate of aggregation and on the rate of protein synthesis. In the cell, several mechanisms, including "folding helpers" seem to have evolved, which influence these processes and thereby prevent unproductive side reactions.

Publication Types:
- Review

PMID: 1367356 [PubMed - indexed for MEDLINE]

Display Abstract   Show 20   Sort by   Send to

Write to the Help Desk
NCBI | NLM | NIH
Department of Health & Human Services
Privacy Statement | Freedom of Information Act | Disclaimer

Aug 14 2006 08:07:58

http://www.ncbi.nlm.nih.gov/entrez/query.fcgi?CMD=Display&DB=pubmed   8/31/2006

Refolding of Denatured and Denatured/Reduced Lysozyme at High Concentrations*

Bakthisaran Raman, Tangirala Ramakrishna, and Ch. Mohan Rao‡

From the Centre for Cellular and Molecular Biology, Hyderabad 500 007, India

Refolding of proteins at high concentrations often results in aggregation. To gain insight into the molecular aspects of refolding and to improve the yield of active protein, we have studied the refolding of lysozyme either from its denatured state or from its denatured/reduced state. Refolding of denatured lysozyme, even at 1 mg/ml, yields fully active enzyme without aggregation. However, refolding of denatured/reduced lysozyme into buffer that lacks thiol/disulfide reagents leads to aggregation. Thiol/disulfide redox reagents such as cysteine/cystine and reduced/oxidized glutathione facilitate the renaturation, with the yield depending on their absolute concentrations. We have obtained an ~70% renaturation yield upon refolding of lysozyme at 150 μg/ml. The cysteine/cystine redox system is more efficient compared with the glutathione redox system. When lysozyme is refolded in the absence of redox reagents, a transient intermediate that has regained a significant amount of secondary structure is formed. The tryptophans in this intermediate are as exposed to water as in the fully unfolded protein. It shows increased exposure of hydrophobic surfaces compared with the native or completely unfolded enzyme. This aggregation-prone intermediate folds to active enzyme upon addition of oxidized glutathione before the aggregation process starts. These properties of the intermediate in the refolding pathway of lysozyme are similar to those proposed for the molten globule.

Understanding molecular details of the formation of functional three-dimensional structures, from the one-dimensional information contained in the genetic material, is still one of the major challenges of biology. Anfinsen (1), 3 decades ago, showed that the amino acid sequence dictates the three-dimensional native structure of a protein. Since then, there has been significant progress, particularly due to the availability of recombinant DNA technology tools. Under conditions favoring folding, unfolded states of a protein rapidly (10–50 ms) collapse to a compact-intermediate state, briefly visiting other intermediate states en route (2, 3). Such a compact-intermediate state, termed molten globule (3–6), is believed to adopt much of the secondary structure of the native protein, to be compact with respect to the unfolded states, and to possess little or no tertiary structure. Conversion of the compact-intermediate state to the native structure determines the overall rate of folding of a protein. Most of the partially folded states, including the molten-globule state, expose hydrophobic surfaces and have a

tendency to aggregate or to interact with hydrophobic surfaces in general. Molecular chaperones provide proper hydrophobic surfaces to interact with such partially folded states of proteins, prevent aggregation, and help in proper folding of proteins (2, 7–10).

With the advent of recombinant DNA technology, it is now possible to express a gene of interest in a foreign cell and to translate it into a polypeptide chain. However, extensive production of functionally active protein has been limited due to the formation of protein aggregates or inclusion bodies (11, 12). Inclusion bodies, aggregates of incompletely folded chains (13), are often partially or completely denatured using denaturants like urea and guanidine hydrochloride and then subjected to refolding (14).

Many proteins can be refolded properly without any external assistance at low concentrations. However, it is a common observation that the yield of renatured protein decreases when the concentration of the protein to be refolded increases (15–21). Kinetic competition between two types of interactions (interchain and intrachain) occurs during the refolding of a protein (20, 22). Unimolecular intrachain interactions largely lead to the native state, while multimolecular interchain interactions would be expected to increase with the concentration of the refolding protein and therefore lead to misfolding and aggregation (21). Thus, the efficacy of refolding depends on the partitioning of the folding protein between productive pathways leading to the native state and nonproductive pathways leading to misfolding and aggregation. Studies on the kinetics of competition between renaturation and aggregation during the refolding of lysozyme have shown that aggregation occurs very early during refolding through nonspecific hydrophobic interactions (21).

We have studied refolding of hen egg white lysozyme at high concentrations (at which earlier studies showed aggregation) using reduced/oxidized glutathione (GSH/GSSG), cysteine/cystine, and reduced/oxidized dithiothreitol (DTT/ODTT)[1] redox systems. We have observed an intermediate in the refolding pathway of lysozyme possessing a significant amount of secondary structure and significantly higher exposed hydrophobic surfaces, which can be refolded to its active form in the presence of GSSG or cystine.

EXPERIMENTAL PROCEDURES

Materials—Hen egg white lysozyme, L-cystine, DL-cystine hydrochloride, L-cysteine, DTT, ODTT, and *Micrococcus lysodeikticus* cells were purchased from Sigma. GSH and GSSG were procured from SISCO Research Laboratory (Bombay, India). Guanidine hydrochloride was purchased from Serva (Heidelberg, Germany). All other chemicals used in this study were of analytical grade. Lysozyme was further purified by Bio-Rex 70 column chromatography as described by Saxena and Wetlaufer (23).

Preparation of Denatured and Denatured/Reduced Enzymes—Dena-

[1] The abbreviations used are: DTT, dithiothreitol; ODTT, oxidized dithiothreitol; HPLC, high pressure liquid chromatography.

Docket No.: 00131-00350-US

Exhibit 12

Refolding of Lysozyme

tured lysozyme was prepared by dissolving 12 mg of enzyme in 1 ml of 50 mM Tris-HCl buffer (pH 8.3) containing 6 M guanidine hydrochloride and incubating at 25 °C for 15 h. Denatured/reduced lysozyme was prepared by dissolving the enzyme in the same buffer that also contained the reducing agent, 100 mM DTT. The lysozyme concentration was estimated by absorbance at 280 nm for a 1% solution as 26.3 (24). The stock of denatured or denatured/reduced protein was diluted, just before refolding, with 50 mM Tris-HCl buffer (pH 8.3) containing 6 M guanidine hydrochloride to obtain denatured or denatured/reduced protein stocks of required concentrations. We avoided the step of exchanging the denaturant with 0.1 M acetic acid, which was included in most of the earlier investigations, since our interest was to study the refolding of the enzymes from their fully denatured/reduced state. It is important to note that lysozyme regains partial secondary structure in 0.1 M acetic acid (23), and a concentration-dependent association of acid-denatured polypeptide chains has been described for several proteins (25, 26).

Refolding of Denatured and Denatured/Reduced Enzymes—Refolding of the enzyme was achieved by adding 25 µl of the denatured or denatured/reduced enzyme stock in denaturing buffer to 0.5 ml of refolding buffer (100 mM Tris acetate (pH 8.1)) either in the absence or presence of the required amounts of thiol/disulfide redox reagents in Eppendorf tubes. The sample was vortexed immediately for a brief period of 15 s and incubated at 25 °C for at least 5 h. L-Cystine is sparingly soluble in water at room temperature, and its solubility is known to increase at alkaline pH. To prepare a 1 mM cystine stock solution in 100 mM Tris acetate (pH 8.2), the suspension was incubated at 60 °C for ~5 min. Clear solution was obtained and brought back to room temperature. DL-Cystine hydrochloride dissolves freely in the buffer.

Kinetics of Renaturation—Refolding of denatured/reduced enzymes was carried out as described above. Small aliquots were withdrawn from the reaction mixture at different time intervals, and enzyme activity was measured immediately.

Kinetics of Aggregation—Refolding of denatured/reduced enzymes was performed in the absorption cuvette as described above. Turbidity of the sample was measured with time by monitoring the absorbance of the sample at 450 nm in a Hitachi U-2000 UV-visible spectrophotometer.

Enzyme Assays—Lysozyme activity was determined at 25 °C essentially as described by Fischer *et al.* (27). The rate of enzymatic lysis of *M. lysodeikticus* cells, suspended in 0.1 M phosphate buffer (pH 6.3), was obtained by measuring the decrease in turbidity of the cell suspension at 450 nm as a function of time using a Hitachi U-2000 UV-visible spectrophotometer. The percentage renaturation yield in the refolding studies was calculated with respect to the activity of the native enzyme.

Studies on the Early Folding Intermediate—Denatured/reduced lysozyme was refolded at 100 µg/ml (final concentration) in 100 mM Tris acetate (pH 8.1) lacking thiol/disulfide reagents; fluorescence and circular dichroism spectra were recorded 2 min after initiation of refolding and were completed within 5 min of initiation of refolding. These early recordings represent spectra of an "intermediate." The fluorescence spectra were recorded in a Hitachi F-4000 fluorescence spectrophotometer. The intrinsic fluorescence spectra of the native and denatured/reduced enzymes and the intermediate were recorded with a scan speed of 60 nm/min and 5 and 3 nm excitation and emission band passes, respectively. The excitation wavelength was set at 295 nm. In another experiment, 10 µl of a 10 mM methanolic solution of the hydrophobic dye 8-anilinonaphthalene-1-sulfonic acid was added to 1 ml of native or refolded enzyme and the intermediate samples. The fluorescence spectra were recorded immediately with the excitation wavelength set at 365 nm and a scan speed of 120 nm/min. All fluorescence spectra were recorded in the correct spectrum mode. Far-UV CD spectra of native and refolded lysozyme and the intermediate were recorded using a Jasco J-20 spectropolarimeter.

To determine whether the intermediate could be renatured, denatured/reduced lysozyme was allowed to refold for a short period of 2 min, allowing the formation of the intermediate. Then, 10 µl of 100 mM GSSG was added to 1 ml of the intermediate, and the sample was incubated at 25 °C. The activity was measured after 3 h.

Studies on Refolded Lysozyme—Denatured/reduced lysozyme was refolded at 100 µg/ml as described above in the presence of 1 mM DL-cystine hydrochloride. The sample was incubated at 25 °C for 5 h and centrifuged at 4000 × *g* to remove insoluble material. Far-UV CD spectra of this sample and the native enzyme were recorded. Reverse-phase HPLC was also performed on an analytical C₁₈ column with a 0–100% acetonitrile gradient and a flow rate of 1 ml/min.
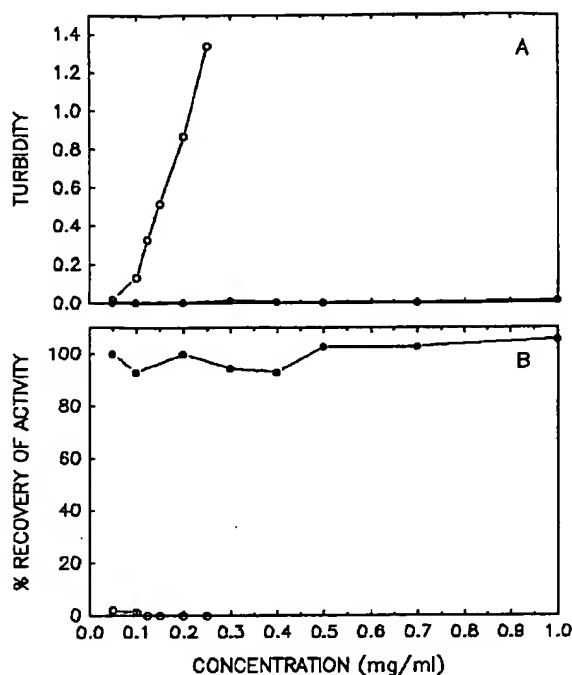

FIG. 1. **Refolding of denatured (●) and denatured/reduced (O) lysozyme at different concentrations.** The refolding buffer contained no thiol/disulfide redox reagents. *A*, turbidity of the samples was measured as the absorbance at 450 nm. *B*, shown is the percentage recovery of activity with respect to the activity of native lysozyme.

RESULTS AND DISCUSSION

Lysozyme is one of the most extensively studied (21, 23, 28–31) enzymes for its refolding properties. Several low molecular weight thiol/disulfide redox pairs such as reduced and oxidized glutathione, reduced and oxidized dithiothreitol, cysteine and cystine, and cystamine and cysteamine have been shown to accelerate the oxidative refolding of lysozyme (23). At low concentrations (~14 µg/ml), lysozyme has been shown to refold to its native state, however with varying renaturation yields (21, 23, 28–31). As the concentration of the enzyme to be refolded increases, the renaturation yield drastically decreases due to misfolding or aggregation (21).

We studied the refolding of denatured and denatured/reduced lysozyme at high concentrations. Refolding of denatured lysozyme even at 1 mg/ml does not result in any aggregation (Fig. 1*A*). Almost 100% activity of the enzyme is recovered (Fig. 1*B*). However, denatured/reduced lysozyme does not refold to its active form when the refolding buffer lacks thiol/disulfide reagents. Even at the lowest concentration studied (50 µg/ml), refolding of denatured/reduced lysozyme results in aggregation as shown in Fig. 1*A*. Lysozyme is known to refold within a few seconds when the disulfide bonds are intact (32), while it takes several minutes when the disulfide bonds are reduced (23). Goldberg and Guillou (33) have shown that a folding intermediate with substantial secondary structure is formed in 4 ms when denatured lysozyme is subjected to refolding, whereas the refolding of lysozyme under conditions that lead to reduction of its disulfide bonds does not exhibit any secondary structural formation in such a time scale. Our results show that denatured lysozyme refolds completely to its active state without any aggregation due to self-association even at concentrations as high as 1 mg/ml. Kumar *et al.* (15) showed that the refolding of denatured but not reduced RNase A at a concentration as high as 20 mg/ml yielded a single peak in sedimen-
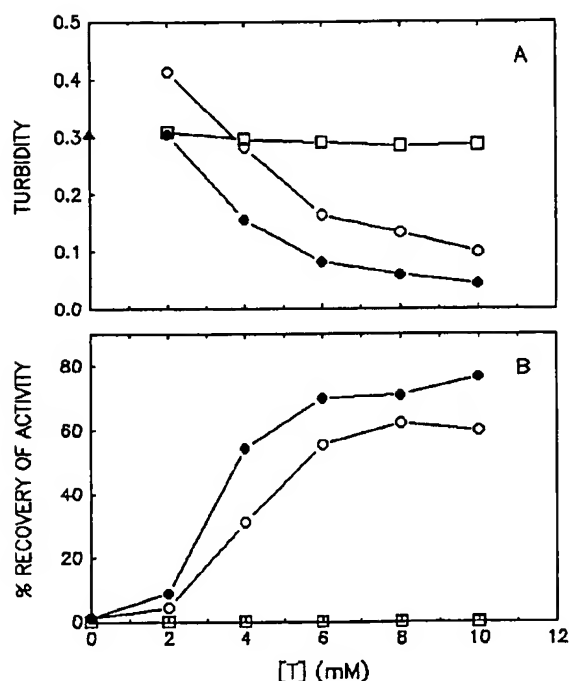
FIG. 2. **Refolding of denatured/reduced lysozyme at 125 μg/ml in the presence of different concentrations of GSH and GSSG (O), cysteine and cystine (●), and DTT and ODTT (□).** The molar ratio of the reduced to oxidized forms was maintained at 10:1. The concentration of the reduced form is given on the *x axis. A,* turbidity profile as a function of the concentration of thiol/disulfide redox reagents. Turbidity was measured as the absorbance at 450 nm. *B,* the percentage recovery of activity with respect to the activity of the native enzyme. *[T]* represents [GSH], [cysteine], or [DTT].
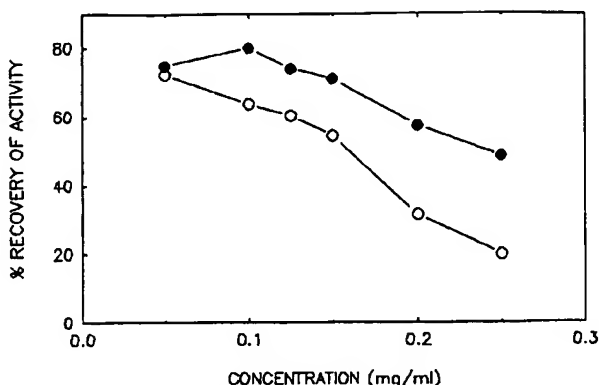

FIG. 3. **Refolding of denatured/reduced lysozyme at different concentrations in the presence of 10 mM GSH and 1 mM GSSG (O) or 10 mM cysteine and 1 mM cystine (●).** The concentrations indicated are the final concentrations of the protein obtained after dilution into the refolding medium. The percentage recovery of activity is with respect to the activity of the native enzyme.

tation analysis with $s_{20,w}$ similar to that of the native enzyme. Native lysozyme does not exhibit self-association at the concentration range used in the present study (35). Thus, it appears that the constraints imposed by the disulfide bonds facilitate a faster rate of secondary structural formation, fewer intermolecular interactions, and productive folding of proteins.

As we have mentioned above, refolding of denatured/reduced lysozyme leads to aggregation of the protein. We studied the effect of thiol/disulfide redox reagents on the refolding of denatured/reduced lysozyme at high concentrations. Fig. 2 shows the effect of absolute concentrations of GSH/GSSG or cysteine/ cystine, maintaining a millimolar ratio of 10:1, on the refolding of denatured/reduced lysozyme at 125 μg/ml. When the refolding buffer lacks these thiol/disulfide redox reagents (*i.e.* at the *y* intercept), the enzyme aggregates to a significant extent as measured by turbidity (Fig. 2*A*), and the renaturation yield is minimal (Fig. 2*B*). The percentage renaturation increases with the increase in concentration of thiol/disulfide reagents in the refolding medium (Fig. 2*B*). To measure the extent of aggregation, we monitored the absorbance at 450 nm as a measure of turbidity of the solutions. Fig. 2 shows that as the concentration of thiol/disulfide reagents increases, the extent of aggregation decreases with a concomitant increase in the percentage renaturation of the enzyme. Under the refolding conditions used in our studies, the DTT/ODTT system, however, did not facilitate renaturation of the enzyme (Fig. 2).

Fig. 3 shows the renaturation yields obtained upon refolding at different concentrations of denatured/reduced lysozyme in the presence of GSH/GSSG and cysteine/cystine reagents. The renaturation yield gradually decreases with an increase in the protein concentration. At the lowest concentration (50 μg/ml),

we obtained 75% renaturation. Earlier studies with a much lower concentration of lysozyme (~14 μg/ml) reported varying renaturation yields, ranging from 35 to 90%, employing different conditions of refolding. However, at concentrations >50 μg/ml, Goldberg *et al.* (21) reported a drastic drop in the renaturation yield; upon refolding lysozyme at 140 μg/ml, they obtained a renaturation yield of only 10%. In an enzyme-assisted folding process, Puig and Gilbert (36) obtained a renaturation yield of ~60% upon refolding lysozyme at 10 μM (140 μg/ml) in the presence of 30 μM (1650 μg/ml) protein-disulfide isomerase, an enzyme found in the lumen of the endoplasmic reticulum (37, 38). Protein-disulfide isomerase catalyzes thiol/ disulfide exchange reactions in the folding of disulfide-containing proteins (39). Under the conditions used in the present study, we were able to obtain renaturation yields of ~70% upon nonenzymatic refolding of lysozyme at concentration as high as 150 μg/ml (see Fig. 3).

We compared the effect of the GSH/GSSG redox system with that of the cysteine/cystine redox system on the refolding of denatured/reduced lysozyme (Figs. 2, 3, and 4). As evident from Figs. 2–4, the cysteine/cystine redox system appears to be more effective than the GSH/GSSG system under the conditions used. In contrast to our observation, Saxena and Wetlaufer (23) found that several thiol/disulfide pairs had about the same efficiency, both in the rate of refolding and in the yield of active lysozyme. We believe that the reason for this difference lies in the concentration of the protein; they studied refolding of lysozyme at a low concentration (14 μg/ml), whereas we used higher concentrations. This is suggested by the data in Fig. 3; at 50 μg/ml, refolding of denatured/reduced lysozyme either in 10 mM GSH, 1 mM GSSG or in 10 mM cysteine, 1 mM cystine results in similar renaturation yields (~75%), whereas at higher concentrations of the protein, the difference in the renaturation yields for the two redox systems is quite significant. Therefore, in the present study, the refolding at higher concentrations of proteins probably differentiates the efficiency of these thiol/disulfide pairs. The reason for the higher efficiency of the cysteine/cystine system over the GSH/GSSG system, however, is not clear. It may be attributed to lesser net ionic charge and the smaller size of cysteine and cystine molecules, which enable these molecules to access the cysteine residues in the partially folded protein better in comparison with relatively highly charged, bulkier GSH and GSSG molecules.

It is interesting to note that oxidized glutathione or cystine alone facilitates the refolding of denatured/reduced lysozyme to
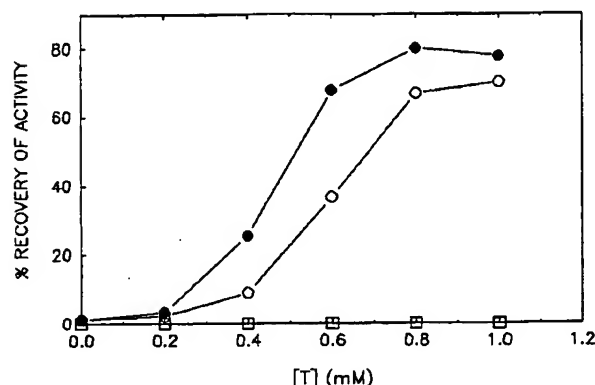
FIG. 4. **Refolding of denatured/reduced lysozyme at 125 μg/ml in the presence of various concentrations of GSSG (O), cystine (●), and ODTT (□).** The percentage recovery of activity is with respect to the activity of the native enzyme. *[T]* represents [GSSG], [cystine] or [ODTT].

WAVELENGTH (nm)

FIG. 5. **Far-UV CD spectra of native (——) and refolded (- - -) lysozyme and the intermediate (- · - ·).** See "Experimental Procedures" for details.

a significant extent as shown in Fig. 4. However, the renaturation yield is very low at lower concentrations of GSSG and is more pronounced at higher concentrations (0.6–1 mM). We also observed that different ratios of oxidized to reduced glutathione have little effect on the renaturation yield of lysozyme (data not shown). These results suggest that redox potential does not affect significantly the refolding of lysozyme. This also suggests that breaking and remaking of disulfide bonds might not be a significant factor in the refolding of lysozyme under the conditions used.

In the present study, we obtained almost 80% recovery of activity on refolding denatured/reduced lysozyme at 100 μg/ml; due to surface denaturation and adsorption of lysozyme on the surface of reaction tubes, some amount of protein is not recovered (36) (in fact, we could observe a thin film of protein on the surface (air/water interface) of the refolded sample that could be removed by centrifugation). The high recovery of activity on refolding lysozyme at appropriate concentrations of thiol/disulfide reagents indicates the recovery of its native structure. We therefore studied the refolded lysozyme for its secondary structure. Fig. 5 shows the far-UV CD spectra of native and refolded lysozyme (see "Experimental Procedures" for details). The far-UV CD spectrum of refolded lysozyme overlaps almost completely with that of native lysozyme within experimental error. The refolded enzyme also elutes with the same retention time as that of the native enzyme on reverse-phase HPLC as shown in Fig. 6. The intrinsic fluorescence of the refolded enzyme and its binding to the hydrophobic dye 8-anilinonaphthalene-1-sulfonic acid are comparable to the native protein (see Figs. 9 and 10). These results clearly demonstrate that the enzyme has almost completely regained its native structure.

We monitored the kinetics of the refolding of denatured/reduced lysozyme at low and high concentrations by measuring the activity of the enzyme as a function of time. Fig. 7 shows the percentage renaturation yield of lysozyme upon refolding at concentrations of 25 and 100 μg/ml in the presence of 10 mM GSH and 1 mM GSSG over a period of 50 min. It is interesting to note that the rate of refolding is relatively lower at the higher concentration of lysozyme.

As mentioned above, higher concentrations of thiol/disulfide reagents suppress the aggregation and improve the renaturation yield in the refolding of proteins at higher concentrations. Thiol/disulfide redox reagents do not have any apparent apolar surfaces, and the mechanism of the observed suppression of aggregation of proteins by the thiol/disulfide reagents may not involve hydrophobic interactions. The kinetics of aggregation of
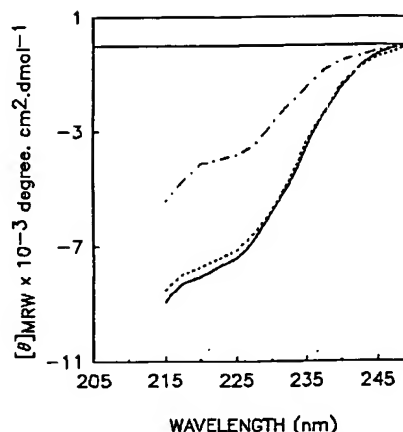
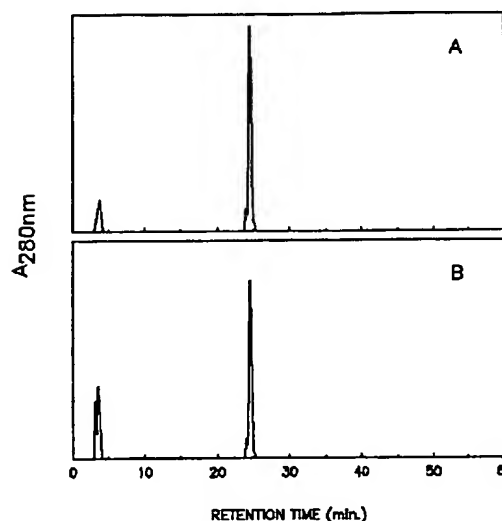

FIG. 6. **Reverse-phase HPLC on a C₁₈ column of native (A) and refolded (B) lysozyme.** An acetonitrile gradient of 0% (at 5 min) to 100% (at 50 min) was used with a flow rate of 1 ml/min. The peaks below 5 min are salt peaks.

denatured/reduced lysozyme upon refolding is shown in Fig. 8. The aggregation is minimum and negligible up to 5 min, and it increases more sharply afterwards. The aggregation is suppressed when the refolding medium contains cystine or GSSG (Fig. 8). This is perhaps due to increased partitioning into proper folding at the expense of the aggregation-prone intermediate.

The data in Fig. 8 show that aggregation is negligible in the first 5 min when lysozyme is refolded at 100 μg/ml in the absence of thiol/disulfide reagents. We therefore studied this sample before the aggregation process starts (between 2 and 5 min after initiation of refolding). The far-UV CD spectrum of this sample is shown in Fig. 5. It is evident from Fig. 5 that a significant amount of secondary structure is regained. Because of the low concentration of the protein sample (and pronounced aggregation observed at higher concentrations), we could not record the near-UV CD spectrum. However, the fluorescence spectrum of this sample shows an emission maximum of 348 nm; the fluorescence spectra of denatured and denatured/reduced protein show emission maxima of 350 nm, while native lysozyme shows an emission maximum of 337 nm (Fig. 9). This
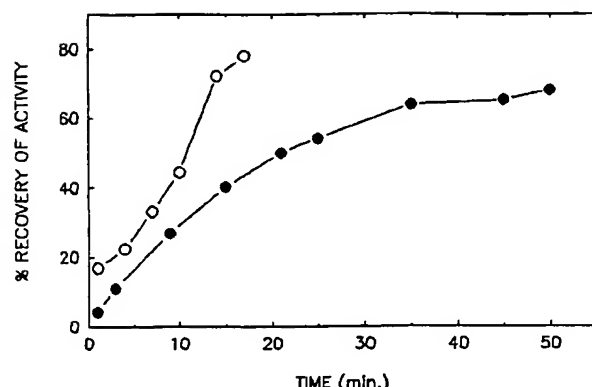
FIG. 7. Kinetics of refolding of denatured/reduced lysozyme at 25 (O) and 100 (●) µg/ml. The refolding medium contained 1 mM GSSG. The percentage recovery of activity is with respect to the activity of the native enzyme.

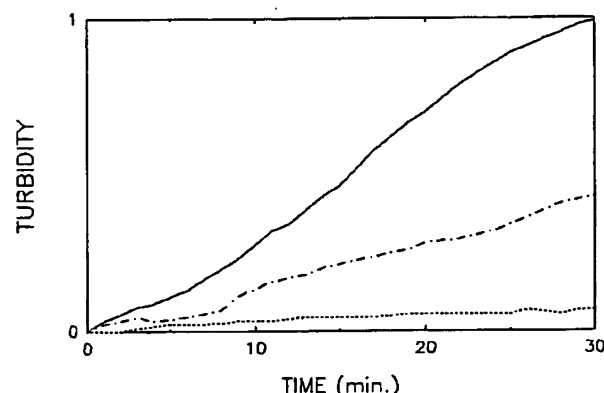FIG. 8. Kinetics of aggregation of denatured/reduced lysozyme upon refolding at 100 (-·-·) and 125 (———) µg/ml in 0.1 M Tris acetate (pH 8.2) lacking redox reagents and in buffer containing 1 mM cystine (---). The extent of aggregation was measured as turbidity of the solutions. Turbidity was measured as the absorbance at 450 nm.

FIG. 9. Intrinsic fluorescence spectra of native (———), denatured or denatured/reduced (-·-·), and refolded (-··-) lysozyme and the intermediate (---). Spectra were recorded with an excitation wavelength of 295 nm and using excitation and emission band passes of 5 and 3 nm, respectively.

FIG. 10. Fluorescence spectra of 8-anilinonaphthalene-1-sulfonic acid-bound native (———), denatured or denatured/reduced (···), and refolded ([-··-]) lysozyme and the intermediate (---). Spectra were recorded at a scan speed of 120 nm/min with data collection at every 0.5 s. The excitation and emission band passes were 5 and 3 nm, respectively, and the excitation wavelength was set at 365 nm.

reveals that the tryptophans of the intermediate are exposed to water, similar to those of the unfolded protein. The hydrophobic dye 8-anilinonaphthalene-1-sulfonic acid binds with much more avidity to this intermediate state (Fig. 10) than to the native, denatured/reduced, or refolded enzyme. We investigated whether this intermediate state can be directed to active enzyme upon addition of oxidized glutathione. Upon addition of GSSG to a final concentration of 1 mM and incubation for ~3 h, almost 60% of the activity was regained. Thus, lysozyme in this state may be characterized as an intermediate in its refolding pathway. The fate of this intermediate depends on the relative rates of (i) aggregation and (ii) proper refolding. The latter process can be favored by the presence GSSG or cystine. Kuwajima *et al.* (32) carried out kinetic studies using stop-flow CD on the refolding of lysozyme and the homologous protein α-lactalbumin at 4.5 °C by measuring changes in the aromatic and peptide regions and observed a kinetic molten-globule intermediate. The native tertiary structure in both proteins was completely absent, while they had almost complete backbone secondary structure. The presence of a stable, partially folded, molten globule-like state, both for lysozyme and α-lactalbumin, has also been demonstrated during trifluoroethanol-induced unfolding (40, 41). The early intermediate obtained by us upon refolding lysozyme in the absence of redox reagents also possesses substantial secondary structure and exhibits intrinsic
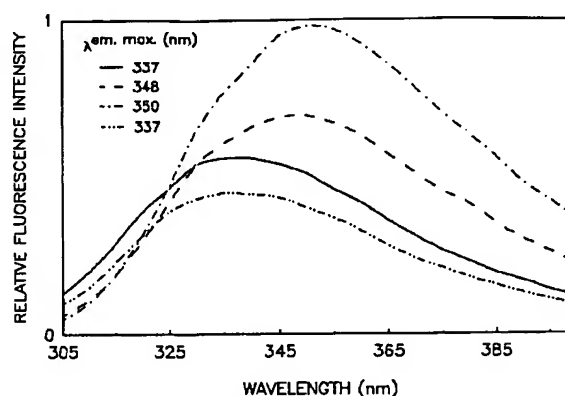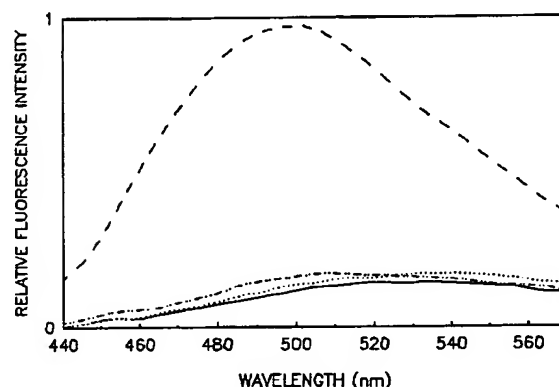
fluorescence similar to that of the fully unfolded protein. The binding of 8-anilinonaphthalene-1-sulfonic acid to this intermediate is severalfold higher than that to the native or fully unfolded enzyme as usually observed for the molten-globule state (34). These properties of the intermediate are similar to those proposed for the molten-globule intermediate of proteins.

We have demonstrated that denatured/reduced lysozyme can be refolded at high concentrations with good renaturation yields at appropriate concentrations of thiol/disulfide reagents in the refolding buffer. The cysteine/cystine redox system appears to be more efficient than the GSH/GSSG system. We have observed an intermediate, formed early during the refolding of lysozyme, before the pairing of disulfide bonds occurs that has properties similar to those of a molten globule. This intermediate is prone to aggregation, but in the presence of GSSG, can be refolded to active enzyme. These results should prove useful in understanding intermediates in the pathway of protein folding.

REFERENCES

1. Anfinsen, C. B. (1973) *Science* 181, 223–230
2. Creighton, T. E. (1990) *Biochem. J.* 270, 1–16
3. Landry, S. J., and Gierasch, L. M. (1994) *Annu. Rev. Biophys. Biomol. Struct.* 23, 645–669
4. Baldwin, R. L. (1993) *Curr. Opin. Struct. Biol.* 3, 84–91

5. Kuwajima, K. (1989) *Proteins Struct. Funct. Genet.* **6**, 87–103
6. Ptitsyn, O. B. (1995) *Adv. Protein Chem.* **47**, 83–229
7. Hartl, F. U., Martin, J., and Neupert, W. (1992) *Annu. Rev. Biophys. Biomol. Struct.* **21**, 293–322
8. Agard, D. A. (1993) *Science* **260**, 1903–1904
9. Craig, E. A. (1993) *Science* **260**, 1902–1903
10. Hendrick, J. P., and Hartl, F. U. (1993) *Annu. Rev. Biochem.* **62**, 349–384
11. Marston, F. A. O. (1986) *Biochem. J.* **240**, 1–12
12. Jaenicke, R. (1987) *Prog. Biophys. Mol. Biol.* **49**, 117–237
13. Haase-Pettingell, C. A., and King, J. (1988) *J. Biol. Chem.* **263**, 4977–4983
14. Kane, J. F., and Hartley, D. L. (1988) *Trends Biotechnol.* **6**, 87–101
15. Kumar, T. K. S., Gopalakrishna, K., Ramakrishna, T., and Pandit, M. W. (1994) *Int. J. Biol. Macromol.* **16**, 171–176
16. Jaenicke, R. (1974) *Eur. J. Biochem.* **46**, 149–155
17. Teipel, J. W., and Koshland, D. A., Jr. (1971) *Biochemistry* **10**, 792–805
18. London, J., Skrzynia, C., and Goldberg, M. E. (1974) *Eur. J. Biochem.* **47**, 409–415
19. Orsini, G., Skrzynia, C., and Goldberg, M. E. (1975) *Eur. J. Biochem.* **59**, 433–440
20. Zettlmeissl, G., Rudolph, R., and Jaenicke, R. (1979) *Biochemistry* **18**, 5567–5571
21. Goldberg, M. E., Rudolph, R., and Jaenicke, R. (1991) *Biochemistry* **30**, 2790–2797
22. Orsini, G., and Goldberg, M. E. (1978) *J. Biol. Chem.* **253**, 3453–3458
23. Saxena, V. P., and Wetlaufer, D. B. (1970) *Biochemistry* **9**, 5015–5022
24. Sophianopoulos, A. J., Rhodes, C. K., Holcomb, D. N., and van Holde, K. E.

(1962) *J. Biol. Chem.* **237**, 1107–1112
25. Rudolph, R., and Jaenicke, R. (1976) *Eur. J. Biochem.* **63**, 409–417
26. Goto, Y., and Fink, A. L. (1989) *Biochemistry* **28**, 945–952
27. Fischer, B., Perry, B., Sumner, I., and Goodenough, P. (1992) *Protein Eng.* **5**, 593–596
28. Perraudin, J. P., Torchia, T. E., and Wetlaufer, D. B. (1983) *J. Biol. Chem.* **258**, 11834–11839
29. Anderson, W. L., and Wetlaufer, D. B. (1976) *J. Biol. Chem.* **251**, 3147–3153
30. Fischer, B., Sumner, I., and Goodenough, P. (1992) *Arch. Biochem. Biophys.* **298**, 361–364
31. Fischer, B., Sumner, I., and Goodenough, P. (1993) *Arch. Biochem. Biophys.* **306**, 183–187
32. Kuwajima, K., Hiraoka, Y., Ikeguchi, M., and Sugai, S. (1985) *Biochemistry* **24**, 874–881
33. Goldberg, M. E., and Guillou, Y. (1994) *Protein Sci.* **3**, 883–887
34. Semisotnov, G. V., Rodionova, N. A., Razgulyaev, O. I., Uversky, V. N., Gripas, A. F., and Gilmanshin, R. L. (1991) *Biopolymers* **31**, 119–128
35. Wills, P. R., Nichol, L. W., and Siezen, R. J. (1980) *Biophys. Chem.* **11**, 71–82
36. Puig, A., and Gilbert, H. F. (1994) *J. Biol. Chem.* **269**, 7764–7771
37. Noiva, R., and Lennarz, W. J. (1992) *J. Biol. Chem.* **267**, 3553–3556
38. Freedman, R. B. (1989) *Cell* **57**, 1069–1072
39. Lyles, M. M., and Gilbert, H. F. (1991) *Biochemistry* **30**, 613–619
40. Buck, M., Radford, S. E., and Dobson, C. M. (1993) *Biochemistry* **32**, 669–678
41. Alexandrescu, A. T., Ng, Y.-L., and Dobson, C. M. (1994) *J. Mol. Biol.* **235**, 587–599

Refolding of recombinant proteins
Eliana De Bernardez Clark

Expression of recombinant proteins as inclusion bodies
in bacteria is one of the most efficient ways to produce
cloned proteins, as long as the inclusion body protein can
be successfully refolded. Aggregation is the leading cause
of decreased refolding yields. Developments during the past
year have advanced our understanding of the mechanism
of aggregation in *in vitro* protein folding. New additives to
prevent aggregation have been added to a growing list. A
wealth of literature on the role of chaperones and foldases in
in vivo protein folding has triggered the development of new
additives and processes that mimic chaperone activity *in vitro*.

Addresses
Department of Chemical Engineering, Tufts University, Medford,
MA 02155, USA; e-mail: edeberna@tufts.edu

Abbreviations
DTT   dithiotreitol
GdmCl   guanidinium chloride

Introduction
Expression of cloned genes in bacteria is widely used
both in industry, for the production of pharmaceutical
proteins, and in research, for the production of proteins
for structural and/or biochemical studies. Bacteria produce
large quantities of recombinant proteins in rapid, often
inexpensive, fermentation processes; however, the product
of interest is frequently deposited in insoluble inactive
aggregates or inclusion bodies. The general strategy
used to recover active protein from inclusion bodies
involves three steps: firstly, inclusion body isolation and
washing; secondly, solubilization of the aggregated protein,
which causes denaturation; and finally, refolding of the
solubilized protein. While the efficiency of the first two
steps can be relatively high, folding yields may be limited
by the production of inactive misfolded species as well
as aggregates.

When the formation of inclusion bodies was first observed
almost two decades ago, existing protein folding protocols
were not, in most cases, applicable to the folding of recom-
binant mammalian proteins, which are in most cases mul-
tidomain, oligomeric, and/or disulphide bonded proteins.
Existing protein folding protocols had been developed to
characterize folding intermediates and investigate folding
pathways of small, monomeric proteins. When applied to
the refolding of inclusion body proteins, these protocols
failed to produce active proteins with significant yields.
Even today, the literature on identification of protein

folding intermediates and the elucidation of folding
pathways deals mostly with small monomeric proteins
that have either intact or no disulphide bonds [1]. For
many years, eukaryotic expression hosts which produced
soluble secreted recombinant proteins became favored
over bacterial hosts because of the difficulties encountered
when refolding inclusion body proteins; however, careful
examination of the folding conditions allowed researchers
to find ways to refold multidomain disulphide bonded
proteins with relatively high yields. Most of the original
work on inclusion body protein folding can be found in
the patent literature starting around 1985 [2].

The recent literature includes many examples in which
recombinant proteins have been produced by refold-
ing from inclusion bodies. Some of these applications
demonstrate the use of suboptimal refolding protocols
to produce small quantities of protein for structural
and/or biochemical studies. Other applications deal with
commercial processes. To be acceptable for commercial
applications, refolding processes must be fast, inexpensive
and highly efficient. This review focuses on recent
developments in the optimization of refolding processes
with emphasis on methodologies applicable to large-scale
protein production. Since most proteins of commercial
value are secreted in their natural host and are likely to
contain disulphide bonds, this review emphasizes recent
progress in protein refolding with concomitant disulphide
bond formation, also called oxidative protein refolding.

Inclusion body isolation and solubilization
Expression of recombinant proteins as inclusion bodies
can be advantageous due to the very high levels of
enriched protein produced and the protection of the
protein product from proteolytic degradation. In addition,
when producing a recombinant product which, when
active, can be toxic or lethal to the host cell, inclusion
body production may be the best available method. Cells
containing inclusion bodies are typically disrupted by high
pressure homogenization and the resulting suspension is
centrifuged to remove the soluble fraction. Occasionally a
lytic enzyme, such as lysozyme, may be added before cell
disruption to increase efficiency and reduce power require-
ments. The resulting inclusion body-containing pellet is
washed with buffers containing either low concentrations
of chaotropic agents, such as urea or guanidinium chloride
(GdmCl), or detergents, such as Triton X-100 [3•,4,5•]
and sodium deoxycholate [4,6,7]. This washing step is
designed to remove contaminants, especially proteins, that
may have adsorbed onto the hydrophobic inclusion bodies
during processing, and could affect protein refolding
yield. Alternatively, sucrose gradient centrifugation may be
performed to purify inclusion bodies and separate them
from other cellular components [4,P1]. After washing,

inclusion bodies are solubilized using strong denaturants, such as urea, GdmCl, or thiocyanate salts, or detergents, such as SDS [8*,P1], n-cetyl trimethylammonium chloride [4], sarkosyl [6], or sodium n-laurosyl sarcosine [7], and a reducing agent, such as β-mercaptoethanol, dithiotreitol (DTT), dithioerythritol, or cysteine. Temperatures above 30°C are typically used to facilitate the solubilization process. A chelating agent, such as EDTA or EGTA, can be included in the solubilization buffer to scavenge metal ions, which could cause unwanted oxidation reactions. Solubilization can also be accomplished by the addition of acids, such as 70% formic acid [5*]. Alternatively, for periplasmic inclusion bodies the recombinant protein may be recovered by *in-situ* solubilization [P2*] in which the denaturant and reducing agent are added to the broth at the end of the fermentation process, and the cell debris is separated from the soluble material by aqueous two-phase extraction.

Solubilized inclusion body proteins can be contaminated with varying levels of host proteins, nucleic acids, and cell membrane components. It is thought that the presence of these microbial contaminants may induce aggregation during refolding, thus reducing overall yields. Maachupalli-Reddy *et al.* [9*] showed that whereas non-proteinaceous contaminants have little effect on renaturation yields, aggregation of protein contaminants can result in significant losses by triggering co-aggregation of the desired protein. Thus, some inclusion body processes include a purification step prior to refolding. Typically this step may be ion exchange [4,10], size exclusion [P3*,11], metal affinity [12], or reverse phase chromatography [P3*]. A common feature of these chromatographic steps is that they all operate with buffers that keep the protein in the denatured reduced state. If the solubilized protein is to be stored for later use, it may typically be exchanged into an acidic buffer, such as 10% acetic acid or 5–10 mM HCl [P3*,13] and freeze-dried. Exposure to low pH may result, for some proteins, in the formation of partially folded intermediates unable to refold to the native active configuration [14]. In this case, the lyophilized protein should be resolubilized using chaotropic agents or detergents, before refolding is attempted.

Renaturation of the solubilized protein

Several methods, including dilution, dialysis, diafiltration, gel filtration, and immobilization onto a solid support, may be employed to remove or reduce excess denaturing and reducing agents, allowing proteins to renature. Dilution of the denatured solution directly into renaturation buffer is the easiest process. In dialysis, the denatured protein solution is dialyzed against renaturation buffer. Because dialysis is based on the diffusion of smaller molecules and ions through membranes, it may be too slow to be used in commercial scale production of proteins. In addition, exposure of the protein to intermediate concentration of denaturants for a prolonged period of time may cause aggregation. Diafiltration is a faster, therefore,

more practical membrane-based alternative because the rate of denaturant removal is not diffusion limited, the driving force being pressure difference; however, as the driving force for buffer exchange is the pressure drop across the membrane, accumulation of denatured protein on the membrane may limit its application due to excessive fouling. Gel filtration chromatography has been successfully used to renature secretory leukocyte protease inhibitor, carbonic anhydrase and lysozyme [P4,15–17]; however, problems in flow through the column may arise due to protein aggregation upon buffer exchange. Aggregation in a chromatographic column can be prevented by immobilizing individual polypeptide chains onto the matrix [12,13,18]. Potential complications may arise if folding of the protein is inhibited by binding to the solid support, which could be prevented by using fusion proteins [19,20*]. In addition to buffer exchange, column chromatography allows for some degree of purification of the desired product.

In the case of disulphide bonded proteins, renaturation buffers must promote disulphide bond formation (oxidation). The most common methods used to promote oxidation during refolding are: air oxidation; the oxido shuffling system; the use of mixed disulphides; and oxidation of sulphonated proteins. Although, oxidation with air or oxygen in the presence of trace amounts of metal ions is simple and inexpensive [P2*,21*], renaturation rates and yields can be low. Higher oxidation rates and yields can be obtained by utilizing 'oxido shuffling' reagents, low molecular weight thiols in reduced and oxidized forms, which allow for both formation and reshuffling of disulphide bonds, which can alter configurations. The most common oxido shuffling reagents are reduced and oxidized glutathione (GSH/GSSG), but the pairs cysteine/cystine, cysteamine/cystamine, DTT/oxidized glutathione, and dithioerythritol/oxidized glutathione have also been utilized. Typically a 1–3 mM reduced thiol and a 10:1 to 5:1 ratio of reduced to oxidized thiol are used to promote proper disulphide bonding [21*]. More recently, we have shown that optimum renaturation yields are obtained when the ratio of reduced to oxidized thiol is anywhere between 3:1 and 1:1 [22*]. A disadvantage of the oxido shuffling system over the use of air oxidation, is the high cost of some of the reagents, particularly oxidized glutathione.

Another strategy employed to oxidize proteins during folding is the formation of mixed disulphides between oxidized glutathione and reduced protein before renaturation [3*]. Formation of mixed disulphides increases the solubility of the denatured protein by increasing the hydrophilic character of the polypeptide chain. Disulphide bond formation is then promoted by adding catalytic amounts of a reducing agent in the renaturation step. A similar protection of thiol groups during solubilization can be achieved by sulphonation of the denatured protein, in which a reducing agent and sodium sulphite are used

to cleave disulphide bonds and protect the resulting thiol groups as sulphonates [P3•,5•]. Under renaturation conditions, the protection groups are removed by oxidation in the presence of small amounts of a reducing agent to promote disulphide bond reshuffling.

Competition between folding and aggregation

Formation of off-pathway species, such as incorrectly folded species and aggregates, are the cause of decreased renaturation yields. Because aggregation is an intermolecular phenomenon, it is highly protein concentration dependent. The most direct means of minimizing aggregation is by decreasing protein concentration. It has been suggested that optimum recovery yields can be expected if the protein concentration is in the range of 10–50 μg/ml [21•]. Renaturation at such low protein concentrations requires large volumes of refolding buffer, driving production costs upward.

The key to a successful commercial refolding process lies in achieving high yields while refolding at high protein concentrations. One solution involves using either slow continuous or discontinuous addition of denatured protein to refolding buffer [3•]. Enough time is allowed between additions for the protein to fold past the early stages in the folding pathway, when it is susceptible to aggregation. The components of the solution containing the denatured protein must be carefully examined to avoid detrimental effects due to their accumulation in the refolding solution after multiple addition steps. Another alternative for decreasing protein aggregation while folding at relatively high protein concentrations (up to 4 mg/ml for carbonic anhydrase II) is to use the temperature-leap tactic [23], in which the protein is allowed to refold at low temperatures, to minimize aggregation, and then the temperature is rapidly raised to promote fast folding after the intermediates responsible for aggregation have been depleted. A third method involves folding by dilution to final denaturant concentrations that are high enough to solubilize aggregates but low enough to promote proper folding. We have shown that the oxidative renaturation of lysozyme can be carried out at protein concentrations of up to 5 mg/ml with very high yields in the presence of 1–2 M GdmCl [22•]. An alternative method which also exposes the refolding protein to intermediate denaturant concentrations was developed by Maeda et al. [24]. In this method, renaturation is started by dialysis against a buffer containing high denaturant concentration (8 M urea) and thiol/disulphide exchange reagents, and the denaturant concentration in the dialysis buffer is gradually diluted using buffer without denaturant. Using this method, Maeda et al. [24] were able to refold immunoglobulin G at concentrations above 1 mg/ml with yields as high as 70%. For proteins that do not tend to aggregate at intermediate denaturant concentrations, the slow dialysis method can successfully prevent aggregation by exposing the protein to a slow decrease in denaturant concentration. For proteins that aggregate at intermediate denaturant concentrations, fast or slow dilution of denatured protein into renaturation buffer, rather than slow dialysis, is the refolding method of choice.

As aggregation is the major cause behind low renaturation yields, elucidating the aggregation pathway may hold the key to successful protein refolding at moderate to high protein concentrations. Intermediates with hydrophobic patches exposed to the solvent play a crucial role in the partition between native and aggregated conformations. Folding intermediates are believed to possess significant elements of secondary structure but little of the native tertiary structure. Due to the expanded volume of these intermediates, hydrophobic patches, which may normally be buried in the native state, are exposed to the solvent. When hydrophobic regions on separate polypeptide chains interact, intermediates are diverted off the correct folding pathway into aggregates. The so called 'molten globule' intermediate is believed to play a major role in the kinetics of folding [25] and probably plays a role in aggregation. Despite the controversy over the nature of this intermediate (on-pathway versus off-pathway) [26•] from a kinetic point of view, intermolecular association of molten globule-like intermediates may be the starting point of the aggregation pathway. On the other hand, Yon [27] suggests that intermolecular associations responsible for aggregate formation may arise from fluctuating species that precede the molten-globule state.

Pioneer work by Goldberg et al. [28] shed light into the nature of interactions responsible for aggregation during folding. They showed that incorrect disulphide bonding may not be the major cause of aggregation because aggregates were formed even when a carboxymethylated protein was folded, that is, all cysteines are blocked from forming disulphide bonds. They also showed that aggregation is a non-specific phenomenon. On the other hand, Speed et al. [29•] recently reported that in mixed folding experiments using the P22 tailspike and coat proteins, folding intermediates of the two proteins did not coaggregate, but rather that they preferred to self-associate, suggesting that aggregation is a specific phenomenon. Since they only analyzed soluble aggregates, Speed et al. [29•] suggest that it is possible that larger aggregates could grow by a different mechanism involving non-specific interactions.

More recently, Maachupalli-Reddy et al. [9•] provided new evidence of the non-specific nature of the aggregation reaction by conducting mixed oxidative renaturation studies with hen egg-white lysozyme and three other proteins: β-galactosidase, bovine serum albumin, and ribonuclease A. They found that foreign proteins that have a tendency to aggregate when folded in isolation, such as β-galactosidase and bovine serum albumin, significantly decreased lysozyme renaturation yields by promoting aggregation in mixed folding experiments. On the other hand, ribonuclease A, which does not

significantly aggregate upon folding in isolation, did not affect lysozyme renaturation yields in mixed folding experiments. We have recently conducted experiments trying to understand the role that disulphide bonding plays in the aggregation pathway [30]. We found that aggregation is fast and that aggregate concentration does not significantly increase beyond the first minute of renaturation. Hydrophobic interactions, and not disulphide bonding, were found to be the major cause of aggregation. Under renaturation conditions that promote disulphide bonding, however, aggregate size, but not concentration, was found to increase due to disulphide bond formation, resulting in covalently bonded aggregates. Based on these results, it is possible to speculate that in mixed folding experiments, in which two or more proteins are simultaneously refolded, small soluble aggregates may form due to specific interactions that are hydrophobic in nature, and large heterogeneous aggregates may grow via disulphide bonding of unpaired cysteines, thus reconciling the conflicting observations of Speed *et al.* [29•] and Maachupalli-Reddy *et al.* [9•] on the specific/non-specific nature of aggregates.

An examination of aggregation data for the P22 tailspike protein, combined with the postulation of three possible mathematical models to describe the aggregation process, led Speed *et al.* [31] to conclude that aggregates grow via a cluster–cluster multimerization mechanism in which multimers of any size associate to form a larger aggregate. Aggregation is not mediated by the sequential addition of monomeric subunits and does not stop when the concentration of monomeric subunits is depleted. This confirms the observation [30] that aggregation is fast, and that aggregate size, rather than total aggregate concentration, increases as time progresses.

Based on the hypothesis that aggregation is caused by interactions between hydrophobic patches in partially folded polypeptide chains, it is possible to envision strategies to decrease aggregate formation. A careful examination of structural and amino acid sequence data can lead to the identification of hydrophobic patches within the protein molecule that could participate in intermolecular interactions. Mutations causing the disruption of such hydrophobic patches may reduce aggregation. This strategy was tested by Plückthun and co-workers [32,33•] who identified mutations located in turns of the protein and in hydrophobic patches which led to decreased *in vitro* and *in vivo* aggregation of recombinant antibody fragments. A second strategy involves the use of antibodies which preferentially bind hydrophobic patches away from the active site to protect the protein from intermolecular associations leading to aggregation. This strategy was tested by Katzav-Gozansky *et al.* [34•] who showed that carboxypeptidase A aggregation can be prevented using specific monoclonal antibodies. Interestingly, Plückthun's group [32,33•] mutated amino acids likely to be on the surface of the native protein, while Solomon and co-workers

[34•] raised their antibodies using native antigents. These results seem to indicate that intermediates responsible for aggregation may have more native-like structural features than currently speculated.

Improving renaturation yields

A simpler strategy to prevent aggregation by interfering with intermolecular hydrophobic interactions is to use additives, small molecules that are relatively inexpensive and easy to remove once refolding goes to completion. A variety of additives have been tested for their ability to prevent aggregation. They may act by stabilizing the native state, by preferentially destabilizing incorrectly folded molecules, by increasing the solubility of folding intermediates, or by increasing the solubility of the unfolded state. In general, these additives do not seem to accelerate the rate of folding, but they do inhibit the unwanted aggregation reaction. Additives that have been shown to promote higher refolding yields are listed in Table 1.

As Table 1 indicates, surfactants and detergents have proven to be very efficient folding aids, and have been shown to work with a variety of proteins, in particular multimeric disulphide bonded ones. Correct disulphide bond formation by thiol/disulphide exchange using oxido shuffling systems and air oxidation have been shown to be promoted in the presence of detergents [7,8•,35•]. One drawback of the use of surfactants and detergents is that they are difficult to remove, a direct result of their ability to bind to proteins and to form micelles. Much easier to remove, low denaturant concentrations and L-arginine have shown excellent folding enhancing capabilities (Table 1); however, because they are used in the molar concentration range, they may interfere with the assembly of oligomeric proteins.

As *in vivo* folding and aggregation processes are modulated by the presence of chaperones and foldases in the cellular environment, it is not surprising that such proteins can also impact the competition between folding and aggregation in *in vitro* protein folding [36•]. Chaperones and foldases, however, are proteins that need to be removed from the renaturation solution at the end of the refolding process, and may be costly to produce unless a recovery-reuse scheme can be implemented [37]. A practical solution to this problem was proposed and implemented by Altamirano *et al.* [38•] who used immobilized mini-chaperones to promote proper folding of several proteins which proved difficult to refold by other means. The immobilized mini-chaperones consisted of fragments of GroEL attached to chromatographic resins. The technique is only applicable to GroEL substrates and has not been tested under oxidative renaturation conditions.

In an attempt to mimic the GroEL-GroES chaperonin action, Rozema and Gellman [35•,39] developed a folding strategy in which the denatured protein is first exposed

Table 1

In vitro folding aids.

Additive	Protein	Reference
Non-denaturing concentrations of chaotropic agents		
GdmCl	P. fluorescens lipase	[10]
	Hen egg-white lysozyme	[22•]
	Carbonic anhydrase II	[41]
	Interferon-β-polypeptides	[P1]
Urea	Porcine growth hormone	[4]
	Hen egg-white lysozyme	[42•]
	IGF-I	[P2•]
	Interferon-β-polypeptides	[P1]
L-arginine	P. fluorescens lipase	[10]
	Fab fragments	[14]
	Hen egg-white lysozyme	[22•]
	α-glucosidase	[20•]
Salts		
Ammonium sulphate	Hen egg-white lysozyme	[42•]
Sugars		
Glycerol	P. fluorescens lipase	[10]
	Hen egg-white lysozyme	[42•]
	IGF-I	[P2•]
Sucrose	IGF-I	[P2•]
Glucose	Hen egg-white lysozyme	[42•]
N-acetyl glucosamine	Hen egg-white lysozyme	[42•]
Sarcosine	Hen egg-white lysozyme	[42•]
Detergents and surfactants		
Chaps	TGF-β-like proteins	[P3•]
	Carbonic anhydrase II	[41]
Tween	Human growth hormone	[44]
SDS	Interferon-β-polypeptides	[P1]
Sarkosyl	RNA polymerase σ factor	[6]
Sodium lauorsylsarcosine	Single chain Fv fragment	[7]
Dodecyl maltoside	Class II MHC	[8•]
Triton X-100	Carbonic anhydrase II	[41]
Polyethylene glycol	Carbonic anhydrase II	[41]
Octaethylene glycol monolauryl	Carbonic anhydrase II	[41]
Phospholipids	Hen egg-white lysozyme	[9•]
	TGF-β-like proteins	[P3•]
Sulphobetaines	Hen egg-white lysozyme	[43]
	β-D-galactosidase	[43]
Short chain alcohols		
n-pentanol	Carbonic anhydrase II	[41]
n-hexanol	Carbonic anhydrase II	[41]
cyclohexanol	Carbonic anhydrase II	[41]

to a detergent-containing solution to prevent aggregation, followed by stripping of the detergent with cyclodextrin to promote folding. The technique has been named 'artificial chaperone-assisted refolding' and has been applied to the refolding of carbonic anhydrase B [39], and the oxidative renaturation of lysozyme [35•]. This procedure has also been shown to work in the refolding MM-creatine kinase [40].

Conclusions

Inclusion body protein refolding used to be considered a difficult task. A protocol that worked for one protein did not work for others. Finding the right conditions to fold a given protein was a trial and error process in which existing methods were tried until a successful one was found. This was in part due to our lack of understanding of the competition between folding and aggregation in *in vitro* protein folding. Despite this lack of knowledge,

many efficient refolding process have been developed in which aggregation is reduced by the use of additives that interfere with intermolecular interactions responsible for aggregation. As more and more additives are added to the list, there is a pressing need to characterize the aggregation process at the molecular level in order to select the right additive. Advances in our understanding of the aggregation pathway combined with knowledge on the role that chaperones play in *in vivo* protein folding provide the tools that will allow us to develop efficient refolding processes. Among these developments, finding sites on the protein molecule that interact with molecular chaperones, and identifying protein regions involved in intermolecular interactions will provide a rational basis for finding specific mutations and designing small binding molecules that prevent aggregation.

References and recommended reading

Papers of particular interest, published within the annual period of review, have been highlighted as:

• of special interest
•• of outstanding interest

1. Clarke AR, Waltho JP: Protein folding pathways and intermediates. Curr Opin Biotechnol 1997, 8:400-405.

2. Herman R: Protein Folding. Munich: European Patent Office; 1993. [EPO Applied Technology Series vol 12.]

3. Rudolph R, Böhm G, Lilie H, Jaenicke R: Folding proteins.
• In Protein Function. A Practical Approach, edn 2. Edited by Creighton TE. New York: IRL Press; 1997:57-99.
This chapter covers relevant topics and techniques in protein unfolding/folding. It contains protocols for cell lysis, isolation of inclusion bodies, and renaturation of solubilized proteins with special emphasis on the renaturation of disulphide bonded proteins. It also covers monitoring of protein folding, kinetics and equilibrium considerations, folding and association of oligomeric proteins, the effects of ligands and the effect of auxiliary proteins assisting protein folding.

4. Cardamone M, Puri NK, Brandon MR: Comparing the refolding and reoxidation of recombinant porcine growth hormone from a urea denatured state and from Escherichia coli inclusion bodies. Biochemistry 1995, 34:5773-5794.

5. Cowley DJ, Mackin RB: Expression, purification and
• characterization of recombinant human proinsulin. FEBS Lett 1997, 402:124-130.
E. coli derived recombinant human proinsulin produced in inclusion bodies was solubilized with 70% formic acid and cleaved with cyanogen bromide. After solvent evaporation and freeze-drying, the lyophilized protein was dissolved in 7 M urea and subjected to oxidative sulphitolysis. The sulphonated material was purified by anion exchange, and refolded at pH 10.5 in the presence of air and β-mercaptoethanol. The refolded proinsulin contained the correct disulphide bond pattern.

6. Burgess RR: Purification of overproduced Escherichia coli RNA polymerase σ factors by solubilizing inclusion bodies and refolding from sarkosyl. Methods Enzymol 1996, 273:145-149.

7. Kurucz I, Titus JA, Jost CA, Segal DM: Correct disulphide pairing and efficient refolding of detergent-solubilized single-chain Fv proteins from bacterial inclusion bodies. Mol Immunol 1995, 12:1443-1452.

8. Stöckel J, Döring K, Malotka J, Jähnig F, Dornmair K: Pathway of
• detergent-mediated and peptide ligand-mediated refolding of heterodimer class II major histocompatibility complex (MHC) molecules. Eur J Biochem 1997, 248:684-691.
An in depth discussion of the mechanism of detergent-mediated protein folding of a heterodimeric disulphide bonded protein with four domains. The contributions of detergent headgroup and aliphatic tail to the stabilization of folding intermediates are dissected. Optimal detergent concentration decreases with increasing critical micelle concentration. Formation of secondary structure occurs early in the folding pathway when the denaturing detergent SDS is replaced by a mild detergent. Tertiary structure formation and heterodimer

association occurs later in the folding pathway concomitantly with disulphide bond formation.

9. Maachupalli-Reddy J, Kelley BD, De Bernardez Clark E: **Effect of**
• **inclusion body contaminants on the oxidative renaturation of hen egg white lysozyme.** *Biotechnol Prog* 1997, 13:144-150.
This paper shows that non-proteinaceous contaminants, such as plasmid DNA, ribosomal RNA, and lipopolysaccharides, have little effect on protein renaturation. Phospholipids improve folding yields by about 15%. Proteinaceous contaminants, on the other hand, can have a significant detrimental effect on folding yields by causing co-aggregation of the protein of interest. The paper also shows that contaminants affect the overall rate of the aggregation reaction without affecting the folding rate.

10. Ahn JH, Lee YP, Rhee JS: **Investigation of refolding condition for Pseudomonas fluorescens lipase by response surface methodology.** *J Biotechnol* 1997, 54:151-160.

11. Simmons T, Newhouse YM, Arnold KS, Innerarity TL, Weisgraber KH: **Human low density lipoprotein receptor fragment. Successful refolding of a functionally active ligand-binding domain produced in Escherichia coli.** *J Biol Chem* 1997, 272:25531-25536.

12. Negro A, Onisto M, Grassato L, Caenazzo C, Garbisa S: **Recombinant human TIMP-3 from Escherichia coli: synthesis, refolding, physico-chemical and functional insights.** *Protein Eng* 1997, 10:593-599.

13. Kim S, Baum J, Anderson S: **Production of correctly folded recombinant [¹³C,¹⁵N] enriched guinea pig [Val90]-α-lactalbumin.** *Protein Eng* 1997, 10:455-462.

14. Buchner J, Rudolph R: **Renaturation, purification and characterization of recombinant Fab fragments produced in Escherichia coli.** *Biotechnol* 1991, 9:157-162.

15. Hamaker KH, Liu J, Seely RJ, Ladisch CM, Ladisch MR: **Chromatography for rapid buffer exchange and refolding of secretory leukocyte protease inhibitor.** *Biotechnol Prog* 1996, 12:184-189.

16. Batas B, Jones HR, Chaudhuri JB: **Studies of the hydrodynamic volume changes that occur during refolding of lysozyme using size-exclusion chromatography.** *J Chromatog A* 1997, 766:109-119.

17. Batas B, Chaudhuri JB: **Protein refolding at high concentration using size-exclusion chromatography.** *Biotechnol Bioeng* 1996, 50:16-23.

18. Qiu H, Wen D, Belanger A, Bunn HF: **Over-expression and refolding of biologically active human erythropoietin from E. coli.** *Protein Eng* 1997, 10(suppl):33.

19. Stempfer G, Rudolph R: **Improved refolding of a matrix-bound fusion protein.** *Ann N Y Acad Sci* 1996, 782:506-512.

20. Stempfer G, Höll-Neugebauer B, Rudolph R: **Improved refolding**
• **of an immobilized fusion protein.** *Nat Biotechnol* 1996, 14:329-334.
The authors demonstrate a strategy to prevent aggregation upon folding by physically isolating protein molecules from each other through immobilizing onto a solid support. In this technique, the protein of interest is produced as a fusion protein with either an amino- or a carboxy-terminal hexa-arginine peptide. The denatured protein is attached to a solid support containing polyanionic groups and renaturation on the immobilized protein is performed by removal of the denaturant. The effect of ionic strength, addition of ethylene glycol and support material are thoroughly investigated.

21. Rudolph R, Lilie H: **In vitro folding of inclusion body proteins.**
• *FASEB J* 1996, 10:49-56.
An excellent review with 80 references detailing key aspects of expression and refolding of inclusion body proteins.

22. Hevehan D, De Bernardez Clark E: **Oxidative renaturation of**
• **lysozyme at high concentrations.** *Biotechnol Bioeng* 1997, 54:221-230.
This paper shows that it is possible to refold a disulphide-bonded protein with very high yields at high protein concentrations (up to 5 mg/ml) by addition of non-denaturing concentrations of the chaotropic agent guanidinium chloride (GdmCl). Increasing GdmCl concentrations decreased both the rate of the folding and aggregation reactions, with a stronger effect on aggregation. The paper also shows that GdmCl is as efficient as L-arginine in decreasing aggregation while resulting in faster folding rates.

23. Xie Y, Wetlaufer DB: **Control of aggregation in protein folding: the temperature-leap tactic.** *Protein Sci* 1996, 5:517-523.

24. Maeda Y, Ueda T, Imoto T: **Effective renaturation of denatured and reduced immunoglobulin G in vitro without assistance of chaperone.** *Protein Eng* 1996, 9:95-100.

25. Ptitsyn OB, Bychkova VE, Uversky VN: **Kinetic and equilibrium folding intermediates.** *Philos Trans R Soc Lond B Biol Sci* 1995, 348:35-41.

26. Creighton TE: **How important is the molten globule for correct**
• **protein folding?** *Trends Biochem Sci* 1997, 22:6-10.
In this paper, TE Creighton analyzes experimental observations of the oxidative refolding of α-lactalbumin obtained in his laboratory and by other investigators. He shows that, contrary to what is widely believed, the molten globule has little native-like topology and it could be an off-pathway, non productive species, rather than the key to rapid folding.

27. Yon JM: **The specificity of protein aggregation.** *Nat Biotechnol* 1996, 14:1231.

28. Goldberg ME, Rudolph R, Jaenicke R: **A kinetic study of the competition between renaturation and aggregation during the refolding of denatured-reduced egg white lysozyme.** *Biochemistry* 1991, 30:2790-2797.

29. Speed MA, Wang DIC, King J: **Specific aggregation of partially**
• **folded polypeptide chains: the molecular basis of inclusion body composition.** *Nat Biotechnol* 1996, 14:1283-1287.
The authors refolded a mixture of P22 tailspike and coat proteins under conditions which promote aggregation of both proteins. Co-aggregation of the proteins was not observed indicating that aggregation is due to specific interactions. As only soluble multimeric species were analyzed, the possibility of formation of heterogeneous insoluble aggregates cannot be excluded.

30. De Bernardez Clark E, Hevehan D, Szela S, Maachupalli-Reddy J: **Oxidative renaturation of hen egg-white lysozyme. Folding vs. aggregation.** *Biotechnol Prog* 1998, 14:47-54.

31. Speed MA, King J, Wang DIC: **Polymerization mechanism of polypeptide chain aggregation.** *Biotechnol Bioeng* 1997, 54:333-343.

32. Knappik A, Plückthun A: **Engineered turns of a recombinant antibody improve its in vivo folding.** *Protein Eng* 1995, 8:81-89.

33. Nieba L, Honegger A, Krebber C, Plückthun A: **Disrupting**
• **the hydrophobic patches at the antibody variable/constant domain interface: improved in vivo folding and physical characterization of an engineered scFv fragment.** *Protein Eng* 1997, 10:435-444.
Amino acid mutations away from the antibody fragment binding site resulted in decreased aggregation rates in vitro. Mutations were performed on exposed hydrophobic residues which are adjacent to another exposed hydrophobic residue in order to disrupt hydrophobic patches. The paper also explores the role of these mutations on in vivo folding and aggregation of the resulting scFv fragments.

34. Katzav-Gozansky T, Hanan E, Solomon B: **Effect of monoclonal**
• **antibodies in preventing carboxypeptidase A aggregation.** *Biotechnol Appl Biochem* 1996, 23:227-230.
This paper shows that certain monoclonal antibodies that bind to the antigen at locations removed from the active site, are capable of promoting proper folding by decreasing aggregation. Thus, monoclonal antibodies can be used as folding additives to prevent aggregation, and as tools to identify sites where protein aggregation may be initiated.

35. Rozema D, Gellman SH: **Artificial chaperone-assisted refolding**
• **of denatured-reduced lysozyme: modulation of the competition between renaturation and aggregation.** *Biochemistry* 1996, 35:15760-15771.
The artificial chaperone strategy consists of refolding by dilution in the presence of a detergent followed by stripping of the detergent using methyl-β-cyclodextrin. Only ionic detergents are effective in the role of artificial chaperones. Lysozyme is not active in the presence of detergent, and activity is recovered only after the stripping step. Thiol/disulphide reagents can be added either in the dilution step (in the presence of detergent) or in the stripping step. Higher yields are obtained when thiol/disulphide exchange occurs in the presence of detergents.

36. Thomas JG, Ayling A, Baneyx F: **Molecular chaperones, folding**
• **catalysts, and the recovery of active recombinant proteins from E. coli. To fold or to refold.** *Appl Biochem Biotechnol* 1997, 66:197-238.
A detailed review of the role of chaperones and foldases on in vivo and in vitro protein folding. Includes an extensive list of relevant references.

37. King J: **Refolding with a piece of the ring.** *Nat Biotechnol* 1997, 15:514-515.

38. Altamirano M, Golbik R, Zahn R, Bucle AM, Fersht AR: **Refolding**
• **chromatography with immobilized mini-chaperones.** *Proc Natl Acad Sci USA* 1997, 94:3576-3578.
The authors demonstrate the practical use of the GroEL apical domain (residues 191-376) and the core of the apical domain (residues 191-345) as folding enhancers in the renaturation of several difficult to refold proteins. The mini-chaperones are immobilized on chromatographic resins and

chromatography can be conducted in both elution and batch modes. The technique only works with proteins that are known to be GroEL substrates. Its applicability in the oxidative renaturation of proteins is not demonstrated.

39. Rozema D, Gellman SH: **Artificial chaperone-assisted refolding of carbonic anhydrase B.** *J Biol Chem* 1996, 271:3478-3487.

40. Couthon F, Clottes E, Vial C: **Refolding of SDS- and thermally denatured MM-creatine kinase using cyclodextrins.** *Biochem Biophys Res Commun* 1996, 227:854-860.

41. Wetlaufer DB, Xie Y: **Control of aggregation in protein refolding: a variety of surfactants promote renaturation of carbonic anhydrase II.** *Protein Sci* 1995, 4:1535-1543.

42. Maeda Y, Yamada H, Ueda T, Imoto T: **Effect of additives on the renaturation of reduced lysozyme in the presence of 4 M urea.** *Protein Eng* 1996, 9:461-465.
Increasing concentrations of additives such as sarcosine, glycerol, ammonium sulphate, glucose and N-acetyl glucosamine resulted in improved refolding rates (except for glycerol) and yields in the oxidative renaturation of lysozyme. Sarcosine was the most effective folding enhancer.

43. Goldberg ME, Expert-Bezanion N, Vuillard L, Rabilloud T: **Non-detergent sulphobetaines: a new class of molecules that facilitate** *in vitro* **protein renaturation.** *Fold Design* 1996, 1:21-27.

44. Bam NB, Cleland JL, Randolph TW: **Molten globule intermediate of recombinant human growth hormone: stabilization with surfactants.** *Biotechnol Prog* 1996, 12:801-809.

Patents

P1. Dorin G, McAlary P, Wong K: **Bacterial production of hydrophobic polypeptides.** *World (WO) Patent* 1996, 96/39523.

P2. Builder S, Hart R, Lester P, Reifsnyder D: **Refolding of misfolded
•   insulin-like growth factor-I.** *US Patent* 1997, 5 663 304.
A method is disclosed in which the oxidative renaturation of insulin-like growth factor-I (IGF-I) is conducted using oxygen and in the presence of low copper or manganese concentrations, an alcoholic or polar aprotic solvent (such as 20% ethanol), an effective amount of chaotropic agent (such as 2 M urea), an effective amount of an alkaline earth, alkali metal, or ammonium salt (such as 1 M NaCl), an optional osmolyte (such as glycerol), and a reducing agent (such as 1 mM DTT). An extensive factorial design analysis of the effects of IGF-I concentration, salt type and concentration, urea, ethanol and glycerol concentrations on folding yield is also included.

P3. Cerletti N, McMaster GK, Cox D, Schmitz A, Meyback B: **Process
•   for refolding recombinantly produced TGF-β-like proteins.** *US Patent* 1997, 5 650 494.
Methods to improve the oxidative renaturation yields of dimeric forms of transforming growth factor β-like proteins are disclosed. The procedure requires the use of mild detergents, such as 3-(3-chlolamidopropyl) dimethylammonio-1-propane sulphonate. Several methods for thiol/disulphide exchange are disclosed. These include the use of reduced and oxidized glutathione, thioredoxin, and folding from a S-sulphonate monomer.

P4. Seely R, Ladisch M: **Process for protein refolding by means of buffer exchange using a continuous stationary phase capable of separating proteins from salt.** *World (WO) Patent* 1997, 97/04003.

Exhibit 14

Association-induced folding of globular proteins

Vladimir N. Uversky*†‡, Daniel J. Segel§, Sebastian Doniach§ and Anthony L. Fink†¶

*Department of Chemistry and Biochemistry, University of California, Santa Cruz, CA 95064; †Institute for Biological Instrumentation, Russian Academy of Sciences, 142292 Pushchino, Moscow Region, Russia; and §Department of Physics, Stanford University, Stanford, CA 94305

ABSTRACT   It has generally been assumed that the aggregation of partially folded intermediates during protein refolding results in the termination of further protein folding. We show here, however, that under some conditions the association of partially folded intermediates can induce additional structure leading to soluble aggregates with many native-like properties. The amount of secondary structure in a monomeric, partially folded intermediate of staphylococcal nuclease was found to double on formation of soluble aggregates at high protein or salt concentrations. In addition, more globularity, as determined from Kratky plots of small-angle x-ray scattering data, was also noted in the associated states.

Protein association (aggregation) is a major biomedical and biotechnological problem. Diseases such as the amyloidoses, prion diseases, and cataracts are caused by protein association, as are several diseases involving inclusion bodies or other amorphous deposits (e. g. inclusion body myositis, light chain deposition disease, Huntington's disease) (1, 2). Formation of inclusion bodies is a common problem in the production of recombinant proteins (3–5). The storage and delivery of protein drugs are also often complicated by the association process. Protein refolding is often also accompanied by aggregation, especially at higher protein concentrations, which has been attributed to the association of partially folded intermediates (6–11).

Partially folded intermediates have been detected under both transient and equilibrium protein folding conditions (12–15). The structural properties of such intermediates are diverse, ranging from substantially unfolded to almost as structured as the native state (15). We have previously established that acid-unfolded staphylococcal nuclease (pH 2.5) can be transformed into one of three partially folded intermediates, depending on the nature and concentration of anions added to neutralize the repulsive effect from the net positive charges in the acid-unfolded polypeptide chain (16–17). Such partially folded species have a strong propensity to aggregate: for both apomyoglobin and staphylococcal nuclease (SNase) we have observed that the propensity to associate decreased with increasing structural content, and the least structured intermediates were monomeric only at rather dilute concentrations.

We present here results of the effect of association on the structural properties of a partially folded intermediate of SNase.

MATERIALS AND METHODS

SNase. SNase was grown and purified from a cloned gene kindly supplied by D. Shortle (Johns Hopkins Univ. School of Medicine). The homogeneity of the protein samples was checked electrophoretically by using the PhastSystem (Phar-

macia). Protein concentrations were determined from the published molar extinction coefficient. Salt titrations at low pH were carried out by making a series of solutions of desired salt concentration and adjusting the pH value with HCl or NaOH. Samples were incubated overnight before measurements. Sodium sulfate was from Sigma. The pH values were measured with a microcombination glass electrode [Microelectrodes (Londonderry, NH), model MI-410].

Circular Dichroism (CD). CD data were collected on an Aviv 60DS CD spectrometer at 23°C. Far-UV spectra from 185–260 nm were collected with 5 sec per point signal averaging; θ_{222} measurements were taken in kinetics mode with the signal averaged over 120 sec. A 0.1-cm fixed pathlength cell was used. The fraction of native secondary structure was estimated as $N_{ss}\% = ([\theta]_{222} - [\theta]_{222}^U)/([\theta]_{222}^N - [\theta]_{222}^U)$, where $[\theta]_{222}$ is the molar ellipticity value at given conditions, while $[\theta]_{222}^U$ and $[\theta]_{222}^N$ are its values in completely unfolded and native states, respectively.

Small-Angle X-Ray Scattering (SAXS). Solution x-ray scattering experiments were carried out at the Stanford Synchrotron Radiation Laboratory on Beam Line 4–2. A flow-cell with 10-μm thick mica windows, a pathlength of 1.3 mm, and a sample capacity of 45 μl was used to reduce extended exposure of the sample to radiation. The sample cell was thermostatted and maintained at 20°C. For Kratky plots the scattering data were plotted as $I(Q) \times Q^2$ vs. Q, where $I(Q)$ is the x-ray scattering intensity, $Q = 4\pi \sin\theta/\lambda$ is the momentum transfer, and 2θ and λ are the scattering angle and the wavelength of the x-rays, respectively.

RESULTS

When a salt-free solution of SNase is titrated from neutral pH to low pH the protein unfolds in a very cooperative process with a midpoint of pH 4. The addition of various anions at pH 2.5 leads to the formation of one of three possible partially folded intermediates (16–17). In the present work we have focused on the least structured partially folded nonglobular intermediate, A_1, which is induced by chloride or sulfate ions. At pH 2.5 and 250 mM Na_2SO_4, and low protein concentrations, SNase is monomeric and ~50% folded, based on the amount of secondary structure and the radius of gyration (ref. 16 and manuscript in preparation). The inset to Fig. 1 shows the θ_{222} as the acid-unfolded state (U_A) is titrated with sodium sulfate: the initial transition, complete by 100 mM sulfate, corresponds to the conversion of U_A to monomeric A_1 (see also Fig. 2B); the second transition, complete by 0.8 M sulfate, demonstrates the effect of increasing ionic strength, and corresponds to salt-induced dimerization (see below).
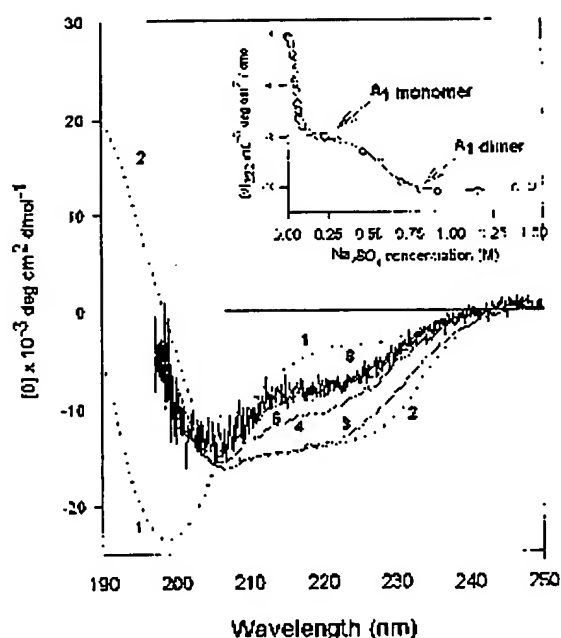
FIG. 1. The effect of protein and salt concentration on the secondary structure content of the A₁ intermediate of SNase. The inset shows the sulfate titration of U_A at 0.15 mg/ml protein (see text). The CD spectra show the increase in secondary structure as protein concentration is increased. Spectrum 1 is the U_A, pH 2.5, no salt; spectrum 2 is the native state, pH 7.5. Spectra 3–6 of the A₁ state were collected under the same conditions (pH 2.5 and 250 mM Na_2SO_4) but at different protein concentrations: spectrum 6, the noisy curve, at 0.08 mg/ml; spectrum 5 at 0.21 mg/ml; spectrum 4 at 0.52 mg/ml; and spectrum 3 at 3.92 mg/ml.

The effect of increasing protein concentration on the secondary structure of the partially folded intermediate is also shown in Fig. 1: the far-UV CD spectra of the A₁ state of SNase (pH 2.5, 250 mM sodium sulfate) at protein concentrations below 0.2 mg/ml (spectra 5 and 6) where the species is monomeric, indicate the conformation is substantially unfolded (≈50% as folded as the native state, as measured by θ_{222}), compared with the native state. SAXS studies showed that under these conditions (≤0.2 mg/ml) the SNase intermediates are monomeric.

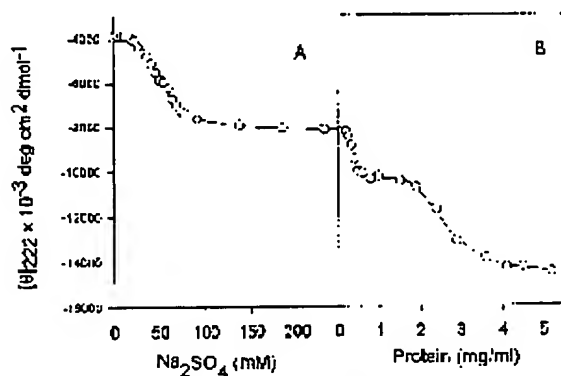FIG. 2. Anion- and protein-induced secondary structure in acid-unfolded SNase (pH 2.5). (A) the effect of increasing Na_2SO_4 at low protein concentration (0.15 mg/ml). (B) The effect of increasing protein concentration at fixed sulfate (250 mM), leading to association. All measurements were carried out at 23°C.

At higher concentrations of protein two transitions were observed by far-UV CD (Fig. 2B). The first of these transitions was complete by a protein concentration of ≈0.5 mg/ml, and led to the formation of a new species (spectrum 4) with considerably more secondary structure, ≈70% of the θ_{222} of the native structure. SAXS data (see below) and size-exclusion HPLC showed that under these conditions the SNase was predominantly dimeric. Further increase in the protein concentration induced a second transition leading to formation of larger soluble aggregates with more secondary structure content. Above 4 mg/ml protein the CD spectrum (spectrum 3) is almost identical to that of the native protein!

Fig. 2 depicts the formation of secondary structure in staphylococcal nuclease at acid pH. As with many other proteins the addition of anions to U_A leads to increased secondary structure due to screening of the positive charges (18–19). Increasing the sulfate concentration from ≈25 to ≈75 mM transforms the acid-unfolded state into the least structured partially folded conformation, A₁, while further increase in anion content up to 250 mM sulfate had little effect (Fig. 2A). Increasing the protein concentration at fixed sulfate concentration (250 mM) induces additional secondary structure (Fig. 2B). This figure clearly shows that the process of association-induced secondary structure formation has sequential (biphasic) character. First, increasing the protein concentration from ≈0.2 to ≈0.5 mg/ml leads to the transition to an intermediate state with more secondary structure. This intermediate exists at moderate protein concentrations (up to 1.5 mg/ml) and then it, in turn, is transformed to a new species with native-like secondary structure. Based on SAXS (see below) and size-exclusion HPLC data (not shown), the species at the end of the sulfate titration is monomeric, whereas the species at moderately high protein concentrations is dimeric, and at high protein concentrations is multimeric. The transition in Fig. 2A, and the second transition in Fig. 2B, were fully reversible, whereas the first transition in Fig. 2B was not (although this is probably a kinetic effect).

There are two particularly noteworthy points. (i) The apparently native-like conformation (as well as the other less structured intermediates) lacks the unique tertiary structure characteristic of native SNase, i.e., its near-UV CD spectrum is that of the unfolded molecule (data not shown). (ii) The dimeric intermediate described here is rather close in its structural properties to the monomeric species observed for acid-unfolded SNase in the presence of trifluoroacetate, the A₂ state (17).

As the intensity of the far UV CD signal is sensitive to each type of ordered secondary structure, it is difficult to separate the contributions of inter- and intramolecular interactions in the process of the association-induced secondary structure formation. To aid in clarifying this point we have used SAXS that can give information about the size, compactness and shape of the scattering molecule (20). In addition it has been shown that analysis of the scattering data in the form of a Kratky plot can provide information about the globularity of the molecule (20–23). The Kratky plot for the native protein will show a characteristic maximum, while for the unfolded polypeptide there will be no maximum (21–23). Partially folded conformations will exhibit a Kratky plot with a maximum whose magnitude depends on their degree of compactness (22).

Fig. 3 shows Kratky plots for staphylococcal nuclease under different experimental conditions. Curves 1 and 5 represent the scattering profiles for acid-unfolded (pH 2.5, no salt) and native (pH 7.5) protein, respectively. The native protein shows the characteristic maximum, while the acid-unfolded SNase scatters as a Gaussian chain, consistent with the lack of a globular core. Curve 2 is for the monomeric form of the A₁ partially folded intermediate [0.2 mg/ml (pH 2.5) and 250 mM Na_2SO_4], and shows that in this conformational state the
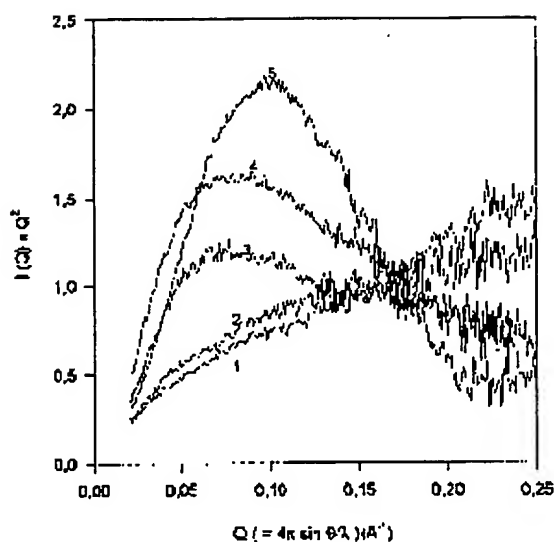
FIG. 3. Kratky plots for SNase in the different conformational states at 20°C: *1*, pH 2.5, no salt (acid-unfolded state); *2*, pH 2.5, 250 mM Na_2SO_4, protein concentration is 0.2 mg/ml (A_1 state); *3*, pH 2.5, 250 mM Na_2SO_4, protein concentration is 0.55 mg/ml (dimerized A_1 state); *4*, pH 2.5, 250 mM Na_2SO_4, protein concentration is 3.55 mg/ml (oligomeric A_1 state); *5*, pH 7.5 (native state).

molecule has no significant globular structure, i.e., the Kratky plot is very similar to that for the unfolded protein. The lack of globular structure attributed to the monomeric intermediate correlates well with recent work by using poly-L-lysine and poly-L-glutamic acid as models in which it was established that formation of intramolecular α-helical elements joined by flexible coils without formation of a hydrophobic core (globular structure) does not affect the shape and intensity of the Kratky plot (23). At the same time Fig. 3 clearly shows that an increase in protein concentration under these conditions leads to the appearance of globular structure (curves 3 and 4), with the amount of globular structure increasing with increasing protein concentration.

This effect cannot be explained just by the association-induced formation of intermolecular interactions: such intermolecular associations of proteins usually lead to the formation of β-sheet structure (11). However, it has been shown that for poly-L-lysine in the β-sheet conformation, the Kratky plot is quantitatively similar to the plot for a Gaussian chain and notably different from the globular one (23). It is known that the β-sheet conformation of poly-L-lysine is formed mostly due to intermolecular interactions (24) (as a consequence, polypeptides in this conformation have no globular core). Therefore, the increase in concentration of the partially folded intermediate induces not only formation of intermolecular structure but leads also to the appearance of new intramolecular structure within an individual protein molecule, as manifested by both increased secondary structure and globular core.

SAXS data are very sensitive to intermolecular protein association. The value of forward-scattered intensity ($I(Q)$ as $Q \rightarrow 0$) is proportional to the square of the molecular weight of the molecule (20). I(0) for a pure dimer sample will therefore be twice that for a sample with the same number of monomers because each dimer will scatter four times as strongly, but there will be half as many as in the pure monomer sample. Our results are consistent with the conclusion that SNase molecules are predominantly monomeric in all three anion-induced intermediates: A_1; A_2 (acid-unfolded SNase in the presence of trifluoroacetate); and A_3 (formed in the

presence of trichloroacetate at low protein concentrations, ≤0.2 mg/ml); as well as in the native and acid-unfolded states. The increase in protein concentration (0.5–2.0 mg/ml) at moderate sulfate (0.25 M) or Cl^- (0.9 M) leads to a 2-fold increase in $I(0)$ (from ~3.6 to ~7.1). Increasing concentrations of these anions at high protein concentrations results in the much larger increases in $I(0)$. For example, at the end of second association-induced transition (0.25 M SO_4^{2-}, 4.0 mg/ml) $I(0)$ is 31.3, which would imply the formation of octamers if the sample is monodisperse. Further increases in protein concentration lead to further increases in the value of $I(0)$, and ultimately the protein precipitates (data not shown).

The results can be summarized, Fig. 4, in the form of a protein and sulfate-dependent conformational "phase" diagram for the association-induced conformational transitions in SNase at low pH. The solid-line boundaries between different conformations are constructed on the basis of the midpoint values of the corresponding Na_2SO_4-induced transitions at fixed protein concentrations, or those of transitions induced by the increasing in protein concentration at fixed sulfate content. Unfolded monomers exist at low sulfate concentration in a wide range of protein concentrations. Partially folded, loosely packed (nonglobular) monomers (A_1), appear in dilute protein solutions when the sulfate concentration increases. Globular (more tightly packed) dimers with larger secondary structure are formed in more concentrated protein solutions with sulfate concentrations >150 mM. Higher multimers with the largest structural order exist in a limited range of high protein and sulfate concentrations. Finally, the shaded area represents the conditions where precipitation occurs. As noted, most of these boundaries reflect reversible transitions.

DISCUSSION

We believe that the monomeric A_1 intermediate corresponds to molecules containing a core of native-like secondary struc-
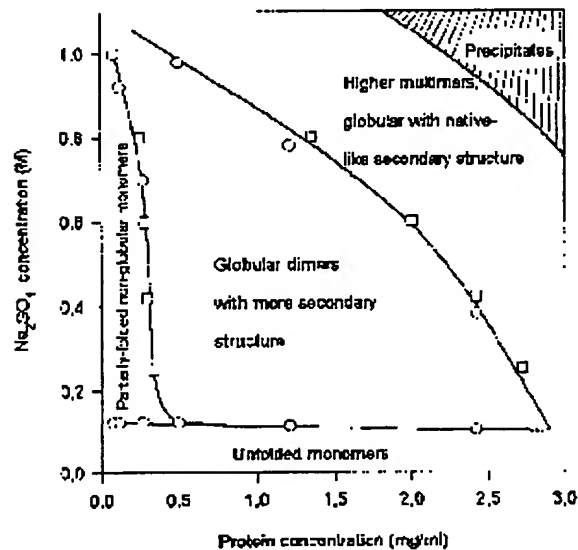

FIG. 4. Sulfate- and protein concentration-dependent conformational "phase" diagram for the conformational states of staphylococcal nuclease at 23°C and pH 2.5. The conformational space consists of U_A, A_1, globular dimers with more secondary structure than the monomer, and globular oligomers with native-like secondary structure content. The continuous lines show the boundaries between these states. Boundaries were determined on the basis of the midpoint (C_m) values of the corresponding Na_2SO_4-induced transitions at fixed protein concentrations (squares), or midpoint (C_m) values of transitions induced by the increasing in protein concentration at fixed sulfate content (circles). The shaded area represents the conditions at which precipitation occurs.

ture with the remainder of the polypeptide chain in a relatively disordered state (which may have regions flickering in and out of native-like secondary structure). The lack of globularity (a tightly packed core) shown by the Kratky plots for A_1 indicate that this core is rather small and loosely packed. Two regions in SNase have been suggested to be the initially formed core, the $n2$-helix and the $\beta2$- and $\beta3$-sheets (25): these are thus logical regions of structure in the proposed core in A_1.

The data show that a partially folded intermediate, with only 50% of the native-like secondary structure in its monomeric form, gains additional secondary structure on association to form dimers or higher multimers, as the protein concentration is increased. Although the multimeric aggregates have native-like secondary structure they lack the characteristic tertiary structure of the native conformation, as revealed by their lack of near-UV CD signal. The Kratky plots indicate that the structure is nevertheless tightly packed.

There are two possible models to explain these observations: (i) association of the monomers occurs first and leads to the induction of the additional structure, or (ii) the higher concentration of protein or salt increases the population of more structured intermediates that then associate. Although the data do not allow an unambiguous choice, we favor the former for several reasons. In a sense these models represent extremes of a continuum, and the question boils down to whether the hydrophobic surfaces involved in association reflect transient or stable regions of the monomeric intermediate structure.

It is most likely that the intermolecular association reflects specific interactions between hydrophobic surfaces of one partially folded molecule with those of another, where these specific interactions are ones that normally occur intramolecularly and lead to the formation of the native state, i.e., in a sense the association arises from nonproductive (intermolecular) interactions that normally are formed (intramolecularly) on the pathway to the native state. In other words if we consider the monomeric native state to arise by the coalescence of structural building blocks (subdomains) in an intramolecular fashion, the aggregates arise by these same interactions but in an intermolecular fashion. Thus the dimers may represent a form of domain swapping (26) in which regions of one A_1 intermediate molecule interact with a second molecule in a specific interaction that results in additional secondary structure formation. In this regard it is interesting to note that a dimeric species of SNase has been reported (27). It is noteworthy that the A_1 dimer is particularly stable.

Although it is well known that peptides with high helical propensity will associate and thus stabilize the helical structure at high peptide concentrations (28, 29), this is the first report that the association or aggregation of a partially folded intermediate of a protein containing a variety of types of secondary structure leads to the formation of additional secondary structure. It is conceivable that the association arises from interactions of amphiphilic helices in the intermediate (possibly only present transiently), analogous to the association of helical peptides, but the CD difference spectra show no evidence of significant increased helix content on association. In addition, the starting point in the present case is a stable partially folded intermediate with substantial structure, in contrast to helical peptide case.

It is not clear how widespread the phenomenon of association-induced secondary structure formation may be, nor if it is physiologically significant. However, the fact that inclusion bodies may have substantial native-like secondary structure (30) could be one consequence. On the other hand, one of the characteristics of aggregated proteins (such as inclusion bod-

ies, folding aggregates, and amyloid) is the presence of β-structure (11), and the association-induced structure in the case of SNase does not seem to involve significant nonnative β-sheet structure. The CD difference spectrum between monomeric A_1 and its dimer is consistent with an increase in β-structure, but the transition from the dimer to higher multimers is more complex, and as noted, results in formation of a CD spectrum similar to that of the native state. Thus it is possible that the association of SNase reported here represents a more specific type of interaction than that typically found in protein aggregation.

1. Carrell, R. W. & Lomas, D. A. (1997) *Lancet* **350**, 134–138.
2. Thomas, P. J., Qu, B. H. & Pedersen, P. L. (1995) *Trends Biochem. Sci.* **20**, 456–459.
3. Marston, F. A. O. (1986) *Biochem. J.* **240**, 1–12.
4. Schein, C. H. (1989) *Bio/Technology* **7**, 1141–1149.
5. Wetzel, R. (1992) in *Stability of Protein Pharmaceuticals, Part B: In Vivo Pathways of Degradation and Strategies for Protein Stabilization*, eds. Ahern, T. J. & Manning, M. C. (Plenum, New York), Vol. 3, pp. 43–48.
6. London, J., Skrzynia, C. & Goldberg, M. E. (1974) *Eur. J. Biochem.* **47**, 409–415.
7. Zettlmeissl, G., Rudolph, R. & Jaenicke, R. (1979) *Biochemistry* **18**, 5567–5571.
8. Jaenicke, R. (1995) *Phil. Trans. R. Soc. London B* **348**, 97–105.
9. DeYoung, L. R., Fink, A. L. & Dill, K. A. (1993) *Acc. Chem. Res.* **26**, 614–620.
10. Mitraki, A. & King, J. (1989) *Bio/Technology* **7**, 690–697.
11. Fink, A. L. (1998) *Folding Design* **3**, R9–R15.
12. Kuwajima, K. (1989) *Proteins* **6**, 87–103.
13. Kim, P. S. & Baldwin, R. L. (1990) *Annu. Rev. Biochem.* **59**, 631–660.
14. Ptitsyn O. B. (1995) *Adv. Protein Chem.* **47**, 83–229.
15. Fink, A. L. (1995) *Annu. Rev. Biophys. Biomol. Struct.* **24**, 495–522.
16. Fink, A. L., Calciano, L. J., Goto, Y., Nishimura, M. & Swedberg, S. A. (1993) *Protein Sci.* **2**, 1155–1160.
17. Uversky, V. N. Karnoup, A. S., Segel, D. J., Seshadri, S., Doniach, S. & Fink, A. L. (1998) *J. Mol. Biol.*, in press.
18. Goto, Y., Takahashi, N. & Fink, A. L. (1990) *Biochemistry* **29**, 3480–3488.
19. Fink, A. L., Calciano, L. J., Goto, Y., Kurotsu, T. & Palleros, D. R. (1994) *Biochemistry* **33**, 12504–12511.
20. Glatter, O. & Kratky, O. (1982) *Small Angle X-Ray Scattering* (Academic, New York), p. 515.
21. Kataoka, M., Hagihara, Y., Mihara, K. & Goto, Y. (1993) *J. Mol. Biol.* **229**, 591–596.
22. Doniach, S., Bascle, J., Garel, T. & Orland, H. (1995) *J. Mol. Biol.* **254**, 960–967.
23. Semisotnov, G. V., Kihara, H., Kotova, N. V., Kimura, K., Amemiya, Y., Wakabayashi, K., Serdynk, I. N., Timchenko, A. A., Chiba, K., Nikaido, K., Ikura, T. & Kuwajima, K. (1996) *J. Mol. Biol.* **262**, 559–574.
24. Adler, A. J., Greenfield, N. J. & Fasman, G. D. (1973) *Methods Enzymol.* **27**, 675–735.
25. Wang Y. & Shortle D. (1995) *Biochemistry* **34**, 15895–15905.
26. Bennett, M. J., Schlunegger, M. P. & Eisenberg, D. (1995) *Protein Sci.* **4**, 2455–2468.
27. Green, S. M., Gittis, A. G., Meeker, A. K. & Lattman, E. E. (1995) *Nat. Struct. Biol.* **2**, 746–751.
28. Yoshida, K., Shibata, T., Masai, J., Sato, K., Noguti, T., Go, M. & Yanagawa, H. (1993) *Biochemistry* **32**, 2162–2166.
29. Kaiser, E. T. & Kezdy, F. J. (1984) *Science* **223**, 249–55.
30. Oberg, K., Chrunyk, B. A., Wetzel, R. & Fink, A. L. (1994) *Biochemistry* **33**, 2628–2634.

Exhibit 15

The Renaturation of Reduced Chymotrypsinogen A in Guanidine HCl

REFOLDING *VERSUS* AGGREGATION*

GILBERT ORSINI‡ AND MICHEL E. GOLDBERG

From the Unité de Biochimie Cellulaire, Département de Biochimie et Génétique Microbienne, Institut Pasteur, 75015 Paris, France

The refolding and reoxidation of fully reduced and denatured chymotrypsinogen A have been studied in the presence of low concentrations of guanidine HCl or urea. Renaturation yields of 60 to 70% were observed when the reoxidation was facilitated by mixtures of reduced and oxidized glutathione. Refolding occurred within a narrow range of denaturant concentration (1.0 to 1.3 M guanidine HCl and 2 M urea) in which the native protein was shown to be stable, and the reduced protein was shown to regain the correct disulfide pairing. Renatured chymotrypsinogen is indistinguishable from the native zymogen in chromatographic behavior, potential chymotryptic activity, sedimentation coefficient, and spectral properties. The kinetics of renaturation were determined. Some of the protein species obtained at various times of renaturation were characterized as incorrectly oxidized molecules which could be renatured by thiol-catalyzed interchange of disulfide bonds.

Reduction of the five disulfide bonds of chymotrypsinogen in 6 M guanidine HCl leads to the maximally unfolded state of this protein (1). Equilibrium studies have shown that the two state approximation accounts for the thermal denaturation of chymotrypsinogen with disulfide bonds intact (2, 3). Full reversibility of the reaction has been observed under a given set of pH and ionic strength conditions (4). With disulfide bonds reduced, however, the denatured protein is notoriously insoluble in aqueous buffers (5). Even at very low protein concentration, extremely stable protein aggregates are formed and prevent the renaturation of the reduced protein in solution (6). To demonstrate the ability of reduced chymotrypsinogen to refold in solution, it was therefore necessary to circumvent the formation of insoluble aggregates. This could be achieved by dialysis of the reduced protein to remove guanidine HCl in

the presence of thiol-disulfide reagents (7). However, the denaturant concentration and the oxidation-reduction potential of the solution constantly varied throughout the dialysis during which the renaturation occurred. Therefore these critical experimental variables could not be adequately controlled during the refolding. Furthermore, dialysis is a slow process which precludes direct observation of the renaturation kinetics. It thus appeared desirable to develop a method suitable for the study of the kinetics of refolding and reoxidation of reduced chymotrypsinogen under controlled conditions.

In the present investigation, it will be shown that, after dilution and incubation of the denatured and reduced protein in an appropriate buffer, the kinetics of the regain of native conformation can conveniently be monitored by chemically blocking the renaturation process. The structural properties of the protein in the renaturation buffer were studied. The influence of low concentrations of guanidine HCl or urea and of mixtures of GSH and GSSG on the renaturation process were investigated and are discussed in terms of a plausible pathway for the refolding of reduced chymotrypsinogen in solution.

EXPERIMENTAL PROCEDURES

Materials—Bovine chymotrypsinogen A was obtained from Worthington (crystallized five times) and from Sigma (crystallized six times). L-1-Tosylamido-2-phenylethyl chloromethyl ketone-treated trypsin was from Worthington. Diisopropylfluorophosphate was from Koch-Light. *N*-Acetyl-L-tyrosine ethyl ester was from Fluka. Reduced dithiothreitol and *N*-ethylmaleimide were from Sigma. GSH and GSSG were from Boehringer Mannheim. Urea was a Hopkin and Williams product. Guanidine HCl was from Carlo Erba; for the spectrophotometrically monitored denaturation and ultracentrifugation experiments, ultra pure guanidine HCl from Schwarz/Mann was used. Carboxymethylcellulose was the microgranular CM-52 form from Whatman.

Chymotrypsinogen Assay: Renaturation Yield—Chymotrypsinogen concentration was determined and the zymogen was activated as described previously (7). When activated at protein concentrations higher than 0.15 mg/ml, chymotrypsinogen showed a potential catalytic rate constant of 210 to 220 s⁻¹, in accordance with that of δ-chymotrypsin for *N*-acetyl-L-tyrosine ethyl ester (8). However, when activated at the zymogen concentrations used in the renaturation experiments, 0.015 to 0.040 mg/ml, native chymotrypsinogen showed an apparent potential catalytic rate constant of only 120 to 140 s⁻¹ because, under these conditions, the activation reaction is slow and second order (9). This reflects the low affinity of the zymogen for trypsin (10). For this reason, renaturation yields were expressed as the percentage of the potential specific activity of the reduced-

reoxidized zymogen relative to that of denatured-renatured chymotrypsinogen with disulfide bonds intact at the same protein concentration (7). With the restriction mentioned above, the renaturation of denatured chymotrypsinogen (with SS bonds intact) is quantitative (90 to 100%).

Denaturation and Reduction of Chymotrypsinogen — Chymotrypsinogen (6 to 8 mg/ml) was denatured (with SS bonds intact) in 6.0 M guanidine HCl, 0.1 M Tris-HCl, 2 mM EDTA, pH 8.5, at room temperature.

Reduction of SS bonds was obtained by a 4-h incubation of denatured chymotrypsinogen with 20 to 30 mM dithiothreitol in stoppered tubes under nitrogen. Complete reduction (10 ± 0.2 —SH groups/mol of protein) was verified as described previously (7).

Renaturation of Reduced Chymotrypsinogen — Reduced chymotrypsinogen was renatured by dilution to a final protein concentration of 0.015 to 0.080 mg/ml into buffered solutions containing various concentrations of guanidine HCl (or urea) and of GSH and GSSG (7, 11), at 6–8°C. Denatured chymotrypsinogen (with SS bonds intact) was diluted in parallel to the same final protein concentration in 1.2 M guanidine HCl solution in the absence of the thiol-disulfide reagents. Stock solutions of guanidine-HCl and urea were freshly prepared in 50 mM Tris-HCl, 2 mM EDTA, pH 8.2. Guanidine HCl concentrations were routinely checked by refractometry (12). GSH concentrations were measured by the method of Ellman (13).

Stopping Renaturation of Reduced Chymotrypsinogen — During the renaturation of the reduced protein, the reaction was stopped at selected intervals by a modification of the method of Hantgan *et al.* (14). GSH and the unreacted protein thiols were alkylated with N-ethylmaleimide at pH 8.2 at 6°C. With 1 mM GSH, N-ethylmaleimide was added in a 5-fold molar excess; when 5 mM GSH was used, the reagent was in 2-fold molar excess. In either case, titration of the thiol groups (13) showed that alkylation was complete within the first minute following the addition of N-ethylmaleimide to the renaturation mixture. Addition of 10 mM N-ethylmaleimide to the control showed that the zymogen with SS bonds intact is totally unaffected by the reagent as evidenced by its unchanged potential specific activity after dialysis and activation.

Dialysis of Renatured Zymogen — Dialysis of the renatured zymogen was routinely carried out to remove guanidine HCl prior to activation. This was mandatory, as guanidinium ion was found to inhibit the activation reaction. The 5-ml aliquots were dialyzed overnight at 4°C against 2 liters of 10 mM Tris-HCl, pH 8.0.

Chromatography of Reduced-renatured Chymotrypsinogen — To concentrate reduced-renatured chymotrypsinogen, a modification of the chromatographic method described by Wilcox (8) was used. A small column (0.8 × 8.0 cm) of carboxymethylcellulose was prepared and equilibrated with a 20 mM potassium phosphate buffer, pH 6.2, at 4°C. 1.5 mg of reduced chymotrypsinogen was renatured as described above and dialyzed against the column buffer. This material was applied to the column and the protein retained on the cellulose was eluted by application of 0.2 M KCl in the same buffer. The protein was dialyzed against 10 mM Tris-HCl buffer, pH 8.0, before spectral and activability measurements.

Ultraviolet Absorption Measurements — Difference denaturation spectra of chymotrypsinogen in guanidine HCl (15) were obtained with a Cary 17 spectrophotometer equipped with thermostated reference and sample compartments. The protein concentration was 0.5 mg/ml. At equilibrium, the difference absorbances at 293 nm (16) were analyzed in terms of a two-state model for the denaturation of chymotrypsinogen. f_{obs}, the observed extent of denaturation (17), was taken as $f_{obs} = (y - y_N)/(y_D - y_N)$ in which $(y - y_N)$ is the difference absorbance at a given guanidine-HCl concentration and $(y_D - y_N)$ is the difference absorbance before (y_N) and after (y_D) the transition and obtained by linear extrapolation.

Ultracentrifugation — The sedimentation coefficients of reduced-renatured and denatured-renatured chymotrypsinogen (with SS bonds intact) were determined in 1.2 M guanidine HCl, 10 mM Tris-HCl, pH 8.2, by sedimentation velocity measurements at 20°C and 55,000 rpm in an MSE Centriscan 75 ultracentrifuge using 20-mm optical path cells. The data of Kawahara and Tanford (18) were used to correct the observed sedimentation coefficients for the viscosity and density of guanidine HCl, assuming the partial specific volume of the protein to be 0.721 ml/g (19) in the solvent used.

RESULTS

Kinetics of Renaturation of Reduced Chymotrypsinogen — To investigate the kinetics of refolding and reoxidation of the reduced zymogen, it was necessary to be able to stop the renaturation at any point of the reaction. This could hopefully be achieved by blocking the thiol-disulfide reagents required for the renaturation of this protein (7). To test this possibility, the denatured-reduced protein was diluted into a buffer containing a mixture of GSH and GSSG, and low concentrations of guanidine HCl which have been reported to permit the renaturation of reduced chymotrypsinogen (7). At various times of incubation, N-ethylmaleimide, chosen because of its high reactivity toward thiols (14, 20), was added to aliquots of the renaturation mixture. Because guanidine HCl was found to strongly inhibit the activation of chymotrypsinogen, the protein was then dialyzed and the extent of renaturation was determined by assay of the chymotrypsin activity after activation. Fig. 1 shows the kinetics observed when the renaturation was carried out under the optimal conditions. It indicates that alkylation efficiently stops the reaction. A control (Fig. 1) verified that when alkylation was omitted before dialysis, the renaturation went to completion because disulfide interchange occurred during the dialysis.

Purification of Reduced-renatured Chymotrypsinogen — Activation of the zymogen has been used in this study as a convenient measure of the renaturation of the reduced protein. It was therefore necessary to verify that the observed renaturation yields actually corresponded to the formation of zymogen molecules capable of activation into fully active chymotrypsin. For this purpose, 1.5 mg of the reduced protein were renatured at a protein concentration of 0.03 mg/ml and the renaturation was stopped by alkylation as described above. The observed renaturation yield was 55%. This material was placed on a carboxymethylcellulose column (see "Experimental Procedures"). Some protein was not retained by the column and was discarded. The adsorbed protein was eluted and was found to correspond, on a weight basis, to 50% of the protein placed on the column. By this procedure, purified reduced-renatured zymogen could be obtained at a higher protein concentration (0.25 mg/ml) than that used during the renaturation. Upon activation, the eluted protein yielded chymotrypsin with a catalytic activity of 210 s⁻¹, a value close to that of δ-chymotrypsin (8). Moreover, this zymogen with full potential activity
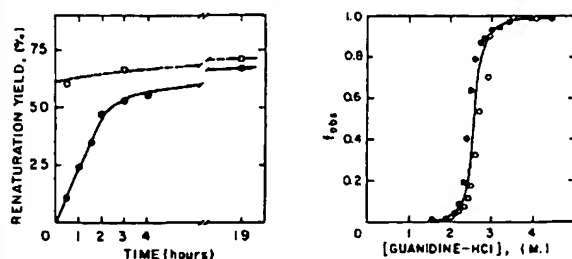

FIG. 1 (*left*). Kinetics of renaturation of reduced chymotrypsinogen in 1.2 M guanidine HCl. At zero time, reduced chymotrypsinogen (6.1 mg/ml) was diluted to 0.030 mg/ml into 50 mM Tris-HCl buffer, pH 8.2, 2 mM EDTA, containing 1.2 M guanidine HCl, 1 mM GSH, and 1 mM GSSG. At the indicated times (●), portions of the reaction mixture were made 5 mM in N-ethylmaleimide, dialyzed, and tested for activability. As a control (○), portions of the reaction mixture were dialyzed at the indicated times without being alkylated.

FIG. 2 (*right*). Equilibrium denaturation and renaturation transition of chymotrypsinogen in guanidine HCl. The buffer was 0.1 M Tris-HCl, pH 8.2, at 25°C. The transition was followed by difference absorbance at 293 nm. f_{obs} is the observed extent of denaturation, normalized as described under "Experimental Procedures." ●, unfolding of native chymotrypsinogen; ○, refolding of chymotrypsinogen previously unfolded in 4.1 M guanidine HCl, 0.1 M Tris-HCl, pH 8.2.

showed the typical ultraviolet spectrum of native chymotrypsinogen (21).

The 50% recovery of a protein indistinguishable from native chymotrypsinogen closely parallels the 55% renaturation yield determined at low protein concentration, thus showing that the activability test is indeed a correct measure of the renaturation of the reduced protein.

Conformation of Reduced-Renatured Chymotrypsinogen in Renaturation Solvent During its incubation in the renaturation mixture, reduced chymotrypsinogen becomes insensitive to alkylation (Fig. 1). This strongly suggests that it is able to form the native disulfide pairing in 1.2 M guanidine HCl. It was however desirable to test whether the protein molecules ultimately characterized as renatured had already formed their SS bonds before the dialysis. These molecules might be insensitive to N-ethylmaleimide because of the inaccessibility of cysteine residues buried within the protein interior. Several experiments were carried out to test this possibility. At various times of the renaturation, N-ethylmaleimide was added, and the protein was then denatured in the presence of excess of this reagent (to expose and alkylate any buried cysteine residue) and renatured by dialysis in the absence of GSH. After this treatment, only correctly and completely reoxidized molecules are likely to recover the native structure. The results of this test are shown in Table I. 85% of the renaturing molecules were unaffected by reaction with 2 mM N-ethylmaleimide in 4.1 M guanidine HCl at 6°C. Identical results were obtained when the renaturing zymogen and excess N-ethylmaleimide were transferred from 1.2 to 3.5 M guanidine HCl at 25°C for 5 min. Since under these conditions the unfolding rate constant for chymotrypsinogen is 3 ± 0.5 min^{-1} (Fig. 3, see below) there is little doubt that any buried cysteine would have been exposed and alkylated by N-ethylmaleimide during this treatment.

The effectiveness of these solvent perturbations in exposing buried cysteines was verified by testing the sensitivity of native chymotrypsinogen to SS bond interchange followed by alkylation. Whereas the native zymogen was insensitive to SS bond interchange in 1.2 M guanidine HCl, a 5-min incubation in 3.5 M guanidine HCl in the presence of 0.6 mM GSH and GSSG followed by alkylation resulted in a 70 to 80% irreversible inactivation of the protein. That this inactivation was due to the scrambling of SS bonds was confirmed by the fact that

TABLE I

Unfolding in presence of N-ethylmaleimide of reduced-renatured chymotrypsinogen

Reduced chymotrypsinogen was renatured by dilution under the same conditions as in Fig. 1. An aliquot was dialyzed without being previously alkylated and used as a control relative to which the renaturation yields were expressed. At 60, 120, and 180 min during the renaturation kinetics (columns A, B, and C, respectively), portions of the renaturation mixture were made 5 mM in N-ethylmaleimide and diluted with guanidine HCl to the final conditions indicated in the first column. These aliquots were incubated for 2 h at 6°C prior to dialysis. Protein concentration was 0.038 mg/ml during the renaturation and 0.018 mg/ml during the incubation with 2 mM N-ethylmaleimide.

Final conditions after alkylation	Maximum renaturation yield		
	Column A	Column B	Column C
	%		
1.2 M guanidine HCl, 2 mM N-ethylmaleimide	34	52	72
4.1 M guanidine HCl, 2 mM N-ethylmaleimide	29	43	60

under the same conditions, but in the absence of GSH and GSSG, complete reversibility of the denaturation of the zymogen was observed.

Taken together, these results clearly indicate that the activatable protein which accumulates in 1.2 M guanidine-HCl (Fig. 1) has already formed the native set of SS bonds when N-ethylmaleimide is added. This fraction of the protein population is therefore likely to be in a conformation closely resembling that of native chymotrypsinogen.

Two independent criteria were used to confirm the above expectation. It was first verified that native chymotrypsinogen is stable in the presence of 1.2 M guanidine HCl. For this purpose, the unfolding transition of chymotrypsinogen in guanidine-HCl was investigated by measuring the 293 nm difference absorption band accompanying the denaturation of this protein (see "Experimental Procedures"). Fig. 2 shows the equilibrium unfolding and refolding transitions of chymotrypsinogen in guanidine HCl. At equilibrium, the transitions have a midpoint near 2.6 M guanidine HCl.[1] The midpoint of the transition could also be determined as the guanidine HCl concentration for which the unfolding and refolding rate constants are equal. Fig. 3 shows that this is the case for 2.8 M guanidine HCl, a value which is not significantly different from that found at equilibrium. Thus, the unfolding transition appears to occur well above 1.2 M guanidine HCl as both equilibrium and kinetic determinations failed to show detectable unfolding of chymotrypsinogen at and below 2 M guanidine HCl. It therefore can be concluded that the reduced zymogen refolds in the presence of guanidine HCl concentrations in which the native protein exhibits full stability.

As a second conformational test, the sedimentation behavior of the reduced-renatured protein was studied in the presence of 1.2 M guanidine HCl. For this purpose, the reduced zymogen was renatured (at a protein concentration of 0.08 mg/ml) during 20 h after which the renaturation was stopped by alkylation. The renaturation yield, determined after dialysis of an aliquot, was 45%. Another aliquot of the renaturation mixture was dialyzed against 1.2 M guanidine-HCl to remove the excess of N-ethylmaleimide and centrifuged in this solvent. During acceleration of the rotor 50 to 60% of the material rapidly sedimented as heterogeneous aggregates. The 40 to 50% remaining protein sedimented as a homogeneous species with a sedimentation coefficient $s_{20,w} = 2.4$ S. Under identical conditions, denatured-renatured chymotrypsinogen (with SS bonds intact) showed only the slow sedimenting homogeneous boundary. Its sedimentation coefficient ($s_{20,w} = 2.6$ S) was, within experimental error, identical with that found for the reduced-renatured species and to that of the native protein (23).

This result clearly shows that aggregation which prevents the renaturation of the reduced protein occurs in guanidine-HCl and confirms that the correct refolding of the monomeric protein molecules, which are shown to be renatured after removal of guanidine HCl, has already occurred in 1.2 M guanidine HCl.

Renaturation of Wrongly Oxidized Protein Molecules – The efficiency of N-ethylmaleimide in stopping the renaturation reaction could be attributed to two distinct causes. This reagent alkylates incompletely oxidized protein molecules thus irreversibly preventing their renaturation. Alterna-

[1] It should be noted that the unfolding and refolding transitions of the protein do not exactly coincide (Fig. 2). Most probably, this is due to a slow aggregation of the protein, upon transfer to denaturant concentrations between 2.2 and 2.5 M. Further work is in progress to elucidate this point.

Refolding of Reduced Chymotrypsinogen

tively, alkylation of GSH prevents the necessary disulfide bond rearrangements of incorrectly oxidized protein species. If such incorrectly oxidized molecules were present in the renaturation mixture after alkylation, they should undergo renaturation upon addition of thiols. Fig. 4 shows that this is indeed the case. After alkylation, a second addition of GSH entails a significant increase of the renaturation level com-
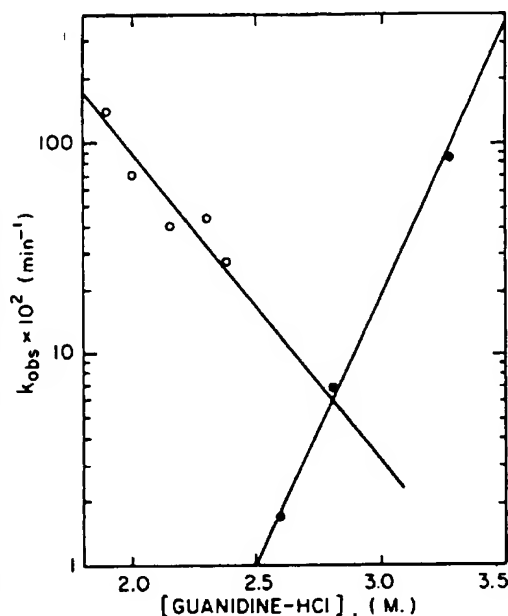
pared to that of the alkylated control, thus indicating the presence of wrongly oxidized molecules within the pool of non-native protein species. It is not known at present if the incorrectly oxidized species contain native SS bonds and hence if they are on a relatively direct refolding pathway.

Dependence of Renaturation Yield upon Renaturation Conditions — The effect of denaturant concentration on the renaturation of the reduced zymogen was investigated. Fig. 5 shows that optimal renaturation yields of 60 to 70% could be obtained only within a narrow range of guanidine HCl concentrations (1.0 to 1.3 M). With urea, the same concentration dependence was observed, 2 M being the optimal urea concentration, although yields were somewhat lower than with guanidine HCl. To test whether this was due to the difference in ionic strength between these denaturants, the efficiency of urea was also measured in the presence of KCl. Fig. 6 shows that the addition of 1 M KCl to the urea renaturation buffer resulted in a shift of the optimal urea concentration from 2 to 3 M with no increase of the renaturation yield.

The dependence of the renaturation yield on the concentra-

FIG. 3. Dependence on guanidine HCl concentration of the first order unfolding and refolding rate constants of chymotrypsinogen. The kinetics of unfolding and refolding of chymotrypsinogen were followed by the time-dependence of the difference absorbance at 293 nm (see "Experimental Procedures"). First order kinetics were observed to at least 90% of completion of both the unfolding and the refolding reactions. The logarithms of the first-order unfolding (●) and refolding (O) rate constants are plotted as a function of the final concentration of guanidine HCl (22).
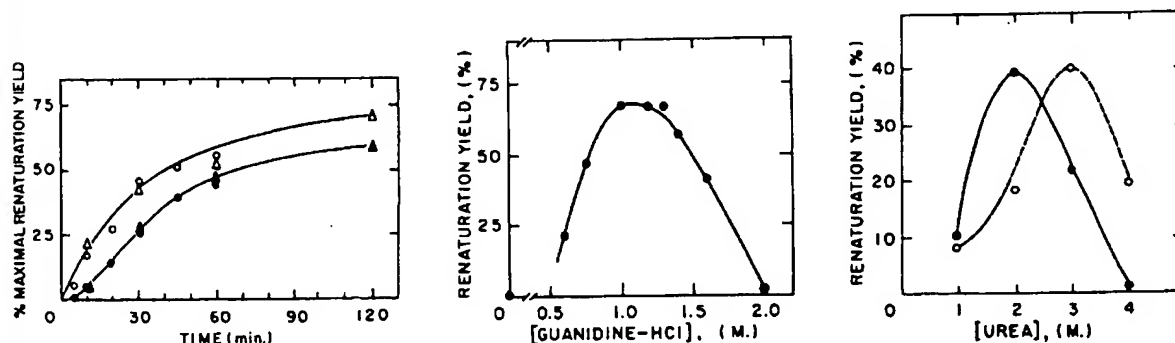
TABLE II

Dependence on GSH and GSSG concentrations of renaturation of reduced chymotrypsinogen

Reduced chymotrypsinogen was diluted in 1.2 M guanidine HCl solutions containing the indicated concentrations of GSH and GSSG. After 4 h at 6°C, the reaction was stopped by alkylation with 10 mM N-ethylmaleimide and the protein mixtures were dialyzed and activated as described under "Experimental Procedures."

GSH	GSSG	Renaturation yield
mM	mM	%
1	0.1	0
1	0.5	45
1	1	50
1	2	35
1	5	0
0.1	1	35
0.5	1	45
2	1	45
5	1	15
5	0.5	10

FIG. 4 (*left*). The renaturation of wrongly oxidized protein molecules. Reduced chymotrypsinogen was renatured by dilution under the same conditions as in Fig. 1. At the indicated times (●, ▲) portions of the renaturation mixture were made 5 mM in N-ethylmaleimide. O and △ indicate aliquots to which 5 min after alkylation GSH was added to 5 mM total concentration. The measured final concentrations of the additives were zero for N-ethylmaleimide and 1 mM GSH. *Triangles* and *circles* correspond to two independent series of experiments. For each experiment, the maximum renaturation yield was obtained by a 20-h incubation of the reduced zymogen in the renaturation mixture, followed by dialysis without alkylation.

FIG. 5 (*center*). The effect of guanidine HCl on the renaturation

of reduced chymotrypsinogen. Reduced chymotrypsinogen was renatured during 20 h by dilution into 50 mM Tris-HCl buffer, pH 8.2-2 mM EDTA, containing guanidine HCl at the indicated concentrations and 1 mM GSH and GSSG. The reaction was stopped by alkylation and the renaturation yield determined after dialysis of the protein.

FIG. 6 (*right*). The effect of urea on the renaturation of reduced chymotrypsinogen. Reduced chymotrypsinogen was renatured during 5 h by dilution into the indicated concentrations of urea in the absence (●) or in the presence (O) of 1.0 M KCl. Other conditions were as in Fig. 5.

tions of GSH and GSSG is summarized in Table II. A broad optimum centered around 1 mM GSH and GSSG ensures a 50% renaturation yield after a 4-h renaturation of the reduced zymogen. Much longer incubation times (24 to 68 h) in the presence of nonoptimal concentrations of the thiol-disulfide reagents did not significantly increase the low yields obtained under the same conditions after the 4-h incubation, thus indicating that the GSH-GSSG mixture would act essentially upon the kinetics of the renaturation reaction.

DISCUSSION

The renaturation of reduced chymotrypsinogen had already been obtained through indirect methods necessitated by its marked insolubility. Covalent immobilization on insoluble supports (24), chemical modification, or removal of the denaturant by dialysis (7). The method presently described has distinct advantages over the previously developed ones. It is simple and does not involve a chemical modification of the native zymogen. Moreover, it permits a direct use of the standard procedures of protein physical chemistry to monitor the refolding of the protein and to elucidate the relationship existing between folding and aggregation.

In the present study, the renaturation of reduced chymotrypsinogen has been investigated under controlled conditions. In the renaturation solvent (1.2 M guanidine HCl or 2 M urea) the refolding and reoxidation are shown to be effective and essentially two classes of stable protein species are found at the end of the reactions: fully renatured chymotrypsinogen and heterogeneous aggregates. In the solvent used for the renaturation of reduced chymotrypsinogen, the denatured zymogen with SS bonds intact is shown to refold rapidly and completely with no detectable aggregation. In the same way, the native zymogen is shown to be totally resistant to the irreversible scrambling of SS bonds in 1.2 M guanidine-HCl. These observations demonstrate that once formed during the renaturation, the native oxidized molecules can no longer form aggregates. Similarly, once formed, the aggregates cannot lead to the native state. If such were the case, the formation of native (oxidized) chymotrypsinogen from the aggregates which, as discussed above, would be irreversible in the renaturation buffer, would continuously draw the aggregated species toward the native form with a 100% final renaturation yield. This prediction is clearly incompatible with the results reported above. Thus no interconversion between native and aggregated molecules occurs in the renaturation solvent. Consequently, rather than being limited by an equilibrium between the native and aggregated forms, the incomplete renaturation of reduced chymotrypsinogen appears to result from a competition between irreversible pathways leading to the formation of the native and aggregated species, respectively. In this view, the simplest interpretation of the favorable effect of guanidine HCl or urea on the renaturation is that they act on the relative rates of formation of the aggregates on the one hand and of the refolded species on the other. This kinetic effect would presumably be produced in the early stages of the refolding (25).

The same interpretation readily accounts for the critical dependence of the renaturation on the denaturant concentration. Below the optimal concentration, aggregation kinetically overcomes refolding whereas above this optimum the initially reduced protein is kept in an unfolded state.

In the early stages of refolding, an unfolded polypeptide chain can be viewed as "collapsing" into a compact globular structure (26) with a major hydrophobic contribution to this

initial process (27). Such a model may well account for the "choice" offered to unfolded reduced chymotrypsinogen between the two distinct pathways suggested above, refolding or aggregation.

A further question is the role of disulfide bond formation in this choice. A relatively broad concentration range of both GSSG and GSH is shown to ensure significant renaturation yields, thus suggesting that the formation of native disulfide bonds as such is not an essential factor for the process under consideration. Even though tentative, this conclusion is in line with observations on the refolding of reduced RNase. The early manifestation of a low, but detectable enzymic activity has been shown to correspond to essentially reduced active RNase molecules, the refolding of which occurs prior to the formation of SS bonds (28). According to this model, during the renaturation of the reduced zymogen disulfide bond formation would occur after the initial choice made between either folding toward the native conformation or interactions leading to aggregation. The reoxidation involves the reshuffling of incorrect disulfide bonds, as is generally observed in the renaturation of reduced proteins (11, 29).

The physical basis for the interaction between proteins and guanidine HCl or urea is still poorly understood (30, 31). This warrants some caution in the interpretation of the fact that these denaturants permit, under restricted conditions, the refolding of reduced chymotrypsinogen. One essential feature of this effect is that it appears to be rather specific. Low concentrations of urea have been shown to trap denatured β-galactosidase and tryptophanase into incorrectly folded and aggregated states (32, 33). Conversely, low concentrations of guanidine HCl or urea have been shown to favor the refolding of bovine and human carbonic anhydrases (34, 35) as well as that of a fragment of a myeloma protein containing the antibody combining site (36). As in the presently illustrated case of reduced chymotrypsinogen, low amounts of denaturants permit the correct refolding of these proteins instead of their aggregation. It is hoped that the specificity of guanidine-HCl or urea in the refolding of reduced chymotrypsinogen can provide an experimental handle for a further investigation of the early steps of protein folding.

REFERENCES

1. Tanford, C., Kawahara, K., and Lapanje, S. (1967) *J. Am. Chem. Soc.* 89, 729–736
2. Brandts, J. F. (1964) *J. Am. Chem. Soc.* 86, 4302–4314
3. Jackson, W. M., and Brandts, J. F. (1970) *Biochemistry* 9, 2294–2301
4. Eisenberg, M. A., and Schwert, G. W. (1951) *J. Gen. Physiol.* 34, 583–606
5. Hapner, K. D., and Wilcox, P. E. (1970) *Biochemistry* 9, 4470–4480
6. Brown, J. C., and Horton, H. R. (1972) *Proc. Soc. Exp. Biol. Med.* 140, 1451–1455
7. Orsini, G., Skrzynia, C., and Goldberg, M. E. (1975) *Eur. J. Biochem.* 59, 433–440
8. Wilcox, P. E. (1970) *Methods Enzymol.* 19, 64–108
9. McClure, W. O., and Edelman, G. M. (1967) *Biochemistry* 6, 567–572
10. Abita, J. P., Delaage, M., and Lazdunski, M. (1969) *Eur. J. Biochem.* 8, 314–324
11. Saxena, V. P., and Wetlaufer, D. B. (1970) *Biochemistry* 9, 5015–5023
12. Nozaki, Y. (1972) *Methods Enzymol.* 26, 43–50
13. Ellman, G. L. (1959) *Arch. Biochem. Biophys.* 82, 70–77
14. Hantgan, R. R., Hammes, G. G., and Scheraga, H. A. (1974)

Biochemistry 13, 3421-3431
15. Chervenka, C. H. (1959) *Biochim. Biophys. Acta* 31, 85-95
16. Brandts, J., and Lumry, R. (1963) *J. Phys. Chem.* 67, 1484-1494
17. Tanford, C. (1968) *Adv. Protein Chem.* 23, 121-282
18. Kawahara, K., and Tanford, C. (1966) *J. Biol. Chem.* 241, 3228-3232
19. Schwert, G. W. (1951) *J. Biol. Chem.* 190, 799-806
20. Riordan, J. F., and Vallee, B. L. (1967) *Methods Enzymol.* 11, 541-548
21. Chervenka, C. H., and Wilcox, P. E. (1956) *J. Biol. Chem.* 222, 621-634
22. Tanford, C. (1970) *Adv. Protein Chem.* 24, 1-95
23. Wilcox, P. E., Kraut, J., Wade, R. D., and Neurath, H. (1957) *Biochim. Biophys. Acta* 24, 72-78
24. Brown, J. C., Swaisgood, H. E., and Horton, H. R. (1972) *Biochem. Biophys. Res. Commun.* 48, 1068-1073
25. Lumry, R., and Eyring, H. (1954) *J. Phys. Chem.* 58, 110-120
26. Levitt, M., and Warshel, A. (1975) *Nature* 253, 694-698

27. Chothia, C., and Janin, J. (1975) *Nature* 256, 705-708
28. Garel, J. R. (1978) *J. Mol. Biol.* 118, 331-345
29. Creighton, T. E. (1977) *J. Mol. Biol.* 113, 329-341
30. Roseman, M., and Jencks, W. P. (1975) *J. Am. Chem. Soc.* 97, 631-640
31. Franks, F., and Eagland, D. (1975) *CRC Crit. Rev. Biochem.* 3, 165-219
32. Goldberg, M. E. (1973) in *Dynamic Aspects of Conformation Changes in Biological Macromolecules* (Sadron, C., ed) pp. 57-65, D. Reithel Publishing Company, Dordrecht
33. London, J., Skrzynia, C., and Goldberg, M. E. (1974) *Eur. J. Biochem.* 47, 409-415
34. Wong, K.-P., and Tanford, C. (1973) *J. Biol. Chem.* 248, 8518-8523
35. Carlsson, U., Aasa, R., Henderson, L. E., Jonsson, B. H., and Lindskog, S. (1975) *Eur. J. Biochem.* 52, 25-36
36. Hochman, J., Gavish, M., Inbar, D., and Givol, D. (1976) *Biochemistry* 15, 2706-2710

All Databases | PubMed | Nucleotide | Protein | Genome | Structure | OMIM | PMC | Journals | Book

Search PubMed for Go Clear

Limits | Preview/Index | History | Clipboard | Details

Display Abstract | Show 20 | Sort by | Send to

All: 1 | Review: 0

About Entrez

Text Version

Entrez PubMed
Overview
Help | FAQ
Tutorials
New/Noteworthy
E-Utilities

PubMed Services
Journals Database
MeSH Database
Single Citation Matcher
Batch Citation Matcher
Clinical Queries
Special Queries
LinkOut
My NCBI

Related Resources
Order Documents
NLM Mobile
NLM Catalog
NLM Gateway
TOXNET
Consumer Health
Clinical Alerts
ClinicalTrials.gov
PubMed Central

1: Arch Biochem Biophys. 1993 Oct;306(1):183-7.   Related Articles, Links

ELSEVIER
FULL-TEXT ARTICLE

Renaturation of lysozyme--temperature dependence of renaturation rate, renaturation yield, and aggregation: identification of hydrophobic folding intermediates.

Fischer B, Sumner I, Goodenough P.

AFRC Institute of Food Research, Department of Protein Engineering, Earley Gate, Reading, England.

Renaturation of denatured-reduced hen egg white lysozyme was analyzed at temperatures between 4 and 70 degrees C using the reduced/oxidized glutathione renaturation system. With an increase in temperature to 50 degrees C both renaturation rate constant and renaturation yield increased while formation of aggregates decreased. Denatured-reduced lysozyme and early folding intermediates were less stable against heat than native lysozyme at temperatures above 60 degrees C. Renaturation at 70 degrees C resulted in no reconstitution of lysozyme activity but the highest level of aggregation. Renaturation of denatured-reduced hen egg white lysozyme was further analyzed in the presence of the hydrophobicity-indicating fluorescence dye 1-anilinonaphalene-8-sulfonate at temperatures between 10 and 40 degrees C. The change in fluorescence intensity, the generation of enzyme activity, renaturation yield, and the formation of aggregates were studied. The results showed that early folding intermediates possess a strong hydrophobic nature. With an increase in temperature both the renaturation rate and the decay rate of hydrophobicity-mediated fluorescence increased. Consequently, with increasing temperature, accumulation of hydrophobic folding intermediates and formation of insoluble aggregates decreased, leading to an increase in the renaturation yield.

PMID: 8215401 [PubMed - indexed for MEDLINE]

Display Abstract | Show 20 | Sort by | Send to

Exhibit 17

Folding and aggregation of TEM β-lactamase: Analogies with the formation of inclusion bodies in *Escherichia coli*

GEORGE GEORGIOU,[1] PASCAL VALAX,[1] MARC OSTERMEIER,[1]
AND PAUL M. HOROWITZ[2]

[1] Department of Chemical Engineering, University of Texas, Austin, Texas 78712
[2] Department of Biochemistry, University of Texas Health Science Center at San Antonio, San Antonio, Texas 78284

Abstract

The enzyme TEM β-lactamase has been used as a model for understanding the pathway leading to formation of inclusion bodies in *Escherichia coli*. The equilibrium denaturation of TEM β-lactamase revealed that an intermediate that has lost enzymatic activity, native protein fluorescence, and UV absorption, but retains 60% of the native circular dichroism signal, becomes populated at intermediate (1.0–1.4 M) concentrations of guanidium chloride (GdmCl). This species exhibits a large increase in bis-1-anilino-8-naphthalene sulfonic acid fluorescence, indicating the presence of exposed hydrophobic surfaces. When TEM β-lactamase was unfolded in different initial concentrations of GdmCl and refolded to the same final conditions by dialysis a distinct minimum in the yield of active protein was observed for initial concentrations of GdmCl in the 1.0–1.5 M range. It was shown that the lower reactivation yield was solely due to the formation of noncovalently linked aggregates. We propose that the aggregation of TEM β-lactamase involves the association of a compact state having partially exposed hydrophobic surfaces. This hypothesis is consistent with our recent findings that TEM β-lactamase inclusion bodies contains extensive secondary structure (Przybycien TM, Dunn JP, Valax P, Georgiou G, 1994, *Protein Eng* 7:131–136). Finally, we have also shown that protein aggregation was enhanced at higher temperatures and in the presence of 5 mM dithiothreitol and was inhibited by the addition of sucrose. These conditions exert a similar effect on the formation of inclusion bodies in vivo.

Keywords: β-lactamase; inclusion bodies; molten globule; protein folding

In recent years it has become apparent that the tendency of proteins to aggregate is of considerable significance for the physiology of the cell as well as for numerous applications in biotechnology (DeYoung et al., 1993). Protein aggregates are formed in vivo as a result of mutations that affect the folding pathway, expression of heterologous polypeptides, or exposure of the cell to certain environmental stresses. Expression of heterologous genes in *Escherichia coli* and other gram-negative bacteria is often accompanied by the formation of micron-size aggregates or inclusion bodies (Mitraki & King, 1989; De Bernardez-Clark & Georgiou, 1991). Whether a protein will fold to its native state or aggregate to form inclusion bodies depends on a variety of physicochemical and physiological parameters, including interactions with chaperones, the growth temperature, level of protein synthesis, and the concentration of small solutes in the in vivo folding environment (Schein & Noteborn, 1988; Bowden & Georgiou, 1990; Blum et al., 1992).

Little is known regarding the mechanism of protein aggregation in the cell. It is generally accepted that aggregation and folding are competing processes with the former exhibiting higher order kinetics and thus becoming favored at elevated protein concentrations. A central question is at what point does the folding pathway branch off. Is aggregation the result of specific complementary interactions between late, nativelike, folding intermediates, or is it simply a consequence of the insolubility of either the unfolded or native state? Earlier in vitro studies produced somewhat conflicting answers (London et al., 1974; Goldberg et al., 1991). However, there is mounting evidence that in vivo protein aggregation, as manifested by the formation of inclusion bodies, is a highly specific process resulting from the association of intermediates having appreciable secondary struc-

ture. Seminal studies by King and coworkers revealed that conditional mutations in the tailspike protein of phage P22 influence the extent of aggregation in vivo and folding pathway in vitro but not the stability and solubility of the native state (Mitraki et al., 1991, 1993). Amino acid substitutions that specifically affect the folding pathway in the cell and are manifested by a change in the propensity to form inclusion bodies have also been isolated in other proteins (Mitraki & King, 1992; Rinas et al., 1992; Chrunyk et al., 1993; Wetzel, 1994).

The TEM β-lactamase is exported across the cytoplasmic membrane and is found in soluble form in the periplasmic space when expressed from its native promoter in pBR322-type vectors. Inclusion bodies are formed upon overexpression from a strong promoter and at elevated temperatures when TEM β-lactamase is secreted via an OmpA leader peptide (Georgiou et al., 1986; Bowden & Georgiou, 1990). Signal peptide deletions that abolish export lead to massive aggregation in the cytoplasm in the form of highly regular, cylindrical inclusion bodies (Bowden et al., 1991). Conditions that affect the formation of TEM β-lactamase inclusion bodies include the growth temperature, the addition of nonmetabolizable sugars in the culture medium, and host mutations that impair the formation of disulfide bonds (Bowden & Georgiou, 1990; Chalmers et al., 1990; M. Ostermeier, unpubl. obs.).

In this work we have investigated the equilibrium denaturation, the folding kinetics, and the aggregation of TEM β-lactamase in vitro. We present evidence that aggregation is initiated by the association of a molten globule-like folding intermediate. This result is consistent with the spectroscopic analysis of the secondary structure of TEM β-lactamase in E. coli inclusion bodies, which revealed the presence of appreciable nativelike structure in the aggregated polypeptide chains (Przybycien et al., 1994). Thus, the aggregation of TEM β-lactamase, both in vitro and in vivo, appears to arise from specific interactions of nativelike intermediates. Furthermore, we demonstrate that conditions which have been shown to inhibit the formation of inclusion bodies in E. coli exert a similar effect on aggregation in vitro.

Fig. 1. A: Equilibrium denaturation curves for TEM β-lactamase as measured by fluorescence intensity (■); CD at 222 nm (O); enzymatic activity (●); and Bis-ANS fluorescence (▲). **B:** Comparison of equilibrium curves measured by fluorescence intensity (squares) and Bis-ANS binding (triangles). Open symbols: data obtained with 5 mM DTT; closed symbols: data obtained without DTT.

Results

Folding equilibrium

The GdmCl-induced unfolding transition of purified TEM β-lactamase at room temperature (23 °C) was monitored by different techniques and the results are shown in Figure 1A. Unfolding was found to be completely reversible up to concentrations of 4 mg/mL (see below). The change in fluorescence intensity as a function of denaturant concentration could be represented reasonably well by a sigmoidal transition with a midpoint at 0.87 M GdmCl. No change in the protein fluorescence was observed at denaturant concentrations higher than 1.2 M. A coincident, 2-state-like transition ($C_m = 0.86$ M) was also detected by UV difference spectroscopy at 286.5 nm, the wavelength for $\Delta\epsilon_{max}$ (Valax & Georgiou, 1991). The change in β-lactamase specific activity using penicillin G as the substrate also exhibited a similar dependence on the concentration of denaturant with detectable activity measurable in up to 1.5 M GdmCl.

Complex changes in the protein were detected by far-UV circular dichroism (Fig. 1A). The initial transition which accounted for approximately 40% of the total signal, was sigmoidal and
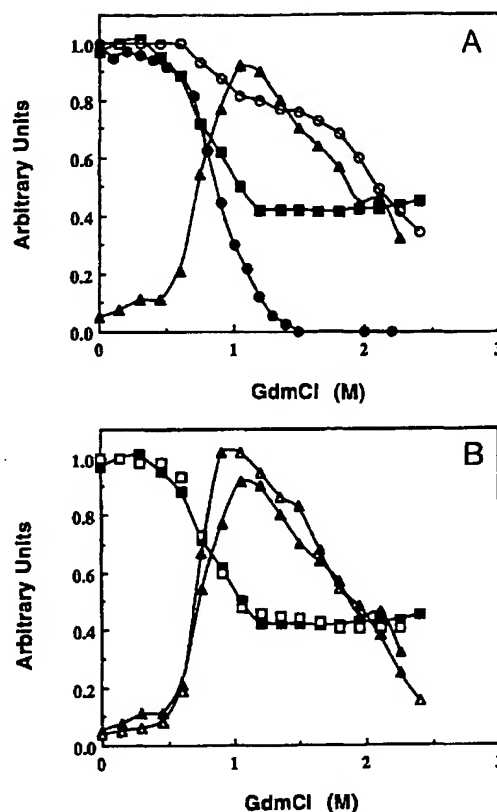
centered around 0.8 M GdmCl. This was followed by a plateau between 1.0 and 1.5 M GdmCl and a second, broader transition. The presence of the plateau in the CD signal indicates the existence of a populated intermediate state having appreciable secondary structure. The characteristics of this intermediate were further examined by the binding of the fluorescent probe Bis-ANS. This reporter molecule exhibits little fluorescence in aqueous solutions but becomes highly fluorescent upon binding to organized hydrophobic regions in proteins (Horowitz & Butler 1993). The wavelength for maximum Bis-ANS fluorescence was independent of the GdmCl concentration indicating that the addition of the probe did not cause conformational changes in the protein. However, the Bis-ANS fluorescence intensity increased sharply at concentrations beyond 0.5 M with a maximum observed at 1.1 M GdmCl. Higher concentrations of denaturant led to a gradual decrease in the Bis-ANS fluorescence, which paralleled the loss of the far-UV CD signal and presumably reflects the global unfolding of the protein.

To investigate the significance of the single disulfide bond of β-lactamase in unfolding, the protein was reduced by incubating in 5 mM DTT for 12 h. At that point, over 95% of the cys-

teines were present in the free thiol form as determined by sulfhydryl titration using Ellman's reagent. The denaturation curves obtained by monitoring the change in fluorescence intensity (Fig. 1B), the far-UV CD signal, and the UV adsorption of the protein in DTT (data not shown) were indistinguishable from those of the oxidized protein. The overall profiles of Bis-ANS fluorescence were also quite similar, but the reduced protein exhibited a small, yet reproducible increase in the Bis-ANS fluorescence in the 0.7–1.4 M GdmCl region. The maximum Bis-ANS fluorescence was observed in 1.0 M GdmCl and was 15% higher following reduction with DTT.

β-Lactamase aggregation upon refolding

Unfolding of the reduced protein in 3 M GdmCl followed by dilution with buffer to a final protein concentration of 3 mg/mL resulted in the appearance of light scattering material as soon as the concentration of GdmCl was reduced below 1.5 M (M. Ostermeier, unpubl. data). The soluble TEM β-lactamase obtained after dilution had a specific activity identical to the authentic protein and eluted as a single symmetric peak by gel filtration HPLC (Valax, 1993). Light scattering material consisted of large protein aggregates, which could be easily collected by centrifugation. Nonreducing SDS-PAGE revealed no evidence of intermolecular disulfide bonds among the polypeptide chains in the aggregate. Prolonged incubation in phosphate buffer did not result in any appreciable release of protein from the aggregates (P. Valax, unpubl. obs.). Light scattering material did not form even after prolonged incubation in 3 M GdmCl.

Aggregation depends strongly on the protein concentration, which changes in the course of refolding experiments initiated by dilution from denaturant solutions. It was of interest to examine the extent of aggregation and the reversibility of the refolding process under conditions where the protein concentration is kept constant throughout the experiment. For this purpose, known amounts of TEM β-lactamase were first equilibrated in 3 M GdmCl and then the concentration of denaturant was reduced to the same final value (0.02 M GdmCl) by dialysis. Within experimental error, the fraction of the protein that was soluble after refolding was equal to the reactivation yield. The reactivation yield is defined as the enzymatic activity following refolding over the activity in a sample of identical protein concentration that was treated in the same way as the samples that were subjected to refolding except that the denaturant was omitted.

Figure 2 shows the fraction of the initial β-lactamase activity recovered at 23 °C and 37 °C as a function of the protein concentration. As expected, the extent of reactivation of TEM β-lactamase depended strongly on both the temperature and the protein concentration. At 37 °C and protein concentrations higher than 0.5 mg/mL, the decrease in the yield of active protein was accompanied by the formation of aggregated material. In contrast, at 23 °C aggregation could not be detected up to 4 mg/mL. At both temperatures, under conditions where refolding was no longer completely reversible, the recovery yield upon refolding was linearly dependent on the protein concentration. Irreversibilities were solely due to aggregation, as there was no evidence of multimeric species in solution and the specific activity of the refolded protein was identical to the native TEM β-lactamase.
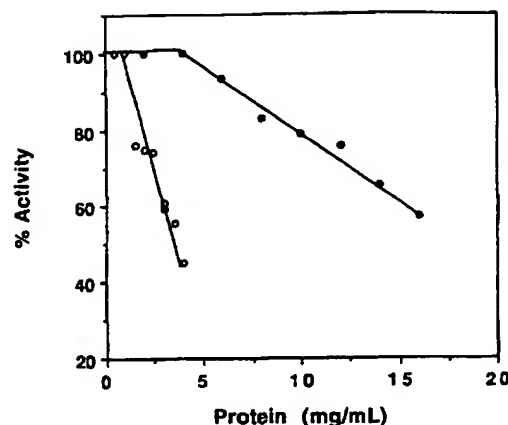

Fig. 2. Effect of protein concentration on the recovery of enzymatic activity of reduced TEM β-lactamase unfolded in 3 mM GdmCl for 3 h followed by removal of the denaturant by dialysis to a final denaturant concentration of 0.02 M. ●, 23 °C; O, 37 °C.

The activity recovered upon refolding at 37 °C was strongly dependent on the initial GdmCl concentration (Fig. 3). Incubation of native protein in GdmCl concentrations between 1.0 and 1.4 M prior to dialysis resulted in only about 5% recovery of the enzymatic activity compared to 60% when the initial GdmCl concentration was 3 M or higher. However, no such minimum in the recovered activity was observed at 23 °C even though the protein concentration for these experiments was 3 times higher.

All subsequent experiments were conducted at 37 °C to allow direct comparison with the formation of TEM β-lactamase inclusion bodies in the periplasmic space of *E. coli*. When unfolding and dialysis were conducted under nonreducing conditions, the activity yield was substantially higher for all initial GdmCl concentrations (Fig. 4). Nevertheless, both in the absence and in the presence of DTT, the refolding yield exhibited a minimum at an initial GdmCl concentration of 1.4 M.
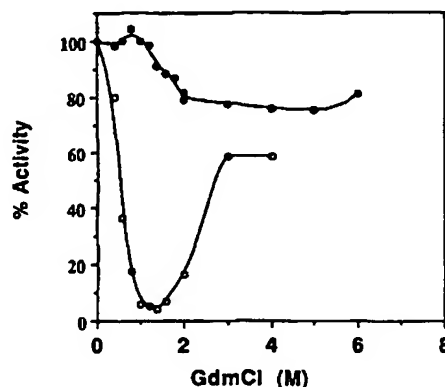

Fig. 3. Recovery of enzymatic activity of reduced TEM β-lactamase unfolded in different initial concentrations of GdmCl and refolded by dialysis to a final denaturant concentration of 0.02 M. ●, 23 °C, 10 mg/mL protein; O, 37 °C, 3 mg/mL protein.
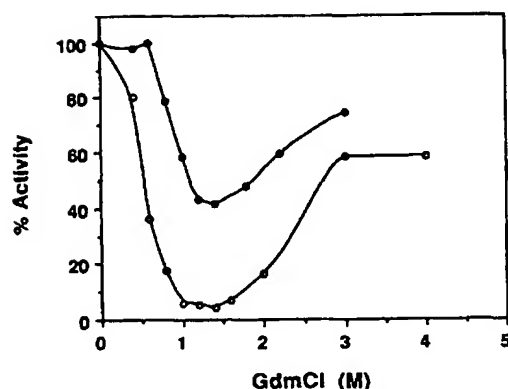
Fig. 4. Recovery of enzymatic activity of β-lactamase at 37 °C in the presence or absence of 5 mM DTT. A solution of 3 mg/mL of protein was incubated in different initial concentrations of GdmCl and refolded by dialysis to a final denaturant concentration of 0.02 M. ●, with 5 mM DTT; O, without DTT.

The addition of moderate concentrations of sucrose in the growth medium has been shown to inhibit the aggregation of TEM β-lactamase in the periplasmic space of *E. coli* grown at 37 °C (Bowden & Georgiou, 1990). At a TEM β-lactamase concentration of 3 mg/mL, the presence of 0.6 M sucrose resulted in a moderate increase in the recovery of correctly folded, active protein upon refolding from solutions containing >0.5 M GdmCl (Fig. 5). The effect of sucrose was most pronounced when refolding was initiated from the completely unfolded state. For protein unfolded in 3 M GdmCl, the protein concentration at which aggregation became apparent increased with increasing concentrations of sucrose in the range of 0–0.6 M (Valax, 1993). Surprisingly however, the addition of sucrose to protein samples equilibrated in less than 0.5 M GdmCl resulted in a decrease in the refolding yield. This result is puzzling because at such low denaturant concentrations the native conformation is well populated (Fig. 1) and sucrose is known to enhance the stability of the native state.
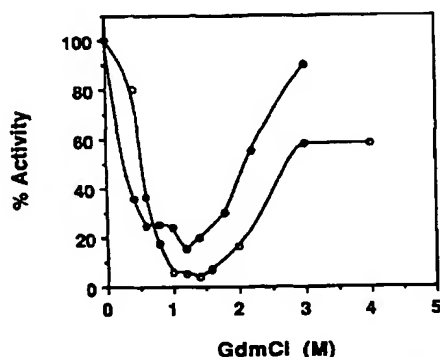
Folding kinetics

The reactivation of β-lactamase from denaturant solutions, as monitored by fluorescence, exhibits a fast phase, which accounts for around 50% of the final specific activity and is complete within the dead time of the experiment, followed by a slower phase (Laminet & Plückthun, 1989). The kinetics of the slow phase in refolding from 3 M GdmCl were monitored by the change in fluorescence intensity at 345 nm. For all final GdmCl concentrations tested, the data for the recovery of more than 90–95% of the fluorescence intensity of the native protein could be fitted by a first-order rate expression. Both the amplitude and the rate constant for the slow phase in folding were dependent on the final GdmCl concentration (Table 1). The amplitude decreased to zero for final GdmCl concentrations >0.6 M. The slow phase in the folding of the reduced protein also exhibited first-order kinetics, but the amplitude was larger and the rate constant smaller. At low final GdmCl concentrations, folding was faster for the oxidized TEM β-lactamase, but the rate constants in the presence and absence of DTT became indistinguishable when the protein was diluted into 0.75 M GdmCl.

The formation of folding intermediates that bind to Bis-ANS were determined as follows. The protein was equilibrated in 3 M GdmCl and then refolding was initiated by dilution to different final concentrations of denaturant. Bis-ANS was added to the refolding mixture at different times following dilution and the fluorescence intensity at 500 nm was determined. For $t = 0$ min, Bis-ANS was present in the dilution buffer. A Bis-ANS binding species was found to form within the dead time for these experiments. Figure 6 shows that the maximum amount of Bis-ANS binding increases for the first few minutes after the initiation of folding and then decreases slowly. The intensity and time of addition of the probe for maximum of Bis-ANS fluorescence was a function of the final GdmCl. Dilution of β-lactamase into 1.8 M GdmCl did not result in any increase in Bis-ANS fluorescence over the basal level at $t = 0$.

Discussion

The changes in the fluorescence intensity, enzymatic activity, and UV adsorption during the unfolding of TEM β-lactamase in GdmCl followed a sigmoidal transition with a mid-point

Fig. 5. Recovery of the enzymatic activity of TEM β-lactamase in 5 mM DTT and in the presence (●) or absence (O) of 0.6 M sucrose. The experimental conditions were as in Figure 4.

Table 1. *Amplitudes of the fast phase and rate constants for the slow phase in the folding of β-lactamase from 3 M GuHCl to the indicated final concentrations in the presence or absence of 5 mM DTT*

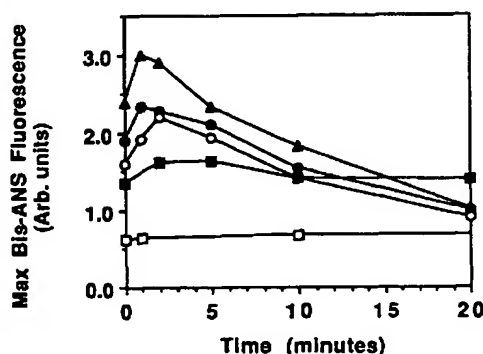| GuHCl (M)	DTT	Amplitude (fraction of the total transition)	k (min^{-1})
0.30	+	0.43 ± 0.015	0.120 ± 0.003
0.45	+	0.36 ± 0.02	0.107 ± 0.001
0.60	+	0.31 ± 0.012	0.089 ± 0.002
0.75	+	0.28 ± 0.025	0.083 ± 0.003
0.30	−	0.31 ± 0.01	0.182 ± 0.002
0.45	−	0.14 ± 0.01	0.131 ± 0.001
0.60	−	0.03 ± 0.005	0.098 ± 0.006
0.75	−	0.02 ± 0.01	0.078 ± 0.002

Fig. 6. Maximum fluorescence due to Bis-ANS binding. A final concentration of 1 μM Bis-ANS was added at different times after dilution of a solution of 0.3 mg/mL of reduced β-lactamase unfolded in 3 M GdmCl to different final concentrations of denaturant. ▲, 0.3 M; ●, 0.45 M GdmCl; ○, 0.45 M GdmCl, no DTT; ■, 0.75 M GdmCl; □, 1.85 M GdmCl.

around 0.85–0.9 M. The loss of enzymatic activity and tryptophan fluorescence indicate that the end of this transition is marked by a significant change in tertiary structure. However, the far-UV CD signal revealed the existence of an intermediate state, which is populated at GdmCl concentrations between 1.1 and 1.5 M and has about 60% of the secondary structure of the native protein. The appearance of this intermediate is accompanied by a marked increase in Bis-ANS fluorescence, a probe that binds preferentially to organized hydrophobic surfaces. The presence of significant secondary structure and exposed hydrophobic surfaces concomitant with the loss of native tertiary structure is consistent with the appearance of a compact intermediate or "molten-globule" state (Ptitsyn et al., 1990; Fink, 1994). Compact folding intermediates have also been detected in 3 other class A β-lactamases, from *Staphylococcus aureus*, *Bacillus licheniformis*, and *Bacillus cereus* under conditions of low denaturant concentration, in acid or high salt (Robson & Pain, 1976; Goto & Fink, 1989; Ptitsyn et al., 1990; Calciano et al., 1993). These enzymes share a high degree of topological similarity with the TEM β-lactamase, but with several subdomains existing in different relative orientations (Jelsch et al., 1992; Strynadka et al., 1992). The compact intermediate form of the *B. licheniformis* enzyme at low pH has been characterized in detail (Calciano et al., 1993). It has a Stokes radius that is only about 10% larger than that of the native protein, binds ANS, and has a high degree of secondary structure. The characteristics of the compact state of *B. licheniformis* β-lactamase suggest that subdomains with native secondary structure are present, but at least some tertiary interactions have been lost, leading to some expansion of the molecule (Fink, 1994). Given the homology and structural similarity between the native *B. licheniformis* enzyme and TEM β-lactamase, it is reasonable to postulate that the intermediate we detected in low GdmCl concentrations adopts a similar conformation.

TEM β-lactamase contains a single disulfide bond between Cys[77] and Cys[123]. Replacement of one or both cysteines by site-specific mutagenesis affects the stability but not the enzymatic activity of the protein (Schultz et al., 1987; Laminet & Plückthun, 1989). When the disulfide bond was reduced by DTT, the

denaturation transition was not affected except that an increase in Bis-ANS binding at low GdmCl concentrations was observed. Cys[77] and Cys[123] form a disulfide bond connecting helices h2 and h4 (Jelsch et al., 1992). Reduction of the disulfide bond presumably leads to loss of stabilizing interactions in the helix-dominated subdomain of β-lactamase (residues 61–211) and increased solvent exposure of the hydrophobic residues in helix h2.

A protein species that exhibits strong binding to Bis-ANS is formed very early upon dilution from 3 M GdmCl (Fig. 6). When the probe is added directly in the diluting buffer, a rapid increase in fluorescence occurs and is complete within 10 s (within the dead time for these experiments). An additional, more gradual increase in fluorescence is complete within 45 s, depending on the final GdmCl concentration, followed by a gradual decrease as the protein reaches the native state. Ptitsyn et al. (1990) have observed similar changes in the binding of Bis-ANS during the folding of the *S. aureus* β-lactamase. They proposed that the Bis-ANS binding species, which is formed early on in the reaction, corresponds to a folding intermediate with the characteristics of the molten globule. It is tempting to speculate that the binding of Bis-ANS to TEM β-lactamase reflects the formation of a molten globule-like species, in analogy with the *S. aureus* enzyme.

The maximum Bis-ANS binding was dependent on the final GdmCl concentration and on the time of addition of Bis-ANS. Maximum Bis-ANS fluorescence was observed within the first few minutes after folding commences. This reflects a rapid increase in organized hydrophobic surfaces during the early steps in the folding transition, which coincides with the fast phase detected by the change in protein intrinsic fluorescence. The early steps are followed by a slower transition manifested by progressively lower Bis-ANS binding and a first-order change in the protein intrinsic fluorescence.

Both the amplitude and the rate constant for the transition monitored by the intrinsic fluorescence depend on the final GdmCl concentration. The rate constant for the slow phase observed with the reduced protein is greater than for the oxidized TEM β-lactamase. A possible explanation is that the presence of the disulfide bond facilitates alignment of the 2 helices in the active site subdomain of the protein and expedites the formation of native secondary structure. Interestingly, the amplitude of the fast phase was greater for the reduced protein than for the oxidized protein.

At relatively higher protein concentrations (3 mg/mL), dilution of the unfolded protein to GdmCl concentrations lower than 1.5 M resulted in the formation of light scattering material in the solution. The parameters that influence protein aggregation upon refolding were investigated by employing diafiltration to lower the denaturant concentration. This allowed the refolding to proceed to the same final conditions while keeping the protein concentration constant throughout the experiment. Neither aggregation nor any decrease in the reactivation of reduced β-lactamase upon refolding from 3 M GdmCl were evident even at relatively high protein concentrations: 0.5 mg/mL at 37 °C and 4.0 mg/mL at 23 °C. At higher protein concentration the reactivation yield varied linearly with the amount of protein. The slope of the reactivation versus protein concentration curve increased substantially at 37 °C.

The reactivation yield was strongly dependent on the initial GdmCl concentration at which TEM β-lactamase had been in-

cubated prior to refolding. At 37 °C, starting with 3 mg/mL of protein that had been equilibrated in 1.0–1.4 M GdmCl, the recovery of active β-lactamase was only 5% compared to over 60% recovery when refolding was initiated from the unfolded state (i.e., in 3 M GdmCl). A similar dependence of the reversibility of refolding on the initial concentration of denaturant has been observed with other proteins, such as horse muscle phosphoglycerate kinase (Mitraki et al., 1987), rhodanese (Horowitz & Criscimagna, 1986), and human growth hormone (De Felippis et al., 1993). The reactivation yield of horse muscle phosphoglycerate kinase at 23 °C exhibited a sharp trough when refolding was initiated from 0.7 ± 0.1 M GdmCl. This phenomenon was shown to result from the aggregation of an intermediate that becomes populated in moderate denaturant concentrations and exhibits a reduced degree of α-helix formation relative to the native state. In the case of rhodanese, the aggregation of the sulfur-free enzyme in GdmCl induced minor changes in overall structure, but led to a substantial increase in the exposure of apolar surfaces of the protein as evidenced by the binding of ANS. In a similar fashion the aggregation of TEM β-lactamase is enhanced drastically in the presence of around 0.9–1.4 M GdmCl, conditions that favor the formation of the compact intermediates having exposed hydrophobic surfaces. The near absence of aggregation at the lower temperatures further supports the hypothesis that the self-association of β-lactamase is driven by hydrophobic forces (Mitraki et al., 1987).

The reduced protein exhibited both higher Bis-ANS binding and showed a lower protein yield upon refolding. As discussed above, this greater tendency to aggregation may be related to increased exposure of the hydrophobic face of helix h2 in the reduced protein. Also, the addition of sucrose resulted in some increase in the reactivation yield, the magnitude of which depends on the initial denaturant concentration. Sugars can affect the folding reaction in a complex manner (Hurle et al., 1987). Specifically, the inhibition of protein aggregation may be related to one of the following processes: (1) viscosity effects that lower the rate constant for the high-order reactions responsible for protein self-association; (2) stabilization of the native state; (3) acceleration of the rate-limiting step in folding effectively decreasing the concentration of the aggregation-prone intermediate. Although we have not attempted to determine the relative contribution of these 3 mechanisms, preliminary results in our laboratory have shown that sucrose increases the rate of refolding of β-lactamase from 3 M GdmCl as well as the stability of the native state (Valax & Georgiou, 1991; Valax, 1993).

How do these observations correlate with the formation of β-lactamase inclusion bodies in *E. coli*? We have shown earlier that the formation of inclusion bodies occurs when the protein is overexpressed, it is completely suppressed when the cells are grown at 23 °C, and it is enhanced in *dsbA* mutant strains where the formation of disulfide bonds is impaired (Bowden & Georgiou, 1990; Chalmers et al., 1990; Bowden et al., 1991; M. Ostermeier & G. Georgiou, unpubl. results). Clearly, these results bear strong similarities with the finding reported here for the purified protein. In vivo aggregation can also be inhibited completely by growing the cells in the presence of nonmetabolizable sugars. Bowden and Georgiou (1990) showed that the addition of sugars affects neither protein synthesis nor the kinetics of pre-β-lactamase processing and suggested they must influence the folding pathway of the mature polypeptide. We found that the addition of sucrose also inhibits aggregation in vitro; however,

the effect was not as dramatic as would have been expected based on the in vivo data. Regardless, the analogies between the in vitro results and the formation of inclusion bodies is quite striking. It is tempting to speculate that the formation of β-lactamase inclusion bodies is dictated solely by the amino acid sequence of the protein. However, the generality of this hypothesis is tempered by observations that the expression of β-lactamase with a heterologous leader peptide results in a massive increase in inclusion body formation (Bowden & Georgiou, 1990). Thus, at least under some physiological conditions, other factors must play a role in the aggregation of TEM β-lactamase in vivo.

Inclusion bodies often contain minor amounts of other proteins. With some care, such protein aggregates can be separated from other cellular components and thus, the conformation of the aggregated polypeptide chains can be analyzed by spectroscopic techniques applicable to particulate samples. Recently, the secondary structure of β-lactamase and interleukin 1β in inclusion bodies was determined by Raman and attenuated total internal reflectance FTIR spectroscopies, respectively (Oberg et al., 1994; Przybycien et al., 1994). Aggregates of both proteins exhibited extensive secondary structure. Clearly, the aggregation of IL-1β and β-lactamase in *E. coli* must be the result of interactions among folding intermediates in which extensive secondary structure has already formed. For interleukin 1β, the secondary structure in inclusion bodies was very similar to the native protein. In contrast, the β-lactamase inclusion bodies exhibited an increase in β-sheet content at the expenses of helical structure. Such differences relative to the native protein are expected given that the aggregation of β-lactamase most likely involves partially folded intermediate(s). Evidently, this is not the case for the in vivo aggregation of interleukin 1β; for this protein, self-association must involve an almost completely native intermediate. Similarly, inclusion bodies formed by cellulase consist of essentially native protein and exhibit full enzymatic activity (Tokatlidis et al., 1991). It appears that there are at least 2 classes of inclusion bodies: the first class results from the association of nativelike intermediates as is the case for interleukin 1β and cellulase; the second class of inclusion bodies, which is represented by TEM β-lactamase, involves the association of a compact state having extensive secondary structure, but not necessarily nativelike tertiary interactions.

Although the completely denatured TEM β-lactamase in 3 M GdmCl was not susceptible to aggregation, the data presented in this work do not completely rule out the possibility that in vitro aggregation involves the self-association of the denatured state rather than a low solubility intermediate. This is because populations of denatured molecules can be present even under conditions that favor the native state (De Young et al., 1993). However, given that the inclusion bodies formed in *E. coli* have considerable secondary structure, and because protein aggregation in vivo and in vitro appear to have many similarities, the hypothesis that the aggregation of TEM β-lactamase involves an insoluble denatured state does not appear likely.

Materials and methods

β-Lactamase purification

β-Lactamase was purified from the periplasmic fraction of *E. coli* RB791(lacIq8) cells transformed with plasmid pJG108 (Bowden et al., 1991). The cells were grown at 30 °C in M9 salts

supplemented with 0.2% glucose, 0.2% casein, and 100 μg/mL of ampicillin. The cultures were induced with 10^{-4} M isopropyl-β-D-thiogalactoside at an OD_{600} of about 0.35. Under these conditions, β-lactamase accumulates in soluble form at a level exceeding 30% of the total cell protein and no accumulation of unprocessed pre-β-lactamase precursor is observed (Valax & Georgiou, 1993). After overnight growth, the cells were harvested by centrifugation at 10,000 × g for 10 min, resuspended in 10 mM Tris acetate buffer, pH 8.0, containing 0.75 M sucrose, and then converted to spheroplasts according to the procedure described by Osborn and Munson (1976). The spheroplasts were centrifuged at 8,000 × g for 15 min and the supernatant was saved and dialyzed overnight against 4 L of 100 mM sodium acetate, pH 7.5, with 400 mM NaCl. The protein was then purified on a Chelating Sepharose FF (Pharmacia, Inc.) column. Prior to loading, the column was washed with 300 mL of buffer A, pH 7.5, containing 50 mM EDTA, and equilibrated with 300 mL of solution A, pH 4.0. Zn^{+2} was loaded onto the packing by flowing 300 mL of buffer A, pH 4.0, containing 5 g/L of $ZnCl_2$. The spheroplast supernatant was loaded directly onto the column at a flow rate of 2 mL/min. After washing with 60 mL of buffer A, pH 7.5, to elute weakly bound protein, the column was eluted with a linear gradient from pH 7.5 to pH 4.0, developed over 80 min, and was finally washed with 60 mL of buffer A, pH 4.0. The active fractions were pooled and dialyzed against 50 mM potassium phosphate, pH 7.0. Approximately 250 mg of β-lactamase was recovered from a 2-L culture. β-Lactamase was found to be more than 95% pure as determined by densitometry of 15% acrylamide SDS-PAGE gels. For long-term storage, the enzyme was diluted in 50 mM KH_2PO_4 buffer, pH 7.0, at a concentration of 1 mg/mL, and was rapidly frozen in dry ice and kept at −70 °C. Under these conditions the enzyme remained fully active for several months.

Unfolding equilibrium measurements

Protein intrinsic fluorescence spectra were determined in an SLM SPF-500C spectrofluorometer using an excitation wavelength of 280 nm. The emission spectra were scanned from 310 to 480 nm. For equilibrium measurements, TEM β-lactamase at a concentration of 60 μg/mL was incubated with varying concentrations of GdmCl for 3 h. The temperature was controlled at 23 °C using a thermostated compartment and an associated water bath. The maximum difference in the fluorescence intensity of the native and denatured protein, in the presence or absence or 6 M GdmCl respectively, was detected at 345 nm (Valax & Georgiou, 1991).

Hydrophobic surface exposure to the solvent was monitored using the fluorescent probe Bis-ANS (Horowitz & Butler, 1993). TEM β-lactamase at a concentration of 60 μg/mL was equilibrated with GdmCl as above, Bis-ANS was added to a final concentration of 10 μM, and the fluorescence emission spectra were scanned from 400 and 600 nm using an excitation wavelength of 395 nm. CD spectra were recorded with a Jasco J500 spectropolarimeter with a model J-500 data processing unit. A protein concentration of 0.3 mg/mL was used for all experiments. The protein solution was equilibrated in the denaturant solution for at least 3 h prior to spectra collection.

The folding equilibria for the reduced TEM β-lactamase were monitored as described above except that all buffers were thoroughly degassed and the protein samples were equilibrated in

the presence of 5 mM dithiothreitol. Sulfhydryl titration using Ellman's reagent confirmed that the single disulfide bond in β-lactamase is completely reduced under these conditions (Valax, 1993).

Folding kinetics

TEM β-lactamase was incubated for 3 h at room temperature in 50 mM potassium phosphate buffer containing 3 M GdmCl with or without 5 mM DTT. The samples were then diluted to various final GdmCl concentrations by the addition of potassium phosphate buffer, pH 7.0, with or without DTT and GdmCl. For all experiments, the final protein concentration after dilution was 60 μg/mL. Protein folding was monitored by measuring the change in fluorescence at 345 nm using an excitation wavelength of 280 nm.

To measure the kinetics of Bis-ANS binding, unfolded TEM β-lactamase in 3 M GdmCl was diluted with buffer to different final GdmCl concentrations as above, and Bis-ANS at a final concentration of 1 μM was added at different times after the initiation of refolding. The intensity of fluorescence emission was recorded at 500 nm with an excitation wavelength of 395 nm.

Protein renaturation

Known amounts of TEM β-lactamase were lyophilized and redissolved in 50 mM potassium phosphate, pH 6.0, containing various concentrations of GdmCl in the presence or absence of 5 mM DTT, as required. The samples were dialyzed against the same solution for 3 h at room temperature in a Pierce microdialyzer model 500. Subsequently, the protein was renatured by dialyzing against phosphate buffer without GdmCl. In all experiments, the final GdmCl concentration was 0.02 M. Following renaturation, the dialysates were centrifuged at 10,000 rpm for 20 min in an Eppendorf microcentrifuge tube at 4 °C and the activity remaining in the supernatant was determined. The pellets were washed in 50 mM potassium phosphate, pH 6.0, and resuspended in the same buffer by vortexing. For all experiments the activity in the wash was less than 5% of the activity found in the supernatant immediately after dialysis. No β-lactamase activity was detected after additional washing of the aggregated pellet.

General methods

β-Lactamase activities were determined spectrophotometrically using penicillin G as the substrate (Valax, 1993). All activity data reported are the average of 3 measurements. Protein concentrations were calculated using an extinction coefficient of $\epsilon_{281} = 29,400$ M^{-1} cm^{-1} (Sigal et al., 1984).

Acknowledgments

References

Blum P, Velligan M, Lin N, Matin A. 1992. DnaK-mediated alterations in human growth hormone protein inclusion bodies. *Bio/Technology 10*:301-304.

Bowden GA, Georgiou G. 1990. Folding and aggregation of β-lactamase in the periplasmic space of *Escherichia coli*. *J Biol Chem 265*:16760–16766.

Bowden GA, Paredes AM, Georgiou G. 1991. Structure and morphology of inclusion bodies in *Escherichia coli*. *Bio/Technology 9*:725–730.

Calciano LJ, Escobar WA, Millhauser GL, Miick SM, Rubaloff J, Todd PA, Fink AL. 1993. Side-chain mobility of β-lactamase A state probed by electron spin resonance spectroscopy. *Biochemistry 32*:5644–5649.

Chalmers JJ, Kim E, Telford JN, Wong EY, Tacon WC, Shuler ML, Wilson DB. 1990. Effects of temperature on *Escherichia coli* overproducing β-lactamase or human epidermal growth factor. *Appl Environ Microbiol 56*:104–111.

Chrunyk BA, Evans J, Lillquist J, Young P, Wetzel R. 1993. Inclusion body formation and protein stability in sequence variants of interleukin 1β. *J Biol Chem 268*:18053–18061.

De Bernardez-Clark E, Georgiou G. 1991. Inclusion bodies and recovery of proteins from the aggregated state. In: Georgiou G, De Bernardez-Clark E, eds. *Protein refolding. ACS Symposium Series 470*. Washington, D.C.: American Chemical Society. pp 97–109.

De Felippis MR, Alter LA, Pekar AH, Havel HA, Brems DN. 1993. Evidence for a self-associating equilibrium intermediate during folding of human growth hormone. *Biochemistry 32*:1555–1562.

De Young LR, Fink AL, Dill K. 1993. Aggregation of globular proteins. *Acc Chem Res 26*:614–620.

Fink AL. 1994. Compact intermediate states in protein folding. In: Roy S, ed. *Sub-cellular biochemistry: Protein structure, function and engineering*. Forthcoming.

Georgiou G, Telford JN, Shuler ML, Wilson DB. 1986. Localization of inclusion bodies in *Escherichia coli* overproducing β-lactamase or alkaline phosphatase. *Appl Environ Microbiol 52*:1157–1161.

Goldberg ME, Rudolph R, Jaenicke R. 1991. A kinetic study of the competition between renaturation and aggregation during the refolding of denatured-reduced egg white lysozyme. *Biochemistry 30*:2790–2797.

Goto Y, Fink AL. 1989. Conformational states of β-lactamase: Molten globule states at acidic and alkaline pH with high salt. *Biochemistry 28*:945–952.

Horowitz PM, Butler M. 1993. Interactive intermediates are formed during the urea unfolding of rhodanese. *J Biol Chem 268*:2500–2504.

Horowitz PM, Criscimagna NL. 1986. Low concentrations of guanidium chloride expose apolar surfaces and cause differential perturbation in catalytic intermediates of rhodanese. *J Biol Chem 261*:15652–15658.

Hurle MR, Michelotti GA, Crisanti MM, Matthews CR. 1987. Characterization of a slow folding reaction for the α subunit of tryptophan synthase. *Proteins Struct Funct Genet 2*:54–63.

Jelsch C, Mourey L, Mason JM, Samana JP. 1992. Crystal structure of *Escherichia coli* TEM1 β-lactamase at 1.8 Å resolution. *Proteins Struct Funct Genet 16*:364–383.

Laminet AA, Plückthun A. 1989. The precursor of β-lactamase: Purification, properties and folding kinetics. *EMBO J 8*:1469–1477.

London J, Skrzynia C, Goldberg ME. 1974. Renaturation of *Escherichia coli* tryptophanase after exposure to 8 M urea. *Eur J Biochem 47*:409–415.

Mitraki A, Betton JM, Desmadril M, Yon JM. 1987. Quasi-irreversibility

in the unfolding–refolding transition of phosphoglycerate kinase induced by guanidine hydrochloride. *Eur J Biochem 163*:29–34.

Mitraki A, Danner M, King J, Seckler R. 1993. Temperature sensitive mutations and second site suppressor substitutions affect the folding of the P22 tailspike protein in vitro. *J Biol Chem 268*:20071–20075.

Mitraki A, Fane B, Haase Pettingell C, Sturtevant J, King J. 1991. Global suppression of protein folding defects and inclusion body formation. *Science 253*:54–58.

Mitraki A, King J. 1989. Protein folding intermediates and inclusion body formation. *Bio/Technology 7*:690–697.

Mitraki A, King J. 1992. Amino acid substitutions influencing intracellular protein folding pathways. *FEBS Lett 307*:20–25.

Oberg K, Chrunyk BA, Wetzel RB, Fink AL. 1994. Native-like secondary structure in interleukin 1β inclusion bodies by attenuated total reflectance FTIR. *Biochemistry 33*:2628–2634.

Osborn MJ, Munson R. 1976. Separation of the inner (cytoplasmic) and outer membranes of gram-negative bacteria. *Methods Enzymol 31*:642–653.

Przybycien TM, Dunn JP, Valax P, Georgiou G. 1994. Secondary structure characterization of β-lactamase inclusion bodies. *Protein Eng 7*:131–136.

Ptitsyn OB, Pain RH, Semisotnov GV, Zerovnik E, Razgulyaev OI. 1990. Evidence for a molten globule state as a general intermediate in protein folding. *FEBS Lett 262*:20–24.

Rinas U, Tsai LB, Lyons D, Fox GM, Stearns G, Fieschko J, Fenton D, Bailey JE. 1992. Cysteine to serine substitutions in basic fibroblast growth factor: Effect on inclusion body formatin and proteolytic susceptibility during in vitro refolding. *Bio/Technology 10*:435–440.

Robson B, Pain RH. 1976. The mechanism of folding of globular proteins. *Biochem J 155*:331–344.

Schein CN, Noteborn MHM. 1988. Formation of soluble recombinant proteins in *Escherichia coli* is favored by lower growth temperature. *Bio/Technology 6*:291–294.

Schultz SC, Dalbadie-McFarland G, Neitzel JJ, Richards JH. 1987. Stability of wild type and mutant RTEM-1 β-lactamases: Effect of the disulfide bond. *Proteins Struct Funct Genet 2*:290–297.

Sigal IS, DeGrado WF, Thomas BJ, Petteway SR Jr. 1984. Purification and properties of thiol β-lactamase. *J Biol Chem 259*:5327–5332.

Strynadka NC, Adachi H, Jensen SE, Johns K, Sielecki A, Betzel C, Sutoh K, James NG. 1992. Molecular structure of the acyl enzyme intermediate in β-lactam hydrolysis at 1.7 Å resolution. *Nature 359*:700–705.

Tokatlidis K, Dhurjati P, Millet J, Beguin P, Aubert JP. 1991. High activity of inclusion bodies formed in *Escherichia coli* overproducing *Clostridium thermocellum* endoglucanase D. *FEBS Lett 282*:205–208.

Valax P. 1993. In vivo and in vitro folding and aggregation of *Escherichia coli* β-lactamase [thesis]. Austin: University of Texas at Austin.

Valax P, Georgiou G. 1991. Folding and aggregation of RTEM β-lactamase. In: Georgiou G, De Bernardez-Clark E, eds. *Protein refolding. ACS Symposium Series 470*. Washington, D.C.: American Chemical Society. pp 97–109.

Valax P, Georgiou G. 1993. Molecular characterization of protein inclusion bodies in *Escherichia coli*: I. Composition. *Biotechnol Prog 9*:539–547.

Wetzel R. 1994. Mutations and off-pathway aggregation of proteins. *Trends Biotechnol 12*:193–198.

Exhibit 18

NCBI PubMed www.pubmed.gov

| All Databases | PubMed | Nucleotide | Protein | Genome | Structure | OMIM | PMC | Journals | Bool |

Search PubMed for Go Clear

Limits   Preview/Index   History   Clipboard   Details

Display Abstract   Show 20   Sort by   Send to

All: 1   Review: 0

About Entrez

Text Version

Entrez PubMed
Overview
Help | FAQ
Tutorials
New/Noteworthy
E-Utilities

PubMed Services
Journals Database
MeSH Database
Single Citation Matcher
Batch Citation Matcher
Clinical Queries
Special Queries
LinkOut
My NCBI

Related Resources
Order Documents
NLM Mobile
NLM Catalog
NLM Gateway
TOXNET
Consumer Health
Clinical Alerts
ClinicalTrials.gov
PubMed Central

1: Biotechnol Prog. 1998 Jan-Feb;14(1):47-54.   Related Articles, Links

ACS PUBLICATIONS
HIGH QUALITY HIGH IMPACT

Oxidative renaturation of hen egg-white lysozyme. Folding vs aggregation.

De Bernardez Clark E, Hevehan D, Szela S, Maachupalli-Reddy J.

Department of Chemical Engineering, Tufts University, Medford, Massachusetts 02155, USA. edeberna@tufts.edu

Since the inception of recombinant DNA technology, different strategies have been developed in the isolation, renaturation, and native disulfide bond formation of proteins produced as insoluble inclusion bodies in Escherichia coli. One of the major challenges in optimizing renaturation processes is to prevent the formation of off-pathway inactive and aggregated species. On the basis of a simplified kinetic model describing the competition between folding and aggregation, it was possible to analyze the effects of denaturant and thiol/disulfide concentrations on this competition. Although higher guanidinium chloride (GdmCl) concentrations resulted in higher renaturation yields, the folding rate was negatively affected, indicating an optimum range of GdmCl for optimum renaturation rates and yields. Similarly, higher total glutathione concentrations resulted in higher yields but decreased rates, also indicating an optimum total glutathione concentration for optimum renaturation rates and yields (6-16 mM), with an optimum ratio of reduced to oxidized glutathione between 1 and 3. To characterize the nature of aggregates, aggregation experiments were performed under different oxidizing/reducing conditions. It is shown that hydrophobic interactions between partially folded polypeptide chains are the major cause of aggregation. Aggregation is fast and aggregate concentration does not significantly increase beyond the first minute of renaturation. Under conditions which promote disulfide bonding, aggregate size, but not concentration, may increase due to disulfide bond formation, resulting in covalently bonded aggregates.

PMID: 9496669 [PubMed - indexed for MEDLINE]

Exhibit 22

[Sign In] [Rec

Pub Med
www.pubmed.gov

| All Databases | PubMed | Nucleotide | Protein | Genome | Structure | OMIM | PMC | Journals | B |

Search PubMed ⬚ for Teschke CM AND 468   Go | Clear | Save S

Limits   Preview/Index   History   Clipboard   Details

Display Abstract   Show 20   Sort by   Send to

About Entrez

Text Version

All: 1   Review: 1   ☒

Entrez PubMed
Overview
Help | FAQ
Tutorials
New/Noteworthy
E-Utilities

PubMed Services
Journals Database
MeSH Database
Single Citation Matcher
Batch Citation Matcher
Clinical Queries
Special Queries
LinkOut
My NCBI

Related Resources
Order Documents
NLM Mobile
NLM Catalog
NLM Gateway
TOXNET
Consumer Health
Clinical Alerts
ClinicalTrials.gov
PubMed Central

1: Curr Opin Biotechnol. 1992 Oct;3(5):468-73.   Related Articles, Links

Folding and assembly of oligomeric proteins in Escherichia coli.

Teschke CM, King J.

Department of Biology, Massachusetts Institute of Technology, Cambridge 02139.

High levels of expression of oligomeric proteins in heterologous systems are frequently associated with misfolding and accumulation of the polypeptides in inclusion bodies. This reflects aspects of the folding and assembly pathways of oligomeric proteins, which generally proceed from either folding intermediates or native-like metastable species that are not in their final conformation. Methods for optimizing the yield of correctly assembled oligomers are discussed.

Publication Types:
- Review

PMID: 1368931 [PubMed - indexed for MEDLINE]

Display Abstract   Show 20   Sort by   Send to

Aug 14 2006 08:07:58

Exhibit 23

NCBI Pub**M**ed
www.pubmed.gov

| All Databases | PubMed | Nucleotide | Protein | Genome | Structure | OMIM | PMC | Journals | Bool |

Search PubMed   for   Go Clear

Limits   Preview/Index   History   Clipboard   Details

Display Abstract   Show 20   Sort by   Send to

About Entrez

Text Version

All: 1   Review: 0

Entrez PubMed
Overview
Help | FAQ
Tutorials
New/Noteworthy
E-Utilities

PubMed Services
Journals Database
MeSH Database
Single Citation Matcher
Batch Citation Matcher
Clinical Queries
Special Queries
LinkOut
My NCBI

Related Resources
Order Documents
NLM Mobile
NLM Catalog
NLM Gateway
TOXNET
Consumer Health
Clinical Alerts
ClinicalTrials.gov
PubMed Central

Transient association of the first intermediate during the refolding of bovine carbonic anhydrase B.

Cleland JL, Wang DI.

Biotechnology Process Engineering Center, Department of Chemical Engineering, Cambridge, Massachusetts 02139.

Many proteins which aggregate during refolding may form transiently populated aggregated states which do not reduce the final recovery of active species. However, the transient association of a folding intermediate will result in reduced refolding rates if the dissociation process occurs slowly. Previous studies on the refolding and aggregation of bovine carbonic anhydrase B (CAB) have shown that the molten globule first intermediate on the CAB folding pathway will form dimers and trimers prior to the formation of large aggregates (Cleland, J. L.; Wang, D. I. C. Biochemistry 1990, 29, 11072-11078; Cleland, J. L.; Wang, D. I. C. In Protein Refolding; Georgiou, G., De-Bernardez-Clark, E., Eds.; ACS Symposium Series 470; American Chemical Society: Washington, DC, 1991; pp 169-179). Refolding of CAB from 5 M guanidine hydrochloride (GuHCl) was achieved at conditions ([CAB]f = 10-33 microM, [GuHCl]f = 1.0 M) which allowed complete recovery of active protein as well as the formation of a transiently populated dimer of the molten globule intermediate on the refolding pathway. A kinetic analysis of CAB refolding provided insight into the mechanism of the association phenomenon. Using the kinetic results, a model of the refolding with transient association was constructed. By adjusting a single variable, the dimer dissociation rate constant, the model prediction fit both the experimentally determined active protein and dimer concentrations. The model developed in this analysis should also be applicable to the refolding of proteins which have been observed to form aggregates during refolding. In particular, the transient association of hydrophobic folding intermediates may also occur during the refolding of other proteins.(ABSTRACT TRUNCATED AT 250 WORDS)

NCBI PubMed www.pubmed.gov

A service of the National Library of
and the National Institutes

[Sign In] [Reg

| All Databases | PubMed | Nucleotide | Protein | Genome | Structure | OMIM | PMC | Journals | B |

Search PubMed for Rudolph R AND 5572   Go Clear Save S

Limits Preview/Index History Clipboard Details

Display Abstract   Show 20 Sort by   Send to

All: 1   Review: 0

1: Biochemistry. 1979 Dec 11;18(25):5572-5.

Related Articles, Links

Reconstitution of lactic dehydrogenase. Noncovalent aggregation vs. reactivation. 2. Reactivation of irreversibly denatured aggregates.

Rudolph R, Zettlmeissl G, Jaenicke R.

Noncovalent aggregation is a side reaction in the process of reconstitution of oligomeric enzymes (e.g., lactic dehydrogenase) after preceding dissociation, denaturation, and deactivation. The aggregation product is of high molecular weight and composed of monomers which are trapped in a minium of conformational energy different from the one characterizing the native enzyme. This energy minimum is protected by a high activation energy of dissociation such that the aggregates are perfectly stable under nondenaturing conditions, and their degradation is provided only by applying strong denaturants, e.g., 6 M guanidine hydrochloride at neutral or acidic pH. The product of the slow redissolution process is the monomeric enzyme in its random configuration, which may be reactivated by diluting the denaturant under optimum conditions of reconstitution. The yield and the kinetics of reactivation of lactic dehydrogenase from pig skeletal muscle are not affected by the preceding aggregation-degradation cycle and are independent of different modes of aggregate formation (e.g., by renaturation at high enzyme concentration or heat aggregation). The kinetics of reactivation may be described by one single rate-determining bimolecular step with $k2 = 3.9 \times 10(4)$ M-1 s-1 at zero guanidine concentration. The reactivated enzyme consists of the native tetramer, characterized by enzymatic and physical properties identical with those observed for the enzyme in its initial native state.

PMID: 518856 [PubMed - indexed for MEDLINE]

Display Abstract   Show 20 Sort by   Send to

Write to the Help Desk
NCBI | NLM | NIH
Department of Health & Human Services
Privacy Statement | Freedom of Information Act | Disclaimer

http://www.ncbi.nlm.nih.gov/entrez/query.fcgi?CMD=Display&DB=pubmed   8/31/2006

NCBI PubMed www.pubmed.gov

A service of the National Library of
and the National Institutes

[Sign In] [Rec

| All Databases | PubMed | Nucleotide | Protein | Genome | Structure | OMIM | PMC | Journals | B |

Search PubMed for Fink AL AND R9   Go Clear Save S

Limits   Preview/Index   History   Clipboard   Details

Display Abstract   Show 20   Sort by   Send to

About Entrez

Text Version

All: 1   Review: 1

Entrez PubMed
Overview
Help | FAQ
Tutorials
New/Noteworthy
E-Utilities

PubMed Services
Journals Database
MeSH Database
Single Citation Matcher
Batch Citation Matcher
Clinical Queries
Special Queries
LinkOut
My NCBI

Related Resources
Order Documents
NLM Mobile
NLM Catalog
NLM Gateway
TOXNET
Consumer Health
Clinical Alerts
ClinicalTrials.gov
PubMed Central

1: Fold Des. 1998;3(1):R9-23.

Related Articles, Links

Protein aggregation: folding aggregates, inclusion bodies and amyloid.

Fink AL.

Department of Chemistry and Biochemistry, University of California, Santa
Cruz 95064, USA. enzyme@cats.ucsc.edu

Aggregation results in the formation of inclusion bodies, amyloid fibrils and
folding aggregates. Substantial data support the hypothesis that partially
folded intermediates are key precursors to aggregates, that aggregation
involves specific intermolecular interactions and that most aggregates
involve beta sheets.

Publication Types:
- Review

PMID: 9502314 [PubMed - indexed for MEDLINE]

Display Abstract   Show 20   Sort by   Send to

Aug 14 2006 08:07:58

Exhibit 26

[Sign In] [Rec

| All Databases | PubMed | Nucleotide | Protein | Genome | Structure | OMIM | PMC | Journals | B |

Search PubMed ⬚ for Oberg K AND 2628   Go Clear Save Sᴇ

Limits   Preview/Index   History   Clipboard   Details

Display | Abstract   Show 20 Sort by   Send to

All: 1   Review: 0 ☒

About Entrez

Text Version

Entrez PubMed
Overview
Help | FAQ
Tutorials
New/Noteworthy
E-Utilities

PubMed Services
Journals Database
MeSH Database
Single Citation Matcher
Batch Citation Matcher
Clinical Queries
Special Queries
LinkOut
My NCBI

Related Resources
Order Documents
NLM Mobile
NLM Catalog
NLM Gateway
TOXNET
Consumer Health
Clinical Alerts
ClinicalTrials.gov
PubMed Central

1: Biochemistry. 1994 Mar 8;33(9):2628-34.   Related Articles, Links

Nativelike secondary structure in interleukin-1 beta inclusion bodies by attenuated total reflectance FTIR.

Oberg K, Chrunyk BA, Wetzel R, Fink AL.

Department of Chemistry and Biochemistry, University of California, Santa Cruz 95064.

Attenuated total reflectance FTIR has been used to study the structure of human interleukin-1 beta in inclusion bodies (IBs) and other aggregated forms. The secondary structure composition of native wild-type IL-1 beta determined by FTIR is in excellent agreement with that previously determined by crystallography and NMR: 52% beta-sheet, 25% loop/irregular structure, and 23% turn. Remarkably, IL-1 beta inclusion bodies exhibit secondary structural composition very similar to that of the native protein. The results indicate that the IBs form from a folding intermediate that has nativelike secondary structure. The secondary structure content of aggregated IL-1 beta, formed either in refolding or by thermal denaturation, was identical within experimental error to that of the IB, indicating that these aggregates were formed from intermediates with structures similar to that of the inclusion body.

PMID: 8117725 [PubMed - indexed for MEDLINE]

Display | Abstract   Show 20 Sort by   Send to

Aug 14 2006 08:07:58

Exhibit 27

NCBI **PubMed**
www.pubmed.gov

| All Databases | PubMed | Nucleotide | Protein | Genome | Structure | OMIM | PMC | Journals | B |

Search PubMed ___ for Kendrick BS AND 1069 ___ Go | Clear | Save S<

Limits Preview/Index History Clipboard Details

Display | Abstract ___ Show | 20 ___ Sort by ___ Send to

All: 1   Review: 0

About Entrez

Text Version

Entrez PubMed
Overview
Help | FAQ
Tutorials
New/Noteworthy
E-Utilities

PubMed Services
Journals Database
MeSH Database
Single Citation Matcher
Batch Citation Matcher
Clinical Queries
Special Queries
LinkOut
My NCBI

Related Resources
Order Documents
NLM Mobile
NLM Catalog
NLM Gateway
TOXNET
Consumer Health
Clinical Alerts
ClinicalTrials.gov
PubMed Central

1: <u>J Pharm Sci.</u> 1998 Sep;87(9):1069-76.   Related Articles, Links

FULL TEXT AVAILABLE ONLINE
interScience

Aggregation of recombinant human interferon gamma: kinetics and structural transitions.

<u>Kendrick BS</u>, <u>Cleland JL</u>, <u>Lam X</u>, <u>Nguyen T</u>, <u>Randolph TW</u>, <u>Manning MC</u>, <u>Carpenter JF</u>.

Department of Pharmaceutical Sciences, University of Colorado Health Sciences Center, Campus Box C238, Denver, Colorado 80262, USA.

Protein aggregation is a complex phenomenon that can occur in vitro and in vivo, usually resulting in the loss of the protein's biological activity. While many aggregation studies focus on a mechanism due to a specific stress, this study focuses on the general nature of aggregation. Recombinant human interferon-gamma (rhIFN-gamma) provides an ideal model for studying protein aggregation, as it has a tendency to aggregate under mild denaturing stresses (low denaturant concentration, temperature below the Tm, and below pH 5). All of the aggregates induced by these stresses have a similar structure (high in intermolecular beta-sheet content and a large loss of alpha-helix) as determined by infrared and circular dichroism spectroscopy. Thermally induced and denaturant-induced aggregation processes follow first-order kinetics under the conditions of this study. Spectroscopic and kinetic data suggest that rhIFN-gamma aggregates through an intermediate form possessing a large amount of residual secondary structure. In contrast to the aggregates formed under denaturing stresses, the salted-out protein has a remarkably nativelike secondary structure.

PMID: 9724556 [PubMed - indexed for MEDLINE]

Display | Abstract ___ Show | 20 ___ Sort by ___ Send to

Exhibit 28

Chaperone-Mediated Protein Folding

ANTHONY L. FINK

Department of Chemistry and Biochemistry, The University of California, Santa Cruz, California

Fink, Anthony L. Chaperone-Mediated Protein Folding. *Physiol. Rev.* 79: 425–449, 1999.–The folding of most newly synthesized proteins in the cell requires the interaction of a variety of protein cofactors known as molecular chaperones. These molecules recognize and bind to nascent polypeptide chains and partially folded intermediates of proteins, preventing their aggregation and misfolding. There are several families of chaperones; those most involved in protein folding are the 40-kDa heat shock protein (HSP40; DnaJ), 60-kDa heat shock protein (HSP60; GroEL), and 70-kDa heat shock protein (HSP70; DnaK) families. The availability of high-resolution structures has facilitated a more detailed understanding of the complex chaperone machinery and mechanisms, including the ATP-dependent reaction cycles of the GroEL and HSP70 chaperones. For both of these chaperones, the binding of ATP triggers a critical conformational change leading to release of the bound substrate protein. Whereas the main role of the HSP70/HSP40 chaperone system is to minimize aggregation of newly synthesized proteins, the HSP60 chaperones also facilitate the actual folding process by providing a secluded environment for individual folding molecules and may also promote the unfolding and refolding of misfolded intermediates.

I. INTRODUCTION

The basic paradigm of molecular chaperones is that they recognize and selectively bind nonnative, but not native, proteins to form relatively stable complexes (48). In most cases, the complexes are dissociated by the binding and hydrolysis of ATP. In addition, there are "specific" molecular chaperones that typically are involved in the assembly of particular multiprotein complexes. Molecular chaperones comprise several highly conserved families of unrelated proteins; many chaperones are also heat shock (stress) proteins. The ubiquitous role of molecular chaperones continues to unfold with more discoveries each year. In the context of in vivo protein folding, chaperones prevent irreversible aggregation of nonnative conformations and keep proteins on the productive folding pathway. In addition, they may maintain newly synthesized proteins in an unfolded conformation suitable for trans-

location across membranes and bind to nonnative proteins during cellular stress, among other functions. It is likely that most, if not all, cellular proteins will interact with a chaperone at some stage of their lifetime.

The focus of this review is on the functional contribution of chaperones to in vivo protein folding and assembly, especially those chaperones that are promiscuous, in that they show broad specificity for binding nonnative proteins. In addition to several specialized review articles on chaperones, e.g., References 11, 49, 50, 53, 76, 77, 90, 144, 164, 190, 191, 226, 228, 252, there have been two recent monographs published on the subject (60, 150). This review is of necessity selective; the main goal is to furnish an up-to-date overview of the role of the major molecular chaperones involved in protein folding. In view of the vast array of literature on molecular chaperones, and the ease of access to literature citations using the Internet, this article should not be viewed as exhaustive.

Why do we need chaperones? After all, a basic tenet of in vitro protein folding has been the seminal work of Anfinsen (2), which demonstrated that formation of the native protein from the unfolded state is a spontaneous process determined by the global free energy minimum. The results indicated that the native state of small globular proteins is determined by their amino acid sequence. However, the experimental conditions necessary to successfully fold many proteins, especially larger ones, in vitro, are very constrictive, usually requiring very low protein concentration and long incubation times and are usually unphysiological (e.g., relatively low temperatures). In contrast, most cells operate at ambient or homeothermically set temperatures (e.g., 37°C) where the hydrophobic effect will be stronger and thus protein denaturation and aggregation will be bigger problems, and the time-frame available for successful folding is short. Thus there is the need for additional factors for the successful folding of many proteins in vivo. When one considers the crowded cellular environment within a cell, it becomes clear that in vitro folding experiments at low protein concentrations are poor models for what happens in the cell, where a newly synthesized protein is in an environment with little or no "free" water, very high concentrations of other proteins and metabolites, and typically membranes, cytoskeletal elements, and other cellular components. Thus the need for chaperones *1)* to prevent aggregation and misfolding during the folding of newly synthesized chains, *2)* to prevent nonproductive interactions with other cell components, *3)* to direct the assembly of larger proteins and multiprotein complexes, and *4)* during exposure to stresses that cause previously folded proteins to unfold, becomes evident. In the few cases where folding has been studied both in vivo and in vitro, it appears that the folding pathways are similar (148, 190).

Cells have solved the problem of misfolding and aggregation, to a considerable extent at least, through the participation of molecular chaperones in the in vivo folding process. Many investigations in the past few years have confirmed the critical role of molecular chaperones in protein folding in the cell. Although much has been learned about the function of chaperones in protein folding, and the general outline of the process is thought to be understood, there are still many important unresolved issues, and new chaperones and cochaperones are still being discovered.

The molecular chaperones involved in the folding of newly synthesized proteins recognize nonnative substrate proteins predominantly via their exposed hydrophobic residues. The major chaperone classes are 40-kDa heat shock protein (HSP40; the DnaJ family), 60-kDa heat shock protein [HSP60; including GroEL and the T-complex polypeptide 1 (TCP-1) ring complexes], 70-kDa heat shock protein (HSP70), and 90-kDa heat shock protein (HSP90). All these chaperones can prevent the aggregation of at least some unfolded proteins. For HSP60 and HSP70, their activity is modulated by the binding and hydrolysis of ATP. The HSP70 (DnaK in *Escherichia coli*) bind to nascent polypeptide chains on ribosomes, preventing their premature folding, misfolding, or aggregation, as well as to newly synthesized proteins in the process of translocation from the cytosol into the mitochondria and the endoplasmic reticulum (ER). The HSP70 are regulated by HSP40 (DnaJ or its homologs). The HSP60 are large oligomeric ring-shaped proteins known as chaperonins that bind partially folded intermediates, preventing their aggregation, and facilitating their folding and assembly. This family is composed of GroEL-like proteins in eubacteria, mitochondria, and chloroplasts and the TCP-1 (CCT or TRiC) family in the eukaryotic cytosol and the archaea. The HSP60 (GroEL in *E. coli*) are large, usually tetradecameric proteins with a central cavity in which nonnative protein structures bind. The HSP60 are found in all biological compartments except the ER. The HSP60 are regulated by a cochaperone, chaperonin 10 (cpn10) (GroES in *E. coli*). In addition to preventing aggregation, it has been suggested that HSP60 may permit misfolded structures to unfold and refold. The HSP90 are associated with a number of proteins and play important roles in modulating their activity, most notably the steroid receptors. A number of other proteins involved in the folding of many newly synthesized proteins are often considered to be molecular chaperones; these include protein disulfide isomerase and peptidyl prolyl isomerase, which catalyze the rearrangement of disulfide bonds and isomerization of peptide bonds around Pro residues, respectively, and are perhaps better considered to be folding catalysts rather than chaperones. As mentioned previously, there are also a number of more specific chaperones that are involved in the folding/assembly of

only one, or a very limited number, of particular substrate proteins.

Chaperones are catalysts in the sense that they transiently interact with their substrate proteins but are not present in the final folded product, and also in that they increase the yield of folded protein. However, there is no good evidence that they actually enhance the spontaneous rate of folding itself, although they may appear to do this by minimizing off-pathway reactions.

A brief perusal of the literature demonstrates that our knowledge of molecular chaperones is growing at an enormous pace. To put these new discoveries in context, a few more general points are worthy of note. Although in many respects the field of molecular chaperones can now be considered a mature one, in that it has passed its first decade of life, and the broad outlines, at least, are reasonably well established, there are still many outstanding questions. Furthermore, there are many areas of considerable controversy, and many of these relate to fundamental questions. For example, we do not yet know with certainty whether all newly synthesized proteins interact with chaperones, although it is likely that they do. We certainly do not know much about all the interactions between the various chaperones themselves, as well as with newly synthesized proteins or other chaperone target proteins. As discussed in this review, there are significant controversies concerning which chaperones interact first with nascent polypeptides, and even whether all nascent polypeptides interact with chaperones. The GroEL family of chaperones has been intensively studied, especially in the context of in vitro protein folding, yet it is not clear just how important a role this family (the cpn60 chaperonins and their TCP-1 eukaryotic homologs) play in the folding of most proteins in the cell. We are only now beginning to get a picture of the apparently ubiquitous role of the HSP90 family in many critical processes in the cell, especially those involving protein-protein interactions. Recently, several new "accessory" proteins have been discovered, which apparently act as "cochaperones." Again, their significance to protein folding and denaturation in the cell in general is unclear at the present time; they may be highly specialized or may turn out to be critical in a broad range of cellular processes involving chaperones. Although some of the chaperones clearly are important in preventing protein aggregation, there is as yet no good evidence that chaperones play a role significant in the opposite side of this equation, namely, in solubilizing protein aggregates, although it would seem likely that this may in fact be a function of some chaperones. Even at the level of the specific mechanisms of chaperone function, there are many controversial aspects, and those in the field know there have been some quite rancorous discussions over competing mechanisms. Thus the molecular chaperone field is one in which there are still many outstanding questions, including some quite

fundamental ones. Consequently, chaperone scientists are likely to remain busy for a long time to come.

We begin with a brief review of the current understanding of in vitro protein folding and the potential for aggregation and misfolding.

II. IN VITRO PROTEIN FOLDING

Despite the fact that in vitro folding may not exactly mimic folding in the cell, it is minimally a good model for in vivo protein folding and has the critical advantage that a very wide variety of biophysical methods may be applied to provide a detailed knowledge of the folding pathway, kinetics, and energetics. Significant increases in our understanding of the folding process have occurred in the past few years, especially through the application of sophisticated new techniques, and these have been summarized in recent reviews (28, 29, 43, 44, 51, 56, 57, 177, 186, 255, 267). Both in vivo and in vitro, proteins fold remarkably rapidly, indicating that the folding pathway is directed in some way. Many studies have revealed intermediates during in vitro protein folding experiments; it is not clear, and is very difficult to establish experimentally, whether these are on- or off-pathway species. Although it is becoming apparent that in some cases these may be off-pathway species (208), some appear to be true intermediates on the productive folding pathway, consistent with rugged energy landscapes (248).

Small proteins may, under appropriate conditions, fold to the native state within a few tens of milliseconds with no detectable intermediates (177, 210). Such folding is consistent with smooth funnel energy landscape models (248), i.e., no intermediates, but could also reflect very fast folding with intermediates of sufficiently short lifetimes that they are not detected by current methods (44). However, for many systems there is substantial experimental data to support the presence of partially folded intermediates during folding. Although stopped-flow circular dichroism kinetics investigations reveal substantial secondary structure formation within a few milliseconds of the initiation of folding, most proteins take much longer to achieve the native state (seconds or longer).

The earliest stages of folding involve hydrophobic collapse to a relatively compact state and formation of metastable secondary structure. It is not clear if collapse or secondary structure occur simultaneously or if one precedes the other. It is most likely that both proceed concurrently. Certainly secondary structural units may be formed on a microsecond time scale (24). There is no conclusive data yet available on how fast the collapse occurs.

The nature of this initial collapsed state will vary depending on the conditions and the particular protein, but in general, it will consist of a very large number of

substates. Further condensation will lead to one or more particularly stable intermediates; again depending on the particular protein, the intermediate(s) will have regions of unique structure, especially in terms of the compactness, amount of secondary structure, and topology. It is very likely that in most cases these intermediates will consist of a core of nativelike structure with the remainder of the protein in varying degrees of disorder. Regions of the nonordered chain are probably flickering in and out of their nativelike secondary structure conformation. At least some proteins fold via a hierarchical path in which additional structural units coalesce to an initially formed core with nativelike structure (61).

It is now clear, based on investigations of transient and equilibrium intermediates in vitro, that partially folded intermediates, as found with newly synthesized proteins in the cell, are particularly prone to aggregate, probably via specific intermolecular interactions between hydrophobic surfaces of structural subunits (59, 255). The intermediates are more prone to aggregate than the unfolded state because in the latter the hydrophobic side chains are scattered relatively randomly in many small hydrophobic regions, whereas in the partially folded intermediates, there will be large patches of contiguous surface hydrophobicity that will have a much stronger propensity for aggregation. The tendency of partially folded intermediates to associate or aggregate is exacerbated as the protein concentration increases. The growing recognition of the critical importance of protein aggregation has resulted in a number of reviews (42, 59, 112, 253–255).

A. Molecular Chaperones and Protein Aggregation

Both in vivo and in vitro the transition of a protein from the unfolded to folded state frequently results in the formation of partially folded intermediate states that have a very strong propensity to aggregate. In vivo this may lead to formation of inclusion bodies, especially when overexpression occurs. Members of the HSP60 and HSP70 molecular chaperone families seem to be most directly, and most generally, involved in preventing this. Current understanding of the role of HSP70 in protein folding suggests that the chaperone sequesters the unfolded or partially folded protein, thereby preventing its aggregation, but does not actively participate in the folding process; subsequent binding of ATP leads to release of the substrate protein in a nonnative conformation (144, 146, 166, 167). The *E. coli* HSP60 chaperone GroEL and its eukaryotic homologs facilitate protein folding by binding partially folded intermediates (or partially folded domains of large multidomain proteins) in their large central cavity (see sect. vB). Folding can thus occur in a situation where aggregation is precluded (144, 229). The general outline is summarized in Figure 1.
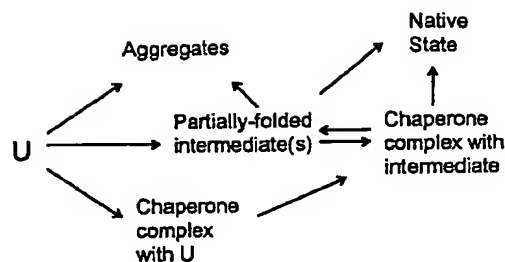

FIG. 1. General outline of chaperone-mediated protein folding in a cell. U represents nascent polypeptide or newly synthesized protein. Chaperones include 40-, 60-, and 70-kDa heat shock proteins, protein disulfide isomerase, and peptidyl prolyl isomerase or trigger factor. For multisubunit proteins, the situation is more complex and not yet well understood.

It is likely that a significant factor in the formation of in vivo aggregates, such as inclusion bodies, is a lack of available molecular chaperones, usually due to either the rapid rate of protein synthesis, the formation of long-lived folding intermediates, or a combination of both. Either situation could lead to saturation of the available chaperones. The longer a protein takes to fold spontaneously, the longer it is likely to remain associated with the HSP60 and HSP70 chaperones. Some proteins fold fast and may have partially folded intermediates that have little propensity to aggregate, thus requiring little or no chaperone assistance and little tendency to form inclusion bodies.

Several experiments have been conducted in which overexpression of various combinations of the DnaK and GroEL chaperone systems decreases the amount of aggregation (8, 72, 81, 134, 229). For example, newly synthesized proteins in *E. coli* were shown to aggregate extensively when the *rpoH* mutation was present (81). This mutation in the RNA polymerase σ^{32}-subunit, which is responsible for heat shock promotor recognition, leads to a lack of heat shock proteins. Although growth is normal at 30°C, on elevating the temperature to 42°C, the cell is unable to produce sufficient chaperones and massive aggregation is observed. Overproduction of either GroEL and GroES, or DnaK and DnaJ, significantly decreases the aggregation at 42°C. If overexpressed together, the four chaperones are able to suppress most of the aggregation. The data suggest that the GroEL/GroES and the DnaK/DnaJ chaperone systems have complementary functions in the folding and assembly of most proteins. In addition, for in vitro aggregating systems, the presence of various chaperones increases the yield of soluble or native protein (16, 18, 97, 221). There have been conflicting reports as to whether the DnaK or GroEL systems, individually or together, yield the optimal amount of renaturation. It appears that in some cases all the chaperones are required for maximal suppression of aggregation, whereas in others either the DnaK system alone, or the GroEL system alone, was effective (229). It

is possible that the two systems interact at different stages of folding, and thus different results may be observed depending on the particular system (16).

III. MOLECULAR CHAPERONES INVOLVED IN IN VIVO PROTEIN FOLDING

The major classes of general chaperones are the HSP40, HSP60, HSP70, HSP90, 100-kDa heat shock protein (HSP100), and the small heat shock proteins. Recent investigations have shown that not only do the major classes of chaperones often function with protein cofactors, but direct interactions between members of the HSP40, HSP70, and HSP90 families may be frequent. This section provides a brief description of the main families of molecular chaperones involved in protein folding in the cell.

A. Small Heat Shock Proteins and α-Crystallins

The small heat shock protein (HSP) and α-crystallin family consists of 12- to 43-kDa proteins that assemble into large multimeric structures and contain a conserved COOH-terminal region termed the α-crystallin domain. Many of the small HSP are produced only under stress conditions. They have been shown to function in vitro as chaperones by preventing protein aggregation in an ATP-independent manner. Several recent reviews have been published (19, 47, 113, 197). The role of small HSP in protein folding in vivo is unclear, but it seems unlikely that they are major players; this probably reflects the fact that release of bound, denatured proteins from the small heat shock proteins is very slow or nonexistent. For the α-crystallins in the eye lens, a major role is to bind denatured proteins and prevent their aggregation (which would result in cataracts). The small HSP bind denatured proteins tightly, but there is little evidence at present that they normally release the bound material subsequently. It has been proposed that their major function may be in times of stress when they bind denatured proteins and prevent their aggregation. Subsequently, when the stress is removed, these complexes may provide a reservoir for the HSP70 chaperone machinery to renature the bound proteins (47). The small HSP exhibit high affinity for partially folded intermediates but show no apparent substrate specificity and are only functional in the oligomeric form (131). Little is known about the mechanism of action of the small HSP; it has been suggested that the substrate protein coats the outside of the large chaperone multimer (133) and that hydrophobic interactions are critical in substrate binding. Several models have been proposed for the quaternary structure of the small HSP, but no consensus exists. A model in which small HSP prevent protein aggregation and may facilitate substrate refolding in con-

junction with other molecular chaperones has recently been proposed (133).

B. HSP40 Family

The HSP40 or DnaJ family consists of over 100 members, defined by the presence of a highly conserved J domain of ~78 residues (DnaJ from *E. coli* has 376 amino acids) (131). Proteins in this family typically consist of several domains, e.g., DnaJ contains at least four conserved regions representing potential functional domains (the J domain, which is linked by a Gly/Phe-rich region to a domain of unknown function, followed by a zinc-finger region, and ending with the COOH-terminal domain, also of unknown function). Much variability is seen in the non-J domains of members of this family. The best studied examples are DnaJ from *E. coli* and several homologs from yeast, such as Mdj1 and Ydj1 (33, 34, 189). The best defined role thus far for the HSP40 is as a cochaperone for HSP70; however, even this function is not well understood, and there is evidence to indicate that DnaJ and other members of the HSP40 family are chaperones in their own right, binding to at least some unfolded proteins and nascent chains (94). The details of the putative role of DnaJ in protein folding are described in sections IV and V. In *E. coli*, DnaK, DnaJ, and GrpE cooperate synergistically in a variety of biological functions, including protein folding. The properties of DnaJ and its homologs have been reviewed previously (23, 34, 131, 260).

Little is known about the structural features of DnaJ that are involved in its interaction with DnaK and unfolded proteins. Analysis of DnaJ fragments showed that both the NH₂-terminal J domain and the adjacent glycine/phenylalanine-rich region are required for interactions with DnaK (117) and to stimulate the ATPase activity of DnaK (220). The G/F motif of DnaJ is also involved in modulating the substrate binding activity of DnaK (246). However, only complete DnaJ is functional with DnaK and GrpE in refolding denatured firefly luciferase. Binding experiments and cross-linking studies indicate that the zinc fingerlike domain is required for DnaJ to bind to nonnative proteins (220).

Nuclear magnetic resonance spectroscopy has been used to determine the three-dimensional structure of the J domain in DnaJ from *E. coli* and humans (101, 181, 222). The structure is dominated by two long helices, with a hydrophobic core of highly conserved side chains. The residues believed responsible for the specificity of the interaction between DnaJ and its homologs with their corresponding HSP70 partners comprise a conserved His-Pro-Asp sequence that extends out from the core of the structure (171, 181). A peptide containing this sequence inhibited the Ydj1 stimulation of HSP70 ATPase activity but did not prevent binding of nonnative substrate pro-

teins, indicating that DnaJ interacts with HSP70 at a site distinct from the peptide binding site (238). The adjacent Gly/Phe-rich domain in DnaJ is disordered and flexible in solution (222).

The major effect of DnaJ on the functional cycle of DnaK is the significant stimulation of the ATPase rate-limiting step, γ-phosphate cleavage, leading to stabilization of DnaK-ADP-substrate protein complexes (146). Both prokaryotic and eukaryotic forms of HSP40 interact with HSP70 in the presence of ATP to suppress protein aggregation (32). It has been proposed that HSP40 is required for the efficient binding of substrate protein to HSP70 through the stimulation of its ATPase activity (see sect. vA) (147).

It has been suggested DnaJ acts directly as a molecular chaperone in that it binds to certain denatured substrate proteins such as firefly luciferase (130, 220, 221), and even some specific folded proteins such as the σ^{32}-heat shock transcription factor or the λP DNA replication protein, but not "normal" native proteins (41, 262). However, DnaJ binds to σ^{32} at a different site than that to which DnaK binds. The yeast DnaJ homolog Ydj1 was found to bind to denatured rhodanese but not unfolded reduced carboxymethylated α-lactalbumin (32, 35). As discussed in section IV, DnaJ or HSP40 has been proposed to bind to nascent polypeptides to prevent their premature folding and to target HSP70 to them (70). However, unambiguous data to support this role are scant. In yeast, DnaJ and its homologs are required not only for protein folding but also for selective ubiquitin-dependent degradation of abnormally folded proteins (132).

Significant specificity in the interactions between members of the HSP70, DnaJ, and GrpE families has been observed (40). As noted, the interaction between a given HSP70 and its interacting DnaJ is determined by the J domain (198). Recently, evidence for interactions between DnaJ homologs and HSP90 have been reported (118). It has also been suggested that DnaJ possesses an active dithiol/disulfide group and may catalyze protein disulfide formation, reduction, and isomerization (38).

C. HSP60 Family

Under the rubric of the HSP60 or chaperonin family, we consider both the GroEL and TCP-1 ring complex families. Unfortunately, different research groups have used different names for the TCP-1 ring complex, e.g., TRiC (for TCP-1 ring complex) and CCT (for chaperonin containing TCP-1). Other members include the Rubisco subunit binding protein and thermophilic factor 55 from archaea. GroEL and its homologs are found in prokaryotes, chloroplasts, and mitochondria, whereas TCP-1 and its homologs are found in the eukaryotic cytosol. Many of the HSP60 chaperones are also known as chap-

eronins (cpn60) and are ring-shaped oligomeric protein complexes with a large central cavity in which nonnative proteins can bind. In bacteria, at least, HSP60 require a cochaperonin, GroES (cpn10), for full function. The term *chaperonin* was originally coined by Ellis (48) to refer to non-heat-induced HSP60.

GroEL is probably the most studied of all molecular chaperones; in combination with its cochaperonin GroES and ATP, it facilitates protein folding, not only by preventing aggregation but also by simultaneously allowing partially folded intermediates to fold in an environment conducive to stabilizing the native state. It has been suggested that GroEL may also function by unfolding misfolded states so as to allow their productive refolding (268, 269). Members of the HSP60 family are also involved in the assembly of large multiprotein complexes such as Rubisco (27, 243). The availability of a high-resolution crystallographic structure, in conjunction with mutagenesis studies, has helped in the elucidation of the details of the reaction cycle (see sect. vB). However, there are still many points of controversy, reflecting the complexity of the mechanism of this large chaperone. Recent reviews include References 53, 105, 108, 144.

The structure of the *E. coli* chaperonin GroEL has been solved by X-ray crystallography (9, 12, 263) and electron microscopy (196) and consists of 14 identical subunits in two stacked heptameric rings, each containing a central cavity. Substantial structural information about GroEL, GroES, and related chaperonins is available from the chaperonin web home page: http://bioc09.uthscsa.edu/~seale/Chap/struc.html. Each subunit consists of three domains: the equatorial, the intermediate, and the apical. The latter, forming the mouth of the central cavity, undergoes major conformational changes on binding of ATP and the cochaperonin GroES, which lead to substantial changes in the hydrophobic nature of the cavity (263) (Fig. 2). In particular, the relatively hydrophobic cavity lining to which the unfolded substrate protein binds before GroES binding becomes much more polar, coincident with a substantial increase in the size of the cavity. The hydrophobic polypeptide-binding site on the cavity-lining surface of the apical domain was identified with the help of various mutants (54). These same residues are also essential for binding of the cochaperonin GroES, which is required for productive polypeptide release.

The identity of amino acid residues at the nucleotide-binding sites of GroEL/GroES was determined by photoaffinity labeling with 2-azido-ATP (13). The labeled site is located at the GroEL/GroEL subunit interface, and labeling of the cochaperonin GroES occurred through a conserved proline. The 2.4-Å crystal structure of the bacterial chaperonin GroEL complexed with adenosine 5'-O-(3-thiotriphosphate) bound to each subunit shows that ATP binds in a pocket with a unique nucleotide-binding
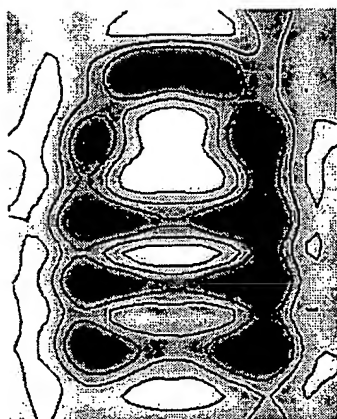
FIG. 2. Structure of GroEL/GroES based on electron diffraction. A cross section through a stacked GroES/GroEL/GroEL unit is shown. Main features starting at top are GroES; enlarged cavity; boundary between stacked GroEL units, flanked by equatorial domains; and smaller cavity, with apical domain pointing inward. Major change in cavity size upon binding GroES is clearly visible. [From Chen et al. (26).]

motif, whose primary sequence is highly conserved among chaperonins (9).

The 45-Å-diameter cavity in GroEL is large enough to accommodate proteins of 40–50 kDa and, as noted, is larger when capped by the GroES heptamer. Conformational changes are observed on binding nucleotides or GroES. The hydrophobic nature of the central cavity in GroEL (in the absence of the cochaperonin) presumably accounts for the lack of affinity for native proteins. GroES enhances the cooperativity of ATP binding and hydrolysis by GroEL and is necessary for the release and folding of many GroEL substrates. The crystallographic structure of GroES is known to high resolution (110). GroES has a highly mobile and accessible polypeptide loop whose mobility and accessibility are lost upon formation of the GroES/GroEL complex (128, 129).

The TCP-1 is a heteroligomeric 970-kDa complex containing several structurally related subunits of 52–65 kDa found in the eukaryotic cytosol. These are assembled into a ring complex that resembles the GroEL double ring (69, 121, 187). In vitro, the TCP-1 ring complex appears to function independently of a small cochaperonin protein such as GroES. Thus far, TCP-1 complexes have been shown to be involved in the folding of very few proteins in the eukaryotic cytosol.

The major difference between TCP-1 complexes and GroEL is the heteroligomeric nature of the TCP-1 ring complex; at least eight subunit species that are encoded by unique genes are known (216). The genes are calculated to have diverged around the starting point of the eukaryotic lineage and share ~30% amino acid identity. It has been proposed that this complexity may have evolved to cope with the folding and assembly of complex proteins in eukaryotic cells (122). Although each TCP-1 sub-

unit is highly diverged from each other, individually they are quite homologous, suggesting that each subunit has a specific, independent function (30a,121).

D. HSP70 Family

The HSP70 are a family of molecular chaperones that are involved in protein folding and several other cellular functions and that exhibit weak ATPase activity. The HSP70 chaperones are composed of two major functional domains. The NH_2-terminal, highly conserved ATPase domain binds ADP and ATP very tightly (in the presence of Mg^{2+} and K^+) and hydrolyzes ATP, whereas the COOH-terminal domain is required for polypeptide binding. Cooperation of both domains is needed for protein folding. Several recent reviews summarize the role of HSP70 molecular chaperones in protein folding (58, 75, 83, 90, 100, 144). Many of the functions of the E. coli HSP70, DnaK, require two cofactors, DnaJ (see sect. mB) and GrpE (see sect. mJ). The majority of in vitro studies on HSP70 have been with DnaK.

The HSP70 family is very large, with most organisms having multiple members; most eukaryotes have at least a dozen or more different HSP70, found in a variety of cellular compartments. Some of the better known mammalian members are HSC70 (or HSP73), the constitutive cytosolic member; HSP70 (or HSP72), the stress-induced cytosolic form; BiP (or Grp78), the ER form; and mHSP70 (or mito-HSP70, or Grp75), the mitochondrial form. In yeast the homologs of HSC70 and BiP are known as Ssa1–4 and Kar2. In E. coli, the major form of HSP70 is DnaK. Here we will use the term HSP70 to refer to any member of the family.

The crystallographic structures of the bovine HSC70 ATPase domain, the DnaK peptide-binding domain complexed with a peptide substrate, and most recently the human HSP70 ATPase domain have been determined (63, 214, 272). The ATPase domain, which is structurally similar to actin and hexokinase, consists of four smaller domains forming two lobes with a deep cleft within which the MgATP and MgADP bind. The structure of the peptide-binding domain consists of a β-sandwich subdomain followed by α-helical segments. The peptide is bound to DnaK in an extended conformation through a channel defined by loops from the β-sandwich. An α-helical domain (the flap or latch) is believed to stabilize the complex but does not contact the peptide directly. Only five residues of the substrate protein make significant contacts with HSP70, explaining the previously observed specificity for short, hydrophobic peptides, with a strong preference for hydrophobic residues such as Leu in the central region and a strong unfavorable interaction with negatively charged residues (7, 64, 80, 225). A model in which the flap over the substrate binding pocket could be

in either an open conformation (to allow entry and egress of substrates) or closed conformation (to form a stable complex) has been suggested to account for the high- and low-affinity states of HSP70 (272).

Recently, the substrate specificity of DnaK has been mapped out in detail by screening an immobilized peptide library (192), following up on earlier peptide-scanning experiments (7). DnaK binding sites in protein sequences occurred statistically every 36 residues. In the folded proteins, these sites are mostly buried, and the majority are found in β-sheets. The binding motif consists of a hydrophobic core of four to five residues enriched particularly in Leu, but also in Ile, Val, Phe, and Tyr, and two flanking regions enriched in basic residues. Acidic residues are excluded from the core and disfavored in flanking regions. On the basis of these data, an algorithm was established that predicts DnaK binding sites in protein sequences with high accuracy (192).

The HSP70 preferentially bind unfolded or partially folded proteins and do not bind normal native proteins (although there are a few specific interactions with proteins in their native states, such as clathrin and σ^{32}). It is likely that only some newly synthesized proteins require the assistance of chaperones. In coimmunoprecipitation studies with anti-HSP70 antibodies and pulse-chase labeling, it was observed that smaller proteins were disproportionately absent, suggesting that they may fold more rapidly, either with or without the assistance of HSP70 (5).

In fact, there is some evidence to support the notion that HSP70 may not interact with short-lived partially folded intermediates (218). The HSP70 inhibits the refolding of the mitochondrial isozyme of aspartate aminotransferase (AAT), but not the cytosolic homolog. This has been attributed to HSP70 binding to a long-lived early folding intermediate in the folding of mitochondrial AAT, for which the analogous cytosolic isozyme intermediate is shorter lived and rapidly transforms to a more nativelike species that does not bind to HSP70 (3). Because there will always be a kinetic competition between spontaneous folding and chaperone binding, intermediates with shorter lifetimes than that required for binding to HSP70 would not form a complex with the chaperone (Fig. 3).

The rapid binding kinetics for substrate proteins to DnaK-ATP (199) suggest that ATP-bound DnaK is the primary form initiating interaction with substrates for chaperone activity. The resulting DnaK-ATP-substrate complexes, however, are also characterized by rapid dissociation of bound substrate but can be stabilized by hydrolysis of the ATP (stimulated to a small extent by the substrate itself, or to a large extent by DnaJ; Ref. 146). The ATP-induced protein-HSP70 complex dissociation results from a conformational change induced in HSP70 by ATP binding. This conformational change decreases the affinity of HSP70 for nonnative substrate proteins and leads to their dissociation (166). Because the binding of
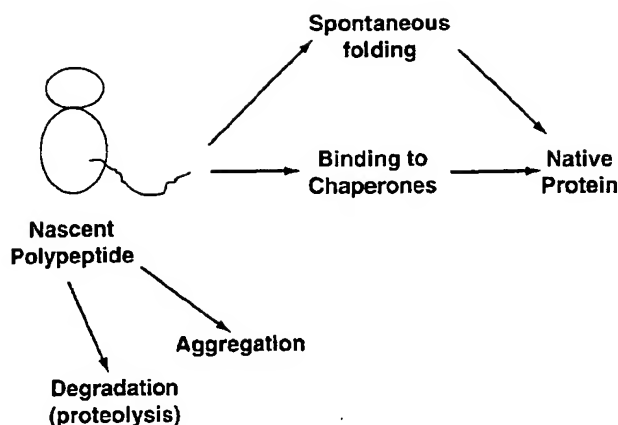

FIG. 3. A newly synthesized protein, whether still associated with ribosome or released, faces several competing pathways. It is likely that in the absence of chaperones, aggregation or other forms of misfolding would be the major pathway for many proteins.

ATP occurs in the NH_2-terminal domain and peptide binding is in the COOH-terminal domain, it is clear that strong coupling between the two functional domains must exist.

Under appropriate conditions, DnaK undergoes autophosphorylation (137). It is not yet clear if this is of physiological significance. At the moment, there is no good evidence that it is. However, GrpE and synthetic peptides have been observed to inhibit the phosphorylation (the effectiveness of a given peptide correlated with its affinity for DnaK), whereas DnaJ had no effect on the reaction (169). Human HSP70 is phosphorylated in vitro in the presence of divalent ions, with calcium being the most effective. Two calcium ions were found in the human ATPase domain structure, and calcium binding may facilitate phosphorylation (214).

Various techniques have shown that HSP70 adopts at least three significantly different conformations, one in the absence of nucleotide, one with ADP bound, and one with ATP bound. Binding of nucleotides or polypeptides alters the conformations of both the nucleotide- and polypeptide-binding domains, further indication that the conformations of these two domains are highly coupled (71).

Recently, a new pair of DnaK/DnaJ-like chaperones has been discovered in *E. coli* (242). Sequence differences between HSC66 and HSC20 compared with other HSP70/HSP40 members suggest that these chaperones may have different peptide binding specificity and be subject to different regulatory mechanisms. In particular, the high level of constitutive expression and lack of significant response to temperature changes suggest that HSC66 and HSC20 may play an important role in the folding of certain newly synthesized proteins under normal cellular conditions.

Details of the mechanism by which HSP70 interact

with newly synthesized and nonnative proteins are given in sections IV and V.A.

E. HSP90 Family

Members of the HSP90 family are highly conserved, essential proteins found in all organisms from bacteria to humans. Examples include the cytosolic form in eukaryotes, HSP90, the ER form, Grp94, and the *E. coli* homolog HtpG. Mammalian HSP90 exist as dimers. Although there are a number of similarities between the activities of HSP90 and HSP70, the former has several identified specific interactions, for example, with cytoskeleton elements, signal transduction proteins (including steroid hormone receptors), and protein kinases (such as the mitogen-activated protein kinase system). HSP90 is frequently found in complexes with other chaperones. In vitro, HSP90 exhibits chaperone activity with diverse proteins, suggesting a general function. The properties of HSP90 have been reviewed (10, 11, 20, 113, 175, 265).

Recently, the crystal structure of the NH$_2$-terminal domain of the yeast HSP90 was solved to reveal a dimeric structure based on a highly twisted 16-stranded β-sheet. The opposing faces of the β-sheet in the dimer define a potential peptide-binding cleft, suggesting that the N domain may serve as a molecular "clamp" in the binding of ligand proteins to HSP90 (179).

There has been a long-standing controversy as to whether HSP90 binds or hydrolyzes ATP. The crystal structures of complexes between the NH$_2$-terminal domain of the yeast HSP90 with ADP/ATP unambiguously show a specific adenine nucleotide binding site, homologous to the ATP-binding site of DNA gyrase B. This site is the same as that identified for binding the antitumor agent geldanamycin, suggesting that geldanamycin acts by blocking the binding of nucleotides to HSP90 and not the binding of incompletely folded substrate proteins as previously suggested. These results strongly suggest the direct involvement of ATP in the function of HSP90 (82, 178).

Even though HSP90 is one of the most abundant chaperones in the cell, its in vivo functions are poorly understood, and little is currently known about its role in chaperoning the folding of newly synthesized proteins, although there are hints that it does not function alone but is associated with several other cofactors. For example, HSP90 performs at least part of its function in a complex with members of the prolyl isomerase family, FKBP52 and p23 (10), and the steroid receptor complex consists of HSP90, HSP70, p48, the cyclophilin Cyp-40, and the associated proteins p23 and p60 (45). Although neither Cyp-40 nor p23 can refold unfolded substrates, in in vitro folding experiments they interact with nonnative proteins and maintain a folding-competent intermediate (67).

A temperature-sensitive mutant of HSP90 in yeast, which rapidly and completely loses activity on shift to high temperatures, has been used to examine the functions of HSP90 in vivo. The results suggested that HSP90 is not required for the de novo folding of most proteins but is required for a specific subset of proteins that have greater difficulty reaching their native conformations (153). In vitro, in the absence of nucleotide, HSP90 can maintain nonnative substrate in a "folding-competent" state that refolds upon addition of HSP70, DnaJ homolog, and nucleotide (66).

F. HSP100 Family

The heat-inducible members of the HSP100 (or Clp) family of proteins have a number of very intriguing properties and share a common function in helping organisms to survive extreme stress (78). They perform a diverse set of functions, including proteolysis. They are highly conserved, present in all organisms, and contain ATP and polypeptide binding sites. Both HSP104 and ClpA form six-membered ring complexes; the diameter of the interior of the rings is much smaller than in GroEL, making it unlikely that the HSP100 function analogously to HSP60. The basic mechanisms by which these chaperones function are not understood. There is some suggestion that HSP104 may act in concert with HSP70 and DnaJ homologs to increase the yields of renatured protein (78). It should be noted that no human analogs of HSP104 have been found.

Unlike HSP60 and HSP70, which are unable to resolubilize aggregated proteins in vitro (with the exception of RNA polymerase), HSP104 has been observed to solubilize thermally aggregated proteins both in vivo and in vitro (170). Interestingly, ClpA can substitute for the ATP-dependent chaperone function of DnaK and DnaJ in the in vitro activation of the plasmid P1 RepA replication initiator protein (257). Another unusual feature of HSP104 is its role in triggering a prionlike disorder in yeast, involving the extrachromosomal elements PSI+ and URE3 (37).

G. Calnexin and Calreticulin

Calnexin is a transmembrane molecular chaperone that resides in the ER. Calreticulin, which has sequence homology with calnexin, is a soluble ER chaperone. Both proteins are involved in the folding and assembly of nascent proteins in the ER in a calcium-dependent manner and play an important role in glycoprotein maturation and quality control in the ER (6, 93, 119, 259).

Most proteins that enter the ER are cotranslationally modified by the addition of a complex carbohydrate structure that undergoes subsequent modification by selective removal of individual hexose residues (219). Both calre-

ticulin and calnexin transiently interact with many newly synthesized proteins in the ER, with some overlap between those proteins that bind to calreticulin and those that bind to calnexin. The specificity of the interaction is determined by the nature of the oligosaccharide and requires the trimming of glucose residues from the asparagine-linked core glycans by glucosidases. Calnexin transiently interacts with newly synthesized glycoproteins, specifically recognizing a monoglucosylated intermediate (162). Its major role appears to be to monitor glycoprotein folding and prevent incompletely folded proteins from leaving the ER. As proposed by Helenius and co-workers (92), carbohydrate processing and folding occur simultaneously; calnexin recognizes and binds the monoglucosylated glycoprotein intermediate of the nascent chain. After the remaining glucose is removed, the glycoprotein is released from calnexin; if it is incompletely folded, it is reglycosylated and rebinds to calnexin. If it is folded it no longer binds to calnexin. Calreticulin is also specific for monoglucosylated glycans (172). The interactions of calreticulin and calnexin with denatured proteins are highly dependent on divalent metal ions or polyamines (261). Calnexin facilitates the folding and assembly of class I histocompatibility molecules and prevents formation of aggregates, showing that it functions as a molecular chaperone (241). Protein folding in the ER is also discussed in section IVA.

H. Protein Disulfide Isomerase

Protein disulfide isomerase (PDI) is a critical cofactor in the folding of many proteins that are found in the ER (65, 77, 143, 176). Many secreted proteins have multiple disulfide bonds, presenting potential problems for correct disulfide pairing during folding. In vitro studies of the refolding of reduced proteins show that disulfide bond formation occurs rapidly and is followed much more slowly by thiol-disulfide rearrangement leading to the correct disulfide pairings. Thus catalysis of oxidative folding is necessary in vivo to rapidly generate the correct disulfide bonds in newly synthesized proteins. In the eukaryotic ER, PDI fulfills this function. Its concentration can reach close to millimolar levels. The properties of PDI have recently been reviewed (245). In addition to strong affinity for unfolded proteins and peptides, it binds many relatively hydrophobic molecules such as steroid and thyroid hormones. Hence, it is not surprising that PDI has been reported to have chaperone-like activity at high concentrations (such as inhibition of aggregation) distinct from its disulfide bond interactions (22, 180, 209).

Protein disulfide isomerase has two catalytic sites situated in two domains homologous to thioredoxin, one near the NH$_2$ terminus and the other near the COOH terminus. The thioredoxin domains, by themselves, can catalyze disulfide formation, but they are unable to catalyze disulfide isomerizations (36).

I. Peptidyl Prolyl Isomerase/Trigger Factor

Under in vitro (and presumably in vivo) conditions, proline *cis-trans* isomerization may become rate limiting in the folding of proteins; in many cases, the presence of peptidyl prolyl isomerase (PPI) will enhance the rate of folding. Peptidyl prolyl isomerases are ubiquitous enzymes found in virtually all organisms and subcellular compartments. Three unrelated families are known: the cyclophilins, the FK506-binding proteins (FKBP), and the parvulins (200). The former two families are also known as immunophilins. The trigger factor is a PPI with somewhat similar activity, and weak homology, to FKBP. Trigger factor is an abundant cytosolic protein originally identified by its ability to maintain the precursor of a secretory protein in a translocation-competent form (31).

Structural studies of the *E. coli* trigger factor reveal a modular structure, composed of three stably folded domains, of which the catalytic one is homologous to FKBP (270). Trigger factor binds partially folded intermediates tightly. Although the isolated catalytic domain of the trigger factor retains full prolyl isomerase activity toward short peptides, its activity toward protein substrates is dramatically reduced, indicating that the polypeptide binding site extends beyond the FKBP domain (201).

Trigger factor has several chaperone-like functions: it binds to nascent cytosolic and secretory polypeptide chains, and it catalyzes protein folding in vitro (98). Trigger factor interacts with GroEL in vivo and promotes its binding to at least some polypeptides; GroEL-trigger factor complexes show much greater affinity for partially folded intermediates than GroEL alone (116). On the basis of studies showing that trigger factor was cross-linked to all tested nascent chains derived from both secreted and cytosolic proteins, it appears that trigger factor may act as a general molecular chaperone in protein synthesis (99, 240).

J. HSP70 Cochaperones

In addition to DnaJ and GrpE, which function as cochaperones with DnaK, and have been known for several years, other protein cofactors that interact with HSP70 have been discovered recently. These include Hip (HSC70-interacting protein), BAG-1, and auxilin. The existence of these cofactors illustrates the complexity of the HSP70 chaperone machinery in cells.

GrpE is a key component of the HSP70 chaperone system for protein folding in bacteria and mitochondria. GrpE acts as a nucleotide exchange factor to control the ATPase activity of DnaK in its reaction cycle, although the

details of its mechanism remain unclear. GrpE has high affinity for monomeric native DnaK, as well as the isolated ATPase domain (185, 202). GrpE has no affinity for ATP or ADP, nor the oligomeric states of DnaK. The nucleotide exchange properties of GrpE are a consequence of the binding of GrpE to DnaK, leading to a conformational change involving the opening of the nucleotide cleft on DnaK, resulting in a low-affinity state for nucleotides. Recently, the crystal structure of GrpE bound to the ATPase domain of the molecular chaperone DnaK has been determined (89). A dimer of GrpE binds asymmetrically to a single molecule of DnaK. The structure of the nucleotide-free ATPase domain complexed with GrpE closely resembles that of the nucleotide-bound mammalian HSP70 homolog, except for an outward rotation of one of the subdomains of the protein. Two long α-helices extend away from the GrpE dimer and suggest an additional role for GrpE in peptide release from DnaK. The functional aspects of GrpE are given in section vA.

Hip is a novel tetrameric cochaperone involved in the regulation of eukaryotic HSC70, distinct from that of bacterial HSP70. It appears to play a role in forming stable HSP70 complexes with substrate proteins. One Hip oligomer binds the ATPase domains of at least two HSC70 molecules, dependent on activation of the HSC70 ATPase by HSP40. Although hydrolysis remains the rate-limiting step in the ATPase cycle, Hip stabilizes the ADP state of HSC70 that has a high affinity for substrate protein. Hip also appears to be a chaperone in its own right, in that it binds to some unfolded proteins (15, 104).

BAG-1 is a recently discovered regulator of HSP70 (216, 271). BAG-1 is an antiapoptotic protein and also interacts with several steroid hormone receptors that require the molecular chaperones HSP70 and HSP90 for activation. The action of BAG-1 is similar to that of GrpE in bacterial cells, in that it binds to the ATPase domain of HSP70 and, in cooperation with HSP40, stimulates the rate of ATP hydrolysis by increasing the rate of release of ADP from HSP70 (103). BAG-1 can be coimmunoprecipitated with HSP70 from cell lysates (223). BAG-1 inhibited the HSP70-mediated in vitro refolding of an unfolded protein substrate. The binding of BAG-1 to one of its known cellular targets, Bcl-2, in cell lysates was found to be dependent on ATP, consistent with the possible involvement of HSP70 in complex formation. The identification of HSP70 as a partner protein for BAG-1 may explain the diverse interactions observed between BAG-1 and several other proteins, including steroid hormone receptors and certain tyrosine kinase growth factor receptors.

Auxilin is a 100-kDa cofactor involved in the HSP70-mediated uncoating of clathrin-coated vesicles (239). Clathrin-coated vesicles transport selected integral membrane proteins from the cell surface and the *trans*-Golgi network to the endosomal system. Before fusing with their target, the vesicles must be stripped of their coats. Auxilin binds with high affinity to assembled clathrin lattices and, in the presence of ATP, recruits HSP70. The presence of a J domain at its COOH terminus indicates that auxilin is a member of the DnaJ family: deletion of the J domain results in the loss of cofactor activity.

A 16-kDa cytosolic protein, called p16, which copurifies with HSC70 from fish liver, has been identified as a member of the Nm23/nucleoside diphosphate kinase family (135). p16 may modulate HSC70 function by maintaining HSC70 in a monomeric state and by dissociating unfolded proteins from HSC70 either through protein-protein interactions or by supplying ATP indirectly through phosphate transfer.

Hop is a recently discovered 60-kDa protein that can form a physical link between HSP70 and HSP90, thus modulating their activities (114). Hop is involved in the refolding of denatured protein in rabbit reticulocyte lysate and stimulates the refolding by HSP70 and Ydj-1 in a purified refolding system. Optimal refolding was observed in the presence of both Hop and HSP90. Hop preferentially formed a complex with ADP-bound HSP70 and also appears to bind to the ADP-bound form of HSP90.

K. Specialized Chaperones

Some molecular chaperones may be highly specific in that they interact with only one, or a very limited number, of target proteins; examples are PapD (127), which is involved in the assembly of bacterial pili, and HSP47, which is involved in the folding and processing of procollagen in the ER. There are many large and complex protein machines in cells: in some of these cases, specific molecular chaperones are involved in their assembly (206). Some of the best-studied systems are bacteriophage capsids and bacterial pili and flagella.

The 47-kDa HSP (HSP47) is an ER-resident chaperone found in collagen-producing cells, where it interacts with procollagen. It has been proposed that it functions as a chaperone regulating procollagen chain folding and/or assembly, but the mechanism is not well understood (152). It is likely that its main function is to prevent aggregation and misfolding of newly synthesized procollagen chains until the correct COOH-terminal associations have been made to yield the collagen triple helix. When HSP47-procollagen complexes reach the *cis*-Golgi network, the chaperone rapidly dissociates. The major interaction site on procollagen has been shown to be the pro-alpha 1 N-propeptide (109).

Receptor-associated protein (RAP) is another example of a specialized molecular chaperone, in this case for the low-density lipoprotein receptor-related protein (LRP), a large receptor that binds multiple ligands. The major role of RAP is to facilitate correct folding of LRP

and to prevent the premature interaction of ligands with LRP (161).

The production of native α/β-tubulin heterodimer depends on the action of cytosolic chaperonin and at least five protein cofactors. These reactions do not depend on ATP hydrolysis (230, 231). The β-tubulin monomer release factor, p14, which catalyzes the release of β-tubulin monomers from intermediate complexes, has recently been shown to be a member of the DnaJ family (141).

There are also a number of chaperones involved in protein export, such as SecB from *E. coli* (88). SecB has two functions: it maintains precursors of some exported proteins in a conformation compatible with export, by preventing them from aggregating or from folding to their native state in the cytoplasm, and it delivers both nascent and completed precursors to SecA, one of the components of the export apparatus associated with the plasma membrane. Only those polypeptides that fold slowly interact significantly with SecB, even though it is able to bind a wide variety of nonnative proteins. Complexes between SecB and substrate proteins are in rapid equilibrium with the free states (236). Thus, unlike the HSP70 and HSP60, in which hydrolysis of ATP is coupled to the binding and release of substrate proteins, SecB does not form stable complexes with substrate proteins. This may reflect the fact that SecB does not mediate protein folding but is specialized for the protein export pathway.

IV. INTERACTIONS OF NASCENT CHAINS WITH CHAPERONES

Fundamental questions in protein biogenesis include at which stage the nascent protein first interacts with molecular chaperones, the identity of the chaperones, and the role of the chaperones in facilitating protein folding. Do they just prevent aggregation and misfolding, or do they play a more active role in the actual folding process? The involvement of chaperones in both co- and posttranslational folding is now clear.

Considerable controversy continues regarding which chaperones are involved in interactions with nascent polypeptide chains. The initial evidence for chaperoning came from studies on the assembly of immunoglobulin light and heavy chains and the involvement of the protein now known as BiP (an HSP70) (85, 151). In a study with major implications for in vivo protein folding and assembly, Welch and co-workers (5) demonstrated that cytosolic forms of HSP70 bind cotranslationally to nascent polypeptide chains and to newly synthesized proteins in the normal (unstressed) cell in an ATP-dependent manner. The association of cytosolic HSP70 with nascent polypeptide in translating ribosomes has subsequently been confirmed in a number of organisms (154).

There have been several reports that a high-molecu-

lar-weight complex of proteins including various chaperones is associated with nascent (or unfolded) polypeptide chains during chain elongation in vitro and in vivo. Early evidence was observed in the renaturation of firefly luciferase in cell-free translation systems (70, 97, 205). Chaperone-stabilized luciferase was associated with high-molecular-weight complexes overlapping the distributions of HSP70, HSP90, and the chaperonin TRiC on gel filtration columns (160). Molecular chaperones that have been implicated include HSP70 (5, 86); HSP70 and HSP40 (123, 154); HSP70, HSP40, and the TCP-1 ring complex chaperonin (70); and HSP70 and HSP90 (46, 205).

In a clever new approach, an antibody to puromycin was used to identify a population of truncated nascent polypeptides that were then probed by immunoprecipitation and chemical cross-linking with several antibodies that recognize the cytosolic chaperones HSP70, CCT (TRiC), HSP40, p48 (Hip), and HSP90, as a means of identifying chaperones bound to the nascent chains (46). The results showed that HSP70 is the predominant chaperone bound to nascent polypeptides. The interaction between HSP70 and nascent polypeptides is apparently dynamic under physiological conditions but can be stabilized by depletion of ATP or by chemical cross-linking. Interestingly, the cytosolic chaperonin CCT (TRiC) was found to bind primarily to full-length, newly synthesized actin and tubulin. Other studies have also implicated the TCP-1 ring complex in the synthesis and assembly of tubulin and actin (69, 215, 264).

This investigation also demonstrated that nascent polypeptides have a strong propensity to bind to many proteins nonspecifically in cell lysates. It is likely that this nonspecific binding is responsible for the reports of additional components in contact with nascent polypeptides (46).

Several studies provide support for cotranslational interactions of molecular chaperones with nascent polypeptide chains, especially HSP70 and perhaps HSP40. The interaction of DnaJ with nascent ribosome-bound polypeptide chains as short as 55 residues was reported using firefly luciferase and chloramphenicol acetyltransferase in cross-linking experiments (97). These investigations showed that both folding and subsequent mitochondrial translocation required DnaK, DnaJ, and GrpE and led to the proposal that DnaJ protects nascent polypeptide chains from aggregation and, in cooperation with HSP70, controls their productive folding once a complete polypeptide or a polypeptide domain has been synthesized. Both HSP70 and HSP40 were shown to be associated with nascent polypeptide chains in translating ribosomes, whereas GroEL, although transiently associated with newly synthesized proteins, was absent from the ribosomes, suggesting that HSP70 and HSP40 play an early role in protein folding, whereas GroEL acts at a later stage (70, 72, 173).

Investigations using fluorescent-labeled rhodanese (by the cotranslational incorporation of a coumarin derivative at the NH_2 terminus of the nascent protein) demonstrated the accumulation of full-length but enzymatically inactive polypeptides on the ribosomes. These polypeptides could be activated and released by subsequent incubation with the chaperones DnaJ, DnaK, GrpE, GroEL, GroES, and ATP and release factor. Changes in fluorescence indicated that DnaJ bound to the nascent protein and appeared to be essential for folding of ribosome-bound rhodanese into the native conformation (87, 124, 126).

Further support that folding of nascent proteins can take place on the ribosome comes from studies on partially folded intermediate states of bacteriophage P22 tail-spike protein and the β-subunit of tryptophan synthase, which can be detected while still bound to ribosomes using monoclonal antibodies to the intermediates. The rapid appearance of the intermediates suggests that the nascent chains start folding during their elongation on the ribosomes. The newly synthesized incomplete chains were shown to interact with DnaK but not GroEL while still bound to the ribosome (235).

There has been considerable discussion as to whether GroEL interacts with newly synthesized proteins in a cotranslational or posttranslational manner. As noted above, several studies indicated that DnaK and DnaJ are involved at an early stage in the folding of newly synthesized protein and that GroEL acts at a later stage (72). In a recent investigation in which rhodanese was synthesized in both in bacterial and wheat germ translation extracts, only posttranslational stable complexes with GroEL were found (184). Further evidence consistent with the HSP70 chaperone machinery interacting with newly synthesized proteins before GroEL (or concurrently) comes from investigations on the synthesis of chloramphenicol acetyltransferase in a system genetically depleted of DnaK and DnaJ. Most of the chloramphenicol acetyltransferase failed to assemble into active trimers and accumulated either in a complex with GroEL or as inactive monomer. The addition of DnaK and DnaJ to the system before the start of protein synthesis led to increased formation of native chloramphenicol acetyltransferase (244). Another investigation supporting a place for GroEL in the later stages of the folding of newly synthesized proteins made use of temperature-sensitive lethal mutations in the GroEL gene. After a shift to a nonpermissive temperature, the rate of general translation in the mutant cells was reduced, but a specific group of cytoplasmic proteins failed to fold to their native states (107). The much more limited specificity demonstrated for TCP-1 chaperonins, compared with GroEL, suggests significantly different roles for these two classes of chaperonins in the biosynthesis of proteins. It is likely that the

functional differences reflect underlying structural differences.

Bukau and co-workers (16) have recently suggested that during the folding of newly synthesized proteins, DnaK and GroEL do not act in sequence, but rather the two chaperone systems form a "lateral network of cooperating proteins." There are data to support both this and the sequential models, so the question remains unresolved at present. Another source of controversy relates to the question of how many newly synthesized proteins require the assistance of HSP60 (chaperonins) in folding. Lorimer has calculated that for *E. coli* there is only sufficient GroEL to assist ~5% of newly translated proteins under normal conditions (142). It is therefore likely that most newly synthesized proteins in *E. coli* fold without the assistance of GroEL, and this implies that most proteins fold fast enough that sequestration on DnaK to minimize the concentration of nonchaperone-bound protein suffices to prevent aggregation.

Thus, whereas the overall outline of the process of chaperone-mediated folding of newly synthesized proteins is clear, the details are as yet incompletely resolved. A nascent polypeptide will interact with HSP70 and possibly other chaperones (probably HSP40) as it emerges from the ribosome. The lifetime of HSP70 complexes with substrate proteins under in vivo conditions is not well established but is likely to be comparable to the time for folding of many newly synthesized proteins. Dissociation of the newly synthesized chain from HSP70 after release of the nascent chain from the ribosome sets up a kinetic competition between rebinding to HSP70, binding to HSP60, spontaneous folding, aggregation, or possible even proteolysis (Fig. 3).

It has also been reported that there may be significant differences between folding in prokaryotes and eukaryotes (155). In a eukaryotic translation system, two-domain engineered polypeptides were observed to fold by sequential and cotranslational folding of their domains. However, in *E. coli*, folding of the same proteins was found to be posttranslational and to lead to intramolecular misfolding of the concurrently folding domains (155). In addition, differences between the in vitro and in vivo nature of the interactions of chaperones with actin during refolding from denaturant have been reported (68).

A. Folding in the Endoplasmic Reticulum

The ER is a key compartment in cells that are specialized for protein export and contains many chaperones that are essential for the production of functional proteins for export (250). Folding begins with the insertion of a preprotein into the lumen of the ER and can occur either posttranslationally, in which case the preprotein is completely synthesized on cytosolic ribosomes before being

translocated, or cotranslationally, in which case membrane-associated ribosomes direct the nascent polypeptide chain into the ER concomitant with polypeptide elongation (14). The ER has excellent quality control mechanisms (involving chaperones) that recognize and selectively retain misfolded proteins, which are then either degraded or refolded (30, 149). The concentration of the ER HSP70, BiP, is increased by elevated levels of misfolded proteins in the ER. How the levels of misfolded molecules are monitored and how this information is used to regulate the synthesis of BiP are still poorly understood. Likewise, the mechanisms by which oxidizing potential of the ER environment is regulated, and the misfolded proteins are degraded, are also unknown.

Although some of the major chaperones involved in protein folding in the ER are well studied, e.g., BiP and PDI, it is apparent that more have yet to be characterized. For example, several calcium-dependent putative chaperones have recently been identified using affinity chromatography with denatured-protein columns and elution with ATP (159). These proteins were identified as BiP (grp78), HSP90 (grp94), calreticulin, a novel 46-kDa protein that binds azido-ATP, as well as three members of the thioredoxin superfamily: PDI, ERp72, and a previously reported 50-kDa protein (p50). Because the release of HSP90, PDI, ERp72, calreticulin, and p50 was stimulated by Ca^{2+}, these proteins appear to function as Ca^{2+}-dependent chaperones (159).

Evidence is accumulating that the ER HSP70 chaperone machinery is similar to that in the cytosol and bacteria, in that at least two DnaJ homologs have been found in the ER. For example, a yeast DnaJ homolog, Scj1p, is located in the lumen of the ER where it can interact with Kar2p (the HSP70 of the yeast ER) via the conserved J domain (198). Undoubtedly, chaperone-mediated folding in the lumen of the ER is complex, as revealed by the observation that the interaction of BiP with immunoglobulin light chains during folding suggests that light chains undergo both BiP-dependent and BiP-independent folding steps and that BiP must release the light chains before disulfide bond formation can occur in them (94).

B. Mitochondrial Import/Folding

Molecular chaperones play a critical role in targeting proteins to the mitochondria and the subsequent folding of the imported protein. In support of the endosymbiont theory on the origin of mitochondria, the chaperones of the mitochondria show a high degree of similarity to bacterial molecular chaperones, including a GrpE homolog (mGrpE) (193). The mitochondrial HSP70 (mHSP70) mediates protein transport across the inner membrane and protein folding in the matrix. These two reactions are carried out by two different mHSP70 complexes. The ADP-bound form of mHSP70 favors formation of a complex on the inner membrane; this "import complex" contains mHSP70, its membrane anchor Tim44, and mGrpE (106). The ATP-bound form of mHSP70 favors formation of a complex in the matrix; this "folding complex" contains mHSP70, the mitochondrial DnaJ homolog Mdj1, and mGrpE. A more detailed discussion of the role of chaperones in mitochondrial import and folding can be found in recent reviews (106, 156, 193).

V. MECHANISMS OF CHAPERONE FUNCTION

Considerable effort has been expended over the past few years to understand the mechanistic details of chaperone function. Great progress has been made, although considerable further study is necessary. The two best understood systems are those of HSP70 and GroEL. Even with these, the complexity of the systems, especially due to the interactions with cochaperones and other cofactors, has often led to apparently conflicting hypotheses. An additional source of potential discrepancies in behavior of the chaperones results from the effects of low concentrations of critical contaminants; for example, it has recently been shown that samples of HSP70 and HSP90 are often contaminated with low levels of DnaJ or HSP40, which may profoundly affect the experimental observations (204).

It is convenient to consider the mechanism of action of both HSP70 and GroEL in terms of their reaction cycles. Both of these chaperones require cochaperones for their full function, GroES in the case of GroEL, and HSP40 (or DnaJ) in the case of HSP70. Several theoretical models have been proposed to account for the effects of chaperonins on protein folding (25, 207, 232).

A. HSP70 Reaction Cycle

Several models have been proposed for the reaction cycle of HSP70 (4, 16, 74, 90, 146, 147, 166, 174, 195, 221). The DnaK cycle has been the most studied and is considered here. The reaction cycles for other HSP70 appear to be similar, with the exception that the cofactor GrpE will only be present in bacteria and mitochondria (273).

Although the general features of the HSP70 reaction cycle are established, there is considerable discussion about the details. Many observations indicate that the maximal functional effect of HSP70 requires the presence of DnaJ (or its homologs) (and GrpE in the case of prokaryotes and mitochondria) (73, 102, 136, 203, 217, 221, 249, 258, 274). The reports that DnaJ or HSP40 may bind at least some unfolded substrates are another source of confusion. It is now well established that GrpE and its homologs are nucleotide exchange factors and stimulate the ATPase cycle of DnaK or mHSP70 by increasing the

rate of ADP release (39, 221) and that DnaJ and its homologs function to increase the rate of hydrolysis of HSP70-bound ATP (146, 221). Several studies have suggested that the action of DnaJ and GrpE with DnaK requires substoichiometric levels of the two cofactors (174). This is also consistent with the physiological molar ratios, in which DnaK is in large excess.

It has been shown that HSP70 discriminates between folded and unfolded proteins, normally binding only the latter (168). In fact, it is likely that HSP70 can distinguish between relatively unfolded intermediates and strongly nativelike intermediates and binds only the former. The fact that HSP70 binds to certain proteins in their native state, e.g., clathrin, is assumed to arise from the presence of accessible, unfolded loops. For a given unfolded substrate protein, there will be several potential HSP70 binding sites along the polypeptide chain, of different affinity for the chaperones (192). Both the conformational state of the substrate protein bound to HSP70 and the conformation of the substrate protein on ATP-induced release have been shown to be substantially unfolded (167).

The nature of the bound nucleotide affects the conformation of the chaperone and particularly its affinity for substrate protein. Thus complexes with ATP have low affinity for substrate and those with bound ADP have high affinity (166, 167, 174). The high affinity of HSP70 for nucleotides means that these chaperones will be found as binary complexes with ATP and ADP in the cell. Although the ATP complex binds substrate proteins/peptides much more rapidly than the ADP complex (146, 199, 224), the resulting ternary complex, HSP70-ATP-substrate, also releases the substrate protein very rapidly, and thus no productive complexes with unfolded substrate result (166). In contrast, the HSP70-ADP complex, although binding substrate protein at a slower rate, forms a relatively stable ternary complex, HSP70-ADP-substrate (167). The formation of small amounts of substrate complex when HSP70-ATP and substrate protein are mixed arises from ATP hydrolysis occurring during the reaction (stimulated by the presence of the substrate protein). Thus the formation of relatively long-lived complexes between unfolded proteins and HSP70 requires the presence of the HSP70-ADP-substrate complex. This explains, at least in part, the need for DnaJ and its homologs, since DnaJ significantly stimulates the rate of hydrolysis of ATP bound by HSP70, thus leading to formation of HSP70-ADP (18, 146).

The release of the substrate protein from the HSP70-ADP-substrate complex is triggered by the binding of ATP, which induces a conformational change in the peptide-binding domain (17, 84, 137, 165, 166, 227). On the basis of the crystallographic structure of the peptide-binding domain, the conformational change presumably involves the raising of the flap or latch, which is hypothesized to help maintain the substrate peptide bound (272).
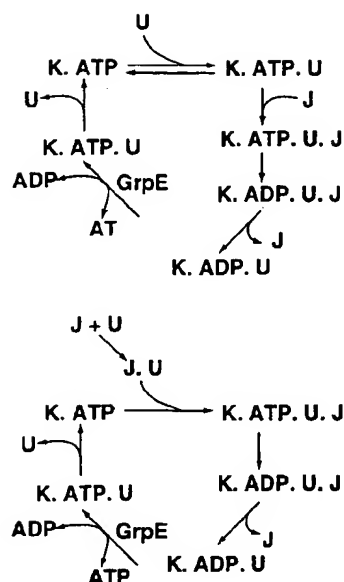
The cycle is completed by rebinding of another substrate protein molecule to the HSP70-ATP complex, or the hydrolysis of the ATP, leading to formation of DnaK-ADP and another conformational change. That substrate protein dissociation precedes ATP hydrolysis was demonstrated by comparison of the corresponding rates, the rate for ATP hydrolysis being significantly slower than that for substrate dissociation (166).

There appear to be several potential pathways for substrate proteins to enter the DnaK reaction cycle: via binding to DnaK-ATP, to DnaK-ATP-DnaJ, to DnaJ (which then binds to DnaK-ATP), to DnaK-ADP, and possibly to DnaK-ADP-DnaJ. The concentrations of the two ternary complexes are expected to be quite low so these are probably not major entry points. The same goes for DnaK-ADP under normal (nonstress) conditions when the levels of DnaK-ATP greatly exceed those of DnaK-ADP. The majority of the data suggest that the DnaK-ATP complex will normally be the main portal for entry to the cycle.

Most of the proposed reaction cycles of HSP70 fall into two broad classes: *1*) those which propose that it is only DnaK (HSP70) with bound ATP which interacts with the unfolded substrate, and that the interaction of this ternary complex with DnaJ (HSP40) leads to rapid ATP hydrolysis (146), and *2*) those which postulate that DnaJ first interacts with an unfolded (nascent) polypeptide, targeting it for binding to DnaK (74, 90, 221). Although there have been several reports that DnaJ (or HSP40) binds to some unfolded proteins (70, 95, 125, 126, 130, 203, 221), unambiguous evidence that DnaJ or its homologs will bind to unfolded proteins in general is currently lacking (240).

In the absence of the cochaperones, substrate protein will cycle on and off the ATP complex and accumulate only in the ADP complex. Although there are conflicting reports regarding the rate-limiting step in the intrinsic HSP70 ATPase activity, the evidence is strongly in favor of rate-limiting cleavage of the γ-phosphate of ATP, both in the absence and presence of DnaJ and substrate protein (115, 146, 147, 227). Both polypeptide substrates and DnaJ homologs stimulate the ATPase activity of HSP70 in *E. coli*, yeast, and human cytosol (147, 273). In the case of the yeast HSP70, Ssa1, the DnaJ homolog Ydj1 also accelerated release of ATP from Ssa1 (273), suggesting a possible explanation for the lack of a GrpE homolog in eukaryotic cytosol.

Thus the major pathway in the DnaK reaction cycle is likely to be the following (Fig. 4A). *1*) DnaK-ATP binds the unfolded substrate protein; the resulting complex may dissociate or bind DnaJ. *2*) The latter complex will undergo rapid DnaJ-stimulated hydrolysis of the ATP to yield a "stable" DnaK-ADP-substrate protein complex (due to the conformational change induced by the ATP→ADP transition), which may or may not also contain the DnaJ. *3*) The ADP dissociates, catalyzed by GrpE,

K. ATP ⇌ K. ATP. U

U ⟶|

K. ATP. U   K. ATP. U. J

ADP⟶⟍GrpE   K. ADP. U. J

AT   ⟍ J

K. ADP. U

J + U

⟍ J. U

K. ATP ⟶ K. ATP. U. J

U ⟶| |

K. ATP. U   K. ADP. U. J

ADP⟶⟍GrpE   ⟍ J

ATP   K. ADP. U

K = DnaK, J + DnaJ, U = substrate protein or peptide

FIG. 4. Models of DnaK (HSP70) reaction cycle. *Top*: cycle starts with substrate protein binding to DnaK-ATP complex. *Bottom*: cycle starts with substrate protein binding to DnaJ. See text for details.

and is replaced by ATP. *4)* This induces a conformational change to the low-affinity form which results in dissociation of the substrate protein, leaving a DnaK-ATP complex. *5)* The latter can then either restart the cycle by binding a substrate protein, or it can undergo ATP hydrolysis to yield a DnaK-ADP complex. This would have to dissociate the ADP and rebind an ATP before entering the productive cycle again. The rates for several of the key steps in the DnaK cycle have been reported (4, 84, 117, 163, 174, 224). Because of the complexity of the system, the measured rates will be very sensitive to the concentrations of all the species involved, as well as the temperature and pH.

The alternative class of models in which DnaJ (or HSP40) acts as the initial chaperone will involve *1)* the unfolded substrate protein binding to DnaJ, which will then *2)* interact with DnaK-ATP, to form a transient HSP70-HSP40-U-ATP complex. This rapidly *3)* undergoes hydrolysis of its ATP, resulting in the formation of a stable HSP70-HSP40-U-ADP complex. It is likely that HSP40 dissociates rapidly from such a complex. Displacement of ADP by ATP (catalyzed by GrpE in bacteria and mitochondria) *4)* triggers the release of substrate protein, thus completing the reaction cycle (Fig. 4*B*).

Some of the newly synthesized proteins released by the HSP70 will fold spontaneously to the native state at a sufficiently fast rate that they neither aggregate nor bind

to another chaperone molecule (either HSP70 or chaperonin) before they are fully folded. However, for some proteins, further interaction with a chaperonin, such as GroEL, is apparently required for complete folding (90, 96).

B. GroEL Reaction Cycle

The GroEL cycle is by far the most studied and best understood chaperonin reaction cycle, yet there are still outstanding questions. A comprehensive review has been published recently (53). For GroEL, the folding reaction is driven by cycles of binding and release of the cochaperone GroES, which alternate with binding and release of the nonnative protein substrate (62, 234). These cycles are driven by ATP binding and hydrolysis that control the conformation of the chaperonin and its affinity for nucleotides and the cochaperonin GroES. There are three major functional states: one in which the unfolded substrate is bound tightly, another in which the substrate protein is trapped in the cavity capped by GroES but in which folding can proceed because the substrate protein is not bound to the walls of the cavity, and a final state in which the substrate protein is "ejected" regardless of whether it is folded or not. Partially folded protein will rebind to the chaperonin, continuing the cycle until folding is complete (145). A distinction has been made between released nonnative conformations that are committed to folding and those that are not. It is assumed that the isolation of a partially folded intermediate in the GroES-capped, relatively polar cavity will lead to significant folding occurring, without competition from aggregation. Mutant chaperonins that are able to trap (bind but not release) substrate protein have proven very useful in such investigations (21, 52, 256).

Although both symmetric and asymmetric complexes of GroEL with GroES have been observed (211, 234, 237), only the latter are believed to be physiologically functional (194, 233) (although the existence of transient symmetric complexes cannot be ruled out). In the asymmetric complexes, the GroEL ring with GroES attached is known as the *cis*-ring, the opposing (distal) ring is the *trans*-ring. The recently determined structure of the GroEL-GroES-(ADP)$_7$ complex revealed that the large rigid-block movements of the intermediate and apical domains in the *cis*-ring allowed bound GroES to stabilize a folding chamber with ADP confined to the *cis*-ring (26, 188, 263). The conformational changes in the apical domains doubled the volume of the central cavity and resulted in burial of the hydrophobic peptide-binding residues at the interface with GroES and between the GroEL subunits. These structural changes result in the enlarged central cavity having a polar surface that favors protein folding (26, 263). The conformational changes induced in GroEL upon
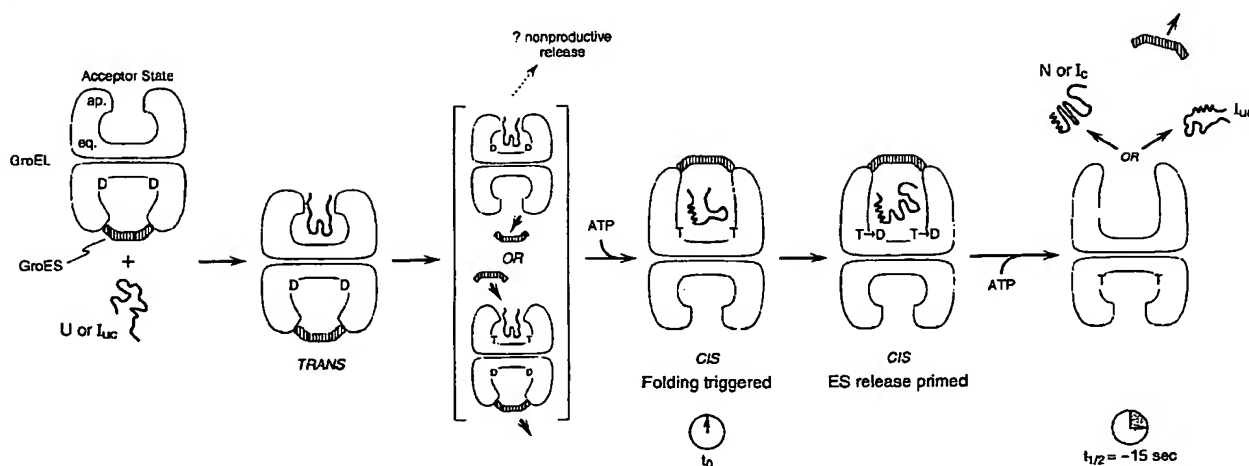
binding of ATP have been observed by several techniques including electron microscopy imaging, X-ray crystallography, and fluorescence labeling (26, 140, 237, 263). In addition, it has been shown that binding of nucleotide to one GroEL ring is strongly favored by GroES binding to the other ring (211). The nucleotides bind to a site near the top of the equatorial domain facing the cavity (9). Under physiological concentrations of chaperonins (equimolar GroEL and GroES) and nucleotides, the predominant species is the asymmetric GroEL-GroES complex (20).

A recent model for the GroEL reaction cycle is shown in Figure 5. It is generally assumed that the asymmetric GroEL-GroES complex is the state that binds substrate protein (211). This species has ADP bound in the ring that is capped by GroES. The substrate protein thus binds to the hydrophobic cavity of the distal ring (20, 53, 145, 251). This *trans*-complex then converts to the *cis*-asymmetric complex in which GroES caps the cavity containing the substrate protein. This intermediate may arise either by a transient symmetric complex with two GroES lids, or by a complex in which the *trans*-GroES dissociates first. Binding of ATP in the *cis*-ring leads to the major conformational changes, especially in the apical domain leading to an increase in the size of the cavity and conversion of its surface to a more polar environment. This leads to dissociation of the substrate protein from its hydrophobic interactions with the lining of the cavity, favoring the folding reaction. Simultaneously, hydrolysis of the ATP in the *trans*-ring leads to the release of GroES and the opportunity for the substrate protein to exit the cavity. If the released substrate protein has not reached the native state, it may rebind for another cycle (53, 55).

Interactions between the two back-to-back rings in

GroEL result in the allosteric regulation of ATP hydrolysis, binding, and release of folding substrates and the cochaperonin GroES. Allosterism in ATP hydrolysis can be described by a model in which each ring of GroEL is in equilibrium between a low-affinity (T) and high-affinity (R) state for ATP, and in which the GroEL double ring is in equilibrium between three states: TT, TR, and RR. Electron microscopy (26, 188) images of all three allosteric states, TT, TR, and RR, have been obtained for various complexes (26). Unfolded substrate proteins bind preferentially to the T state and stimulate the ATPase activity of GroEL by both a direct effect on GroEL and a shift in the equilibrium from the RR state toward the more active TR state (266). GroES promotes the T to R transition of the state distal to GroES in the GroEL-GroES complex. Owing to the relatively low affinity of the R conformation for nonfolded proteins, this transition leads to release of protein substrates from *trans*-ternary complexes of GroEL, GroES, and protein substrate. The role of this release mechanism may be to assist the folding of relatively large proteins that cannot form *cis*-ternary complexes and/or to facilitate degradation of damaged proteins that cannot fold (111, 266). GroEL undergoes a conformational change that is partly maintained after ATP hydrolysis, as long as ADP and P_i are bound to the GroEL ring (140).

There have been several investigations of the rates for individual steps in the GroEL reaction cycle that demonstrate the importance of nucleotide binding and hydrolysis, and GroES binding, on the rate of substrate protein release (79, 91, 138, 139, 157, 182, 212, 234). Horwich and co-workers (21) have shown that under normal conditions the rate of hydrolysis of ATP in the ring *trans* to the bound GroES determines the rate of release of the GroES

and hence the rate of dissociation of the substrate protein. This has been estimated to have a half-life of ~15 s (21). Confirmation that this "timer" sets the length of time for which the folding substrate protein remains in the GroEL cavity comes from observations on the folding of mitochondrial malate dehydrogenase; trapping experiments show that its dwell time on the complex is only 20 s (182). This is in good agreement with both the rate of ATP turnover and the dwell time of GroES on the complex but is much shorter than the time taken for the substrate to commit to the folded state.

Evidence is accumulating to indicate that GroEL is able to unfold misfolded conformations (1, 158, 183, 213, 232, 234, 268). The protection factors for the backbone amide protons of cyclophilin A bound to GroEL have been calculated from measurements of the rates of hydrogen/ deuterium exchange using NMR (158); in contrast to the native structure, similar protection factors were found throughout the sequence consistent with complete unfolding of the substrate protein. Clarke and co-workers (183) studied the GroEL-facilitated folding of mitochondrial malate dehydrogenase and showed that the chaperonin accelerated the dissociation of a misfolded intermediate formed by reversible aggregation of an early partially folded intermediate, through a repeated binding and release cycle coupled to ATP hydrolysis. It is likely that the apparent "unfoldase" activity of GroEL actually arises from its preferential affinity for the unfolded conformation (247). Thus, through mass action, misfolded intermediates will be unfolded and given a new chance to fold productively in the GroEL cavity.

The key factors in the chaperonin cycle therefore are as follows: *1)* nonnative substrate protein binds to the *trans*-ring of GroEL, in which ADP and GroES are bound in the "opposite" GroEL ring. Binding is facilitated by the hydrophobic surfaces of the apical domain lining the cavity in the GroEL ring. *2)* Subsequent ATP binding to the *cis*-ring leads to release of the ADP and GroES, followed by *3)* binding of ATP and GroES to the *cis*-ring results in the massive conformational change leading to the enlarged cavity. This conformational change triggers the release of the substrate protein from the surface of the apical domain and also "starts the clock." *4)* Hydrolysis of the ATP in the *cis*-ring weakens the interaction between GroES and the *cis*-ring, and binding of ATP in the *trans*-ring leads to the complete release of the GroES and substrate protein with a half-life of ~15 s (194).

VI. CONCLUDING REMARKS

Molecular chaperones recognize and bind to nascent polypeptide chains and partially folded intermediates of proteins, preventing their aggregation and misfolding. The folding of most newly synthesized proteins in the cell will involve interaction with one or more chaperones. The chaperones most generally implicated in protein folding are the HSP40 (DnaJ), HSP60 (GroEL), and HSP70 (DnaK) families. Recent investigations using a wide variety of techniques ranging from genetics to biophysics have begun to unravel the complexities of these chaperone machines. At the heart of the general protein folding machinery of the cell are the reaction cycles of HSP60, HSP70, and their cochaperones. For both these chaperone systems, the binding of ATP triggers a critical conformational change ultimately leading to release of the bound substrate protein. Although both chaperone systems minimize aggregation of newly synthesized proteins, the HSP60 chaperones also facilitate the actual folding process by providing a secluded environment for individual folding molecules and may also promote the unfolding and refolding of misfolded intermediates. Different cellular locations, with their different roles in the production of new proteins, have specific chaperone systems tailored to the demands of the specific location (e.g., ER, mitochondria). Because of the critical nature of chaperones in maintaining orderly functioning of the cell, substantial redundancy is found in that multiple versions of chaperones are usually present. For selected proteins, additional specific chaperones are required for their folding and assembly. Although we now have what appears to be a good picture of the general outline of in vivo chaperone-mediated protein folding, it is clear that there are still a very large number of unanswered questions, especially regarding the molecular details.

REFERENCES

1. ACTON, S. L., D. H. WONG, P. PARHAM, F. M. BRODSKY, AND A. P. JACKSON. Alteration of clathrin light chain expression by transfection and gene disruption. *Mol. Biol. Cell* 4: 647–660, 1993.
2. ANFINSEN, C. B. Principles that govern the folding of protein chains. *Science* 181: 223–230, 1973.
3. ARTIGUES, A., A. IRIARTE, AND M. MARTINEZ-CARRION. Refolding intermediates of acid-unfolded mitochondrial aspartate aminotransferase bind to Hsp70. *J. Biol. Chem.* 272: 16852–16861, 1997.
4. BANECKI, B., AND M. ZYLICZ. Real time kinetics of the DnaK/DnaJ/GrpE molecular chaperone machine action. *J. Biol. Chem.* 271: 6137–6143, 1996.
5. BECKMANN, R. P., L. E. MIZZEN, AND W. J. WELCH. Interaction of Hsp 70 with newly synthesized proteins: implications for protein folding and assembly. *Science* 248: 850–854, 1990.
6. BERGERON, J. J., M. B. BRENNER, D. Y. THOMAS, AND D. B. WILLIAMS. Calnexin: a membrane-bound chaperone of the endoplasmic reticulum. *Trends Biochem. Sci.* 19: 124–128, 1994.
7. BLOND-ELGUINDI, S., S. E. CWIRLA, W. J. DOWER, R. J. LIPSHUTZ, S. R. SPRANG, J. F. SAMBROOK, AND M. J. GETHING. Affinity panning of a library of peptides displayed on bacteriophages reveals the binding specificity of BiP. *Cell* 75: 717–728, 1993.
8. BLUM, P., J. ORY, J. BAUERNFEIND, AND J. KRSKA. Physiological consequences of DnaK and DnaJ overproduction in *E. coli*. *J. Bacteriol.* 174: 7436–7444, 1992.
9. BOISVERT, D. C., J. WANG, Z. OTWINOWSKI, A. L. HORWICH, AND P. B. SIGLER. The 2.4 A crystal structure of the bacterial chaperonin GroEL complexed with ATP-γ-S. *Nature Struct. Biol.* 3: 170–177, 1996.
10. BOSE, S., T. WEIKL, H. BUGL, AND J. BUCHNER. Chaperone

function of Hsp90-associated proteins. *Science* 274: 1715–1717, 1996.

11. BOSTON, R. S., P. V. VIITANEN, AND E. VIERLING. Molecular chaperones and protein folding in plants. *Plant Mol. Biol.* 32: 191–222, 1996.

12. BRAIG, K., Z. OTWINOWSKI, R. HEGDE, D. C. BOISVERT, A. JOACHIMIAK, A. L. HORWICH, AND P. B. SIGLER. The crystal structure of the bacterial chaperonin GroEL at 2.8 A. *Nature* 371: 578–586, 1994.

13. BRAMHALL, E. A., R. L. CROSS, S. ROSPERT, N. K. STEEDE, AND S. J. LANDRY. Identification of amino acid residues at nucleotide-binding sites of chaperonin GroEL/GroES and cpn10 by photoaffinity labeling with 2-azido-adenosine 5′-triphosphate. *Eur. J. Biochem.* 244: 627–634, 1997.

14. BRODSKY, J. L. Translocation of proteins across the endoplasmic reticulum membrane. *Int. Rev. Cytol.* 178: 277–328, 1998.

15. BRUCE, B. D., AND J. CHURCHICH. Characterization of the molecular-chaperone function of the heat-shock-cognate-70-interacting protein. *Eur. J. Biochem.* 245: 738–744, 1997.

16. BUCHBERGER, A., H. SCHRODER, T. HESTERKAMP, H. J. SCHONFELD, AND B. BUKAU. Substrate shuttling between the DnaK and GroEL systems indicates a chaperone network promoting protein folding. *J. Mol. Biol.* 261: 328–333, 1996.

17. BUCHBERGER, A., H. THEYSSEN, H. SCHRODER, J. S. McCARTY, G. VIRGALLITA, P. MILKEREIT, J. REINSTEIN, AND B. BUKAU. Nucleotide-induced conformational changes in the ATPase and substrate binding domains of the DnaK chaperone provide evidence for interdomain communication. *J. Biol. Chem.* 270: 16903–16910, 1995.

18. BUCHBERGER, A., A. VALENCIA, R. McMACKEN, C. SANDER, AND B. BUKAU. The chaperone function of DnaK requires the coupling of ATPase activity with substrate binding through residue E171. *EMBO J.* 13: 1687–1695, 1994.

19. BUCHNER, J. Supervising the fold: functional principles of molecular chaperones. *FASEB J.* 10: 10–19, 1996.

20. BURSTON, S. G., AND A. R. CLARKE. Molecular chaperones: physical and mechanistic properties. *Essays Biochem.* 29: 125–136, 1995.

21. BURSTON, S. G., J. S. WEISSMAN, G. W. FARR, W. A. FENTON, AND A. L. HORWICH. Release of both native and non-native proteins from a *cis*-only GroEL ternary complex. *Nature* 383: 96–99, 1996.

22. CAI, H., C. C. WANG, AND C. L. TSOU. Chaperone-like activity of protein disulfide isomerase in the refolding of a protein with no disulfide bonds. *J. Biol. Chem.* 269: 24550–24552, 1994.

23. CAPLAN, A. J., D. M. CYR, AND M. G. DOUGLAS. Eukaryotic homologues of *Escherichia-coli* DnaJ: a diverse protein family that functions with Hsp70 stress proteins. *Mol. Biol. Cell* 4: 555–563, 1993.

24. CHAN, C. K., Y. HU, S. TAKAHASHI, D. L. ROUSSEAU, W. A. EATON, AND J. HOFRICHTER. Submillisecond protein folding kinetics studied by ultrarapid mixing. *Proc. Natl. Acad. Sci. USA* 94: 1779–1784, 1997.

25. CHAN, H. S., AND K. A. DILL. A simple model of chaperonin-mediated protein folding. *Proteins* 24: 345–351, 1996.

26. CHEN, S., A. M. ROSEMAN, A. S. HUNTER, S. P. WOOD, S. G. BURSTON, N. A. RANSON, A. R. CLARKE, AND H. R. SAIBIL. Location of a folding protein and shape changes in GroEL-GroES complexes imaged by cryo-electron microscopy. *Nature* 371: 261–264, 1994.

27. CHENG, M. Y., F. U. HARTL, J. MARTIN, R. A. POLLOCK, F. KALOUSEK, W. NEUPERT, E. M. HALLBERG, R. L. HALLBERG, AND A. L. HORWICH. Mitochondrial heat-shock protein Hsp60 is essential for assembly of proteins imported into yeast mitochondria. *Nature* 337: 620–625, 1989.

28. CLARKE, A. R., AND J. P. WALTHO. Protein folding and intermediates. *Curr. Opin. Biotechnol.* 8: 400–410, 1997.

29. CLARKE, J., L. S. ITZHAKI, AND A. R. FERSHT. Hydrogen exchange at equilibrium: a short cut for analysing protein- folding pathways? *Trends Biochem. Sci.* 22: 284–287, 1997.

30. COX, J. S., R. E. CHAPMAN, AND P. WALTER. The unfolded protein response coordinates the production of endoplasmic reticulum protein and endoplasmic reticulum membrane. *Mol. Biol. Cell* 8: 1805–1814, 1997.

30a. CREUTZ, C. E., A. LIOU, S. L. SNYDER, A. BROWNAWELL, AND K. WILLISON. Identification of the major chromaffin granule-binding protein, chromobindin A, as the cytosolic chaperonin CCT (chaperonin containing TCP-1). *J. Biol. Chem.* 269: 32035–32038, 1994.

31. CROOKE, E., AND W. WICKNER. Trigger factor: a soluble protein that folds pro-OmpA into a membrane. *Proc. Natl. Acad. Sci. USA* 84: 5216–5220, 1987.

32. CYR, D. M. Cooperation of the molecular chaperone Ydj1 with specific Hsp70 homologs to suppress protein aggregation. *FEBS Lett.* 359: 129–132, 1995.

33. CYR, D. M., AND M. G. DOUGLAS. Differential regulation of Hsp70 subfamilies by the eukaryotic DnaJ homologue Ydj1. *J. Biol. Chem.* 269: 9798–9804, 1994.

34. CYR, D. M., T. LANGER, AND M. G. DOUGLAS. DnaJ-like proteins: molecular chaperones and specific regulators of Hsp70. *Trends Biochem. Sci.* 19: 176–181, 1994.

35. CYR, D. M., X. LU, AND M. G. DOUGLAS. Regulation of Hsp70 function by a eukaryotic DnaJ homolog. *J. Biol. Chem.* 267: 20927–20931, 1992.

36. DARBY, N., AND T. E. CREIGHTON. Probing protein folding and stability using disulfide bonds. *Mol. Biotechnol.* 7: 57–77, 1997.

37. DEBBURMAN, S. K., G. J. RAYMOND, B. CAUGHEY, AND S. LINDQUIST. Chaperone-supervised conversion of prion protein to its protease-resistant form. *Proc. Natl. Acad. Sci. USA* 94: 13938–13943, 1997.

38. DE CROUY-CHANEL, A., M. KOHIYAMA, AND G. RICHARME. A novel function of *Escherichia coli* chaperone DnaJ. Protein-disulfide isomerase. *J. Biol. Chem.* 270: 22669–22672, 1995.

39. DEKKER, P. J., AND N. PFANNER. Role of mitochondrial GrpE and phosphate in the ATPase cycle of matrix Hsp70. *J. Mol. Biol.* 270: 321–327, 1997.

40. DELOCHE, O., W. L. KELLEY, AND C. GEORGOPOULOS. Structure-function analyses of the Ssc1p, Mdj1p, and Mge1p *Saccharomyces cerevisiae* mitochondrial proteins in *Escherichia coli*. *J. Bacteriol.* 179: 6066–6075, 1997.

41. DELOCHE, O., K. LIBEREK, M. ZYLICZ, AND C. GEORGOPOULOS. Purification and biochemical properties of *Saccharomyces cerevisiae* Mdj1p, the mitochondrial DnaJ homologue. *J. Biol. Chem.* 272: 28539–28544, 1997.

42. DEYOUNG, L. R., A. L. FINK, AND K. A. DILL. Aggregation of globular proteins. *Acc. Chem. Res.* 26: 614–620, 1993.

43. DILL, K. A., S. BROMBERG, K. Z. YUE, K. M. FIEBIG, D. P. YEE, P. D. THOMAS, AND H. S. CHAN. Principles of protein folding: a perspective from simple exact models. *Protein Sci.* 4: 561–602, 1995.

44. DILL, K. A., AND H. S. CHAN. From Levinthal to pathways to funnels. *Nature Struct. Biol.* 4: 10–19, 1997.

45. DITTMAR, K. D., AND W. B. PRATT. Folding of the glucocorticoid receptor by the reconstituted Hsp90-based chaperone machinery. The initial Hsp90.p60.Hsp70-dependent step is sufficient for creating the steroid binding conformation. *J. Biol. Chem.* 272: 13047–13054, 1997.

46. EGGERS, D. K., W. J. WELCH, AND W. J. HANSEN. Complexes between nascent polypeptides and their molecular chaperones in the cytosol of mammalian cells. *Mol. Biol. Cell* 8: 1559–1573, 1997.

47. EHRNSPERGER, M., M. GAESTEL, AND J. BUCHNER. Structure and function of small heat-shock proteins. In: *Molecular Chaperones in the Life Cycle of Proteins*, edited by A. L. Fink and Y. Goto. New York: Dekker, 1998, p. 533–575.

48. ELLIS, R. J. The molecular chaperone concept. *Semin. Cell Biol.* 1: 1–9, 1990.

49. ELLIS, R. J. Revisiting the Anfinsen cage. *Folding Design* 1: R9–R15, 1996.

50. ELLIS, R. J., AND F. U. HARTL. Protein folding in the cell: competing models of chaperonin function. *FASEB J.* 10: 20–26, 1996.

51. ENGLANDER, S. W., L. MAYNE, Y. BAI, AND T. R. SOSNICK. Hydrogen exchange: the modern legacy of Linderstrom-Lang. *Protein Sci.* 6: 1101–1109, 1997.

52. FARR, G. W., E. C. SCHARL, R. J. SCHUMACHER, S. SONDEK, AND A. L. HORWICH. Chaperonin-mediated folding in the eukaryotic cytosol proceeds through rounds of release of native and nonnative forms. *Cell* 89: 927–937, 1997.

53. FENTON, W. A., AND A. L. HORWICH. GroEL-mediated protein folding. *Protein Sci.* 6: 743–760, 1997.

54. FENTON, W. A., Y. KASHI, K. FURTAK, AND A. L. HORWICH. Residues in chaperonin GroEL required for polypeptide binding and release. *Nature* 371: 614–619, 1994.

55. FENTON, W. A., J. S. WEISSMAN, AND A. L. HORWICH. Putting a lid on protein folding: structure and function of the co-chaperonin, GroES. *Chem. Biol.* 3: 157–161, 1996.

56. FERSHT, A. R. Nucleation mechanisms in protein folding. *Curr. Opin. Struct. Biol.* 7: 3–9, 1997.

57. FINK, A. L. Compact intermediate states in protein folding. *Annu. Rev. Biophys. Biomol. Struct.* 24: 495–522, 1995.

58. FINK, A. L. The Hsp 70 reaction cycle and its role in protein folding. In: *Molecular Chaperones in the Life Cycle of Proteins*, edited by A. L. Fink and Y. Goto New York: Dekker, 1998, p. 123–150.

59. FINK, A. L. Protein aggregation: folding aggregates, inclusion bodies and amyloid. *Folding Design* 3: R9—R15, 1998.

60. FINK, A. L., AND Y. GOTO (Editors). *Molecular Chaperones in the Life Cycle of Proteins.* New York: Dekker, 1998.

61. FINK, A. L., K. A. OBERG, AND S. SESHADRI. Discrete intermediates vs. molten globule models of protein folding: characterization of partially-folded intermediates of apomyoglobin. *Folding Design* 3: 19–25, 1997.

62. FISHER, M. T., AND X. YUAN. The rates of commitment to renaturation of rhodanese and glutamine synthetase in the presence of the GroE chaperonins. *J. Biol. Chem.* 269: 29598–29601, 1994.

63. FLAHERTY, K. M., C. DELUCA-FLAHERTY, AND D. B. McKAY. Three-dimensional structure of the ATPase fragment of a 70K heat-shock protein. *Nature* 346: 623–628, 1990.

64. FLYNN, G. C., J. POHL, M. T. FLOCCO, AND J. E. ROTHMAN. Peptide-binding specificity of the molecular chaperone BiP. *Nature* 353: 726–730, 1991.

65. FREEDMAN, R. B., T. R. HIRST, AND M. F. TUITE. Protein disulphide isomerase: building bridges in protein folding. *Trends Biochem. Sci.* 19: 331–336, 1994.

66. FREEMAN, B. C., AND R. I. MORIMOTO. The human cytosolic molecular chaperones Hsp90, Hsp70 (Hsc70) and Hdj-1 have distinct roles in recognition of a non-native protein and protein refolding. *EMBO J.* 15: 2969–2979, 1996.

67. FREEMAN, B. C., D. O. TOFT, AND R. I. MORIMOTO. Molecular chaperone machines: chaperone activities of the cyclophilin Cyp-40 and the steroid aporeceptor-associated protein p23. *Science* 274: 1718–1720, 1996.

68. FRYDMAN, J., AND F. U. HARTL. Principles of chaperone-assisted protein folding: differences between in vitro and in vivo mechanisms. *Science* 272: 1497–1502, 1996.

69. FRYDMAN, J., E. NIMMESGERN, H. ERDJUMENT-BROMAGE, J. S. WALL, P. TEMPST, AND F.-U. HARTL. Function in protein folding of TriC, a cytosolic ring complex containing tcp-1 and structurally related subunits. *EMBO J.* 11: 4767–4778, 1992.

70. FRYDMAN, J., E. NIMMESGERN, K. OHTSUKA, AND F. U. HARTL. Folding of nascent polypeptide chains in a high molecular mass assembly with molecular chaperones. *Nature* 370: 111–117, 1994.

71. FUNG, K. L., L. HILGENBERG, N. M. WANG, AND W. J. CHIRICO. Conformations of the nucleotide and polypeptide binding domains of a cytosolic Hsp70 molecular chaperone are coupled. *J. Biol. Chem.* 271: 21559–21565, 1996.

72. GAITANARIS, G. A., A. VYSOKANOV, S. C. HUNG, M. E. GOTTESMAN, AND A. GRAGEROV. Successive action of *Escherichia coli* chaperones in vivo. *Mol. Microbiol.* 14: 861–869, 1994.

73. GAMER, J., H. BUJARD, AND B. BUKAU. Physical interaction between heat shock proteins DnaK, DnaJ, and GrpE and the bacterial heat shock transcription factor-sigma(32). *Cell* 69: 833–842, 1992.

74. GAMER, J., G. MULTHAUP, T. TOMOYASU, J. S. McCARTY, S. RUDIGER, H. J. SCHONFELD, C. SCHIRRA, H. BUJARD, AND B. BUKAU. A cycle of binding and release of the DnaK, DnaJ and GrpE chaperones regulates activity of the *Escherichia coli* heat shock transcription factor sigma32. *EMBO J.* 15: 607–617, 1996.

75. GEORGOPOULOS, C., AND W. J. WELCH. Role of the major heat shock proteins as molecular chaperones. *Annu. Rev. Cell Biol.* 9: 601–634, 1993.

76. GETHING, M. J., AND J. SAMBROOK. Protein folding in the cell. *Nature* 355: 33–45, 1992.

77. GILBERT, H. F. Protein disulfide isomerase and assisted protein folding. *J. Biol. Chem.* 272: 29399–29402, 1997.

78. GLOVER, J. R., E. C. SCHIRMER, M. A. SINGER, AND S. L. LINDQUIST. Hsp104. In: *Molecular Chaperones in the Life Cycle of Proteins*, edited by A. L. Fink and Y. Goto. New York: Dekker, 1998, p. 193–224.

79. GOLDBERG, M. S., J. ZHANG, S. SONDEK, C. R. MATTHEWS, R. O. FOX, AND A. L. HORWICH. Native-like structure of a protein-folding intermediate bound to the chaperonin GroEL. *Proc. Natl. Acad. Sci. USA* 94: 1080–1085, 1997.

80. GRAGEROV, A., AND M. E. GOTTESMAN. Different peptide binding specificities of Hsp70 family members. *J. Mol. Biol.* 241: 133–135, 1994.

81. GRAGEROV, A., E. NUDLER, N. KOMISSAROVA, G. A. GAITANARIS, M. E. GOTTESMAN, AND V. NIKIFOROV. Cooperation of GroEL/GroES and DnaK/DnaJ heat shock proteins in preventing protein misfolding in *Escherichia coli*. *Proc. Natl. Acad. Sci. USA* 89: 10341–10344, 1992.

82. GRENERT, J. P., W. P. SULLIVAN, P. FADDEN, T. A. J. HAYSTEAD, J. CLARK, E. MIMNAUGH, H. KRUTZSCH, H. J. OCHEL, T. W. SCHULTE, E. SAUSVILLE, L. M. NECKERS, AND D. O. TOFT. The amino-terminal domain of heat shock protein 90 (hsp90) that binds geldanamycin is an ATP/ADP switch domain that regulates hsp90 conformation. *J. Biol. Chem.* 272: 23843–23850, 1997.

83. HA, J.-H., E. R. JOHNSON, D. B. McKAY, M. C. SOUSA, S. TAKEDA, AND S. M. WILBANKS. Structure and properties of the 70-kilodalton heat-shock proteins. In: *Molecular Chaperones in the Life Cycle of Proteins*, edited by A. L. Fink and Y. Goto. New York: Dekker, 1998, p. 95–122.

84. HA, J. H., AND D. B. McKAY. Kinetics of nucleotide-induced changes in the tryptophan fluorescence of the molecular chaperone Hsc70 and its subfragments suggest the ATP-induced conformational change follows initial ATP binding. *Biochemistry* 34: 11635–11644, 1995.

85. HAAS, I. G., AND M. WABL. Immunoglobulin heavy chain binding protein. *Nature* 306: 387–389, 1983.

86. HANSEN, W. J., V. R. LINGAPPA, AND W. J. WELCH. Complex environment of nascent polypeptide chains. *J. Biol. Chem.* 269: 26610–26613, 1994.

87. HARDESTY, B., W. KUDLICKI, O. W. ODOM, T. ZHANG, D. McCARTHY, AND G. KRAMER. Cotranslational folding of nascent proteins on *Escherichia coli* ribosomes. *Biochem. Cell Biol.* 73: 1199–1207, 1995.

88. HARDY, S. J., AND L. L. RANDALL. Recognition of ligands by SecB, a molecular chaperone involved in bacterial protein export. *Philos. Trans. R. Soc. Lond. B Biol. Sci.* 339: 343–354, 1993.

89. HARRISON, C. J., M. HAYER-HARTL, M. DI LIBERTO, F. HARTL, AND J. KURIYAN. Crystal structure of the nucleotide exchange factor GrpE bound to the ATPase domain of the molecular chaperone DnaK. *Science* 276: 431–435, 1997.

90. HARTL, F. U. Molecular chaperones in cellular protein folding. *Nature* 381: 571–579, 1996.

91. HAYER-HARTL, M. K., J. MARTIN, AND F. U. HARTL. Asymmetrical interaction of GroEL and GroES in the ATPase cycle of assisted protein folding. *Science* 269: 836–841, 1995.

92. HEBERT, D. N., B. FOELLMER, AND A. HELENIUS. Glucose trimming and reglucosylation determine glycoprotein association with calnexin in the endoplasmic reticulum. *Philos. Trans. R. Soc. Lond. B Biol. Sci.* 348: 107–112, 1995.

93. HEBERT, D. N., J. F. SIMONS, J. R. PETERSON, AND A. HELENIUS. Calnexin, calreticulin, and Bip/Kar2p in protein folding. *Cold Spring Harb. Symp. Quant. Biol.* 60: 405–415, 1995.

94. HENDERSHOT, L., J. WEI, J. GAUT, J. MELNICK, S. AVIEL, AND Y. ARGON. Inhibition of immunoglobulin folding and secretion by dominant negative BiP ATPase mutants. *Proc. Natl. Acad. Sci. USA* 93: 5269–5274, 1996.

95. HENDRICK, J. P., AND F. U. HARTL. Molecular chaperone functions of heat-shock proteins. *Annu. Rev. Biochem.* 62: 349–384, 1993.

96. HENDRICK, J. P., AND F. U. HARTL. The role of molecular chaperones in protein folding. *FASEB J.* 9: 1559–1569, 1995.

97. HENDRICK, J. P., T. LANGER, T. A. DAVIS, F. U. HARTL, AND M. WIEDMANN. Control of folding and membrane translocation by

binding of the chaperone DnaJ to nascent polypeptides. *Proc. Natl. Acad. Sci. USA* 90: 10216–10220, 1993.

98. HESTERKAMP, T., AND B. BUKAU. The *Escherichia coli* trigger factor. *FEBS Lett.* 389: 32–34, 1996.

99. HESTERKAMP, T., S. HAUSER, H. LUTCKE, AND B. BUKAU. *Escherichia coli* trigger factor is a prolyl isomerase that associates with nascent polypeptide chains. *Proc. Natl. Acad. Sci. USA* 93: 4437–4441, 1996.

100. HIGHTOWER, L. E., AND S.-M. LEUNG. Substrate-binding specificty of the Hsp70 family. In: *Molecular Chaperones in the Life Cycle of Proteins*, edited by A. L. Fink and Y. Goto. New York: Dekker, 1998, p. 151–168.

101. HILL, R. B., J. M. FLANAGAN, AND J. H. PRESTEGARD. ^{1}H and ^{15}N magnetic resonance assignments, secondary structure, and tertiary fold of *Escherichia coli* DnaJ(1–78). *Biochemistry* 34: 5587–5596, 1995.

102. HOFFMANN, H. J., S. K. LYMAN, C. LU, M. A. PETIT, AND H. ECHOLS. Activity of the Hsp70 chaperone complex–DnaK, DnaJ, and GrpE–in initiating phage lambda DNA replication by sequestering and releasing lambda P protein. *Proc. Natl. Acad. Sci. USA* 89: 12108–12111, 1992.

103. HOHFELD, J., AND S. JENTSCH. GrpE-like regulation of the Hsc70 chaperone by the anti-apoptotic protein BAG-1. *EMBO J.* 16: 6209–6216, 1997.

104. HOHFELD, J., Y. MINAMI, AND F. U. HARTL. Hip, a novel cochaperone involved in the eukaryotic Hsc70/Hsp40 reaction cycle. *Cell* 83: 589–598, 1995.

105. HOROWITZ, P. M. Some structural aspects of chaperonin-assisted folding by GroEL and GroES. In: *Molecular Chaperones in the Life Cycle of Proteins*, edited by A. L. Fink and Y. Goto. New York: Dekker, 1998, p. 275–300.

106. HORST, M., W. OPPLIGER, S. ROSPERT, H. J. SCHONFELD, G. SCHATZ, AND A. AZEM. Sequential action of two Hsp70 complexes during protein import into mitochondria. *EMBO J.* 16: 1842–1849, 1997.

107. HORWICH, A. L., K. B. LOW, W. A. FENTON, I. N. HIRSHFIELD, AND K. FURTAK. Folding in vivo of bacterial cytoplasmic proteins: role of GroEL. *Cell* 74: 909–917, 1993.

108. HORWICH, A. L., AND K. R. WILLISON. Protein folding in the cell: functions of two families of molecular chaperone, Hsp 60 and TF55-TCP1. *Philos. Trans. R. Soc. Lond. B Biol. Sci.* 339: 313–325, 1993.

109. HU, G., T. GURA, B. SABSAY, J. SAUK, S. N. DIXIT, AND A. VEIS. Endoplasmic reticulum protein Hsp47 binds specifically to the N-terminal globular domain of the amino-propeptide of the procollagen I alpha 1 (I)-chain. *J. Cell Biochem.* 59: 350–367, 1995.

110. HUNT, J. F., A. J. WEAVER, S. J. LANDRY, L. GIERASCH, AND J. DEISENHOFER. The crystal structure of the GroES co-chaperonin at 2.8 Å resolution. *Nature* 379: 37–45, 1996.

111. INBAR, E., AND A. HOROVITZ. GroES promotes the T to R transition of the GroEL ring distal to GroES in the GroEL-GroES complex. *Biochemistry* 36: 12276–12281, 1997.

112. JAENICKE, R. Folding and association versus misfolding and aggregation of proteins. *Philos. Trans. R. Soc. Lond. B Biol. Sci.* 348: 97–105, 1995.

113. JAKOB, U., AND J. BUCHNER. Assisting spontaneity: the role of Hsp90 and small Hsps as molecular chaperones. *Trends Biochem. Sci.* 19: 205–211, 1994.

114. JOHNSON, B. D., R. J. SCHUMACHER, E. D. ROSS, AND D. O. TOFT. Hop modulates Hsp70/Hsp90 interactions in protein folding. *J. Biol. Chem.* 273: 3679–3686, 1998.

115. KAMATH-LOEB, A. S., C. Z. LU, W. C. SUH, M. A. LONETTO, AND C. A. GROSS. Analysis of three DnaK mutant proteins suggests that progression through the ATPase cycle requires conformational changes. *J. Biol. Chem.* 270: 30051–30059, 1995.

116. KANDROR, O., M. SHERMAN, R. MOERSCHELL, AND A. L. GOLDBERG. Trigger factor associates with GroEL in vivo and promotes its binding to certain polypeptides. *J. Biol. Chem.* 272: 1730–1734, 1997.

117. KARZAI, A. W., AND R. McMACKEN. A bipartite signaling mechanism involved in DnaJ-mediated activation of the *Escherichia coli* DnaK protein. *J. Biol. Chem.* 271: 11236–11246, 1996.

118. KIMURA, Y., I. YAHARA, AND S. LINDQUIST. Role of the protein

chaperone YDJ1 in establishing Hsp90-mediated signal transduction pathways. *Science* 268: 1362–1365, 1995.

119. KRAUSE, K. H., AND M. MICHALAK. Calreticulin. *Cell* 88: 439–443, 1997.

121. KUBOTA, H., G. HYNES, A. CARNE, A. ASHWORTH, AND K. WILLISON. Identification of six Tcp-1-related genes encoding divergent subunits of the TCP-1-containing chaperonin. *Curr. Biol.* 4: 89–99, 1994.

122. KUBOTA, H., G. HYNES, AND K. WILLISON. The chaperonin containing t-complex polypeptide 1 (TCP-1). Multisubunit machinery assisting in protein folding and assembly in the eukaryotic cytosol. *Eur. J. Biochem.* 230: 3–16, 1995.

123. KUDLICKI, W., J. CHIRGWIN, G. KRAMER, AND B. HARDESTY. Folding of an enzyme into an active conformation while bound as peptidyl-tRNA to the ribosome. *Biochemistry* 34: 14284–14287, 1995.

124. KUDLICKI, W., O. W. ODOM, G. KRAMER, AND B. HARDESTY. Chaperone-dependent folding and activation of ribosome-bound nascent rhodanese. Analysis by fluorescence. *J. Mol. Biol.* 244: 319–331, 1994.

125. KUDLICKI, W., O. W. ODOM, G. KRAMER, AND B. HARDESTY. Binding of an N-terminal rhodanese peptide to DnaJ and to ribosomes. *J. Biol. Chem.* 271: 31160–31166, 1996.

126. KUDLICKI, W., O. W. ODOM, G. KRAMER, B. HARDESTY, G. A. MERRILL, AND P. M. HOROWITZ. The importance of the N-terminal segment for DnaJ-mediated folding of rhodanese while bound to ribosomes as peptidyl-tRNA. *J. Biol. Chem.* 270: 10650–10657, 1995.

127. KUEHN, M. J., D. J. OGG, J. KIHLBERG, L. N. SLONIM, K. FLEMMER, T. BERGFORS, AND S. J. HULTGREN. Structural basis of pilus subunit recognition by the PapD chaperone. *Science* 262: 1234–1241, 1993.

128. LANDRY, S. J., A. TAHER, C. GEORGOPOULOS, AND S. M. VAN DER VIES. Interplay of structure and disorder in cochaperonin mobile loops. *Proc. Natl. Acad. Sci. USA* 93: 11622–11627, 1996.

129. LANDRY, S. J., J. ZEILSTRA-RYALLS, O. FAYET, C. GEORGOPOULOS, AND L. M. GIERASCH. Characterization of a functionally important mobile domain of GroES. *Nature* 364: 255–258, 1993.

130. LANGER, T., C. LU, H. ECHOLS, J. FLANAGAN, M. K. HAYER, AND F.-U. HARTL. Successive action of DnaK, DnaJ and GroEL along the pathway of chaperone-mediated protein folding. *Nature* 356: 683–689, 1992.

131. LAUFEN, T., U. ZUBER, A. BUCHBERGER, AND B. BUKAU. DnaJ proteins In: *Molecular Chaperones in the Life Cycle of Proteins*, edited by A. L. Fink and Y. Goto. New York: Dekker, 1998, p. 241–274.

132. LEE, D. H., M. Y. SHERMAN, AND A. L. GOLDBERG. Involvement of the molecular chaperone Ydj1 in the ubiquitin-dependent degradation of short-lived and abnormal proteins in *Saccharomyces cerevisiae*. *Mol. Cell. Biol.* 16: 4773–4781, 1996.

133. LEE, G. J., A. M. ROSEMAN, H. R. SAIBIL, AND E. VIERLING. A small heat shock protein stably binds heat-denatured model substrates and can maintain a substrate in a folding-competent state. *EMBO J.* 16: 659–671, 1997.

134. LEROUX, M. R., R. MELKI, B. GORDON, G. BATELIER, AND E. P. CANDIDO. Structure-function studies on small heat shock protein oligomeric assembly and interaction with unfolded polypeptides. *J. Biol. Chem.* 272: 24646–24656, 1997.

135. LEUNG, S. M., AND L. E. HIGHTOWER. A 16-kDa protein functions as a new regulatory protein for Hsc70 molecular chaperone and is identified as a member of the Nm23/nucleoside diphosphate kinase family. *J. Biol. Chem.* 272: 2607–2614, 1997.

136. LIBEREK, K., C. GEORGOPOULOS, AND M. ZYLICZ. Role of the *Escherichia coli* DnaK and DnaJ heat shock proteins in the initiation of bacteriophage lambda DNA replication. *Proc. Natl. Acad. Sci. USA* 85: 6632–6636, 1988.

137. LIBEREK, K., J. MARSZALEK, D. ANG, C. GEORGOPOULOS, AND M. ZYLICZ. *Escherichia coli* DnaJ and GrpE heat shock proteins jointly stimulate ATPase activity of DnaK. *Proc. Natl. Acad. Sci. USA* 88: 2874–2878, 1991.

138. LILIE, H., AND J. BUCHNER. Interaction of GroEL with a highly structured folding intermediate: iterative binding cycles do not involve unfolding. *Proc. Natl. Acad. Sci. USA* 92: 8100–8104, 1995.

139. LIN, Z., AND E. EISENSTEIN. Nucleotide binding-promoted conformational changes release a nonnative polypeptide from the *Escherichia coli* chaperonin GroEL. *Proc. Natl. Acad. Sci. USA* 93: 1977–1981, 1996.

140. LLORCA, O., S. MARCO, J. L. CARRASCOSA, AND J. M. VALPUESTA. Conformational changes in the GroEL oligomer during the functional cycle. *J. Struct. Biol.* 118: 31–42, 1997.

141. LLOSA, M., K. ALORIA, R. CAMPO, R. PADILLA, J. AVILA, L. SANCHEZ-PULIDO, AND J. C. ZABALA. The beta-tubulin monomer release factor (p14) has homology with a region of the DnaJ protein. *FEBS Lett.* 397: 283–289, 1996.

142. LORIMER, G. H. A quantitative assessment of the role of the chaperonin proteins in protein folding in vivo. *FASEB J.* 10: 5–9, 1996.

143. LUZ, J. M., AND W. J. LENNARZ. Protein disulfide isomerase: a multifunctional protein of the endoplasmic reticulum. *EXS* 77: 97–117, 1996.

144. MARTIN, J., AND F. U. HARTL. Chaperone-assisted protein folding. *Curr. Opin. Struct. Biol.* 7: 41–52, 1997.

145. MARTIN, J., M. MAYHEW, T. LANGER, AND F. U. HARTL. The reaction cycle of GroEL and GroES in chaperonin-assisted protein folding. *Nature* 366: 228–233, 1993.

146. McCARTY, J. S., A. BUCHBERGER, J. REINSTEIN, AND B. BUKAU. The role of ATP in the functional cycle of the DnaK chaperone system. *J. Mol. Biol.* 249: 126–137, 1995.

147. MINAMI, Y., J. HOHFELD, K. OHTSUKA, AND F. U. HARTL. Regulation of the heat-shock protein 70 reaction cycle by the mammalian DnaJ homolog, Hsp40. *J. Biol. Chem.* 271: 19617–19624, 1996.

148. MITRAKI, A., B. FANE, C. HAASE-PETTINGELL, J. STURTEVANT, AND J. KING. Global suppression of protein folding defects and inclusion body formation. *Science* 253: 54–58, 1991.

149. MORI, K., T. KAWAHARA, H. YOSHIDA, H. YANAGI, AND T. YURA. Signalling from endoplasmic reticulum to nucleus: transcription factor with a basic-leucine zipper motif is required for the unfolded protein-response pathway. *Genes Cells* 1: 803–817, 1996.

150. MORIMOTO, R. I., A. TISSIERES, AND C. GEORGOPOULOS (Editors). *Progress and Perspectives on the Biology of Heat Shock Proteins and Molecular Chaperones.* Cold Spring Harbor, NY: Cold Spring Harbor Laboratory, 1994, p. 1–30.

151. MUNRO, S., AND H. R. PELHAM. An Hsp70-like protein in the ER: identity with the 78 kd glucose-regulated protein and immunoglobulin heavy chain binding protein. *Cell* 46: 291–300, 1986.

152. NAGATA, K., M. SATOH, A. D. MILLER, AND N. HOSOKAWA. Involvement of Hsp47 in the folding and processing of procollagen in the endoplasmic reticulum. In: *Molecular Chaperones in the Life Cycle of Proteins*, edited by A. L. Fink and Y. Goto. New York: Dekker, 1998, p. 225–240.

153. NATHAN, D. F., M. H. VOS, AND S. LINDQUIST. In vivo functions of the *Saccharomyces cerevisiae* Hsp90 chaperone. *Proc. Natl. Acad. Sci. USA* 94: 12949–12956, 1997.

154. NELSON, R. J., T. ZIEGELHOFFER, C. NICOLET, M. WERNER-WASHBURNE, AND E. A. CRAIG. The translation machinery and 70 kd heat shock protein cooperate in protein synthesis. *Cell* 71: 97–105, 1992.

155. NETZER, W. J., AND F. U. HARTL. Recombination of protein domains facilitated by co-translational folding in eukaryotes. *Nature* 388: 343–349, 1997.

156. NEUPERT, W. Protein import into mitochondria. *Annu. Rev. Biochem.* 66: 863–917, 1997.

157. NIEBA, L., S. E. NIEBA-AXMANN, A. PERSSON, M. HAMALAINEN, F. EDEBRATT, A. HANSSON, J. LIDHOLM, K. MAGNUSSON, A. F. KARLSSON, AND A. PLUCKTHUN. BIACORE analysis of histidine-tagged proteins using a chelating NTA sensor chip. *Anal. Biochem.* 252: 217–228, 1997.

158. NIEBA-AXMANN, S. E., M. OTTIGER, K. WUTHRICH, AND A. PLUCKTHUN. Multiple cycles of global unfolding of GroEL-bound cyclophilin A evidenced by NMR. *J. Mol. Biol.* 271: 803–818, 1997.

159. NIGAM, S. K., A. L. GOLDBERG, S. HO, M. F. ROHDE, K. T. BUSH, AND M. Y. U. SHERMAN. A set of endoplasmic reticulum proteins possessing properties of molecular chaperones includes Ca^{2+}-binding proteins and members of the thioredoxin superfamily. *J. Biol. Chem.* 269: 1744–1749, 1994.

160. NIMMESGERN, E., AND F. U. HARTL. ATP-dependent protein re-

folding activity in reticulocyte lysate. Evidence for the participation of different chaperone components. *FEBS Lett.* 331: 25–30, 1993.

161. OBERMOELLER, L. M., I. WARSHAWSKY, M. R. WARDELL, G. BU, AND R. RAPPUOLI. Differential functions of triplicated repeats suggest two independent roles for the receptor-associated protein as a molecular chaperone. Efficient production of heat-labile enterotoxin mutant proteins by overexpression of dsbA in a degP-deficient *Escherichia coli* strain. *Arch. Microbiol.* 167: 280–283, 1997.

162. OU, W. J., P. H. CAMERON, D. Y. THOMAS, AND J. J. BERGERON. Association of folding intermediates of glycoproteins with calnexin during protein maturation. *Virology* 193: 545–562, 1993.

163. PACKSCHIES, L., H. THEYSSEN, A. BUCHBERGER, B. BUKAU, R. S. GOODY, AND J. REINSTEIN. GrpE accelerates nucleotide exchange of the molecular chaperone DnaK with an associative displacement mechanism. *Biochemistry* 36: 3417–3422, 1997.

164. PAHL, A., K. BRUNE, AND H. BANG. Fit for life? Evolution of chaperones and folding catalysts parallels the development of complex organisms. *Cell Stress Chaperones* 2: 78–86, 1997.

165. PALLEROS, D. R., K. L. REID, J. S. McCARTY, G. C. WALKER, AND A. L. FINK. Dnak, Hsp73, and their molten globules. Two different ways heat shock proteins respond to heat. *J. Biol. Chem.* 267: 5279–5285, 1992.

166. PALLEROS, D. R., K. L. REID, L. SHI, W. J. WELCH, AND A. L. FINK. ATP-induced protein Hsp70 complex dissociation requires K⁺ but not ATP hydrolysis. *Nature* 365: 664–666, 1993.

167. PALLEROS, D. R., L. SHI, K. L. REID, AND A. L. FINK. Hsp70-protein complexes. Complex stability and conformation of bound substrate protein. *J. Biol. Chem.* 269: 13107–13114, 1994.

168. PALLEROS, D. R., W. J. WELCH, AND A. L. FINK. Interaction of hsp70 with unfolded proteins: effects of temperature and nucleotides on the kinetics of binding. *Proc. Natl. Acad. Sci. USA* 88: 5719–5723, 1991.

169. PANAGIOTIDIS, C. A., W. F. BURKHOLDER, G. A. GAITANARIS, A. GRAGEROV, M. E. GOTTESMAN, AND S. J. SILVERSTEIN. Inhibition of DnaK autophosphorylation by heat shock proteins and polypeptide substrates. *J. Biol. Chem.* 269: 16643–16647, 1994.

170. PARSELL, D. A., A. S. KOWAL, M. A. SINGER, AND S. LINDQUIST. Protein disaggregation mediated by heat-shock protein Hsp104. *Nature* 372: 475–478, 1994.

171. PELLECCHIA, M., T. SZYPERSKI, D. WALL, C. GEORGOPOULOS, AND K. WUTHRICH. NMR structure of the J-domain and the Gly/Phe-rich region of the *Escherichia coli* DnaJ chaperone. *J. Mol. Biol.* 260: 236–250, 1996.

172. PETERSON, J. R., A. ORA, P. N. VAN, AND A. HELENIUS. Transient, lectin-like association of calreticulin with folding intermediates of cellular and viral glycoproteins. *Mol. Biol. Cell* 6: 1173–1184, 1995.

173. PETIT, M. A., W. BEDALE, J. OSIPIUK, C. LU, M. RAJAGOPALAN, P. McINERNEY, M. F. GOODMAN, AND H. ECHOLS. Sequential folding of UmuC by the Hsp70 and Hsp60 chaperone complexes of *Escherichia coli*. *J. Biol. Chem.* 269: 23824–23829, 1994.

174. PIERPAOLI, E. V., E. SANDMEIER, A. BAICI, H. J. SCHONFELD, S. GISLER, AND P. CHRISTEN. The power stroke of the DnaK/DnaJ/GrpE molecular chaperone system. *J. Mol. Biol.* 269: 757–768, 1997.

175. PRATT, W. B. The role of the Hsp90-based chaperone system in signal transduction by nuclear receptors and receptors signaling via MAP kinase. *Annu. Rev. Pharmacol. Toxicol.* 37: 297–326, 1997.

176. PRIMM, T. P., K. W. WALKER, AND H. F. GILBERT. Facilitated protein aggregation. Effects of calcium on the chaperone and anti-chaperone activity of protein disulfide-isomerase. *J. Biol. Chem.* 271: 33664–33669, 1996.

177. PRIVALOV, P. L. Intermediate states in protein folding. *J. Mol. Biol.* 258: 707–725, 1996.

178. PRODROMOU, C., S. M. ROE, R. O'BRIEN, J. E. LADBURY, P. W. PIPER, AND L. H. PEARL. Identification and structural characterization of the ATP/ADP-binding site in the Hsp90 molecular chaperone. *Cell* 90: 65–75, 1997.

179. PRODROMOU, C., S. M. ROE, P. W. PIPER, AND L. H. PEARL. A molecular clamp in the crystal structure of the N-terminal domain of the yeast Hsp90 chaperone. *Nature Struct. Biol.* 4: 477–482, 1997.

180. PUIG, A., AND H. F. GILBERT. Anti-chaperone behavior of BiP

during the protein disulfide isomerase-catalyzed refolding of reduced denatured lysozyme. *J. Biol. Chem.* 269: 25889–25896, 1994.

181. QIAN, Y. Q., D. PATEL, F. U. HARTL, AND D. J. McCOLL. Nuclear magnetic resonance solution structure of the human Hsp40 (HDJ-1) J-domain. *J. Mol. Biol.* 260: 224–235, 1996.

182. RANSON, N. A., S. G. BURSTON, AND A. R. CLARKE. Binding, encapsulation and ejection: substrate dynamics during a chaperonin-assisted folding reaction. *J. Mol. Biol.* 266: 656–664, 1997.

183. RANSON, N. A., N. J. DUNSTER, S. G. BURSTON, AND A. R. CLARKE. Chaperonins can catalyse the reversal of early aggregation steps when a protein misfolds. *J. Mol. Biol.* 250: 581–586, 1995.

184. REID, B. G., AND G. C. FLYNN. GroEL binds to and unfolds rhodanese posttranslationally. *J. Biol. Chem.* 271: 7212–7217, 1996.

185. REID, K. L., AND A. L. FINK. Physical interactions between members of the DnaK chaperone machinery: characterization of the DnaK-GrpE complex. *Cell Stress Chaperones* 1: 127–137, 1996.

186. RODER, H., AND W. COLON. Kinetic role of early intermediates in protein folding. *Curr. Opin. Struct. Biol.* 7: 15–28, 1997.

187. ROMMELAERE, H., M. VAN TROYS, Y. GAO, R. MELKI, N. J. COWAN, J. VANDEKERCKHOVE, AND C. AMPE. Eukaryotic cytosolic chaperonin contains T-complex polypeptide 1 and seven related subunits. *Proc. Natl. Acad. Sci. USA* 90: 11975–11979, 1993.

188. ROSEMAN, A. M., S. CHEN, H. WHITE, K. BRAIG, AND H. R. SAIBIL. The chaperonin ATPase cycle: mechanism of allosteric switching and movements of substrate-binding domains in GroEL. *Cell* 87: 241–251, 1996.

189. ROWLEY, N., C. PRIP-BUUS, B. WESTERMANN, C. BROWN, E. SCHWARZ, B. BARRELL, AND W. NEUPERT. Mdj1p, a novel chaperone of the DnaJ family, is involved in mitochondrial biogenesis and protein folding. *Cell* 77: 249–259, 1994.

190. RUDDON, R. W., AND E. BEDOWS. Assisted protein folding. *J. Biol. Chem.* 272: 3125–3128, 1997.

191. RUDIGER, S., A. BUCHBERGER, AND B. BUKAU. Interaction of Hsp70 chaperones with substrates. *Nature Struct. Biol.* 4: 342–349, 1997.

192. RUDIGER, S., L. GERMEROTH, J. SCHNEIDER-MERGENER, AND B. BUKAU. Substrate specificity of the DnaK chaperone determined by screening cellulose-bound peptide libraries. *EMBO J.* 16: 1501–1507, 1997.

193. RYAN, M. T., D. J. NAYLOR, P. B. HOJ, M. S. CLARK, AND N. J. HOOGENRAAD. The role of molecular chaperones in mitochondrial protein import and folding. *Int. Rev. Cytol.* 174: 127–193, 1997.

194. RYE, H. S., S. G. BURSTON, W. A. FENTON, J. M. BEECHEM, Z. XU, P. B. SIGLER, AND A. L. HORWICH. Distinct actions of *cis* and *trans* ATP within the double ring of the chaperonin GroEL. *Nature* 388: 792–798, 1997.

195. SADIS, S., AND L. E. HIGHTOWER. Unfolded proteins stimulate molecular chaperone Hsc70 ATPase by accelerating ADP/ATP exchange. *Biochemistry* 31: 9406–9412, 1992.

196. SAIBIL, H. R. What can electron microscopy tell us about chaperoned protein folding? *Folding Design* 1: R45–R49, 1996.

197. SAX, C. M., AND J. PIATIGORSKY. Expression of the alpha-crystallin/small heat-shock protein/molecular. *Adv. Enzymol. Related Areas Mol. Biol.* 69: 155–201, 1994.

198. SCHLENSTEDT, G., S. HARRIS, B. RISSE, R. LILL, AND P. A. SILVER. A yeast DnaJ homologue, Scj1p, can function in the endoplasmic. *J. Cell Biol.* 129: 979–988, 1995.

199. SCHMID, D., A. BAICI, H. GEHRING, AND P. CHRISTEN. Kinetics of molecular chaperone action. *Science* 263: 971–973, 1994.

200. SCHMID, F. X. Catalysis of protein folding by prolyl isomerases In: *Molecular Chaperones in the Life Cycle of Proteins*, edited by A. L. Fink and Y. Goto. New York: Dekker, 1998, p. 361–389.

201. SCHOLZ, C., G. STOLLER, T. ZARNT, G. FISCHER, AND F. X. SCHMID. Cooperation of enzymatic and chaperone functions of trigger factor in the catalysis of protein folding. *J. Bioenerg. Biomembr.* 29: 35–43, 1997.

202. SCHONFELD, H. J., D. SCHMIDT, H. SCHRODER, AND B. BUKAU. The DnaK chaperone system of *Escherichia coli*: quaternary structures and interactions of the DnaK and GrpE components. *J. Biol. Chem.* 270: 2183–2189, 1995.

203. SCHRODER, H., T. LANGER, F. U. HARTL, AND B. BUKAU. DnaK, DnaJ and GrpE form a cellular chaperone machinery capable of

204. SCHUMACHER, R. J., W. J. HANSEN, B. C. FREEMAN, E. AL-NEMRI, G. LITWACK, AND D. O. TOFT. Cooperative action of Hsp70, Hsp90, and DnaJ proteins in protein renaturation. *Biochemistry* 35: 14889–14898, 1996.

205. SCHUMACHER, R. J., R. HURST, W. P. SULLIVAN, N. J. McMAHON, D. O. TOFT, AND R. L. MATTS. ATP-dependent chaperoning activity of reticulocyte lysate. *J. Biol. Chem.* 269: 9493–9499, 1994.

206. SECKLER, R. Assembly of oligomers and multisubunit structures. In: *Molecular Chaperones in the Life Cycle of Proteins*, edited by A. L. Fink and Y. Goto. New York: Dekker, 1998, p. 391–413.

207. SFATOS, C. D., A. M. GUTIN, V. I. ABKEVICH, AND E. I. SHAKH-NOVICH. Simulations of chaperone-assisted folding. *Biochemistry* 35: 334–339, 1996.

208. SILOW, M., AND M. OLIVEBERG. High-energy channeling in protein folding. *Biochemistry* 36: 7633–7637, 1997.

209. SONG, J. L., AND C. C. WANG. Chaperone-like activity of protein disulfide-isomerase in the refolding of rhodanese. *Eur. J. Biochem.* 231: 312–316, 1995.

210. SOSNICK, T. R., L. MAYNE, R. HILLER, AND S. W. ENGLANDER. The barriers in protein folding. *Nature Struct. Biol.* 1: 149–156, 1994.

211. SPARRER, H., AND J. BUCHNER. How GroES regulates binding of nonnative protein to GroEL. *J. Biol. Chem.* 272: 14080–14086, 1997.

212. SPARRER, H., H. LILIE, AND J. BUCHNER. Dynamics of the GroEL-protein complex: effects of nucleotides and folding mutants. *J. Mol. Biol.* 258: 74–87, 1996.

213. SPARRER, H., K. RUTKAT, AND J. BUCHNER. Catalysis of protein folding by symmetric chaperone complexes. *Proc. Natl. Acad. Sci. USA* 94: 1096–1100, 1997.

214. SRIRAM, M., J. OSIPIUK, B. FREEMAN, R. MORIMOTO, AND A. JOACHIMIAK. Human Hsp70 molecular chaperone binds two calcium ions within the ATPase domain. *Structure* 5: 403–414, 1997.

215. STERNLICHT, H., G. W. FARR, M. L. STERNLICHT, J. K. DRISCOLL, K. WILLISON, AND M. B. YAFFE. The T-complex polypeptide 1 complex is a chaperonin for tubulin and actin in vivo. *Proc. Natl. Acad. Sci. USA* 90: 9422–9426, 1993.

216. STOLDT, V., F. RADEMACHER, V. KEHREN, J. F. ERNST, D. A. PEARCE, AND F. SHERMAN. Review: the CCT eukaryotic chaperonin subunits of *Saccharomyces cerevisiae* and other yeasts. *Yeast* 12: 523–529, 1996.

217. STRAUS, D., W. WALTER, AND C. A. GROSS. Dnak, DnaJ, and GrpE heat shock proteins negatively regulate heat shock gene expression by controlling the synthesis and stability of sigma 32. *Genes Dev.* 4: 2202–2209, 1990.

218. STRICKLAND, E., B. H. QU, L. MILLEN, AND P. J. THOMAS. The molecular chaperone Hsc70 assists the in vitro folding of the N-terminal nucleotide-binding domain of the cystic fibrosis transmembrane conductance regulator. *J. Biol. Chem.* 272: 25421–25424, 1997.

219. SUH, K., C. A. GABEL, AND J. E. BERGMANN. Identification of a novel mechanism for the removal of glucose residues. *J. Biol. Chem.* 267: 21671–21677, 1992.

220. SZABO, A., R. KORSZUN, F. U. HARTL, AND J. FLANAGAN. A zinc finger-like domain of the molecular chaperone DnaJ is involved in binding to denatured protein substrates. *EMBO J.* 15: 408–417, 1996.

221. SZABO, A., T. LANGER, H. SCHRODER, J. FLANAGAN, B. BUKAU, AND F. U. HARTL. The ATP hydrolysis-dependent reaction cycle of the *Escherichia coli* Hsp70 system DnaK, DnaJ, and GrpE. *Proc. Natl. Acad. Sci. USA* 91: 10345–10349, 1994.

222. SZYPERSKI, T., M. PELLECCHIA, D. WALL, C. GEORGOPOULOS, AND K. WUTHRICH. NMR structure determination of the *Escherichia coli* DnaJ molecular chaperone: secondary structure and backbone fold of the N-terminal region (residues 2–108) containing the highly conserved J domain. *Proc. Natl. Acad. Sci. USA* 91: 11343–11347, 1994.

223. TAKAYAMA, S., D. N. BIMSTON, S. MATSUZAWA, B. C. FREEMAN, C. AIME-SEMPE, Z. XIE, R. I. MORIMOTO, AND J. C. REED. BAG-1 modulates the chaperone activity of Hsp70/Hsc70. *EMBO J.* 16: 4887–4896, 1997.

224. TAKEDA, S., AND D. B. McKAY. Kinetics of peptide binding to the

bovine 70 kDa heat shock cognate protein, a molecular chaperone. *Biochemistry* 35: 4636–4644, 1996.

225. TAKENAKA, I. M., S. M. LEUNG, S. J. McANDREW, J. P. BROWN, AND L. E. HIGHTOWER. Hsc70-binding peptides selected from a phage display peptide library that resemble organellar targeting sequences. *J. Biol. Chem.* 270: 19839–19844, 1995.

226. TAVARIA, M., T. GABRIELE, I. KOLA, AND R. L. ANDERSON. A hitchhiker's guide to the human Hsp70 family. *Cell Stress Chaperones* 1: 23–28, 1996.

227. THEYSSEN, H., H. P. SCHUSTER, L. PACKSCHIES, B. BUKAU, AND J. REINSTEIN. The second step of ATP binding to DnaK induces peptide release. *J. Mol. Biol.* 263: 657–670, 1996.

228. THOMAS, J. G., A. AYLING, AND F. BANEYX. Molecular chaperones, folding catalysts, and the recovery of active recombinant proteins from *E. coli* to fold or to refold. *Appl. Biochem. Biotechnol.* 66: 197–238, 1997.

229. THOMAS, J. G., AND F. BANEYX. Protein folding in the cytoplasm of *Escherichia coli*: requirements for the DnaK-DnaJ-GrpE and GroEL-GroES molecular chaperone machines. *Mol. Microbiol.* 21: 1185–1196, 1996.

230. TIAN, G., Y. HUANG, H. ROMMELAERE, J. VANDEKERCKHOVE, C. AMPE, AND N. J. COWAN. Pathway leading to correctly folded beta-tubulin. *Cell* 86: 287–296, 1996.

231. TIAN, G., S. A. LEWIS, B. FEIERBACH, T. STEARNS, H. ROMMELAERE, C. AMPE, AND N. J. COWAN. Tubulin subunits exist in an activated conformational state generated and maintained by protein cofactors. *J. Cell Biol.* 138: 821–832, 1997.

232. TODD, M. J., G. H. LORIMER, AND D. THIRUMALAI. Chaperonin-facilitated protein folding: optimization of rate and yield by an iterative annealing mechanism. *Proc. Natl. Acad. Sci. USA* 93: 4030–4035, 1996.

233. TODD, M. J., P. V. VIITANEN, AND G. H. LORIMER. Hydrolysis of adenosine 5'-triphosphate by *Escherichia coli* GroEL: effects of GroES and potassium ion. *Biochemistry* 32: 8560–8567, 1993.

234. TODD, M. J., P. V. VIITANEN, AND G. H. LORIMER. Dynamics of the chaperonin ATPase cycle: implications for facilitated protein folding. *Science* 265: 659–666, 1994.

235. TOKATLIDIS, K., B. FRIGUET, D. DEVILLE-BONNE, F. BALEUX, A. N. FEDOROV, A. NAVON, L. DJAVADI-OHANIANCE, AND M. E. GOLDBERG. Nascent chains: folding and chaperone interaction during elongation on ribosomes. *Philos. Trans. R. Soc. Lond. B Biol. Sci.* 348: 89–95, 1995.

236. TOPPING, T. B., AND L. L. RANDALL. Chaperone SecB from *Escherichia coli* mediates kinetic partitioning via a dynamic equilibrium with its ligands. *J. Biol. Chem.* 272: 19314–19318, 1997.

237. TOROK, Z., L. VIGH, AND P. GOLOUBINOFF. Fluorescence detection of symmetric GroEL₁₄(GroES7)₂ heterooligomers involved in protein release during the chaperonin cycle. *J. Biol. Chem.* 271: 16180–16186, 1996.

238. TSAI, J., AND M. G. DOUGLAS. A conserved HPD sequence of the J-domain is necessary for YDJ1 stimulation of Hsp70 ATPase activity at a site distinct from substrate binding. *J. Biol. Chem.* 271: 9347–9354, 1996.

239. UNGEWICKELL, E., H. UNGEWICKELL, S. E. HOLSTEIN, R. LINDNER, K. PRASAD, W. BAROUCH, B. MARTIN, L. E. GREENE, AND E. EISENBERG. Role of auxilin in uncoating clathrin-coated vesicles. *Nature* 378: 632–635, 1995.

240. VALENT, Q. A., D. A. KENDALL, S. HIGH, R. KUSTERS, B. OUDEGA, AND J. LUIRINK. Early events in preprotein recognition in *E. coli*: interaction of SRP and trigger factor with nascent polypeptides. *EMBO J.* 14: 5494–5505, 1995.

241. VASSILAKOS, A., M. F. COHEN-DOYLE, P. A. PETERSON, M. R. JACKSON, AND D. B. WILLIAMS. The molecular chaperone calnexin facilitates folding and assembly of class I histocompatibility molecules. *EMBO J.* 15: 1495–1506, 1996.

242. VICKERY, L. E., J. J. SILBERG, AND D. T. TA. Hsc66 and Hsc20, a new heat shock cognate molecular chaperone system from *Escherichia coli*. *Protein Sci.* 6: 1047–1056, 1997.

243. VIITANEN P. V., T. H. LUBBEN, J. REED, P. GOLOUBINOFF, D. P. O'KEEFE, AND G. H. LORIMER. Chaperonin-facilitated refolding of ribulosebisphosphate carboxylase and ATP hydrolysis by chaperonin 60 (GroEL) are K⁺ dependent. *Biochemistry* 29: 5665–5671, 1990.

244. VYSOKANOV, A. V. Synthesis of chloramphenicol acetyltransferase in a coupled transcription-translation in vitro system lacking the chaperones DnaK and DnaJ. *FEBS Lett.* 375: 211–214, 1995.

245. WALKER, K. W., AND H. F. GILBERT. Protein disulfide isomerase. In: *Molecular Chaperones in the Life Cycle of Proteins*, edited by A. L. Fink and Y. Goto. New York: Dekker, 1998, p. 331–359.

246. WALL, D., M. ZYLICZ, AND C. GEORGOPOULOS. The conserved G/F motif of the DnaJ chaperone is necessary for the activation of the substrate binding properties of the DnaK chaperone. *J. Biol. Chem.* 270: 2139–2144, 1995.

247. WALTER, S., G. H. LORIMER, AND F. X. SCHMID. A thermodynamic coupling mechanism for GroEL-mediated unfolding. *Proc. Natl. Acad. Sci. USA* 93: 9425–9430, 1996.

248. WANG, J., J. ONUCHIC, AND P. WOLYNES. Statistics of kinetic pathways on biased rough energy landscapes with applications to protein folding. *Phys. Rev. Lett.* 76: 4861–4864, 1996.

249. WAWRZYNOW, A., B. BANECKI, D. WALL, K. LIBEREK, C. GEORGOPOULOS, AND M. ZYLICZ. ATP hydrolysis is required for the DnaJ-dependent activation of DnaK chaperone for binding to both native and denatured protein substrates. *J. Biol. Chem.* 270: 19307–19311, 1995.

250. WEI, J., AND L. M. HENDERSHOT. Protein folding and assembly in the endoplasmic reticulum. *EXS* 77: 41–55, 1996.

251. WEISSMAN, J. S., C. M. HOHL, O. KOVALENKO, Y. KASHI, S. CHEN, K. BRAIG, H. R. SAIBIL, W. A. FENTON, AND A. L. HORWICH. Mechanism of GroEL action: productive release of polypeptide from a sequestered position under GroES. *Cell* 83: 577–587, 1995.

252. WELCH, W. J., AND C. R. BROWN. Influence of molecular and chemical chaperones on protein folding. *Cell Stress Chaperones* 1: 109–115, 1996.

253. WETZEL, R. Principles of protein stability. Part 2: enhanced folding and stabilization of proteins by suppression of aggregation in vitro and in vivo. In: *Protein Engineering: A Practical Approach*, edited by A. R. Rees and M. J. E. Sternberg. New York: Oxford Univ. Press, 1992, p. 191–221.

254. WETZEL, R. Mutations and off-pathway aggregation of proteins. *Trends Biotechnol.* 12: 193–198, 1994.

255. WETZEL, R. For protein misassembly, it's the "I" decade. *Cell* 86: 699–702, 1996.

256. WHITE, Z. W., K. E. FISHER, AND E. EISENSTEIN. A monomeric variant of GroEL binds nucleotides but is inactive as a molecular chaperone. *J. Biol. Chem.* 270: 20404–20409, 1995.

257. WICKNER, S., S. GOTTESMAN, D. SKOWYRA, J. HOSKINS, K. McKENNEY, AND M. R. MAURIZI. A molecular chaperone, ClpA, functions like DnaK and DnaJ. *Proc. Natl. Acad. Sci. USA* 91: 12218–12222, 1994.

258. WILD, J., P. ROSSMEISSL, W. A. WALTER, AND C. A. GROSS. Involvement of the DnaK-DnaJ-GrpE chaperone team in protein secretion in *Escherichia coli*. *J. Bacteriol.* 178: 3608–3613, 1996.

259. WILLIAMS, D. B. The Merck Frosst Award Lecture 1994/La conference Merck Frosst 1994. Calnexin: a molecular chaperone with a taste for carbohydrate. *Biochem. Cell. Biol.* 73: 123–132, 1995.

260. WISNIEWSKI, T., A. GOLABEK, E. MATSUBARA, J. GHISO, AND B. FRANGIONE. Apolipoprotein E: binding to soluble Alzheimer's beta-amyloid. *Biochem. Biophys. Res. Commun.* 192: 359–365, 1993.

261. WIUFF, C., AND G. HOUEN. Cation-dependent interactions of calreticulin with denatured and native proteins. *Acta Chem. Scand.* 50: 788–795, 1996.

262. WU, B., A. WAWRZYNOW, M. ZYLICZ, AND C. GEORGOPOULOS. Structure-function analysis of the *Escherichia coli* GrpE heat shock protein. *EMBO J.* 15: 4806–4816, 1996.

263. XU, Z. H., A. L. HORWICH, AND P. B. SIGLER. The crystal structure of the asymmetric GroEL-GroES-(ADP)₇ chaperonin complex. *Nature* 388: 741–750, 1997.

264. YAFFE, M. B., G. W. FARR, D. MIKLOS, A. L. HORWICH, M. L. STERNLICHT, AND H. STERNLICHT. TCP1 complex is a molecular chaperone in tubulin biogenesis. *Nature* 358: 245–248, 1992.

265. YAHARA, I. Structure and function of the 90-kDa stress protein Hsp90. In: *Molecular Chaperones in the Life Cycle of Proteins*, edited by A. L. Fink and Y. Goto. New York: Dekker, 1998, p. 183–192.

266. YIFRACH, O., AND A. HOROVITZ. Nested cooperativity in the ATPase activity of the oligomeric chaperonin GroEL. *Biochemistry* 34: 5303–5308, 1995.

267. YON, J. M. Protein folding: concepts and perspectives. *Cell. Mol. Life Sci.* 53: 557–567, 1997.

268. ZAHN, R., S. PERRETT, AND A. R. FERSHT. Conformational states bound by the molecular chaperones GroEL and secB: a hidden unfolding (annealing) activity. *J. Mol. Biol.* 261: 43–61, 1996.

269. ZAHN, R., S. PERRETT, G. STENBERG, AND A. R. FERSHT. Catalysis of amide proton exchange by the molecular chaperones GroEL and SecB. *Science* 271: 642–645, 1996.

270. ZARNT, T., T. TRADLER, G. STOLLER, C. SCHOLZ, F. X. SCHMID, AND G. FISCHER. Modular structure of the trigger factor required for high activity in protein folding. *J. Mol. Biol.* 271: 827–837, 1997.

271. ZEINER, M., M. GEBAUER, AND U. GEHRING. Mammalian protein RAP46: an interaction partner and modulator of 70 kDa heat shock proteins. *EMBO J.* 16: 5483–5490, 1997.

272. ZHU, X., X. ZHAO, W. F. BURKHOLDER, A. GRAGEROV, C. M. OGATA, M. E. GOTTESMAN, AND W. A. HENDRICKSON. Structural analysis of substrate binding by the molecular chaperone DnaK. *Science* 272: 1606–1614, 1996.

273. ZIEGELHOFFER, T., P. LOPEZ-BUESA, AND E. A. CRAIG. The dissociation of ATP from hsp70 of *Saccharomyces cerevisiae* is stimulated by both Ydj1p and peptide substrates. *J. Biol. Chem.* 270: 10412–10419, 1995.

274. ZYLICZ, M., T. YAMAMOTO, N. McKITTRICK, S. SELL, AND C. GEORGOPOULOS. Purification and properties of the DnaJ replication protein of *Escherichia coli. J. Biol. Chem.* 260: 7591–7598, 1985.

Docket No.: 00131-00350-US

EMBO WORKSHOP REPORT

Exhibit 29

Protein folding and misfolding inside and outside the cell

Christopher M.Dobson and R.John Ellis

Oxford Centre for Molecular Sciences, University of Oxford, South Parks Road, Oxford OX1 3QT, UK

e-mail: chris.dobson@chem.ox.ac.uk or je@dna.bio.warwick.ac.uk

The workshop was held at St Catherine's College, Oxford, from March 25–28, 1998, and attracted participants from 32 nations. Protein folding is one of the most important processes in biology since it adds functional flesh to the bare bones of genes, but it has traditionally been studied by people separated both intellectually and physically because they are training in different disciplines. The aim of the meeting was to bring together chemists and structural biologists studying how pure, denatured proteins refold spontaneously in the test tube, with biochemists and cell biologists who are concerned with how proteins fold inside living cells and medical scientists interested in the diseases that result when this process goes wrong. In this report we concentrate on general concepts and themes rather than on detailing every contribution.

Many studies have established that the vast majority of denatured protein chains are capable of refolding spontaneously to the correctly folded conformation in the absence of either other macromolecules or energy expenditure. Chris Dobson (Oxford, UK) summarized the increasingly sophisticated physical techniques used to study protein refolding, and stressed the 'new view' of this process as a three-dimensional, downhill energy search by a vast array of different initial conformations that converge by different routes on the unique functional structure. He introduced the fact that such techniques are now becoming applicable to study folding in cell-free translation extracts which are much closer to the intracellular environment than are pure proteins refolding from the denatured state. For example, it is now possible to obtain mass spectra from intact ribosomes and to characterize particular protein components from the spectrum.

There are several possible fates of newly synthesized protein chains inside cells. The major distinction between these fates is whether the chains succeed in folding correctly, or whether the chains aggregate. Aggregation has commonly been regarded as a nuisance which affects *in vitro* protein refolding studies; it is now apparent that aggregation is also a problem for cells. In the intracellular environment, the competition between folding, aggregation and degradation determines whether a polypeptide chain can achieve its functional state with the efficiency required for successful cell growth, or whether it aggregates into a state that causes cellular damage and even death.

John Ellis (Warwick, UK) reviewed evidence that aggregation is a specific process, which may be amplified by the high concentration of identical nascent chains emerging from polysomes, and by the very large increases in association constants produced by the crowding effect of the high concentration of macromolecules in the cytoplasm (340 mg/ml in *Escherichia coli*), an effect yet to be extensively studied on protein refolding *in vitro*. Combating aggregation is one of the major roles of molecular chaperones, of which there are at least 20 structurally distinct families. It is important to appreciate that protein folding occurs in several different intracellular compartments, especially in eukaryotic cells, and that the chaperone complement differs between these compartments. Thus, proteins coevolve with particular chaperones, and for meaningful *in vitro* experiments it is advisable to choose naturally occurring protein–chaperone combinations. A major theme of this workshop was the discussion of the best conceptual and methodological approaches for determining the precise basis of how cells contrive to optimize correct protein folding and reduce aggregation.

How do denatured proteins refold in the test tube?

It has been evident for many years that the sequence of a protein defines its three-dimensional fold. The question of how an unstructured (random coil) polypeptide can rapidly and efficiently find its appropriate fold from the countless alternatives is, however, a problem that has perplexed the scientific community for many years. Considerable progress in understanding this remarkable process has been made recently through a combination of theoretical and experimental advances.

A particularly important theoretical strategy has been to simulate refolding by using 'lattice models' for proteins in which residues are represented as points on a three-dimensional lattice that interact with one another according to defined potential functions. The idea is to devise models simple enough for extensive calculations to be carried out to simulate refolding, yet sufficiently complex to encapsulate key features of real proteins. Martin Karplus (Cambridge, MA) described the results of simulations using such models.

In order to fold successfully, a polypeptide chain must collapse, a process favoured by the burial of hydrophobic sidechains, while forming key contacts between residues which ensure that the native fold is formed efficiently. The simulations suggest that this process can occur for sequences where the formation of native-like interactions stabilizes the folding chain, and where stable misfolded states, which can act as kinetic traps, are avoided. As well as providing insights into the folding process, such simulations allow the results of experimental studies to

be interpreted more fully and permit the rational design of new experimental strategies; the experiments in turn can be used to test and improve the simulations.

A variety of experimental techniques has been developed to study refolding. As well as kinetic experiments, reviewed by Christopher Dobson, a complementary approach is to adjust the solution conditions to generate stable analogues of species likely to be important in the kinetic refolding process. NMR spectroscopy is particularly important in these studies because of its ability to provide structural and dynamical information at the level of individual residues. Peter Wright (La Jolla, CA) described studies of myoglobin where a variety of partially folded states can be stabilized and have been characterized in detail. These experiments have been able to map the development of stable native-like secondary structure, and the reduction in conformational flexibility as the compactness of the protein increases. Further insights into these issues come from molecular dynamics simulations of partially folded states of proteins; Lorna Smith (Oxford, UK) described the results of such approaches with the proteins lysozyme and α-lactalbumin. An important conclusion of this work that correlates well with the experimental data is that the overall fold of a protein can form prior to the generation of specific close-packing of residues that is characteristic of the native protein.

Determining the relationship between sequence and structure is a key aspect of understanding folding, but it is also crucial for the design of novel sequences with specific properties. Luis Serrano (Heidelberg, Germany) described an example of a de novo-designed triple-stranded β-sheet, composed of 16 residues. Sheena Radford (Leeds, UK) described studies using biophysical techniques of the refolding of proteins with different folds, e.g. proteins that are either largely helical or largely sheet. It is now possible to begin to address the issue of the way that evolution has selected a limited, although still large, number of possible folds for polypeptide chains; whether this selection is for ease of folding rather than for stability or functional value is not clear. Oleg Ptitsyn (Bethesda, MD) suggested that key residues in the globin and cytochrome sequences may be conserved in evolution to ensure that rapid folding occurs to a specific structure. These ideas relate closely to those discussed above in terms of simulations, and have also emerged from the elegant protein engineering experiments of Alan Fersht.

In studies of protein refolding, a number of characteristics that result in slow steps and potential misfolding have been recognized. Prominent among these is the need for some proteins to form the correct isomer of peptide bonds involving proline, and the need to form the correct disulfide bonds between cysteine residues. Such problems arise for protein folding in cells, and enzymes exist that catalyse such steps. Robert Freedman (Canterbury, UK) discussed one of the best known such enzymes, protein disulfide isomerase; this enzyme allows the exchange of disulfide bonds among folding chains until the lowest energy state is reached, a feature reminiscent of the earlier steps in folding described above. This topic formed the introduction to sessions concerned with protein folding inside cells.

How do proteins fold inside cells?

As well as enzymes that isomerize covalent bonds in protein chains, cells contain a variety of molecular chaperones that control and assist the folding process.

Previous work suggests that two types of chaperone act sequentially on newly synthesized polypeptides in both the cytoplasm of prokaryotic cells and in the cytosol and mitochondria of eukaryotic cells. Small chaperones (<100 kDa), such as hsp70 (DnaK) and hsp40 (DnaJ), bind to hydrophobic regions on nascent chains to prevent aggregation and premature folding as elongation continues, while large chaperones (>800 kDa), such as GroEL, bind complete, partially folded chains individually in a central cage, where folding proceeds further until the danger of aggregation with similar chains has passed. Some aspects of these views were confirmed and extended, while others were challenged.

Elizabeth Craig (Madison, WI) reported that of the 14 hsp70-like proteins in yeast, it is the two cytosolic SSB proteins, but not the four cytosolic SSA proteins, that bind to both nascent chains and ribosomes. Binding is independent of ATP and occurs even to chains as short as 70 residues, 30–40 of which are buried in the ribosome. There are least twice as many SSB protein molecules as ribosomes in yeast, so in principle every nascent chain could have one SSB attached, but this has not yet been established. On the other hand, Bernd Bukau (Freiburg, Germany) was unable to demonstrate the binding of DnaK or DnaJ to nascent chains in E.coli, but presented genetic evidence that a major role of these chaperones in this organism is to assist the refolding of proteins unfolded by heat stress. Other chaperones such as hsp90 may bind to at least some types of newly synthesized chain. Johannes Buchner (Regensburg, Germany) reported that hsp90 has two distinct chaperone sites; binding by the N-terminal fragment is ATP-dependent and prefers unstructured peptides, while binding by the C-terminal fragment is ATP-independent and prefers partially folded polypeptides.

There is evidence that the GroEL of E.coli binds in vivo to only ~10–15% of all the newly synthesized cytoplasmic chains under normal growth conditions. Arthur Horwich (New Haven, CT) and Ulrich Hartl (Martinsried, Germany) independently reported the identification of some of the natural substrates for this chaperone under such conditions; these include GroEL itself, the three elongation factors, the α chain of RNA polymerase, E3 from pyruvate dehydrogenase and the β subunit of the F_1 ATPase. Hartl reviewed his folding shift hypothesis that proposes an evolutionary shift from a predominantly post-translational type of protein folding in prokaryotes to a predominantly co-translational type of protein folding in eukaryotes. Such a shift could provide the basis for the appearance in eukaryotes of large modular proteins via gene fusion events. In support of this view, Hartl reported that the expression in yeast of a mutant form of GroEL that binds partially folded chains but cannot release them does not affect the growth rate. This observation is consistent with the rapid co-translational folding of most newly synthesized chains that are released from the eukaryotic ribosome in a state not recognized by GroEL. In contrast, the expression of the mutant GroEL in E.coli reduces the growth rate, presumably because ~50% of the newly

synthesized but only partially folded chains bind irreversibly to the mutant GroEL. Boyd Hardesty (Austin, TX) used cell-free translation extracts to show that for newly synthesized rhodanese to fold correctly DnaJ, DnaK + GrpE and then GroEL/ES, must be added in that order, confirming the view that the small chaperones act before the large chaperones. He also presented interesting new data suggesting that the elongation factors Tu and Ts may also act as chaperones since they assist the refolding of denatured rhodanese, provided that GTP is present.

Both Horwich and Hartl support the folding cage model for GroEL action, and Hays Rye (New Haven, CT) presented additional elegant fluorescence energy transfer data in favour of this model, but this view was challenged by Alan Fersht (Cambridge, UK) on the grounds that an apical fragment of GroEL (residues 193–335) complements a temperature-sensitive mutant of *E.coli* at 43°C and enhances the activity of co-expressed GroEL in lethal GroEL knockouts. Whether this complementation requires GroES, the other component required for the cage to function, is not known, and the apical fragment is unable to act like the wild-type GroEL as the only source of GroEL in the cell at permissive temperature. Cell viability rather than growth rates were measured in this study, so the cage might be an efficiency-enhancing device essential for cells to compete in nature rather than an absolute requirement under all conditions. However, it should be noted that in this study the cells always contain at least some GroEL cages.

Helen Saibil (London, UK) presented her latest 9 Å cryoEM pictures of GroEL in action, and stated that she is now certain that the C-terminus forms a barrier between the two rings; this was complemented by a report by Keith Willison (London, UK) of similar large ATP-induced domain movements in the GroEL equivalent in the eukaryotic cytosol, CCT. Willison also suggested that CCT functions as an ATP-loading machine for its main substrate, actin, rather than as a folding cage, since nucleotide-free actin denatures irreversibly at a high rate while actin peptides that bind to CCT are mostly from the surface of the folded molecule.

Instead of folding in the cytosol, an important subset of proteins fold and are glycosylated after transport into the endoplasmic reticulum; this compartment lacks large chaperones of the GroEL type but contains calnexin and calreticulin that chaperone the folding of glycosylated proteins. Ari Helenius (Zürich, Switzerland) studied the effect of glucosidase inhibitors on the *in vivo* folding of a temperature-sensitive mutant of the VSV G protein and concluded that it is the glucose residues that determine its binding to calnexin rather than protein–protein interactions. Ineke Braakman (Amsterdam, The Netherlands) reported that the gp160 envelope protein of HIV undergoes extensive but slow post-translational folding in the ER, the signal peptide being removed only after synthesis is complete.

Walter Neupert (Munich, Germany) reviewed the evidence for the view that unidirectional protein transport into yeast mitochondria requires mitochondrial hsp70 acting as a molecular ratchet; this mechanism is proposed to result in the unfolding of the translocating protein on the cytosolic side of the outer mitochondrial envelope. He also reported the identification of two chaperones called

TIM 10 and TIM 12 in the intermitochondrial membrane space that aid translocation, perhaps by functionally replacing hsp70 which is absent from this compartment. It seems that the list of proteins acting as molecular chaperones is destined to grow still further.

How is protein misfolding linked to disease?

It is increasingly clear that protein folding is not only an essential feature of the conversion of genetic information into biological activity, but is also a key feature in the control and localization of this activity. This conclusion leads naturally to the idea that the failure of proteins to fold, or to fold into an incorrect structure, can be a cause of disease. Cystic fibrosis is an example of a genetic disease where a variant protein (CFTR) is unable to fold correctly to a stable state in the endoplasmic reticulum and fails to reach the plasma membrane, eventually being degraded. Philip Thomas (Dallas, TX) and John Riordan (Scottsdale, AZ) discussed the problem of the misfolding and incorrect trafficking of CFTR mutant proteins and their links with the molecular pathology of the disease. Interestingly, even the wild-type chains do not fold with high efficiency; only ~30% of wild-type chains survive the quality-control mechanisms of the endoplasmic reticulum. It is perhaps not surprising that a wide range of mutations in different regions of the CFTR protein result in significantly reduced levels of activity in sufferers of this condition.

We have noted above that one of the roles of molecular chaperones is to prevent the aggregation of partially folded proteins. The remaining talks at the Workshop focussed on issues of aggregation which, once ignored as a topic of serious study, is now elevated to almost cult status. Jonathan King (Cambridge, MA) described elegant studies showing that misfolded intermediates result in the formation of inclusion bodies in the case of the trimeric phage P22 tail spike protein, a trimeric protein. Interestingly, there is evidence that completion of folding of the protrimer, both *in vivo* and *in vitro*, requires interchain disulfide bond formation, even although the native trimer has no such bonds. Anthony Fink (Santa Cruz, CA) showed how biophysical studies can characterize the structural properties of aggregated proteins, while Jean Baum (Piscataway, NJ) discussed remarkable real-time NMR experiments probing the molecular basis of misfolding of collagen mutants that cause *osteogenesis imperfecta*. Subsequent speakers concentrated on the aggregation of proteins to form amyloid fibrils and plaques.

Amyloid formation is associated with some 20 sporadic, genetic or infectious diseases; remarkably these fibrils have similar morphologies, despite their origin from unrelated polypeptides. Mark Pepys (London, UK) reviewed this topic, pointing out that one of these diseases, Alzheimer's, was estimated to be the most expensive medical problem in the Western world. Byron Caughey (Hamilton, MT) discussed the spongiform encephalopathies, including BSE, scrapie, and CJD, which, of course, are currently of great concern. Max Perutz (Cambridge, UK) described fibrils in Huntington's disease which have many of the characteristics of amyloid. A key issue in such diseases is the mechanism of conversion of soluble proteins into insoluble aggregates. The meeting started with the idea

that protein folding mechanisms are amenable to both theoretical analysis and investigation by biophysical methods; it concluded by discussing how aggregation could also be studied at the molecular level by similar approaches.

A variety of approaches are being applied to this problem. Carol Robinson (Oxford, UK) described incisive experiments using time-of-flight mass spectrometry to probe the nature of amyloidogenic folding intermediates, while Valerie Daggett (Seattle, WA) described molecular dynamics simulations to probe the early steps in the structural conversion associated with these proteins. David Eisenberg (Los Angeles, CA) described crystallographic studies of oligomeric proteins generated by domain swapping that could represent at least the initial events in the structural conversions of some proteins, while Perutz described a possible zipper mechanism. The possibility of a detailed molecular view of amyloid structure was raised by dramatic pictures of fibrils produced from an SH3 domain. These pictures were generated using cryoelectron microscopic image reconstruction techniques and resulted from a collaboration between the groups of Saibil and Dobson.

Will all of this effort give rise to practical benefits in terms of therapeutic treatment? There is justification for some optimism in this area. Pepys discussed several different approaches, including suppression of the production of amyloid precursor, prevention of amyloid formation and stimulation of amyloid degradation. Jeffery Kelly (La Jolla, CA) described strategies to develop drugs to treat amyloidosis resulting from mutations in the transthyretin gene. The idea here is to stabilize the tetrameric form of the protein using analogues of its natural ligand, thyroxine. Caughey described peptides of the prion protein that inhibit the conversion of the full length protein to its amyloidogenic form, while Pepys outlined approaches to tackling amyloid diseases in general by inhibiting SAP, a protein which appears to stabilize the fibrils against degradation. Most encouragingly, Pepys reported that SAP-minus mice show reduced amyloid fibril formation, and has identified a compound 'R' that can strip SAP from the fibrils. These are indications that the long haul from 'theory to therapy' has begun.

Characterization of a Partially Folded Monomer of the DNA-binding Domain of Human Papillomavirus E2 Protein Obtained at High Pressure*

Débora Foguel‡, Jerson L. Silva, and Gonzalo de Prat-Gay§

From the Programa de Biologia Estrutural, Departamento de Bioquímica Médica-ICB, Centro Nacional de Ressonância Magnética Nuclear de Macromoléculas, Universidade Federal do Rio de Janeiro, 21941-590 Rio de Janeiro, Brazil

The pressure-induced dissociation of the dimeric DNA binding domain of the E2 protein of human papillomavirus (E2-DBD) is a reversible process with a K_d of 5.6×10^{-8} M at pH 5.5. The complete exposure of the intersubunit tryptophans to water, together with the concentration dependence of the pressure effect, is indicative of dissociation. Dissociation is accompanied by a decrease in volume of 76 ml/mol, which corresponds to an estimated increase in solvent-exposed area of 2775 Å². There is a decrease in fluorescence polarization of tryptophan overlapping the red shift of fluorescence emission, supporting the idea that dissociation of E2-DBD occurs in parallel with major changes in the tertiary structure. The dimer binds bis(8-anilinonaphthalene-1-sulfonate), and pressure reduces the binding by about 30%, in contrast with the almost complete loss of dye binding in the urea-unfolded state. These results strongly suggest the persistence of substantial residual structure in the high pressure state. Further unfolding of the high pressure state was produced by low concentrations of urea, as evidenced by the complete loss of bis(8-anilinonaphthalene-1-sulfonate) binding with less than 1 M urea. Following pressure dissociation, a partially folded state is also apparent from the distribution of excited state lifetimes of tryptophan. The combined data show that the tryptophans of the protein in the pressure-dissociated state are exposed long enough to undergo solvent relaxation, but the persistence of structure is evident from the observed internal quenching, which is absent in the completely unfolded state. The average rotational relaxation time (derived from polarization and lifetime data) of the pressure-induced monomer is shorter than the urea-denatured state, suggesting that the species obtained under pressure are more compact than that unfolded by urea.

The interaction of proteins with DNA constitutes the basis for the regulation of key biological functions such as gene expression, replication, and recombination. DNA-binding proteins recognize specific stretches of DNA, and the molecular basis for the interactions is currently the focus of intensive research (1, 2). The domains of proteins that interact with DNA are highly variable in folding topology, and thus they can accommodate a large number of functions for the different complexes in both eukaryotic and prokaryotic systems (1, 3). One characteristic of many DNA-binding dimeric proteins is that the structures of the monomers are often highly intertwined (4–8). Studies on several complexes have revealed that both DNA and protein undergo conformational changes upon interaction, especially at the interface, and there is an important free energy coupling among folding, dimerization, and DNA recognition (9–12). In cases where these DNA-binding proteins have been studied, their unfolding by denaturing agents occurs simultaneously with dissociation in a highly concerted manner (13–17).

Human papillomavirus (HPV)[1] infection of the anogenital tract is associated with several premalignant and malignant lesions, especially dysplasia and carcinoma of the uterine cervix (18). The E2 transcriptional transactivator protein (E2-TA) participates in the regulation of the expression of viral genes in papillomavirus (19, 20). The products of the E2 gene are crucial to the life cycle of the virus because they regulate transcription from all viral promoters, which makes E2-TA a potential target for antiviral therapy. The E2 protein is comprised of an N-terminal transactivation domain separated from the C-terminal DNA binding and dimerization domain by a flexible region rich in proline residues (7). The solution structure of the C-terminal DNA binding domain (E2-DBD) from human papillomavirus strain-31 (HPV-31) was recently determined by NMR spectroscopy (21). The urea-induced denaturation of the recombinant E2-DBD from HPV-16 was shown to proceed through a concerted two-state unfolding and dissociation process, with no detectable intermediate species (17). However, investigation of its kinetic folding pathway reveals the presence of a short lived monomeric intermediate (22).

Noncovalent interactions can be reversibly perturbed using high hydrostatic pressure, which allows a thermodynamic characterization of protein folding, protein-protein, and protein-ligand interactions (23, 24). Hydrostatic pressure drives the structure of proteins to a thermodynamic state of smaller volume (23, 25, 26). Protein folding and protein-protein interactions are normally accompanied by an increase in volume because of the combined effects of the formation of solvent-excluding cavities and the release of bound solvent (24). Water is released as nonpolar amino acid residues are buried, as well as when salt linkages are formed. Arc repressor, a small DNA-

[1] The abbreviations used are: E2 transcriptional transactive bis-ANS, bis(8-anilinonaphtha

This paper is availa

binding dimer protein from the bacteriophage P22, has been studied in detail by high pressure, in an attempt to understand interrelationships among protein folding, dimerization, and DNA recognition (9, 11, 15, 16).

In this paper, we study the reversible dissociation of HPV-16 E2-DBD using high pressure in combination with fluorescence spectroscopic techniques. We present evidence for a persistent residual structure in the monomeric denatured state at high pressure and are able to characterize it by Trp fluorescence spectra, polarization, lifetime distribution, stability to urea unfolding, and binding of bis(8-anilinonaphthalene-1-sulfonate) (bis-ANS). The existence of a folded monomeric state of E2-DBD in the absence of denaturants may represent an important target to drug development in addition to being highly relevant to the understanding of the basic principles underlying protein folding mechanisms.

EXPERIMENTAL PROCEDURES

Chemicals—All reagents were of analytical grade. bis-ANS was purchased from Molecular Probes (Eugene, OR). Distilled water was filtered and deionized through a Millipore water purification system.

The C-terminal 80-amino acid (positions 286–365) DNA binding domain of HPV-16 E2 protein was overexpressed in *Escherichia coli* and purified as a soluble, folded dimeric protein (17). As shown previously, the isolated C-domain still retains the ability to dimerize and bind to the DNA (27). Protein concentration was determined using an extinction coefficient of 41,900 M^{-1} cm^{-1} at 280 nm (28).

Spectroscopic Measurements under Pressure—The high pressure cell equipped with optical windows has been described (15) and was purchased from ISS (Champaign, IL). Fluorescence spectra were recorded on an ISSK2 spectrofluorometer (ISS Inc., Champaign, IL). Fluorescence spectra at pressure p were quantified by the center of spectral mass $\langle \nu_p \rangle$.

$$\langle \nu_p \rangle = \Sigma \nu_i \cdot F_i / \Sigma F_i \qquad (Eq. 1)$$

where F_i stands for the fluorescence emitted at wave number ν_i and the summation is carried out over the range of appreciable values of F.

The pressure was increased in steps of 200 bars. At each step, the sample was allowed to equilibrate for 15 min prior to making measurements. There were no time-dependent changes in fluorescence spectra between 10 and 30 min.

Unless otherwise stated, the experiments were performed at 22 °C in the standard buffer: 50 mM bis-Tris-HCl containing 1 mM dithiothreitol and adjusted to the desired pH by the addition of HCl.

Thermodynamic Parameters—The degree of dissociation (α_p) is related to $\langle \nu_p \rangle$ by the expression,

$$\alpha_p = (\langle \nu_p \rangle - \langle \nu_i \rangle)/(\langle \nu_f \rangle - \langle \nu_i \rangle) \qquad (Eq. 2)$$

where $\langle \nu_i \rangle$ and $\langle \nu_f \rangle$ are the initial and final values of the center of spectral mass, respectively, while $\langle \nu_p \rangle$ is the center of spectral mass at pressure p.

The equilibrium constant, and therefore the Gibbs free energy for a monomer-dimer association equilibrium, will depend on the standard volume change (ΔV) of the reaction,

$$K_d(p) = K_{do}\exp(p\Delta V/RT) \qquad (Eq. 3)$$

$$\ln(\alpha_p^2/(1 - \alpha_p)) = p(\Delta V/RT) + \ln(K_{do}/4C) \qquad (Eq. 4)$$

where $K_d(p)$ and K_{do} are the equilibrium constants for dissociation at pressure p and at atmospheric pressure respectively; ΔV is the volume change, α_p is the extent of reaction at pressure p, and C is the protein concentration as dimer. In a dissociation-association process, a change in protein concentration from C_1 to C_2 results in a parallel displacement Δp of the plot of $\ln K_d(p)$ versus p along the pressure axis,

$$\Delta p = (n - 1)(RT/\Delta V_C)\ln(C_2/C_1) \qquad (Eq. 5)$$

where ΔV_c is the volume change of association determined from changes in dissociating pressure with concentration at a constant degree of dissociation, and n is the number of subunits.

Lifetime Measurements—Lifetime measurements were performed in a multifrequency cross-correlation phase and modulation fluorometer (ISS/K2), as described previously (29–31). Samples were excited at 295 nm with a 300-W xenon lamp, and emission was collected using 7–54

and 0–52 filters. For pressure experiments, light scattered from ficol particles was used as reference (15). The choice of fitting with Lorentzian components was based on χ^2 values and plots of weighted residuals.

Fluorescence Anisotropy Measurements—Values of fluorescence anisotropy were measured according to the equation,

$$A = I_{||} - I_{\perp}/I_{||} + 2I_{\perp} \qquad (Eq. 6)$$

where $I_{||}$ and $I_{\perp}$ are the intensities of the emission when the polarizers are oriented parallel or perpendicular to the direction of the polarizer of the excitation, respectively. The errors for the polarization measurements were less than ±0.005.

Average rotational relaxation times ($\langle \rho \rangle$) were calculated from the anisotropy values (A) and from the average lifetime experimentally determined by using the Perrin equation,

$$A_0/(A) = (1 + 3\tau/\langle \rho \rangle) \qquad (Eq. 7)$$

where A_0 is the limiting anisotropy of the fluorophore (0.240), and τ is the fluorescence decay lifetime.

Urea Unfolding of the High Pressure State—To a solution containing the E2-DBD dimer at 1 μM, 10 mM bis-Tris-HCl, 1 mM dithiothreitol, pH 5.5, and 5 μM bis-ANS at 22 °C, different concentrations of urea were added. The mixture was introduced in the high pressure cell, and after a 30-min period of incubation, fluorescence spectra of bis-ANS were recorded. Next, the pressure was taken to 2860 bars, required for attaining the maximum change in the center of spectral mass when monitoring Trp fluorescence in pressure titrations in the absence of bis-ANS. Since the decrease of the fluorescence of E2-bound bis-ANS at high pressure is a slow reaction, we followed the changes in the total fluorescence intensity with time until the completion of the reaction.

RESULTS

Structural Considerations of the E2-DBD—The crystal structure of the E2-DBD from bovine papillomavirus strain-1 revealed a new class of folding topology (7, 32), only shared by the EBNA1 DNA binding domain from the Epstein-Barr virus with no amino acid sequence homology (33). The fold consists of a dimeric eight-stranded β-barrel, with each monomer contributing half of the barrel. Two helices/monomer interact with the outside of the barrel, forming hydrophobic cores: a major α-helix, which forms the DNA binding site, and a minor α-helix at the opposite side (Fig. 1A). The solution structure of the E2-DBD from HPV-31 (80% homology with E2-DBD from HPV-16; Fig. 1B) has been solved recently by NMR methods and has identical folding topology, although some significant differences between solution and crystal structures were observed (21). The dimeric interface is stabilized by intersubunit β-sheet hydrogen bonding and by the packing of hydrophobic residues at the center of the barrel. The formation of the dimer buries 2,567 $Å^2$ of solvent-accessible area in the bovine papillomavirus strain-1 domain, which strongly suggests that any partly folded monomer would have to undergo substantial accommodations in structure (7).

The HPV-16 E2-DBD has three tryptophan residues/monomer, two of which face the central cavity of the barrel that forms the interface between the two monomers in a stacked conformation as shown in the HPV-31 E2-DBD structure (Ref. 21; Fig. 1). The position of tryptophan residues in E2-DBD is unique, in that the indole rings of Trp[87] (monomer 1) and Trp[39] (monomer 1) stack in a characteristic antiparallel fashion; the same occurs with Trp[87] (monomer 2) and Trp[39] (monomer 2). All four base-stacking interactions occur within the dimer interface, giving rise to a favorable aromatic-aromatic interaction. This makes it possible to follow dissociation and unfolding processes using fluorescence, with substantial sensitivity. The third tryptophan residue, Trp[59], which is present in HPV-16 E2-DBD but absent in HPV-31 E2-DBD faces the solvent and is located in the smaller α-helix (Fig. 1).

Pressure Dissociation of the E2-DBD: Concentration Dependence, Reversibility, and Thermodynamic Parameters—To mon-

A

B

```
HPV-31   ATTPIIHLKG   DANILKCLRY   RLSK-YKDLY   EQVSSTWHWT   CTD-GKHKH-
HPV-16   HTTPIVHLKG   DANTLKCLRY   RFKK-HCTLY   TAVSSTWHWT   GHN-VKHKS-
HPV-31   AIVTLTYIST   SQRDDFLHTV   KIPHTVSVST   -GYM-TI
HPV-16   AIVTLTYDSE   WQRDQFLSQV   KIPKTITVST   -GEM-SI
```
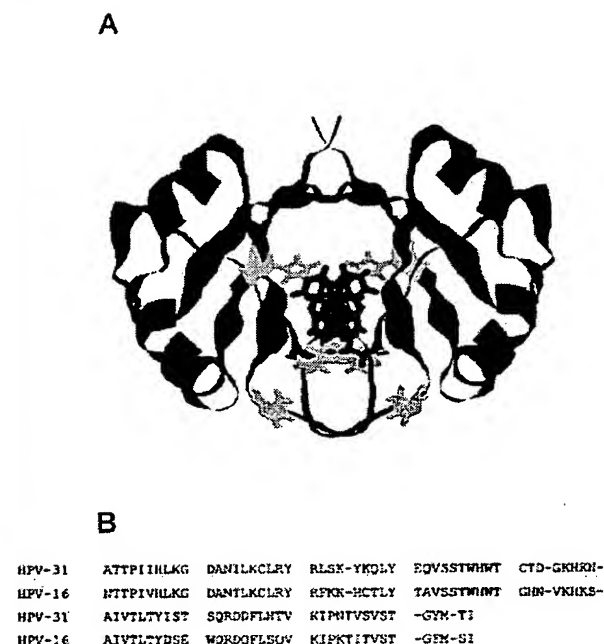
FIG. 1. *A*, ribbon representation of the solution structure of E2-DBD of HPV-31. The monomeric subunits are colored differently. The tryptophans (residues 37 and 39) and histidines (residues 8, 38, 46) are shown in *green* and *yellow*, respectively. The coordinates are from Liang *et al.* (21). The schematic representation was produced by using the program Rasmol. *B*, sequence alignment of the E2-DBD proteins from human papillomaviruses 31 and 16 (Ref. 21).

itor dissociation of E2-DBD under pressure, we followed the shift of the fluorescence emission spectra by measuring changes in the center of spectral mass (see Equation 1). This reveals changes in the environment of the tryptophan residues at the interface, which will eventually become exposed to the solvent. Fig. 2A compares the tryptophan emission spectra of E2 at pH 5.5 and 22 °C in the native state and under denaturing conditions (5 M urea; high hydrostatic pressure). Under high pressure (2.86 kilobars), the tryptophan fluorescence intensity decreased approximately 40%, whereas denaturation induced by urea was not accompanied by significant changes in the total fluorescence intensity. The *inset* of Fig. 2A shows that despite differences in tryptophan fluorescence intensity in urea and under pressure, both conditions caused the same displacement toward the red ($\Delta\lambda_{max} = 10$ nm). In both cases, the final value of center of mass was around 28,600 cm^{-1}, reflecting complete exposure of the tryptophan residues to the aqueous environment upon dissociation by pressure or denaturation by urea. Titration of the changes in center of spectral mass as a function of pressure is shown in Fig. 2B.

The equilibrium dissociation constant and the accompanying volume change for the dimer ⇔ monomer equilibrium were calculated using the equation for dissociation by pressure (Equation 4). Fig. 3A shows the degree of dissociation at each pressure, based on the center-of-mass data at pH 5.5 from Fig. 2B (Equation 2). The values derived from fluorescence anisotropy (*squares*) coincide with those obtained from the changes in fluorescence spectra (*circles*). The intercept of the semilogarithmic plot of these data (Equation 4) yields the dissociation constant (K_d); the slope provides the volume change of association (ΔV) (Fig. 3A, *inset*). The K_d values obtained in this way from both fluorescence spectra and anisotropy data are in excellent agreement with that calculated by Mok *et al.* (17) from urea unfolding experiments (Table I), especially so considering
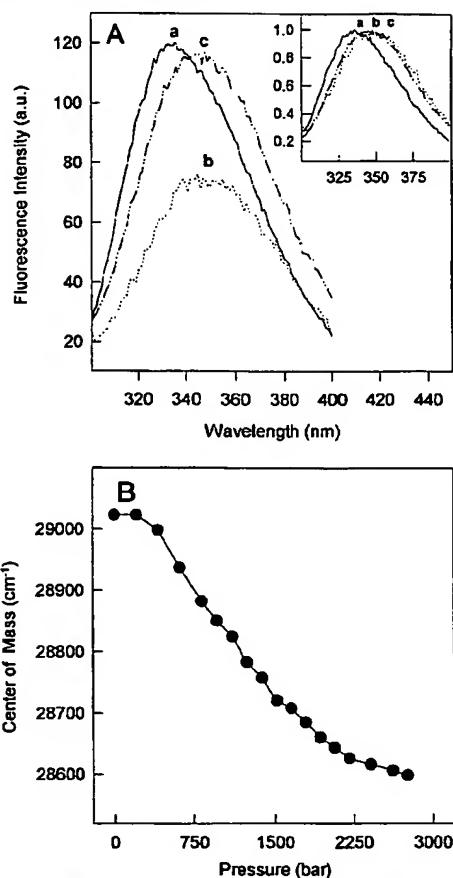
FIG. 2. **Effects of pressure on the intrinsic fluorescence emission of E2-DBD.** *A*, nonnormalized intrinsic fluorescence spectra of E2 (1 μM) at atmospheric pressure (*a*), at 2.9 kilobars (*b*), and at atmospheric pressure in the presence of 5 M urea (*c*), excited at 278 nm in 50 mM bis-Tris-HCl, 1 mM dithiothreitol, pH 5.5. The *inset* shows normalized spectra. *B*, pressure-induced dissociation of E2-DBD as followed by the center of spectral mass change at pH 5.5 at 22 °C. Other conditions were as in *panel A*.

the difference in techniques and the extrapolations to atmospheric pressure and absence of denaturant, respectively. These results show that the previous use of an empirical approach ($\Delta G_u = \Delta G_o + m$[urea]) agrees very well with the thermodynamic relation ($\Delta G_p = \Delta G_o + p\Delta V$) at pH 5.5.

Measurements of changes in volume are inaccessible to most denaturation techniques but are of great importance, since they measure the differences in packing of the states involved, adding valuable information to the thermodynamic characterization. The calculated volume change for the dissociation of E2-DBD by high pressure at 1 μM and pH 5.5 is 76 ml/mol (slope of plot in Fig. 3A), which falls within the range found for other dimers (23).

An independent assessment of dissociation can be obtained from the concentration dependence of the process (Fig. 3B). An increase in E2-DBD concentration promotes a displacement in the $p_{1/2}$ value (the pressure that promotes 50% change) from 1300 bars at 1 μM to 2070 bars at 10 μM E2-DBD. The difference in $p_{1/2}$ between these two experiments ($\Delta p_{1/2} = 770$ bars) allows us to calculate ΔV_c (23), the expected volume change for the dissociation of E2-DBD (Equation 5). The ΔV_c value was 73.2 ml/mol, in very good agreement with the value obtained for ΔV at a fixed protein concentration (76 ml/mol; Fig. 3). A ratio of $\Delta V/\Delta V_c$ that is close to 1 indicates that the dissociation
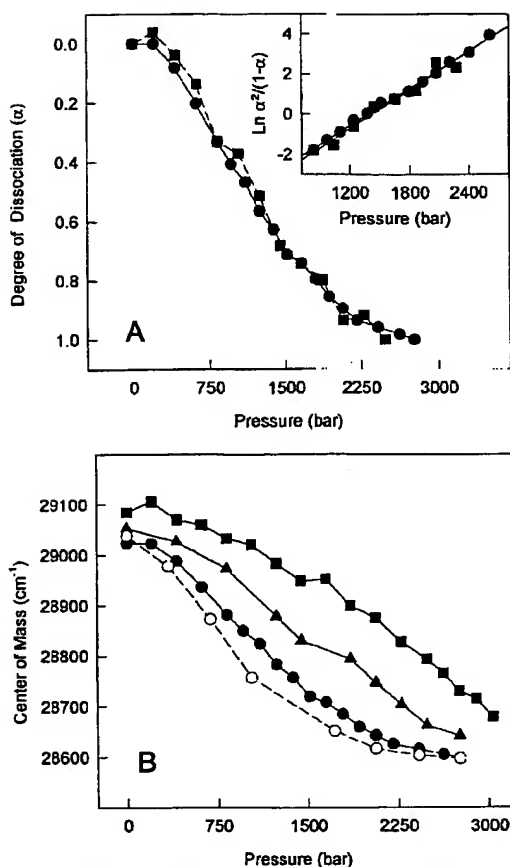
TABLE I

Dissociation constant at atmospheric pressure (K_d) and the volume change of association (ΔV) for the equilibrium $E2_2 \leftrightarrow 2\ E2$ at different pH conditions

E2-DBD, pH 5.5	K_d	ΔV
	M	ml/mol
Values obtained by the center of spectral mass shift	5.6×10^{-8}	76.0 ± 3.5 (5)[a]
Values obtained by the anisotropy change	4.3×10^{-8}	78.5 ± 4.2 (3)[b]
E2-DBD, pH 6.0		
With 0.5 M urea	6.0×10^{-9}	93
With 0.75 M urea	1.0×10^{-8}	100
With 0.95 M urea	5.4×10^{-8}	86
Extrapolated value at 0 M urea (17)	5.5×10^{-8}	

[a] Average and S.D. of five experiments.

[b] Average and S.D. of three experiments.

FIG. 3. *A*, degree of dissociation as a function of pressure at pH 5.5. The extent of dissociation (α) was calculated as described under "Experimental Procedures" (Equation 2) by using the center of mass values from Fig. 2*B* (●). For comparison, the degree of dissociation calculated from the anisotropy changes as a function of pressure (Fig. 7*A*) is also shown (■). *Inset*, a plot of $\ln(\alpha^2/(1 - \alpha))$ *versus* pressure (Equation 4), where the slope gives the volume change of association and the intercept is related to the dissociation constant at atmospheric pressure (Table I). *B*, concentration dependence of the pressure-induced dissociation of E2-DBD. ●, 1 μM; ▲, 5 μM; ■, 10 μM. The shift in the intrinsic fluorescence emission was used to follow dissociation of E2-DBD. The decompression curve at 1 μM protein concentration is also shown (○). All experiments were performed at 22 °C in bis-Tris-HCl 50 mM containing 1 mM dithiothreitol at pH 5.5.

FIG. 4. *A*, effects of pH on the pressure-induced dissociation of E2-DBD at 22 °C. Dissociation of E2-DBD was performed at pH 5.5 (◆); 5.8 (▲); 6.0 (■), and 7.0 (●). Other conditions as in Fig. 2*A*. *B*, apparent volume change of association as a function of the pH calculated from the experiments in Fig. 4*A* using Equation 4 (see "Experimental Procedures").

process complies with the law of mass action in the concentration range analyzed and that there is no significant conformational heterogeneity as observed in multisubunit complexes (34), tetramers (35), and more recently in a dimeric protein (36).

The reversibility of the dissociation process induced by pressure was confirmed by following the spectral change on decompression. The value of center of spectral mass for the Trp emission returns to the initial value (prior to pressure application), with negligible hysteresis (Fig. 3*B*, *open circles*).

The stability of E2-DBD toward pressure denaturation depends markedly on the pH (Fig. 4*A*). At pH 6.0 or 7.0 the process is incomplete, with a decrease in the center of mass of only 200–300 cm^{-1} at 2.86 kilobars, the highest pressure applied. At pH 5.8, the center of mass shift was greater, but only at pH 5.5 is the final value (28,600 cm^{-1}) compatible with the value obtained in urea, indicating complete exposure of tryptophan residues to the solvent. The urea unfolding curves also showed a strong dependence on pH (17). It is noteworthy that at atmospheric pressure, the center of mass of E2-DBD in-

creases from 29,050 cm^{-1} at pH 5.5 to 29,280 cm^{-1} at pH 7.0 (Fig. 4*A*). This result clearly indicates that pH causes a change in the environment of at least one of the Trp residues. The changes in the center of spectral mass with an increase in pH from 5.5 to 7.0, although rather small ($\sim$200 cm^{-1}), are not significantly dependent on protein concentration (not shown). Besides, as previously shown by analytical ultracentrifugation (17), E2-DBD is still a dimer, with no detectable monomers at pH 5.5. These data suggest that an isomerization reaction rather than a dissociation reaction is taking place when the pH
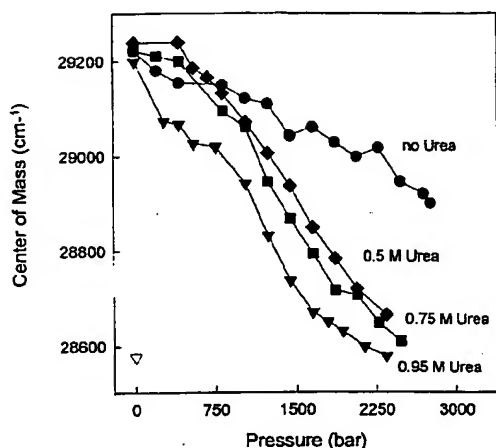
FIG. 5. **Effects of subdenaturing concentrations of urea on the dissociation of E2-DBD by pressure at pH 6.** The center of mass shift was used to follow dissociation in the absence of urea (●) or in the presence of 0.5 M (♦); 0.75 M (■), and 0.95 M (▼) urea. Other conditions were as in Fig. 2A. The isolated *symbol* at the *bottom left* corresponds to the center of mass value of 1 μM E2-DBD in the presence of 6 M urea at atmospheric pressure at the same pH.

FIG. 6. *A*, comparison between urea denaturation and pressure-induced dissociation of E2-DBD, based on tryptophan fluorescence intensity. The tryptophan spectral area ratio is shown as a function of pressure increase (●) or urea addition (O). The ratios were calculated by dividing the area at any given condition by the spectral area at atmospheric pressure or by the area in the absence of urea. Other conditions were as in Fig. 2A. *B*, Lorentzian distribution of Trp fluorescence lifetimes for E2-DBD at atmospheric pressure (——), in the presence of 6 M urea (—) and at 3 kilobars (- - -). Each data point represents the average of five measurements, and the error is smaller than 0.2 degree for the phase and 0.004 for the modulation measurements. The pH was adjusted to 5.5 in all measurements. Other conditions were as under "Experimental Procedures." The protein concentration was 10 μM in all experiments.

is lowered from 7.0 to 5.5. The existence of a predissociated dimer (17, 37) and of a denatured dimer (38) has been demonstrated for the Arc repressor. Fig. 4B shows the change in volume change as a function of pH. At high pH values, the changes induced by pressure are less steep, which results in a smaller volume change (~43 ml/mol). Between pH 6.0 and 5.5 there is an abrupt transition, and ΔV increases to ~80 ml/mol. The presence of a predissociation transition explains the smaller volume changes (less steep dependence on pressure) at high pH values, where the presence of a dimeric intermediate stretches the dissociation curve (16, 23).

Eight histidines out of 10 per dimer of HPV-16 E2-DBD lie at the interface between the two subunits (histidines 8, 38, and 46 are indicated in the E2-DBD structure; Fig. 1). The histidines of each subunit face each other at the interface, especially histidines 8 and 38; if they are protonated, they could destabilize the dimer. This may account for the greater tendency to dissociate at lower pH. Proton dissociation of the histidines, with a pK around 5.8 from Fig. 4B, would suppress the charge repulsion at the interface and engender a tight dimer. These histidines may exert a crucial regulatory effect on the stabilization with a potential effect on sequence-specific DNA binding.

Since the pressure dissociation process was not fully complete at pH 6.0 or 7.0 at the maximum pressures that were attained in Fig. 4A, we repeated the experiment at pH 6.0 with subdenaturing concentrations of urea added to the buffer (Fig. 5). In the presence of 0.5–0.95 M urea, pressure induced a decrease in the center of spectral mass to a value similar to that observed at high urea concentrations at atmospheric pressure or at high pressure at pH 5.5 in Fig. 4A, *i.e.* complete exposure of the Trp side chains to the solvent. From these curves, we calculate the ΔV of association and the K_d at pH 6.0 in the presence of different concentrations of urea (Table I). The K_d values are in good agreement with the value previously obtained from urea unfolding curves (17). Interestingly, the data show that ΔV increases dramatically with the addition of a small concentration of urea (0.5 M urea). The increase in ΔV observed when small amounts of urea are added could reflect an extra transition from "native-like" monomer to an unfolded monomer.

Residual Structure in the High Pressure Monomeric State of E2-DBD—In Fig. 2A, it was shown that the urea-induced denaturation of E2 shifts the spectrum to the red but does not
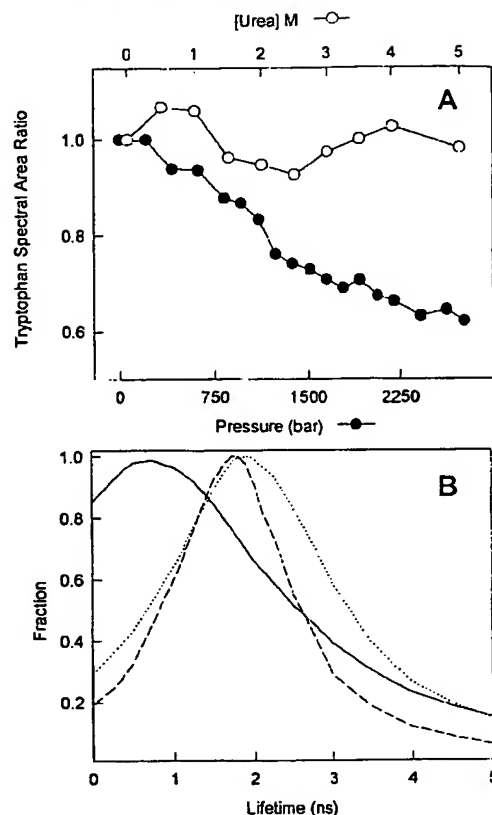
promote any decrease in intensity, whereas dissociation induced by high pressure affects both parameters. Fig. 6A shows the changes in the spectral area of the tryptophan fluorescence emission as a function of pressure or urea. As it is seen, over a broad range of concentrations, urea did not promote changes in tryptophan emission intensity, while pressure provoked a gradual decrease in the fluorescence intensity. The changes in tryptophan fluorescence intensity under high pressure resemble those induced by acid pH (17).

Time-resolved fluorescence measurements allow us to probe the tryptophan environment in the nanosecond time frame, providing a dynamic characterization of the conformational state of a protein (30, 31). Fluorescence lifetime measurements were performed to compare the excited state of the Trp residues of E2-DBD at pH 5.5 in three different states: native state (atmospheric pressure), pressure-dissociated state (2.8 kilobars), and urea-denatured state (Fig. 6B). In the native state, the best fit for the data is achieved by a Lorentzian distribution of lifetimes, rather than discrete exponential decays, centered at 1.745 ns. For the pressure-dissociated state, the distribution of lifetimes shifts to shorter lifetimes, centered at 0.727 ns (Fig.

6B and Table II). The decrease of 2.2-fold in the lifetime value is consistent with the decrease in tryptophan emission that takes place under these conditions (Fig. 6A). On the other hand, the center of the distribution of lifetimes for the urea-denatured state (1.951 ns) is very similar to the native state, consistent with the identical intensities of the native and urea-denatured states. However, for both pressure-dissociated and urea-denatured states, the width of the distribution increases dramatically in comparison with the control at atmospheric pressure and in the absence of denaturant (Fig. 6B; Table II). The dramatic differences between the distribution of lifetimes of the pressure-dissociated and urea-denatured states indicate that the phase space explored by the Trp residues are very different. The shorter lifetimes experienced by the Trp residues in the pressure-dissociated state suggest that a conformation-dependent quenching takes place.

Hydrodynamic Evidence for Residual Structure in the Pressure-dissociated Monomer—To compare the rotational hydrodynamic properties of E2 in the pressure-dissociated and urea-denatured states, fluorescence anisotropy measurements were performed. The steady-state anisotropy value for the dimer at atmospheric pressure was 0.12. The anisotropy decreases to 0.0548 at 2.5 kilobars, suggesting a decrease in the rotational hydrodynamic radius (Fig. 7A). Fig. 7A also shows the decompression curve (open circles), indicating complete reversibility of the dissociation process. Fig. 7B shows the change in anisotropy induced by the increase in urea concentration. At 5 M urea, where the fluorescence spectrum was already shifted completely to the red, the anisotropy was 0.078, significantly higher than the value observed for the pressure-dissociated protein. This result indicates that the urea-denatured form of E2 is more expanded than the pressure-induced monomer. From the changes in anisotropy, in combination with the lifetime measurements, the average rotational relaxation times ($<\rho>$) were determined according to Equation 7 (Table II). The value of $<\rho>$ at atmospheric pressure is consistent with the expected value for a combination of local motions with global rotation of the Trp residues in a protein with the dimensions of

E2-DBD dimer (7, 21). The tryptophans of the pressure-dissociated monomer rotate faster, indicating a more compact state than is seen with the urea-denatured form (Table II). The ΔV and K_d values were 78.5 ml/mol and 4.3×10^{-8} M, respectively, very close to those obtained from the center of mass data (Fig. 3A and Table I).

Persistent Binding of bis-ANS in the Pressure-dissociated State—As part of the characterization of the high pressure state, we made use of the hydrophobic dye bis-ANS, which binds to accessible hydrophobic patches in structured proteins, which translates into a large increase of its fluorescence emission (15, 39, 40). At pH 7.0, the E2-DBD dimer appears to bind two molecules of bis-ANS (40). When the E2-DBD was pressurized in the presence of bis-ANS, there is a 30% decrease in the bis-ANS fluorescence (Fig. 8), whereas the change in the center of spectral mass of the tryptophan residues (not shown) is the same as before. Urea denaturation causes a much larger decrease in the bis-ANS fluorescence, which is compatible with the lack of long range interactions in an unfolded polypeptide (Fig. 8). These data indicate that the protein under pressure retains some degree of long range tertiary interactions, whereas high concentrations of urea (5 M) cause a more extensive unfolding.

Probing the Stability of the Pressure-dissociated State to Urea Unfolding—To gain more insight on the pressure-dissociated state, we analyzed its stability toward urea denaturation. We reasoned that adding increasing concentrations of urea to the state at high pressure, in the presence of bis-ANS, would further decrease the amount of bound bis-ANS consistent with a fully unfolded polypeptide. In this way, we could obtain an estimate of the stability of the species trapped under high pressure. Fig. 9A shows typical traces of the time course of changes in bis-ANS fluorescence of E2-DBD after pressure (2.86 kilobars) is applied, at increasing concentrations of urea.

The bis-ANS fluorescence values obtained after reaching the equilibrium were plotted against urea (Fig. 9B). The structure present at high pressure is completely unfolded at 1 M urea, with an apparent $[U]_{50\%}$ of ~0.25 M. In contrast, the stability of the folded dimer at atmospheric pressure but otherwise similar conditions is much higher ($[U]_{50\%}$ of ~2.5 M, Fig. 9). The species present at 2.6 kilobars in the presence of 1 or 2 M urea could be defined as a largely unfolded state in which the tryptophan residues are completely exposed to the solvent (center of mass equal to 28,600 cm^{-1}) and its bis-ANS binding capacity is almost abolished, as expected for a completely unfolded polypeptide.

DISCUSSION

When studying the folding of dimeric proteins, it is important to determine the hierarchy of stability of possible structures formed in the reaction and to be able to distinguish, when possible, between folding and association events (41). In the particular case of several DNA-binding proteins with structures that are highly intertwined, folding and association are

TABLE II

Comparison of the rotational hydrodynamic properties of E2 in the native, pressure-dissociated, and urea-denatured states

Measurements of anisotropy and lifetime are the average of five measurements. The error for anisotropy was smaller than 0.0005, and the χ^2 values for the fittings of lifetime distribution were typically lower than 5.0.

Condition	Anisotropy	Average lifetime	Distribution width	Rotational relaxation time
		ns	*ns*	*ns*
Native state	0.1210	1.745	1.748	5.32
Pressure-dissociated state	0.0548	0.727	2.752	0.645
Urea-denatured state	0.078	1.951	2.483	2.82

FIG. 7. **Dissociation of E2-DBD based on tryptophan fluorescence anisotropy at pH 5.5 under pressure** (A) **or denaturation in the presence of increasing concentrations of urea** (B). In A, the *open circles* represent the decompression curve. The excitation was set at 295 nm, and the emission was collected through 7-54 and 0-52 cut-off filters. The anisotropy values under pressure were corrected for distortions in the bomb windows.
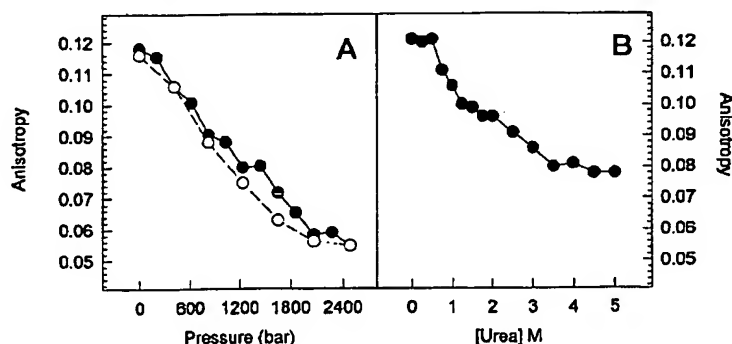
highly coupled processes. A good example is the Arc repressor, in which a highly concerted folding and association process is observed, as determined by fluorescence spectroscopy and NMR (13, 15, 16, 37, 38).

High pressure constitutes a noninvasive technique in which reversible dissociation or denaturation processes can be analyzed on a thermodynamic basis (24). In the present work, we describe the reversible dissociation of E2-DBD by high pressure, and we characterize the partially folded monomers. The Trp fluorescence changes that take place under pressure allow us to determine the volume change of association by applying the thermodynamic principles associated to pressure effects. A substantial fraction of the increase in volume on folding and association of proteins results from the formation of solvent-excluded void volumes. The structural importance of the volume change can be evaluated by comparison with other dimer-monomer dissociation reactions. The volume change of association for E2-DBD (76 ml/mol) is within the same range of that obtained for other dimers (55–170 ml/mol) (for a review, see Ref. 23). However, most of the dimers previously studied were much larger than E2-DBD. Only the Arc repressor was smaller (15). An appropriate way to express the volume change

is to normalize to the molecular weight of the dimer (15, 23), which furnishes the specific volume change. The value obtained for Arc and E2-DBD is much higher than for other dimers. The specific volume change of association is 4.2 μl/g for E2-DBD; 7.69 μl/g for Arc; and 0.688, 1.25, 1.88, and 4.73 μl/g for enolase, hexokinase, tryptophan synthase β_2 subunit, and R17 coat protein dimer, respectively (23). The large change in volume per mass of protein found in Arc, R17 coat protein, and E2-DBD dissociation can be explained by a high degree of interaction of buried amino acid side chains with the solvent under dissociation. The hydration of charges that were involved in salt bridges or the hydration of polar and nonpolar groups results in volume contraction. It is suggested that the partially unfolded states of these three proteins in the monomeric state favor a higher degree of hydration when compared with other dissociation systems. However, the Arc repressor undergoes an almost 2 times greater volume change per mass of protein than does E2-DBD, indicating that in the case of Arc the disruption of the structure under dissociation is more drastic.

An estimate of the solvent-excluded surface can be made from the volume change (42). The volume change obtained experimentally (76 ± 4 ml/mol) for E2-DBD at pH 5.5 corresponds to a decrease in volume of 126 Å^3/dimer dissociated. Considering a nonpolar solvent as a model for calculating linear compressibility, this value corresponds to exposure of 2775 ± 256 Å^2 when E2-DBD dissociates. This value is compatible with the x-ray diffraction structure, which led to the conclusion that 2,467 Å^2 of solvent-accessible area is buried on formation of the dimer (7). This remarkable similarity (within experimental error) between the pressure-dissociated state and that calculated from x-ray diffraction for the native monomer presents further evidence that the monomer retains some tertiary structure; although it is less stable, it still maintains a substantial proportion of hydrophobic residues buried in its interior.

Although the structure of E2-DBD from HPV-16 has not yet been solved, a structure of an equivalent protein from a strain with 80% homology (HPV-31) has been solved by NMR methods and shows the same topology as in the crystal structure of the bovine virus E2-DBD (Fig. 1; Refs. 7 and 21). This confirms that one of the three tryptophan residues/monomer is effectively located at the surface in the minor α-helix, facing the solvent, and the other two are located at the dimeric interface, facing the center of the barrel. It is, therefore, very likely that the buried tryptophan residues are responsible for the change in the fluorescence spectral mass, as they become exposed to the solvent at high pressure or high urea concentration. However, although the tryptophan residues in the pressure-dissociated state undergo solvent relaxation (resulting in a spectral shift as large as that caused by urea denaturation), the lifetime
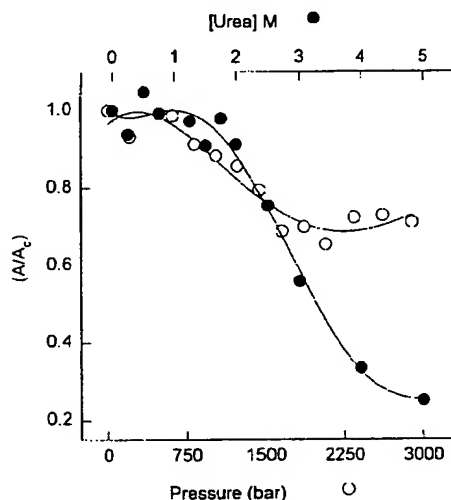

FIG. 8. **Decrease in binding of bis-ANS to E2-DBD as dissociation/denaturation is induced by urea (●) or pressure (○).** The area of the bis-ANS fluorescence spectrum is normalized to A_0, the area obtained at atmospheric pressure in the absence of urea. The difference between the values at 3000 bars and in 5 M urea indicates that different conformations are attained. Protein concentration was 1 μM, and bis-ANS was 5 μM. Excitation was set at 360 nm, and emission was collected in the range 400–600 nm.

FIG. 9. **Effects of subdenaturing concentrations of urea on the intermediate species trapped under pressure.** A, kinetics of E2-DBD denaturation under pressure (2860 bars), based on the decrease in bis-ANS binding in the absence of urea (○) or in the presence of 1 M urea (●) at pH 5.5. The fluorescence of bis-ANS was measured as in Fig. 8. B, urea-induced denaturation of the species trapped under high pressure (●) and of the protein at atmospheric pressure (▲). The end point of each kinetic experiment (see panel A) is plotted as a function of urea concentration. Note that in the presence of 0.75–1.00 M urea, bis-ANS decreases to a value similar to that seen in the presence of 4–5 M urea at atmospheric pressure (▲). Protein concentration was 1 μM, and bis-ANS concentration was 5 μM.
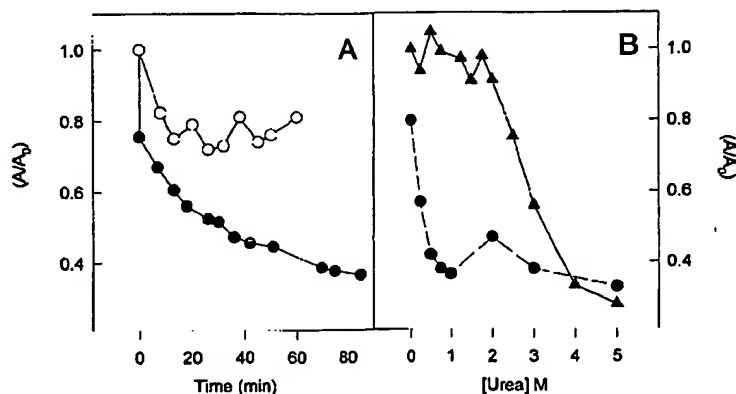
distribution is different from that in the urea-unfolded state. The width of the distribution is broader than in the native state but narrower than in the completely unfolded state. Four lines of evidence distinguish the states attained by pressure and urea: Trp intensity, excited-state lifetime, average rotational relaxation time, and bis-ANS binding. This clearly shows the presence of a state with persistent structure at high pressure. The conformation of E2 trapped under high pressure is more compact than the urea-denatured state, and it retains the ability to bind bis-ANS, features compatible with molten globule-like conformations (43, 44). High pressure has been used to trap molten-globule conformations of different protein systems (15, 24, 45, 46).

The urea-unfolded state virtually binds no bis-ANS, whereas the pressure-dissociated state retains ~70% of its bis-ANS binding capacity. This strongly suggests that there are persistent long-range interactions that allow for the formation of sites where the dye can be inserted. The nature of those sites is unclear. They might lie in an accessible core or in the DNA binding site, since folded E2-DBD binds both ANS and bis-ANS (22, 28). It can be argued that the bis-ANS binding is in fact due in part to a residual native-like conformation of the DNA binding site.

The structure of E2-DBD in the monomeric state under pressure is very unstable: urea titration of the bis-ANS binding reveals a midpoint around 0.25 M urea, in contrast with the 2.5 M for the native state (Fig. 9B). This decreased stability to urea explains why the dissociation constant obtained from extrapolation to zero in the urea-unfolding curves (atmospheric pressure) is similar to that obtained from the pressure-dissociation experiment. The lack of resistance to unfolding of the high pressure state at low urea concentrations can be interpreted as high sensitivity of the global structure to the chemical denaturant or noncooperative unfolding of the local structure that binds bis-ANS. Although we cannot discern between these two explanations due to experimental limitations, the lack of cooperativity is a defining characteristic in molten globule-like conformations (43, 44).

Altogether, our data suggest the following pathway for the reversible dissociation and unfolding of E2-DBD at pH 5.5.

$$(E2)_2 \leftrightarrow 2A \leftrightarrow 2U$$
$$\quad\;\;(1)\quad\;\;\;(2)$$

REACTION 1
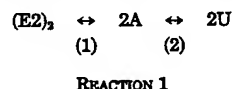
Equilibrium 1 encompasses the process of dissociation of the dimer to partially folded monomers (A) at pH 5.5. Unfolding by high concentrations of urea involves both equilibria. Equilibrium 2 *per se* was monitored by the experiment of Fig. 9, where the pressure-dissociated state was denatured by urea to a completely unfolded species (U). The free energy change for reaction 2 (ΔG_2) is less than 2.0 kcal/mol, indicating that A is relatively unstable.

With the evidence accumulated in the present work, it is tempting to suggest that the monomeric high pressure-dissociated state is related to the nonnative monomeric intermediate species found in kinetic refolding studies (22). The subsequent association of E2-DBD from the monomeric intermediate is slow, consistent with a rearrangement that must take place before the final association/folding step leading to the native dimer, which must involve the acquisition of precise geometric interactions and tight side chain packing (22). Further experiments will be needed to test this hypothesis.

The overall characteristics of the pressure-dissociated state strongly suggest a molten globule-like conformation. The implications of a "structured" monomer in the absence of chemical denaturants or extreme pH conditions contribute to the under-

standing of the equilibrium between folded and unfolded states in conditions that are more compatible with the cellular environment, since pressure is a thermodynamic variable that strictly affects the position of that equilibrium. Further detailed characterization of the structure at high pressure will require the use of high pressure NMR experiments (16). Provided that enough structural detail can be obtained from NMR experiments, future prospects will include the possibility of developing synthetic compounds capable of trapping the monomeric state, of potential therapeutic value against papillomaviruses.

REFERENCES

1. Pabo, C. O., and Sauer, R. T. (1992) *Annu. Rev. Biochem.* **61**, 1053–1095
2. von Hipel, P. H. (1994) *Science* **263**, 769–770
3. Travers, A. (1993) *DNA-Protein Interactions*, Chapman & Hall, Publishers, London
4. Schevitz, R. W., Otwinowski, Z., Joachimiak, A., Lawson, C. L., and Sigler, P. B. (1985) *Nature* **317**, 782–786
5. Jordan, S. R., and Pabo, C. O. (1988) *Science* **242**, 893–899
6. Breg, J. N., van Opheusden, J. H. J., Burgering, M. J. M., Boelens, R., and Kaptein, R. (1990) *Nature* **346**, 586–589
7. Hegde, R. S., Grossman, S. R., Laimins, L. A., and Sigler, P. B. (1992) *Nature* **359**, 505–512
8. Raumann, B. E., Brown, B. M., and Sauer, R. T. (1994) *Curr. Opin. Struct. Biol.* **4**, 36–43
9. Silva, J. L., and Silveira, C. F. (1993) *Protein Sci.* **2**, 945–950
10. Spolar, R. S., and Record, M. T., Jr. (1994) *Science* **263**, 777–784
11. Foguel, D., and Silva, J. L. (1994) *Proc. Natl. Acad. Sci. U. S. A.* **91**, 8244–8247
12. Lundbäck, L., and Härd, T. (1996) *Proc. Natl. Acad. Sci. U. S. A.* **93**, 4754–4759
13. Bowie, J. U., and Sauer, R. T. (1989) *Biochemistry* **28**, 7139–7143
14. Milla, M. E., and Sauer, R. T. (1994) *Biochemistry* **33**, 1125–1133
15. Silva, J. L., Silveira, C. F, Correa, A., and Pontes, L. (1992) *J. Mol. Biol.* **223**, 545–555
16. Peng, X., Jonas, J., and Silva, J. L. (1994) *Biochemistry* **33**, 8323–8329
17. Mok, Y.-K., Prat-Gay, Butler, P. J., and Bycroft, M. (1996) *Prot. Sci.* **5**, 310–319
18. de Villiers, E. M., Wagner, D., and Schneider, A. (1987) *Lancet* **2**, 703–706
19. Ham, J., Dostatni, N., Gauthier, J.-M., and Yaniv, M. (1991) *Trends Biochem. Sci.* **16**, 440–444
20. McBride, A. A., Romanczuk, H., and Howley, P. M. (1991) *J. Biol. Chem.* **266**, 18411–18414
21. Liang, H., Petros, A. M., Meadows, R. P., Yoon, H. S., Egan, D. A., Walter, K., Holzman, T. F., Robins, R., and Fesik, S. W. (1996) *Biochemistry* **35**, 2095–2103
22. Mok, Y.-K., Bycroft, M., and Prat-Gay, G. (1996) *Nat. Struct. Biol.* **3**, 711–717
23. Silva, J. L., and Weber, G. (1993) *Annu. Rev. Phys. Chem.* **44**, 89–113
24. Silva, J. L., Foguel, D., Da Poian, A. T., and Prevelige, P. E. (1996) *Curr. Opin. Struct. Biol.* **6**, 166–175
25. Gross, M., and Jaenicke, R. (1994) *Eur. J. Biochem.* **221**, 617–630
26. Robinson, C. R., and Sligar, S. G. (1995) *Methods Enzymol.* **259**, pp. 395–427, Academic Press, Inc., New York
27. Sander, C. M., and Maitland, N. J. (1994) *Nucleic Acids Res.* **22**, 4890–4897
28. Lima, L. M. T. R., and de Prat-Gay, G. (1997) *J. Biol. Chem.* **272**, 19295–19303
29. Lakowicz, J. R., Laczko, G., Cherek, H., Gratton, E., and Linkeman, M. (1984) *Biophys. J.* **46**, 463–478
30. Alcala, R., Gratton, E., and Prendergast, F. G. (1987) *Biophys. J.* **51**, 597–604
31. Beecham, J. M., Gratton, E., Ameloot, M., Knutson, J. R., and Brand, L. (1991) in *Topics in Fluorescence Spectroscopy* (Lakowicz, J. R., ed) Vol. 2, pp. 241–305, Plenum Publishing Corp., New York
32. Lilley, D. M. J. (1995) *DNA-Protein: Structural Interactions* (Lilley, D. M. J., ed) pp. 1–48, IRL Press, New York
33. Bochkarev, A., Barwell, J., Pfuetzner, R., Furey, W. J., Edwards, A. M., and Frappier, L. D. (1995) *Cell* **83**, 39–46
34. Silva, J. L., Villas-Boas, M., Bonafe, C. F. S., and Meireles, N. C. (1989) *J. Biol. Chem.* **264**, 15863–15868
35. Erijman, L., and Weber, G. (1991) *Biochemistry* **30**, 1595–1599
36. Rietveld, A. M., and Ferreira, S. T. (1996) *Biochemistry* **35**, 7743–7751
37. Burgering, M. J. M., Hald, M., Boelens, R., Breg, J. N., and Kaptein, R. (1995) *Biopolymers* **35**, 217–226
38. Robinson, C. R., Rentzeperis, D., Silva, J. L., and Sauer, R. T. (1997) *J. Mol. Biol.* **273**, 692–700
39. Rosen, C. G., and Weber, G. (1969) *Biochemistry* **8**, 3915–3920
40. Gorovits, B., Raman, C. S, and Horowitz, P. M. (1995) *J. Biol. Chem.* **270**, 2061–2066
41. Neet K. E., and Timm, D. E. (1994) *Protein Sci.* **3**, 2167–2174
42. Foguel, D., Suarez, M. C., Barbosa, C., Rodrigues, J. J., Sorenson, M. M., Smillie, L. B., and Silva, J. L. (1996) *Proc. Natl. Acad. Sci. U. S. A.* **93**, 10642–10646
43. Kim, P. S., and Baldwin, R. L. (1995) *Annu. Rev. Biochem.* **59**, 631–660
44. Haynie, D. T., and Freire, E. (1993) *Proteins Struct. Funct. Genet.* **16**, 115–140
45. Vidugiris, C. A. J., Markley, J. L, and Royer, C. A. (1995) *Biochemistry* **34**, 4909–4912
46. Clery C., Renault, F., and Masson, P. (1995) *FEBS Lett.* **370**, 212–214

Exhibit 31

Pub Med
www.pubmed.gov

| All Databases | PubMed | Nucleotide | Protein | Genome | Structure | OMIM | PMC | Journals | Book |

Search PubMed ___ for ___

Go   Clear

Limits   Preview/Index   History   Clipboard   Details

Display | Abstract   Show 20   Sort by   Send to

About Entrez

Text Version

All: 1   Review: 0

Entrez PubMed
Overview
Help | FAQ
Tutorials
New/Noteworthy
E-Utilities

PubMed Services
Journals Database
MeSH Database
Single Citation Matcher
Batch Citation Matcher
Clinical Queries
Special Queries
LinkOut
My NCBI

Related Resources
Order Documents
NLM Mobile
NLM Catalog
NLM Gateway
TOXNET
Consumer Health
Clinical Alerts
ClinicalTrials.gov
PubMed Central

1: <u>Biochemistry.</u> 1984 Jul 17;23(15):3411-7.   Related Articles, Links

Effect of pressure on the self-association of melittin.

Thompson RB, Lakowicz JR.

The effect of increased hydrostatic pressure (1 bar to 1.8 kbar) on the self-association of melittin was measured by using the fluorescence anisotropy of its single tryptophan residue. The degree of self-association was found to decrease with increasing pressure. The volume change (delta V) for dissociation is surprisingly large. At low pressures, delta V for dissociation is near -150 mL/mol. The magnitude of the volume change decreased with increasing pressure, possibly as a result of pressure-induced compression of free volume trapped at the subunit interface region of the tetramer. Overall, the pressure-dependent association of melittin is comparable to that expected for hydrophobic interactions and to that found for micelle formation by detergents.

PMID: 6466646 [PubMed - indexed for MEDLINE]

Display | Abstract   Show 20   Sort by   Send to

Aug 14 2006 08:07:58

Exhibit 32

A service of the National Library of
and the National Institutes

[Sign In] [Regis

All Databases	PubMed	Nucleotide	Protein	Genome	Structure	OMIM	PMC	Journals	Book

Search PubMed for [   ] Go [Clear]

Limits   Preview/Index   History   Clipboard   Details

Display | Abstract   Show | 20 | Sort by   Send to

All: 1   Review: 0

About Entrez

Text Version

Entrez PubMed
Overview
Help | FAQ
Tutorials
New/Noteworthy
E-Utilities

PubMed Services
Journals Database
MeSH Database
Single Citation Matcher
Batch Citation Matcher
Clinical Queries
Special Queries
LinkOut
My NCBI

Related Resources
Order Documents
NLM Mobile
NLM Catalog
NLM Gateway
TOXNET
Consumer Health
Clinical Alerts
ClinicalTrials.gov
PubMed Central

1: Biochemistry. 1981 Apr 28;20(9):2587-93.   Related Articles, Links

Pressure-induced reversible dissociation of enolase.

Paladini AA Jr, Weber G.

A study of the polarization of the intrinsic fluorescence and the fluorescence of dansyl conjugates of enolase shows that an increase in hydrostatic pressure, in the range of 1 bar-3 kbar, promotes the dissociation of this protein into dimers. The dissociation of oligomeric proteins under pressure is predicted to be a general phenomenon by a model that assumes the existence of small "free volumes" at the intersubunit boundaries. The same model predicts a dependence of the standard volume change in the dissociation reaction upon the pressure, owing to the additional surface compressibility of the monomers, and numerical analysis of the results clearly shows that dependence for enolase. For a midpoint dissociation pressure of 1.5 kbar the standard volume change in the dissociation reaction is delta V p0 = -65 +/- 8 mL mol-1 and the dependence of the volume change upon pressure (dVp0/dp) is approximately -30 mL mol-1 kbar-1. The reversibility of the pressure effects is shown to be better than 95% by either polarization or fluorescence spectrum recovery. The pressure perturbation of the fluorescence polarization is a method of general applicability to studies of protein aggregation, and it can be also of value in characterizing the effect of ligands on the aggregation of oligomeric proteins.

PMID: 7236623 [PubMed - indexed for MEDLINE]

Display | Abstract   Show | 20 | Sort by   Send to

Aug 14 2006 08:07:58

A service of the National Library of
and the National Institutes

[Sign In] [Regis

Pub Med
www.pubmed.gov

| All Databases | PubMed | Nucleotide | Protein | Genome | Structure | OMIM | PMC | Journals | Book |

Search PubMed ___ for ___   Go | Clear |

Limits   Preview/Index   History   Clipboard   Details

Display | Abstract   Show | 20   Sort by   Send to

All: 1   Review: 0

About Entrez

Text Version

Entrez PubMed
Overview
Help | FAQ
Tutorials
New/Noteworthy
E-Utilities

PubMed Services
Journals Database
MeSH Database
Single Citation Matcher
Batch Citation Matcher
Clinical Queries
Special Queries
LinkOut
My NCBI

Related Resources
Order Documents
NLM Mobile
NLM Catalog
NLM Gateway
TOXNET
Consumer Health
Clinical Alerts
ClinicalTrials.gov
PubMed Central

1: Biophys Chem. 1982 Aug;16(1):1-7.   Related Articles, Links

ELSEVIER
FULL-TEXT ARTICLE

Thermodynamics and mechanism of high-pressure deactivation and dissociation of porcine lactic dehydrogenase.

Muller K, Ludemann HD, Jaenicke R.

Lactic dehydrogenase (LDH) from pig heart and pig skeletal muscle can be reversibly dissociated into monomers at high hydrostatic pressure. The reaction can be quantitatively fitted by a reversible consecutive dissociation-unfolding mechanism according to N in equilibrium 4M in equilibrium 4M (where N is the native tetramer, and M and M two different conformations of the monomer) (K. Muller, et al., Biophys. Chem. 14 (1981) 101.). At p less than or equal to 1 kbar, the pressure deactivation of both isoenzymes (H4 and M4) is described by the two-state equilibrium N in equilibrium 4M. From the respective equilibrium constant and the temperature and pressure dependence of the change in free energy, the thermodynamic parameters of the dissociation/deactivation may be determined, e.g., for LDH-M4: delta G_{Diss} = 110 kJ/mol, delta S_{Diss} =-860 J/K per mol, delta H_{Diss}= -124 kJ/mol (enzyme concentration 10 microgram/ml, in Tris-HCl buffer, pH 7.6, I = 0.16 M, 293 K, 0.8 kbar); the dissociation volume is found to be delta V_{Diss} =-420 ml/mol (0.7 less than p less than 0.9 kbar). Measurements using 8-anilino-1-naphthalenesulfonic acid (ANS) as extrinsic fluorophore demonstrate that the occurrence of hydrophobic surface area upon dissociation parallels the decrease in reactivation yield after pressurization beyond 1 kbar. Within the range of reversible deactivation (p less than 1 kbar) no increase in ANS fluorescence is detectable, thus indicating compensatory effects in the process of subunit dissociation. $2H_2O$ is found to stabilize the enzyme towards pressure dissociation, in accordance with the involvement of hydrophobic interactions in the subunit contact of both isoenzymes of LDH.

PMID: 7139038 [PubMed - indexed for MEDLINE]

Display | Abstract   Show | 20   Sort by   Send to

Exhibit 34

PubMed
www.pubmed.gov

| All Databases | PubMed | Nucleotide | Protein | Genome | Structure | OMIM | PMC | Journals | Book |

Search PubMed 　　　for 　　　　　　　　　Go [Clear]

Limits　　Preview/Index　　History　　Clipboard　　Details

Display | Abstract　　　　Show | 20 Sort by　　Send to

About Entrez

Text Version

All: 1　Review: 0

Entrez PubMed
Overview
Help | FAQ
Tutorials
New/Noteworthy
E-Utilities

PubMed Services
Journals Database
MeSH Database
Single Citation Matcher
Batch Citation Matcher
Clinical Queries
Special Queries
LinkOut
My NCBI

Related Resources
Order Documents
NLM Mobile
NLM Catalog
NLM Gateway
TOXNET
Consumer Health
Clinical Alerts
ClinicalTrials.gov
PubMed Central

1: Biochim Biophys Acta. 1978 Dec 20;537(2):386-95.　　Related Articles, Links

Pressure effects on water-swollen elastin. A model for hydrophobic interactions in proteins.

French CJ, Gosline JM.

The effect of pressure on the swelling of elastin in pure water was investigated. Because elastin is a very non-polar protein, and because the swelling of elastin can be directly related to changes in the strength of hydrophobic interactions, we have used elastin as a model to study the effect of pressure on hydrophobic interactions in proteins. The elastin swelling model is particularly useful because it is based on a macromolecular system very similar to a globular protein and not on dilute aqueous solutions of small non-polar compounds. Increased pressure causes elastin to increase its swollen volume, and the observed swelling changes were analyzed in terms of the Flory-Rehner theory (Flory, P.J. and Rehner, Jr., J (1943) J. Chem. Phys. 11, 521--526) for the swelling of kinetically free, random polymer networks. Our calculations provide a measure of the volume change for the process of transferring 1 mol of an average non-polar amino acid side chain from a region where the side chains are surrounded by other non-polar groups and have no contact with water (i.e. a hydrophobic region) into contact with water. The results indicate that there is a small, negative volume change associated with this process, and quantitative estimates indicate that the volume change is of the order of --6 ml/mol side chain. The results support the hypothesis that the free energy required to transfer a non-polar side chain from a hydrophobic region into water becomes less positive (i.e. the hydrophobic interaction becomes weaker) as hydrostatic pressure is increased.

PMID: 728452 [PubMed - indexed for MEDLINE]

Display | Abstract　　　Show | 20 Sort by　　Send to

Write to the Help Desk
NCBI | NLM | NIH
Department of Health & Human Services
Privacy Statement | Freedom of Information Act | Disclaimer

http://www.ncbi.nlm.nih.gov/entrez/query.fcgi?CMD=Display&DB=pubmed　　　　9/1/2006

Aug 14 2006 08:07:58

The pressure dependence of hydrophobic interactions is consistent with the observed pressure denaturation of proteins

(protein folding/protein folding kinetics/hydrophobic effect/activation volumes/protein unfolding)

GERHARD HUMMER*†, SHEKHAR GARDE*‡, ANGEL E. GARCÍA*, MICHAEL E. PAULAITIS§, AND LAWRENCE R. PRATT*

*Theoretical Division, MS K710, Los Alamos National Laboratory, Los Alamos, NM 87545; ‡Center for Molecular and Engineering Thermodynamics, Department of Chemical Engineering, University of Delaware, Newark, DE 19716; and §Department of Chemical Engineering, Johns Hopkins University, Baltimore, MD 21218

ABSTRACT   Proteins can be denatured by pressures of a few hundred MPa. This finding apparently contradicts the most widely used model of protein stability, where the formation of a hydrophobic core drives protein folding. The pressure denaturation puzzle is resolved by focusing on the pressure-dependent transfer of water into the protein interior, in contrast to the transfer of nonpolar residues into water, the approach commonly taken in models of protein unfolding. Pressure denaturation of proteins can then be explained by the pressure destabilization of hydrophobic aggregates by using an information theory model of hydrophobic interactions. Pressure-denatured proteins, unlike heat-denatured proteins, retain a compact structure with water molecules penetrating their core. Activation volumes for hydrophobic contributions to protein folding and unfolding kinetics are positive. Clathrate hydrates are predicted to form by virtually the same mechanism that drives pressure denaturation of proteins.

A decade ago, Walter Kauzmann (1) challenged the commonly held view that a hydrophobic core stabilizes globular proteins, by poignantly remarking that the "liquid-hydrocarbon model (2) fails almost completely when one attempts to extend it to the effects of pressure on protein folding." Although a variety of forces stabilize folded proteins (3–6), the formation of a hydrophobic core is thought to play a dominant role. This view is supported by the temperature dependence of hydrophobic contributions to protein unfolding showing remarkable similarities to the transfer of hydrocarbons from a nonpolar phase into water, notably a convergence of the entropy of transfer (2, 7, 8). However, Kauzmann (1) pointed out that the pressure dependence of protein unfolding is at odds with the hydrophobic-core model: The volume change ΔV upon unfolding is positive at low pressures but negative at pressures of about 100–200 MPa. The transfer of hydrocarbons into water shows exactly the opposite behavior, with ΔV being negative at low pressures and positive at high pressures.

Evidently, pressure unfolding of a protein (9–16) does not correspond to the transfer of a nonpolar molecule from a nonpolar environment into aqueous solution. Unlike heat-denatured proteins, the ensemble of pressure-denatured proteins retains elements of structural organization (13, 17). Consequently, an understanding of the thermodynamics of pressure denaturation might focus on the free energy of water transfer into the hydrophobic core of the protein (18) rather than transfer of nonpolar solutes into water. Our conceptual framework for pressure denaturation is as follows: the protein interior is largely composed of efficiently packed residues,

more likely hydrophobic than those at the surface (19). Increasing hydrostatic pressure then forces water molecules into the protein interior, gradually filling cavities, and eventually breaking the protein structure apart.

We therefore study the effects of pressure on the association of nonpolar residues in water. We use the information theory model of hydrophobic interactions, a unification (20–22) of the Pratt–Chandler (23) and scaled particle theories (24, 25) of hydrophobic effects. The information theory model accounts for the primitive hydrophobic effects of solvation, association, and conformational equilibria of small nonpolar solutes in water (20). We have previously studied the temperature dependence of hydrophobic hydration by using the information theory model (8). This study reproduced the characteristic entropy increase with temperature and entropy convergence at about 400 K, in accord with calorimetry experiments (2). Here, we use the information theory model to predict the association of hydrophobic particles as a function of pressure. Specifically, we focus on the potential of mean force (pmf) between two and three nonpolar solutes (23, 26–32). The effect of water insertion into a nonpolar aggregate is then quantified by calculating the free energy difference between the contact minimum and the solvent-separated minimum in the pmf.

MATERIALS AND METHODS

The information theory model (8, 20, 21) describes the occupancy fluctuations for molecular volumes within liquid water by using the water number density ρ and water-oxygen pair correlation function $g(r)$. The probability p_0 of zero occupancy yields chemical potentials of cavity formation (33–35) for nonpolar solutes,

$$\Delta\mu^{ex} = -k_B T \ln p_0. \qquad [1]$$

In its simplest form, the information theory model utilizes the experimentally accessible first and second moments of the number of solvent centers inside the cavity volume v,

$$\langle n \rangle = \rho v, \qquad [2]$$

$$\langle n(n-1) \rangle = \rho^2 \int_v d\mathbf{r} \int_v d\mathbf{s}\, g(|\mathbf{r} - \mathbf{s}|). \qquad [3]$$

The moments are used as constraints in the maximum-entropy calculation that estimates the probabilities p_n to observe n solvent centers inside the solute cavity v. In its simplest form the p_n are of discrete Gaussian form, $p_n = \exp(\lambda_0 + \lambda_1 n + \lambda_2 n^2)$

with $n = 0, 1, 2, \ldots$, where λ_0, λ_1, λ_2 are Lagrange multipliers to be determined from the constraints of available information and the normalization condition, $\sum_{n=0}^{\infty} p_n = 1$.

The water–oxygen pair correlation functions used in the information theory calculations were determined from Monte Carlo simulations of 256 SPC water molecules (36) at 298 K for densities between 0.975 and 1.2 times the standard density ρ_0 = 997.07 kg·m^{-3} at density intervals of 0.025 ρ_0. Ewald summation was used for electrostatic interactions (37). The pressure p was calculated from $p = \rho k_B T - \langle \partial U / \partial V \rangle$, where the last term is the ensemble average of the volume derivative of the potential energy that contains contributions from the volume dependence of the effective Ewald potential. The pressure behavior of SPC water was found to be in good agreement with experimental data. The isothermal compressibility χ_T at standard density was $\rho_0 k_B T \chi_T = 0.061$, in excellent agreement with the experimental value of 0.062. The pressure at a density 1.2ρ_0 was 725 MPa compared with an experimental pressure of 775 MPa.

RESULTS AND DISCUSSION

Fig. 1 shows the calculated pmfs between two methane-sized cavities (water-oxygen exclusion radius $d = 0.33$ nm) (8, 20) for pressures between -16 to 725 MPa (-0.16 to 7.25 kbar), relative to the solvent-separated minimum. We observe two effects: increasing pressure heightens the desolvation barrier between the solvent-separated and contact minimum, and lowers the pmf at complete cavity overlap ($r \rightarrow 0$). The desolvation-barrier increase follows from the increased energetic cost at high pressure of forming a small void between the two solutes; the free energy decrease at short distances reflects the increased gain in solvation free energy of bringing two cavities to perfect overlap ($r = 0$) with increasing pressure. These opposite trends with pressure lead to a region near $r = d$, where the pmfs cross.

The pmfs shown in Fig. 1 do not contain the contributions of direct methane–methane Lennard–Jones interactions (38). The total pmfs, the sum of direct and solvent contributions (20), are shown in Fig. 2. We observe that increasing pressure destabilizes the contact minimum of the methane–methane pmf at $r \sim 0.39$ nm relative to the solvent-separated minimum at 0.73 nm. Fig. 2 *Inset* shows the free energy difference between the two pmf minima as a function of pressure. Increasing the pressure to about 700 MPa reduces the relative stability of the contact minimum by about 0.35 $k_B T$ (0.9 kJ·mol^{-1}). The results of Monte Carlo simulations (39) show

a similar shift of about 0.25 $k_B T$. Simulations of concentrated methane solutions in water showed the destabilizing effect of pressure on methane aggregates (40): At low pressures, methane aggregates form, suggestive of liquid phase separation; at pressures of a few hundred MPa, those aggregates dissolve.

Methane–methane pmfs are a valuable model for studying interactions of hydrophobic groups. However, many-body contributions beyond pairwise might arise from the packing of hydrophobic side chains in the protein interior. To investigate those many-body contributions, we calculated the pmf of three methane molecules in an equilateral configuration as a function of distance. We find that the three-body pmfs, shown in Fig. 3, are well approximated by the sum of the two-body pmfs. Increasing pressure to 700 MPa again destabilizes the contact minimum relative to the solvent-separated minimum by about 0.83 $k_B T$, with the three-body interactions reducing the pressure destabilization by about 20%.

FIG. 2. Pmf for methane association for varying pressure, including Lennard–Jones and solvent contributions. Results are shown for pressures between -16 and 725 MPa, where arrows indicate changes with increasing pressure. (*Inset*) Difference in free energy between the contact ($r \sim 0.39$ nm) and solvent-separated minimum ($r \sim 0.73$ nm) as a function of pressure. Equilibrium of those two states would also involve an ideal contribution $-\ln(r_2/r_1)^2$ deriving from relative volume changes of spherical shells. Note that the stable contact minimum moves inward slightly with increasing pressure.
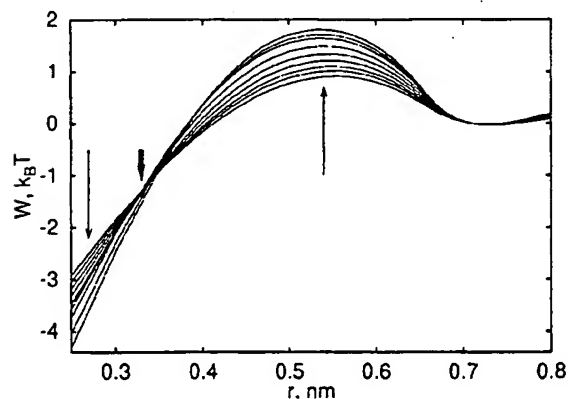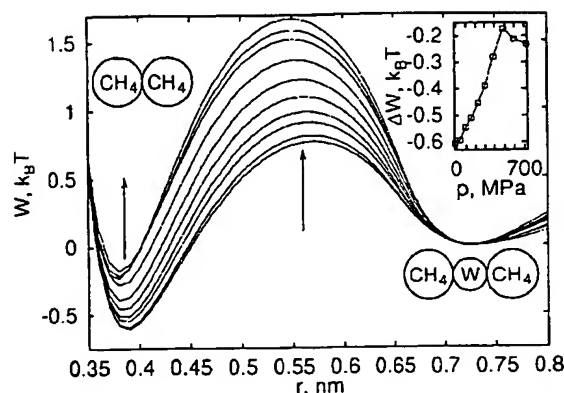

FIG. 1. Pmf between two methane-sized cavities for different pressures, normalized at the solvent-separated minimum. Results are shown for pressures between -16 and 725 MPa. Thin arrows indicate changes with increasing pressure. The thick arrow indicates the crossover region at $r = d$.
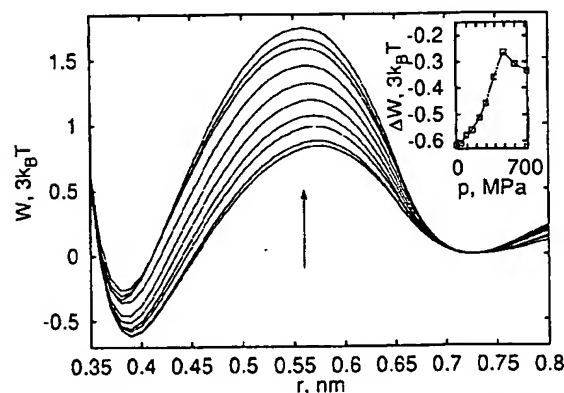

FIG. 3. Pmf for association of three methane molecules in an equilateral configuration for varying pressure, including Lennard–Jones and solvent contributions. Note that the energy unit is $3k_B T$ for comparison with the pair pmfs shown in Fig. 2. The three-body pmfs are shown as a function of the pair distance r for pressures between -16 and 725 MPa, where the arrow indicates changes with increasing pressure. (*Inset*) Difference in free energy between the contact and solvent-separated minimum as a function of pressure.

Consideration of solute-size effects is also important because the effective size of a hydrophobic amino acid side chain is larger than a methane molecule. Inspecting the pressure-dependent pmfs for cavities of sizes d from 0.31 to 0.35 nm, we find that the crossover between the increasing desolvation barrier and decreasing overlap minimum is at a distance $r \approx d$, where $d \approx R_W + R_S$ is approximately the sum of the van der Waals radii of water, R_W, and the solute, R_S. The minimum of the van der Waals interaction between the solutes, on the other side, is at a distance $2R_S$ and thus in the desolvation-barrier region for all solutes larger than water, $R_S > R_W$. For nonpolar particles with contact distances in the desolvation barrier, increasing pressure destabilizes the contact configuration relative to the solvent-separated configuration. As a consequence, the effect of pressure destabilization is expected to be even stronger for interacting nonpolar amino acid side chains compared with methane pairs.

Fig. 4 illustrates kinetic effects expected from the present model. The free-energy differences $\Delta W_f^{\ddagger}$ between the solvent-separated minimum and the desolvation barrier, as well as $\Delta W_u^{\ddagger}$ between the contact minimum and the barrier depend linearly on pressures between 0 and 500 MPa. $\Delta W_f^{\ddagger}$ and $\Delta W_u^{\ddagger}$ correspond to the activation barriers for pressure-induced "folding" and "unfolding" of one hydrophobic contact pair (i.e., the transition from the solvent-separated to the contact minimum and *vice versa*). We define activation volumes as the derivative of the activation barriers with respect to pressure, $\Delta v_{fu}^{\ddagger} = \partial W_{fu}^{\ddagger}/\partial p$. Both activation volumes are positive and approximately independent of pressure in the range 0 to 500 MPa, $\Delta v_f^{\ddagger} = 3.8$ ml/mol and $\Delta v_u^{\ddagger} = 1.6$ ml/mol. Accordingly, pressure slows down the interconversion between the two states.

These results are consistent with an experimental study of the pressure dependence of folding and unfolding rates for staphylococcal nuclease (41). Both the protein folding and unfolding rates decrease with increasing pressure, corresponding to positive activation volumes in a two-state model, $\Delta V_f^{\ddagger} = 92 \pm 4$ ml/mol and $\Delta V_u^{\ddagger} = 20 \pm 3$ ml/mol. In a simplified picture neglecting polar and many-body contributions, the activation volumes for folding and unfolding of staphylococcal nuclease correspond to breaking $\Delta V_{fu}^{\ddagger}/\Delta v_{fu}^{\ddagger} \approx 10$–$25$ hydrophobic contacts upon formation of the transition state. In the crystal structure (42), 155 pairs of carbon atoms (excluding carbonyl carbons) are found within 0.4 nm for all carbon atoms on polar and nonpolar amino acids that are not neighbors along the peptide chain. With the same criterion, 34 nonneighboring amino acids are found to be paired. The energy landscape theory and folding-funnel model predict that approximately 40% of the native contacts between amino acids are broken at the transition state (43, 44). Accordingly, the crude estimate of 10–25 disrupted interactions gives the right order of magnitude. Vidugiris *et al.* (41) also conclude that the transition state corresponds to a collapsed, loosely-packed solvent-excluded structure. This finding agrees with the present model, where the desolvation barrier corresponds to an extended structure (relative to the contact configuration) that does not allow solvent penetration.

The present model, together with the results of Fig. 2, answers the question why "expanded" protein structures that eliminate close hydrophobic contacts are more stable at higher pressures: The protein–water system may be packed more efficiently and have a lower total volume when water molecules are mixed into the structure, swelling the protein globule. Pressure stabilization of clathrate hydrates (45) provides a simple analogous behavior. High pressure stabilizes the crystalline phase that eliminates close solute contacts. But this does not violate the thermodynamic principle that increasing pressure stabilizes the phase of lower volume.

CONCLUSIONS

The results for the pressure dependence of nonpolar interactions have implications on our understanding of protein unfolding thermodynamics, kinetics, and structure. They establish that the model of folded proteins stabilized by a hydrophobic core does not contradict the experimental observations that proteins can be denatured by pressure, thus resolving the pressure denaturation puzzle pointed out by Kauzmann (1). We find that pressure destabilizes the contact configuration of nonpolar molecular groups relative to a solvent-separated configuration. This observation leads to our most significant conclusion regarding the mechanism of pressure denaturation: Pressure denaturation corresponds to the incorporation of water into the protein, whereas heat denaturation corresponds to the transfer of nonpolar groups into water. With increasing pressure, packing forces compete more favorably with the tendency to form a tetrahedral hydrogen bond network (46). The resulting increase in the coordination number causes energetic frustration (47). This in turn reduces the relative cost of inserting water molecules into a nonpolar aggregate, an otherwise unfavorable environment. That insertion of water molecules is manifest in the increasing importance of the solvent-separated minimum in the free energy of association.

Our results lead to a picture of the ensemble of pressure-denatured protein structures, where water molecules penetrate the protein interior. This finding is in agreement with experimental observations (13), most notably the observed increase in the hydrodynamic radius upon denaturation (48, 49) and an increase in the hydrogen-exchange rates of lysozyme and RNase A with pressure (50). This swelling process results in structures with reduced compactness that, however, retain considerably more order than heat-denatured proteins, as probed by NMR experiments of hydrogen exchange (17). Adding glycerol as a cosolvent to water increases the pressure required for denaturation of the Arc repressor (51). An extrapolation to a pure glycerol solvent suggests that the Arc repressor protein could not be pressure denatured in glycerol. Oliveira *et al.* (51) therefore conclude that water is crucial for pressure denaturation, and that the denatured state is solvated. Tryptophan-phosphorescence lifetime studies of dimeric alcohol dehydrogenase under pressures exceeding 250 MPa were interpreted as pressure-induced water penetration into the dimer interface (52).

X-ray crystallography of lysozyme at 100 MPa did not show an increased hydration of the protein interior (53, 54), but that study was carried out at pressures significantly below the denaturation pressure (48, 55, 56). A sharp increase of the hydrodynamic radius of lysozyme has been observed for pressures above about 500–600 MPa (48). The slow rates of
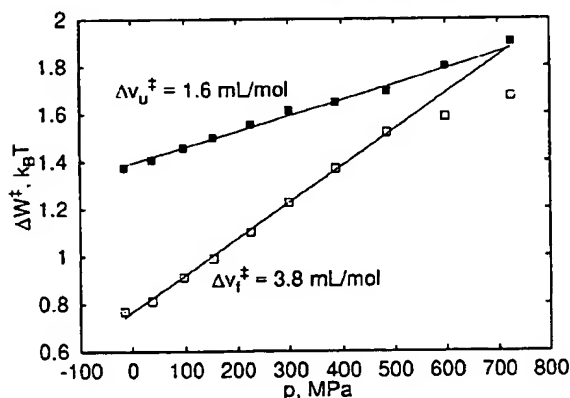

FIG. 4. Activation free energy as a function of pressure. $\Delta W_u^{\ddagger}$ and $\Delta W_f^{\ddagger}$ are the free energy differences of the contact (□) and solvent-separated minima (■), respectively, to the desolvation barrier of the pmf for methane association (Fig. 2). Activation volumes $\Delta v_u^{\ddagger}$ and $\Delta v_f^{\ddagger}$ are derived from a linear fit for pressures between 0 and 500 MPa.

Biophysics: Hummer *et al.*

Proc. Natl. Acad. Sci. USA 95 (1998)   1555

unfolding observed in pressure-jump experiments (41, 57, 58) suggest that sub-nanosecond molecular-dynamics simulations of pressure denaturation (59–62) do not fully cover the relevant time scales, although an increase in the solvent exposure of residues in the hydrophobic core has indeed been observed in an 800-ps simulation calculation (62).

We compared observed activation volumes for folding and unfolding (41) and calculated activation volumes for forming and breaking hydrophobic contacts. From the ratio of those activation volumes, one can estimate that the equivalent of about 10–25 hydrophobic contacts are broken in the transition state of pressure unfolding of staphylococcal nuclease (41). Exploring the characteristics of pressure-denatured proteins in relation to proteins unfolded by temperature or chemical denaturants provides valuable input to theories of protein folding. Bryngelson *et al.* (43) pointed out that pressure can be used to explore the roughness of the folding energy landscape. In agreement with the present model, the experimental data (41) show that pressure slows down folding and unfolding kinetics, corresponding to an increasingly rough landscape.

The swelling of the protein core with increasing pressure will affect protein structure, dynamics, and stability, to be characterized in intensified studies of that largely unexplored thermodynamic dimension, pressure (63). A better understanding of proteins under pressure will also help to elucidate adaptation processes of barophilic organisms, such as those living in the deep sea under pressures of up to about 120 MPa (64–66).

1. Kauzmann, W. (1987) *Nature (London)* **325**, 763–764.
2. Baldwin, R. L. (1986) *Proc. Natl. Acad. Sci. USA* **83**, 8069–8072.
3. Kauzmann, W. (1959) *Adv. Protein Chem.* **14**, 1–63.
4. Dill, K. A. (1990) *Biochemistry* **29**, 7133–7155.
5. Makhatadze, G. I. & Privalov, P. L. (1995) *Adv. Protein Chem.* **47**, 307–425.
6. Lazaridis, T., Archontis, G. & Karplus, M. (1995) *Adv. Protein Chem.* **47**, 231–306.
7. Fu, L. & Freire, E. (1992) *Proc. Natl. Acad. Sci. USA* **89**, 9335–9338.
8. Garde, S., Hummer, G., García, A. E., Paulaitis, M. E. & Pratt, L. R. (1996) *Phys. Rev. Lett.* **77**, 4966–4968.
9. Brandts, J. F., Oliveira, R. J. & Westort, C. (1970) *Biochemistry* **9**, 1038–1047.
10. Zipp, A. & Kauzmann, W. (1973) *Biochemistry* **12**, 4217–4228.
11. Heremans, K. (1982) *Annu. Rev. Biophys. Bioeng.* **11**, 1–21.
12. Weber, G. & Drickamer, H. G. (1983) *Q. Rev. Biophys.* **16**, 89–112.
13. Silva, J. L. & Weber, G. (1993) *Annu. Rev. Phys. Chem.* **44**, 89–113.
14. Jonas, J. & Jonas, A. (1994) *Annu. Rev. Biophys. Biomol. Struct.* **23**, 287–318.
15. Royer, C. A. (1995) *Methods Enzymol.* **259**, 357–377.
16. Silva, J. L., Foguel, D., Da Poian, A. T. & Prevelige, P. E. (1996) *Curr. Opin. Struct. Biol.* **6**, 166–175.
17. Zhang, J., Peng, X., Jonas, A. & Jonas, J. (1995) *Biochemistry* **34**, 8631–8641.
18. Wolfenden, R. & Radzicka, A. (1994) *Science* **265**, 936–937.
19. Richards, F. M. (1974) *J. Mol. Biol.* **82**, 1–14.
20. Hummer, G., Garde, S., García, A. E., Pohorille, A. & Pratt, L. R. (1996) *Proc. Natl. Acad. Sci. USA* **93**, 8951–8955.
21. Berne, B. J. (1996) *Proc. Natl. Acad. Sci. USA* **93**, 8800–8803.
22. Chandler, D. (1993) *Phys. Rev. E* **48**, 2898–2905.
23. Pratt, L. R. & Chandler, D. (1977) *J. Chem. Phys.* **67**, 3683–3704.
24. Pierotti, R. A. (1963) *J. Phys. Chem.* **67**, 1840–1845.
25. Stillinger, F. H. (1973) *J. Solut. Chem.* **2**, 141–158.
26. Pangali, C., Rao, M. & Berne, B. J. (1979) *J. Chem. Phys.* **71**, 2975–2981.
27. Watanabe, K. & Andersen, H. C. (1986) *J. Phys. Chem.* **90**, 795–802.
28. Smith, D. E., Zhang, L. & Haymet, A. D. J. (1992) *J. Am. Chem. Soc.* **114**, 5875–5876.
29. van Belle, D. & Wodak, S. J. (1993) *J. Am. Chem. Soc.* **115**, 647–652.
30. Head-Gordon, T. (1995) *J. Am. Chem. Soc.* **117**, 501–507.
31. Garde, S., Hummer, G. & Paulaitis, M. E. (1996) *Faraday Discuss.* **103**, 125–139.
32. Lüdemann, S., Abseher, R., Schreiber, H. & Steinhauser, O. (1997) *J. Am. Chem. Soc.* **119**, 4206–4213.
33. Pohorille, A. & Pratt, L. R. (1990) *J. Am. Chem. Soc.* **112**, 5066–5074.
34. Pratt, L. R. & Pohorille, A. (1992) *Proc. Natl. Acad. Sci. USA* **89**, 2995–2999.
35. Beutler, T. C., Béguelin, D. R. & van Gunsteren, W. F. (1995) *J. Chem. Phys.* **102**, 3787–3793.
36. Berendsen, H. J. C., Postma, J. P. M., van Gunsteren, W. F. & Hermans, J. (1981) in *Interaction Models for Water in Relation to Protein Hydration*, ed. Pullman, B. (Reidel, Dordrecht, The Netherlands), pp. 331–342.
37. Hummer, G., Pratt, L. R. & García, A. E. (1995) *J. Phys. Chem.* **99**, 14188–14194.
38. Jorgensen, W. L., Madura, J. D. & Swenson, C. J. (1984) *J. Am. Chem. Soc.* **106**, 6638–6646.
39. Payne, V. A., Matubayasi, N., Murphy, L. R. & Levy, R. M. (1997) *J. Phys. Chem. B* **101**, 2054–2060.
40. Wallqvist, A. (1992) *J. Chem. Phys.* **96**, 1657–1658.
41. Vidugiris, G. J. A., Markley, J. L. & Royer, C. A. (1995) *Biochemistry* **34**, 4909–4912.
42. Hynes, T. R. & Fox, R. O. (1991) *Proteins Struct. Funct. Genet.* **10**, 92–105.
43. Bryngelson, J. D., Onuchic, J. N., Socci, N. D. & Wolynes, P. G. (1995) *Proteins Struct. Funct. Genet.* **21**, 167–195.
44. Onuchic, J. N., Socci, N. D., Luthey-Schulten, Z. & Wolynes, P. G. (1996) *Folding Design* **1**, 441–450.
45. Sloan, E. D., Jr. (1990) *Clathrate Hydrates of Natural Gases* (Dekker, New York).
46. Stillinger, F. H. & Rahman, A. (1974) *J. Chem. Phys.* **61**, 4973–4980.
47. Sciortino, F., Geiger, A. & Stanley, H. E. (1991) *Nature (London)* **354**, 218–221.
48. Chryssomallis, G. S., Torgerson, P. M., Drickamer, H. G. & Weber, G. (1981) *Biochemistry* **20**, 3955–3959.
49. Cléry, C., Renault, F. & Masson, P. (1995) *FEBS Lett.* **370**, 212–214.
50. Carter, J. V., Knox, D. G. & Rosenberg, A. (1978) *J. Biol. Chem.* **253**, 1947–1953.
51. Oliveira, A. C., Gaspar, L. P., Da Poian, A. T. & Silva, J. L. (1994) *J. Mol. Biol.* **240**, 184–187.
52. Cioni, P. & Strambini, G. B. (1996) *J. Mol. Biol.* **263**, 789–799.
53. Kundrot, C. E. & Richards, F. M. (1987) *J. Mol. Biol.* **193**, 157–170.
54. Kundrot, C. E. & Richards, F. M. (1988) *J. Mol. Biol.* **200**, 401–410.
55. Li, T. M., Hook, J. W., Drickamer, H. G. & Weber, G. (1976) *Biochemistry* **15**, 5571–5580.
56. Samarasinghe, S. D., Campbell, D. M., Jonas, A. & Jonas, J. (1992) *Biochemistry* **31**, 7773–7778.
57. Vidugiris, G. J. A., Truckses, D. M., Markley, J. L. & Royer, C. A. (1996) *Biochemistry* **35**, 3857–3864.
58. Frye, K. J. & Royer, C. A. (1997) *Protein Sci.* **6**, 789–793.
59. Kitchen, D. B., Reed, L. H. & Levy, R. M. (1992) *Biochemistry* **31**, 10083–10093.
60. Brunne, R. M. & van Gunsteren, W. F. (1993) *FEBS Lett.* **323**, 215–217.
61. Hünenberger, P. H., Mark, A. E. & van Gunsteren, W. F. (1995) *Proteins Struct. Funct. Genet.* **21**, 196–213.
62. Wroblowski, B., Diaz, J. F., Heremans, K. & Engelborghs, Y. (1996) *Proteins Struct. Funct. Genet.* **25**, 446–455.
63. Frauenfelder, H., Alberding, N. A., Ansari, A., Braunstein, D., Cowen, B. R., *et al.* (1990) *J. Phys. Chem.* **94**, 1024–1037.
64. Brooks, J. M., Kennicutt, M. C., Fisher, C. R., Macko, S. A., Cole, K., Childress, J. J., Bidigare, R. R. & Vetter, R. D. (1987) *Science* **238**, 1138–1142.
65. Gross, M. & Jaenicke, R. (1994) *Eur. J. Biochem.* **221**, 617–630.
66. Yayanos, A. A. (1995) *Annu. Rev. Microbiol.* **49**, 777–805.

Exhibit 36

High-Resolution, High-Pressure NMR Studies of Proteins

J. Jonas,* L. Ballard,# and D. Nash#

*Beckman Institute for Advanced Science and Technology, and #Department of Chemistry, School of Chemical Sciences, University of Illinois, Urbana, Illinois 61801 USA

ABSTRACT   Advanced high-resolution NMR spectroscopy, including two-dimensional NMR techniques, combined with high pressure capability, represents a powerful new tool in the study of proteins. This contribution is organized in the following way. First, the specialized instrumentation needed for high-pressure NMR experiments is discussed, with specific emphasis on the design features and performance characteristics of a high-sensitivity, high-resolution, variable-temperature NMR probe operating at 500 MHz and at pressures of up to 500 MPa. An overview of several recent studies using 1D and 2D high-resolution, high-pressure NMR spectroscopy to investigate the pressure-induced reversible unfolding and pressure-assisted cold denaturation of lysozyme, ribonuclease A, and ubiquitin is presented. Specifically, the relationship between the residual secondary structure of pressure-assisted, cold-denatured states and the structure of early folding intermediates is discussed.

INTRODUCTION

Since Anfinsen and colleagues (Anfinsen, 1973) first studied the renaturation of reduced and unfolded ribonuclease A (RNase A), much effort has been expended in attempting to understand the relationships between the amino acid sequence, the structure, and dynamic properties of the native conformation of proteins. Recently, increasing attention has been focused on denatured and partially folded states, because determination of their structure and stability may provide critical insights into the mechanisms of protein folding (Kim and Baldwin, 1990; Creighton, 1993; Buck et al., 1994). The native conformations of hundreds of proteins are known in great detail from structural determinations by x-ray crystallography and, more recently, NMR spectroscopy. However, detailed knowledge of the conformations of denatured and partially folded states is lacking, which is a serious shortcoming in current studies of protein stability and protein folding pathways (Robertson and Baldwin, 1991).

Most studies dealing with protein denaturation have been carried out at atmospheric pressure with various physico-chemical perturbations, such as temperature, pH, or denaturants, as experimental variables. Compared to varying temperature, which produces simultaneous changes in both volume and thermal energy, the use of pressure to study protein solutions perturbs the environment of the protein in a continuous, controlled way by changing only intermolecular distances (Weber and Drickamer, 1983). In addition, by taking advantage of the phase behavior of water (Jonas, 1982), shown in Fig. 1, high pressure can substantially lower the freezing point of an aqueous protein solution. Therefore, by applying high pressure, one can investigate in

detail not only pressure-denatured proteins, but also cold-denatured proteins in aqueous solution.

The great potential of the high-resolution, high-pressure NMR techniques for studies of proteins (Jonas and Jonas, 1994) provided the motivation for our efforts in improving the performance of high-resolution, high-pressure NMR probes. We have discussed our own progress (Ballard et al., 1996) in the development of high-pressure NMR instrumentation, based on the autoclave-style approach, in which both the sample and the RF coil are located in a nonmagnetic, high-pressure vessel. In this contribution we focus on the very recent development (Ballard et al., 1998) of a high-sensitivity, high-resolution NMR probe operating at 500 MHz and at pressures of up to 500 MPa. Such probes are currently being used to obtain conventional 2D NMR spectra (e.g., COSY and NOESY spectra) of proteins on a routine basis.

One major application of NMR to protein chemistry is the use of hydrogen exchange kinetics as a probe of protein structure. Our group has recently applied this method to investigate structure in proteins denatured by high pressure at various temperatures. Previous work (Zhang et al., 1995; Konno et al., 1995; Wong et al., 1996) on pressure and cold denaturation has suggested that these methods can leave appreciable residual structure in proteins, particularly when compared to other methods such as thermal or urea denaturation. In RNase A, for example (Zhang et al., 1995), the extent of residual structure measured by hydrogen exchange methods is similar to that present in molten globules (Buck et al., 1994) and other well-characterized, partially structured proteins. The cold-denatured state of *Streptomyces* subtilisin inhibitor (Konno et al., 1995) shows a smaller radius of gyration by x-ray scattering than the heat- and urea-denatured states do—its value is only marginally (~5%) larger than that of the native state, and is in line with values cited for molten globules and other collapsed unfolded states. As a result, cold denaturation appears to be a milder method of denaturation than the more conventional
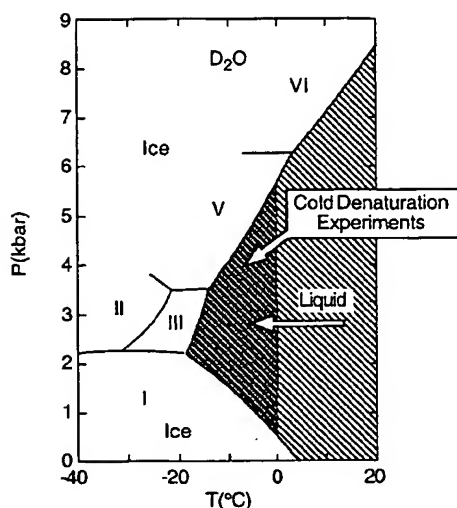
Biophysical Journal

FIGURE 1   High-pressure phase diagram of D_2O (Jonas, 1982).

methods of heat and chemical (e.g., urea) denaturation. In contrast, the recent study of monomeric λ repressor (Huang and Oas, 1996) concludes that the heat- and cold-denaturated states are thermodynamically and conformationally equivalent. However, this observation may be the result of the 3M urea added to the protein solutions used both for cold denaturation (0°C) and heat denaturation (70°C) of λ repressor.

Such results are interesting enough, but they become more important when related to modern protein folding studies. Structures that persist in a protein upon denaturation, even relatively mild denaturation, are likely to be highly stable. If no appreciable barriers exist to the rapid formation of such structures, they should be among the first to appear in the refolding of a protein. Consequently, mildly denatured states may serve as useful models for species present early in refolding, with the advantage that such species could be studied for hours or even days, rather than fractions of a second. There is already considerable evidence that the equilibrium collapsed unfolded states of some proteins, obtained under mildly denaturing conditions, are structurally similar to the early, collapsed states that occur when the protein begins to fold (Fink, 1995; Ptitsyn, 1995). Hence a major motivation for this research (Nash and Jonas, 1997a,b) was to characterize several proteins by cold denaturation and compare them to known species observed during folding.

The proteins discussed here were chosen for several reasons. All three—lysozyme, ribonuclease A, and ubiquitin—are small, well-characterized proteins that have been studied before. The solution NMR structures for all three are known (Di Stefano and Wand, 1987; Redfield and Dobson, 1988; Rico et al., 1991). Numerous studies have been made of all of these proteins in various denatured and partially folded states. For example, the folding pathways and inter-

mediates of ribonuclease A (Udgaonkar and Baldwin, 1990; Houry and Scheraga, 1996) and of lysozyme (Radford et al., 1992) have been described in detail. Various denatured states of ribonuclease A (Robertson and Baldwin, 1991), lysozyme (Buck et al., 1994), and ubiquitin (Harding et al., 1991) are available for comparison. The cold-denatured state of ribonuclease A has been characterized before (Zhang et al., 1995), and evidence for structure in the pressure-denatured state has been described. Furthermore, in the case of ubiquitin, Gladwin and Evans (1996) found no evidence for significant protection from exchange at early stages of folding; therefore, to test the hypothesis of this parallel, we have also investigated hydrogen exchange in the pressure-assisted, cold-denatured state of ubiquitin.

EXPERIMENTAL

The materials and experimental conditions for the various NMR experiments were discussed in detail in the original studies (Zhang et al., 1995; Nash et al., 1996; Nash and Jonas, 1997a,b). The principal NMR system in the laboratory is composed of a General Electric GN-300 NMR console, operating at a proton Larmor frequency of 300 MHz, with an Oxford Instruments wide-bore superconducting magnet (ϕ = 89 mm, 7.04 T). The GN-300 is interfaced to a Tecmag Scorpio data acquisition system for pulse programming and experimental control with MacNMR software. This system was used for some studies of proteins at high pressure and ambient temperature (Ballard et al., 1996), as well as for optimization of cold denaturing conditions (i.e., determination of pressures and temperatures that lead to near-complete cold denaturation) for the hydrogen exchange experiments (Nash et al., 1996; Nash and Jonas, 1997a,b).

The hydraulic pressure generation system was similar to the system described previously (Jonas et al., 1993). As with the earlier system, carbon disulfide (CS_2) was used as the pressure transmitting fluid for proton studies. As an illustration of the quality of high-resolution NMR spectra during high-pressure denaturation experiments, we include Fig. 2 and Fig. 3, which are taken from our earlier studies.

For most of the recent protein studies, more advanced instrumentation (Ballard et al., 1998) was used. For general-purpose studies of proteins, the group has begun using a Varian INOVA wide-bore instrument, adapted to handle high pressure, with a proton frequency of 500 MHz. This instrument is gradually replacing the 300-MHz spectrometer for protein studies because of its higher sensitivity and resolution (Table 1), and is useful for direct measurements at high pressure at temperatures at and above room temperature (range ~0°C to ~60°C).

For lower temperatures, other methods and instruments have been employed. Structure in cold-denatured proteins was assessed by hydrogen exchange techniques, which did not require high pressure to be maintained during measurement. Measurements of the extent of hydrogen exchange in cold-denatured proteins were therefore obtained on spectrometers outside the group laboratory: either a Varian Unity 500 MHz spectrometer (ribonuclease A) or a Varian INOVA 500 MHz narrow-bore spectrometer (lysozyme and ubiquitin), both using a conventional, commercially available NMR probe. Cold-denaturing conditions were obtained at pressures of 2250–3750 bar and temperatures of −13 to −17°C, depending on the protein (Nash et al., 1996; Nash and Jonas, 1997a,b).

It is appropriate at this point to mention several design considerations for high-resolution, high-pressure NMR probes that are to be used for protein studies. The sample size (diameter) should definitely be greater than 5 mm; otherwise the sensitivity of the high-pressure NMR probe will seriously limit the scope of problems to be studied. For a protein it should be possible to obtain good S/N for concentrations in the millimolar (mM) or lower range. Higher concentrations usually result in aggregation and even precipitation of the protein when temperature or pressure is changed.

In our recent experiments (Ballard et al., 1998), we have increased the sensitivity, power, and tuning range of our double-tuned ($^1H/^2H$) NMR
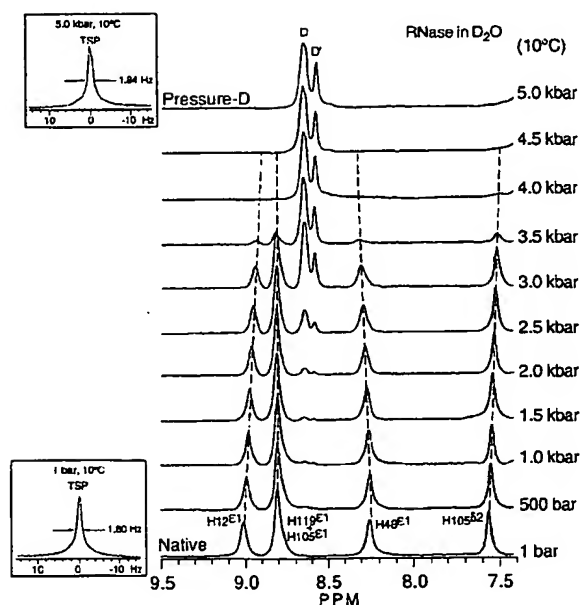
FIGURE 2   Histidine region of the ^{1}H NMR spectra of RNase A in D_2O at various pressures (10°C, pH* 2.0). The standard in the insets is sodium 3-(trimethylsilyl)tetradeuteriopropionate (TSP) (Zhang et al., 1995).
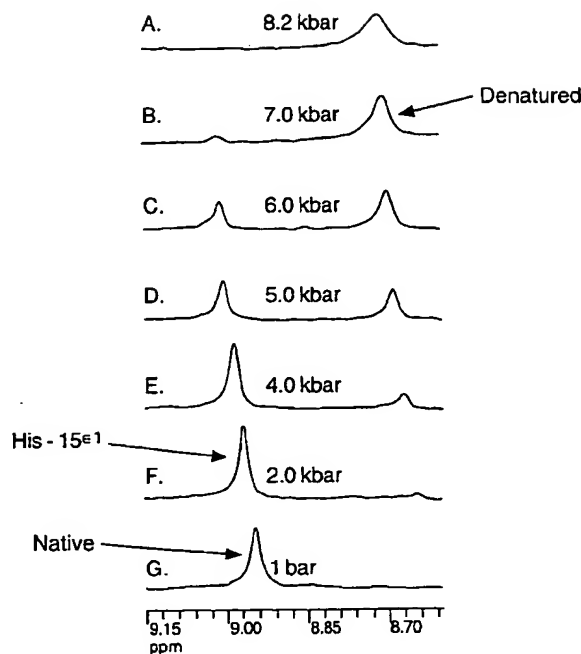

FIGURE 3   Stacked ^{1}H NMR plot of the lysozyme (pH* 2.2, 4 mM protein, 20 mM maleic-2,3-d2 anhydride, 1.5 mM TSP) histidine region at selected pressures at 37.5°C. Note the disappearance of the native His[15] residue peak (~8.95 ppm) and the appearance of the denatured His[15] residue peak (~8.70 ppm) with pressure; complete denaturation is attained between 7 and 8.25 kbar (Ballard et al., 1996).

probes. The pressure vessel, pressure RF feedthroughs, and internal capacitor design concepts described earlier were all incorporated. In contrast, though, the RF coil now consists of a single-turn saddle coil machined from low magnetic susceptibility oxygen-free copper. Table 1 illustrates the significant improvement in sensitivity of the high-pressure NMR probe, when the coil design is changed from a two-turn wire coil to a one-turn machined coil by comparing the sensitivity (S/N ratio) for various high-pressure NMR probes used in our laboratory. For an 8-mm sample diameter, the S/N ratio for a 300-MHz probe increased from 34 to 131, whereas it increased to 260 at 500 MHz. Clearly, the increased frequency of 500 MHz also contributes to the enhanced sensitivity, but the major improvement is due to the RF coil design.

A comparison of the high quality of spectra obtained at 500 MHz with the new probe RF coil design to those obtained at 300 MHz with the earlier coil design is given in Fig. 4. The most important feature is the improved sensitivity, as the aromatic region, 500 MHz N-domain of troponin C F29W with Ca^{2+} was obtained for a 0.4 mM concentration compared to the 300 MHz spectrum, which was obtained for a 0.8 mM concentration of the protein using similar acquisition parameters. Although one can readily appreciate the advantages of higher sensitivity and probe power on dilute biochemical studies using one-pulse methods, we feel that an even more important extension of this work is in the field of high-pressure 2D NMR. As a demonstration of this capability, we include Fig. 5, which shows the 2D NOESY aromatic region of N-domain troponin C F29W at 5 kbar.

RESULTS AND DISCUSSION

The experimental procedures were described in detail in the original studies (Zhang et al., 1995; Nash et al., 1996; Nash and Jonas, 1997a,b) of cold denaturation of ribonuclease A, lysozyme, and ubiquitin. Hydrogen exchange data for proteins are typically expressed in terms of the protection factor $P = k_{rc}/k_{obs}$ for a given amide proton, where k_{obs} is the experimentally measured exchange rate and k_{rc} is the ex-

change rate for a proton in an ideal unstructured polypeptide under the same conditions. P values close to 1 indicate lack of appreciable structure, whereas P values in certain regions of native proteins can exceed 10^6. In partially folded states, such as molten globules (Buck et al., 1994) or the methanol-induced A state of ubiquitin (Pan and Briggs, 1992), P values are intermediate. Typical values in such states range from 1 to several hundred.

The exchange of amide hydrogens in peptides is primarily caused by acid and base, with a small contribution from water, which can act as a weak acid or base (Bai et al., 1993):

$$k = k_a[D^+] + k_b[OD^-] + k_w \qquad (1)$$

TABLE 1   High-pressure NMR probe performance features

Coil design	^{1}H freq. MHz [max. press., bars]	Sample O.D. (mm)	S/N	Ref.
2-Turn wire coil,	300 [9000]	8	34	Ballard et al. (1996)
1-Turn machined coil, 300 MHz	300 [5000]	8	131	Ballard et al. (1998)
1-Turn machine coil, 500 MHz	500 [5000]	8	260	Ballard et al. (1998)

A

1035 bar
500 MHz

7.4 7.2 7.0 6.8 6.6 ppm
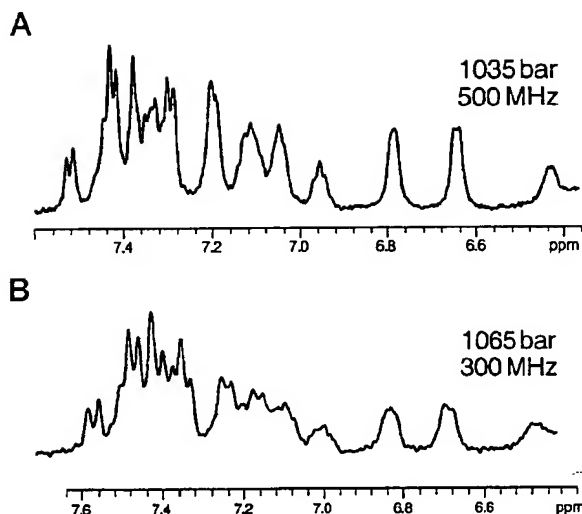
B

1065 bar
300 MHz

7.6 7.4 7.2 7.0 6.8 6.6 ppm

FIGURE 4 Comparison of the 1D proton aromatic region of the NMR spectrum of N-domain troponin C F29W + Ca^{2+} solution (pH* 7.0, 20 mM tris(hydroxymethyl)aminomethane-$d11$, 100 mM potassium chloride, 5 mM dithiothreitol, 2 mM ethylenebis(oxyethylenenitrilo)tetraacetic acid, 8 mM calcium chloride, 1.5 mM TSP) obtained at ~1 kbar pressure and 500 MHz (A) and 300 MHz (B). Spectrum A was obtained for a 0.4 mM protein solution, and spectrum B was recorded for a 0.8 mM protein solution. The number of accumulations was 1024 for both A and B.

Values for the three rate constants are known for reference "random coil" materials, specifically, unstructured oligopeptides and random-coil polypeptides, at 293 K and ambient pressure (Bai et al., 1993). To obtain a value for k_{rc} for cold-denaturing conditions, the reference values were corrected for temperature and pressure by using the activation energies and the activation volumes, respectively:

$$k_i(T) = k_i(T_0)\exp\left(-\frac{E_a}{R}\left[\frac{1}{T} - \frac{1}{T_0}\right]\right) \qquad (2)$$

$$k_i(P) = k_i(P_0)\exp\left(-\frac{(P - P_0)\Delta V^\#}{RT}\right) \qquad (3)$$

where i denotes any of the three individual reactions and E_a and $\Delta V^\#$ are the activation energy and activation volume. The activation volume, defined from

$$\Delta V^\# = -RT\frac{\partial \ln k}{\partial P} \qquad (4)$$

was assumed to be constant, over the pressure range of interest, to derive Eq. 3. This assumption has been shown to be valid over a wide pressure range for k_a and k_b in poly-D,L-lysine (Carter et al., 1978), and because the reaction mechanism for k_w is similar, this is a reasonable assumption here as well. The activation energies for k_a, k_b, and k_w are 14 kcal/mol, 3 kcal/mol, and 19 kcal/mol, respectively (Bai et al., 1993). Activation volumes were obtained from data on model compounds: random coil poly-D,L-lysine for k_a and k_b (Carter et al., 1978), and N-methylacetamide for k_w (Mabry

et al., 1996). The values of $\Delta V^\#$ are 0 ± 1, $+6 \pm 1$, and -9.0 ± 1.8 cm³/mol for k_a, k_b, and k_w, respectively.

Fig. 6 A shows the protection factors in cold-denatured lysozyme ($T = -13°C$, $p = 3750$ bar) as a function of residue number and their correspondence with secondary structural elements in the native state (Nash and Jonas, 1997a); Fig. 7 shows how the protection factors in cold-denatured lysozyme compare with those in various other well-studied denatured states—thermally denatured lysozyme at 69°C, chemically denatured lysozyme in 8 M urea solution, and the acid-denatured state of CM^{6-127} lysozyme, produced by cleaving the disulfide bond between C6 and C127 in native lysozyme (Buck et al., 1994).

From the hydrogen exchange rate data, it is clear that many regions of lysozyme are markedly protected from exchange, with P values exceeding 10, in the cold-denatured state. The range of P factors runs from 1.19 for F3 to 71.0 for R114. Except for a partially folded form observed in 50% trifluoroethanol (Buck et al., 1994), cold-denatured lysozyme is the only form of denatured lysozyme that shows appreciable protection from exchange. Data for heat, urea, and CM^{6-127} lysozyme, analyzed using the same temperature and side chain correction methods used in this study (Buck et al., 1994), show few residues with $P > 5$ (Fig. 6). It should be made clear that the pressure-assisted, cold-denatured state is not a "pure" cold-denatured state, because the pressure affects the protein directly. Nevertheless, any effect that pressure has is clearly very different from that induced by high temperature or chemical denaturants such as urea.

Lysozyme, in its native state, consists of two domains: the α domain, which contains four α-helices, and the β-domain, which contains a three-strand antiparallel β-sheet (Miranker et al., 1991). In the cold-denatured state of lysozyme, protection of amide protons against exchange is largely confined to the α-domain; all four α-helices show appreciable protection ($P > 10$ for at least one residue) from exchange. The most notable protection, involving three residues with $P > 30$, occurs in helix D (residues 108–115). In contrast, most of the β-sheet region (residues 41–60) shows no appreciable protection, with all but two residues having $P < 5$. The persistence of α-helical structure in cold-denatured proteins has been noted before, as in the cold-denatured state of barstar (Wong et al., 1996). An anomalous area of protection occurs at the end of the β-sheet and in the following loop, a region in which residues 60, 61, 63, 64, 65, 76, and 78 were observable. This region is the most highly protected area of cold-denatured lysozyme, after the D helix. It differs from the other highly protected regions in cold-denatured lysozyme, though, by not consisting of a single, well-defined region of secondary structure.

By using pulsed-labeling hydrogen exchange studies and confining exchange to the dead time of their instrumentation (~3.5 ms), Gladwin and Evans (1996) observed relatively early stages in the folding of lysozyme. Slowing of exchange measured during this time can be quantified by

FIGURE 5 2D ^{1}H/^{1}H NOESY aromatic region of N-domain troponin C F29W + Ca^{2+} obtained with the 500-MHz probe (25°C) at 5 kbar. The protein concentration was ~0.6 mm, and the NOESY mixing time was 0.15 s. The composition of the buffer solution was identical to that used in Fig. 4.
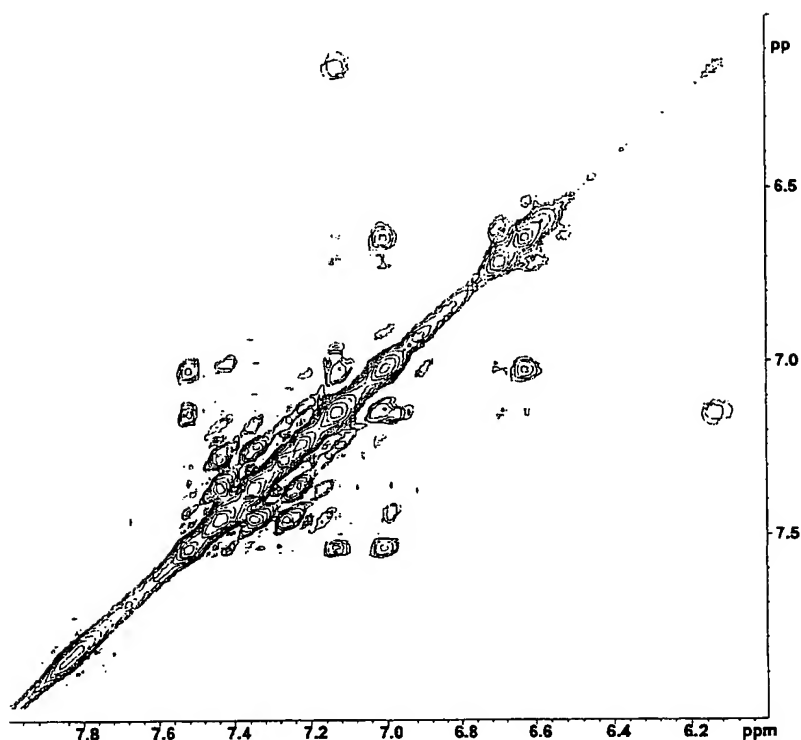
comparing the measured exchange rate to that for a random coil, as in other hydrogen exchange studies. The resulting quantity, although similar to a protection factor, is determined from a rate that changes considerably as the protein refolds; as a result, it is best referred to as a "dead-time inhibition factor" (I_D) rather than a true protection factor (Gladwin and Evans, 1996). Nevertheless, I_D values provide information similar to that provided by P values in equilibrium denatured states. During the first 3.5 ms of folding, lysozyme shows moderate degrees of protection ($I_D > 5$), not only in the α-helices and the C-terminal 3^{10} helix, but also in the loop region from residues 60–65, as well as residue 78 (Gladwin and Evans, 1996). We have thus observed a strong parallel between a stable, denatured form of lysozyme and the transient species observed during folding. Fig. 6 B compares the inhibition of hydrogen exchange observed during the first 3.5 ms of folding (Gladwin and Evans, 1996) to the protection factors obtained for pressure-assisted, cold-denatured lysozyme, as shown in Fig. 6 A.

The range of protection factors observed (Nash et al., 1996) in cold- denatured RNase A (2.8–78) is similar to that present in cold-denatured lysozyme. In contrast to lysozyme, however, the extent of protection in cold-denatured RNase A is less organized. Rather than having large extents of secondary structure protected, such as large portions of the α-helices in lysozyme, the protection in cold-denatured RNase A occurs in small regions, particularly those near disulfide-linked cysteine residues. Fig. 8 plots the protection factors versus residue in pressure-assisted cold-denatured

RNase A on a three-dimensional representation of the native structure. The most notable such region of high protection in RNase A, three residues with $P > 10$, is centered in C84, in the central strand of the large β-sheet. Protection in this β-sheet is highly nonuniform. For example, the region of the first strand from residues 35 to 48 is essentially unprotected ($P < 5$ for all residues), in contrast to the region around C84.

In a qualitative comparison, one can see that the pressure-assisted cold-denatured state exhibits patterns of protection factors (relatively low) resembling the pattern of protection factors observed by Udgaonkar and Baldwin (1990) and Houry and Scheraga (1996) for the folding intermediate of ribonuclease A. Fig. 8 also gives a qualitative comparison of protection factors for the early folding intermediate (Udgaonkar and Baldwin, 1990) and those observed of hydrogen exchange in the pressure-assisted cold-denatured state of ribonuclease A.

In the case of lysozyme and RNase A, the patterns of protection against hydrogen exchange are similar to those observed in early (refolding time <10 ms) folding intermediates for these proteins, leading to the idea that the cold-denatured state is structurally similar to such intermediates. To help test this idea, ubiquitin, which has folding kinetics that are markedly different from those of either RNase A or lysozyme (Briggs and Roder, 1992), was investigated (Nash and Jonas, 1997b). In particular, ubiquitin shows much less evidence of early structure formation than lysozyme; it more closely resembles a random coil.
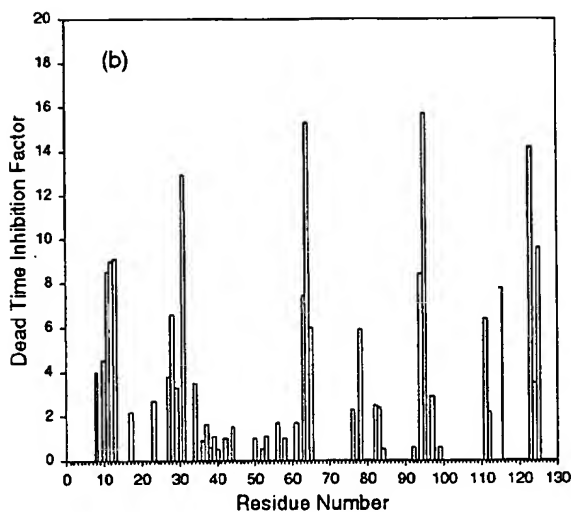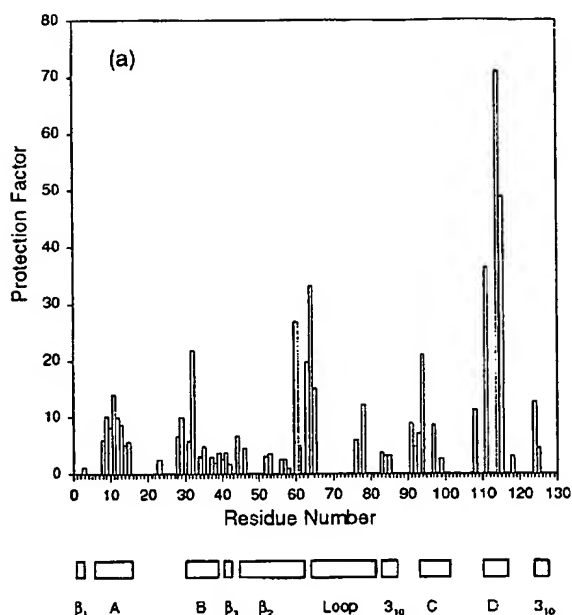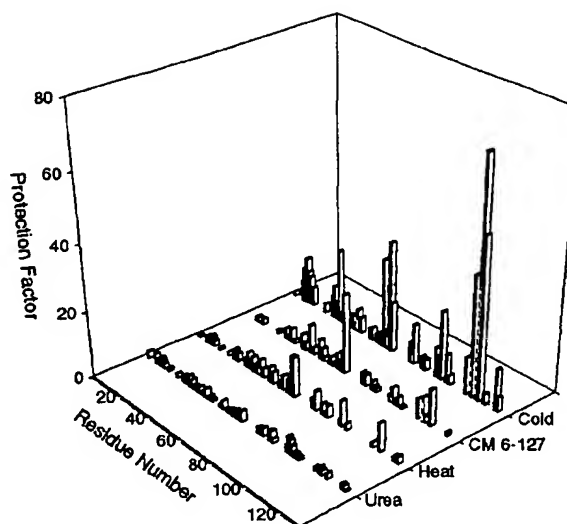
FIGURE 7   Comparison of protection factors observed in various experiments. Data for cold-denatured lysozyme were taken from Nash and Jonas (1997a); data for heat, urea, and acid-denatured CM$^{6-127}$ lysozyme were taken from Buck et al. (1994).

FIGURE 6   (*a*) Protection factors for the pressure-assisted cold-denatured state (p = 3750 bar, T = -13°C) of lysozyme. Secondary structural elements in the native state are indicated below. A–D denote the four α-helices; β_1 and β_2 denote the two- and three-stranded β-sheet regions, respectively. (*b*) Dead-time inhibition factors obtained for the first 3.5 ms of lysozyme folding (Gladwin and Evans, 1996).

change. It is important to point out that in ubiquitin, the same dead-time inhibition study (Gladwin and Evans, 1996) showed no evidence for protection from exchange, with the largest dead-time inhibition factors being ~2 (Fig. 9). Moreover, there was no correlation of even these modestly

Cold-denatured ubiquitin (p = 2250 bar, T = -16°C) shows little deviation from a random coil in its hydrogen exchange kinetics, with no P values above 5 and most below 2. As shown in Fig. 8, these values are typical of highly denatured proteins such as the urea-denatured state of lysozyme. Under other circumstances, however, such as the A state produced by a 60% methanol solution at a pH of 2.0, ubiquitin shows significantly more protection from ex-
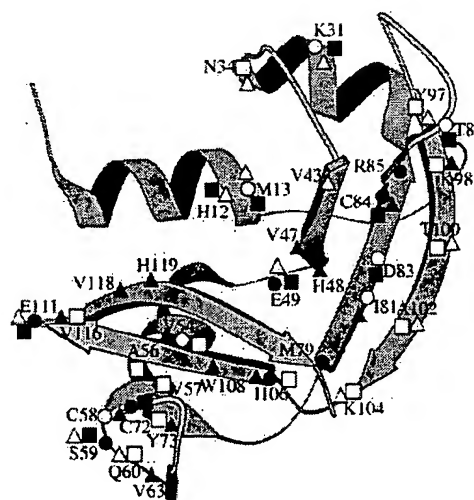
FIGURE 8   Qualitative comparison of protection factors for the pressure-denatured state (Zhang et al., 1995) and pressure-assisted cold-denatured state (Nash and Jonas, 1996) of RNase A compared to protection factors for early folding intermediate for RNase (Udgaonkar and Baldwin, 1990). Amide protons are protected in pressure-denatured state with p > 10, <20 (O); pressure-denatured state with p > 20 (●); cold-denatured state with p > 10, <20 (□); cold-denatured state with p > 20 (■); folding intermediate with "strong" protection (△); and folding intermediate with "weak," "medium," or "ill-defined" protection (▲).
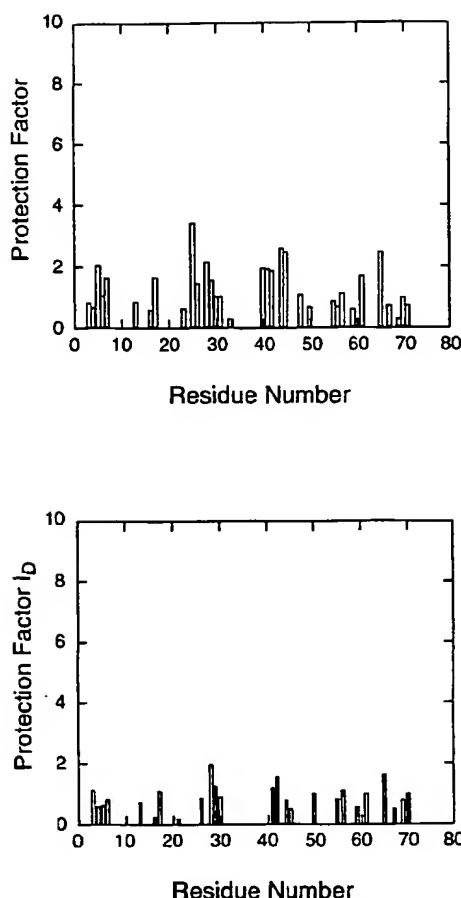
Work is in progress in our laboratory to investigate systematically the pressure- and pressure-assisted cold denaturation of other proteins, to obtain novel information about their folding intermediates, or to simply indicate key stable structures favored preferentially in the folding process. The methods used to investigate these states include both the hydrogen exchange method outlined above and more direct NMR methods (e.g., COSY, NOESY, and TOCSY) using the improved high-pressure NMR probes (Table 1) and the 500-MHz NMR instrument.

FIGURE 9 Protection factors versus residue in pressure-assisted cold-denatured ($T = -16°C$, $p = 2250$ bar) ubiquitin (*A*) compared with dead-time exchange inhibition factors (*B*) (protection factor I_D obtained during the first 3.5 ms of refolding; Gladwin and Evans, 1996).

elevated factors within significant elements of secondary structure, as there were in lysozyme.

The similarity of cold-denatured state protection factors to the protection observed in protein refolding studies has led to the idea that the cold-denatured state is populated by species comprising elements of secondary and perhaps tertiary structure that are comparatively stable. The similarities between the cold-denatured state and the early folding states suggest that these structural elements would be expected to form first during folding. In the case of ubiquitin, the folding reaction appears to proceed in one highly cooperative step, with little of the multiphasic behavior observed in proteins like lysozyme or ribonuclease A. Although a possible intermediate for ubiquitin refolding has been characterized by other means (Khorasanizadeh et al., 1996), the intermediate thus identified shows no protection from hydrogen exchange. The results for the cold-denatured state of ubiquitin parallel these results: there is no partially folded state that is stable enough to be characterized by hydrogen exchange methods when ubiquitin is cold denatured.

REFERENCES

Anfinsen, C. B. 1973. Principles that govern the folding of protein chains. *Science.* 181:223–230.

Bai, Y., J. S. Milne, L. Mayne, and S. W. Englander. 1993. Primary structure effects on peptide group hydrogen exchange. *Proteins Struct. Funct. Genet.* 17:75–86.

Ballard, L., C. Reiner, and J. Jonas. 1996. High-resolution NMR probe for experiments at high pressures. *J. Magn. Res.* 123A:81–86.

Ballard, L., A. Yu, C. Reiner, and J. Jonas. 1998. A high pressure, high resolution NMR probe for experiments at 500 MHz. *J. Magn. Res.* (in press).

Briggs, M. S., and H. Roder. 1992. Early hydrogen-bonding events in the folding reaction of ubiquitin. *Proc. Natl. Acad. Sci. USA.* 89:2017–2021.

Buck, M., S. E. Radford, and C. M. Dobson. 1994. Amide hydrogen exchange in a highly denatured state: hen egg-white lysozyme in urea. *J. Mol. Biol.* 237:247–254.

Carter, J. V., D. G. Knox, and A. Rosenberg. 1978. Pressure effects on folded proteins in solution. *J. Biol. Chem.* 253:1947–1953.

Creighton, T. E. 1993. Proteins, 2nd ed. W. H. Freeman and Company, New York.

Di Stefano, D. L., and A. J. Wand. 1987. Two-dimensional ¹H NMR study of human ubiquitin: a main chain directed assignment and structure analysis. *Biochemistry.* 26:7272–7281.

Fink, A. L. 1995. Compact intermediate states in protein folding. *Annu. Rev. Biophys. Biomol. Struct* 24:495–522.

Gladwin, S. T., and P. A. Evans. 1996. Structure of very early protein folding intermediates: new insights through a variant of hydrogen exchange labeling. *Folding Des.* 1:407–417.

Harding, M. H., D. H. Williams, and D. N. Woolfson. 1991. Characterization of a partially denatured state of a protein by two-dimensional NMR: reduction of the hydrophobic interactions in ubiquitin. *Biochemistry.* 30:3120–3128.

Houry, W. A., and H. A. Scheraga. 1996. Structure of a hydrophobically collapsed intermediate on the conformational folding pathway of ribonuclease A probed by hydrogen-deuterium exchange. *Biochemistry.* 35:11734–11746.

Huang, G. S., and T. G. Oas. 1996. Heat and cold denatured states of monomeric λ repressor are thermodynamically and conformationally equivalent. *Biochemistry.* 35:6173–6180.

Jonas, J. 1982. Nuclear magnetic resonance at high pressure. *Science.* 216:1179–1184.

Jonas, J., and A. Jonas. 1994. High-pressure NMR spectroscopy of proteins and membranes. *Annu. Rev. Biophys. Biomol. Struct.* 23:287–318.

Jonas, J., X. Peng, P. Koziol, C. Reiner, and D. M. Campbell. 1993. High-resolution NMR spectroscopy at high pressures. *J. Magn. Reson.* 102B:299–309.

Khorasanizadeh, S., I. D. Peters, and H. Roder. 1996. Evidence for a three-state model of protein folding from kinetic analysis of ubiquitin variants with altered core residues. *Nature Struct. Biol.* 3:193–205.

Kim, P. S., and R. L. Baldwin. 1990. Intermediates in the folding reactions of small proteins. *Annu. Rev. Biochem.* 59:631–660.

Konno, T., M. Kataoka, Y. Kamatari, K. Kanaori, A. Nosaka, and K. Akasaka. 1995. Solution x-ray scattering analysis of cold-, heat-, and urea-denatured states in a protein, *Streptomyces* subtilisin inhibitor. *J. Mol. Biol.* 251:95–103.

Mabry, S. A., B.-S. Lee, T. Zheng, and J. Jonas. 1996. Determination of the activation volume of the uncatalyzed hydrogen exchange reaction between n-methylacetamide and water. *J. Am. Chem. Soc.* 118:8887–8890.

Miranker, A., S. E. Radford, M. Karplus, and C. M. Dobson. 1991. Demonstration by NMR of folding domains in lysozyme. *Nature.* 349:633–636.

Nash, D., and J. Jonas. 1997a. Structure of pressure-assisted cold denatured lysozyme and comparison with lysozyme folding intermediates. *Biochemistry.* 36:14375–14383.

Nash, D., and J. Jonas. 1997b. Structure of the pressure-assisted cold denatured state of ubiquitin. *Biochem. Biophys. Res. Commun.* 238:289–291.

Nash, D., B.-S. Lee, and J. Jonas. 1996. Hydrogen-exchange kinetics in the cold denatured state of ribonuclease A. *Biochim. Biophys. Acta.* 1297:40–48.

Pan, Y., and M. S. Briggs. 1992. Hydrogen exchange in native and alcohol forms of ubiquitin. *Biochemistry.* 31:11405–11412.

Ptitsyn, O. B. 1995. Structures of folding intermediates. *Curr. Opin. Struct. Biol.* 5:74–78.

Radford, S. E., C. M. Dobson, and P. A. Evans. 1992. The folding of hen lysozyme involves partially structured intermediates and multiple pathways. *Nature.* 358:302–307.

Redfield, C., and C. M. Dobson. 1988. Sequential ^{1}H NMR assignments and secondary structure of hen egg white lysozyme in solution. *Biochemistry.* 27:122–136.

Rico, M., J. Santoro, C. González, M. Bruix, J. L. Neira, J. L. Nieto, and J. Herranz. 1991. 3D structure of bovine pancreatic ribonuclease A in aqueous solution: an approach to tertiary structure determination from a small basis of ^{1}H NMR NOE correlations. *J. Biomol. NMR.* 1:283–298.

Robertson, A. D., and R. L. Baldwin. 1991. Hydrogen exchange in thermally denatured ribonuclease A. *Biochemistry.* 30:9907–9914.

Udgaonkar, J. B., and R. L. Baldwin. 1990. Early folding intermediate of ribonuclease A. *Proc. Natl. Acad. Sci. USA.* 87:8197–8201.

Weber, G., and H. G. Drickamer. 1983. The effect of high pressure upon proteins and other biomolecules. *Q. Rev. Biophys.* 16:89–112.

Wong, K.-B., S. M. V. Freund, and A. R. Fersht. 1996. Cold denaturation of barstar: ^{1}H, ^{15}N, and ^{13}C NMR assignment and characterisation of residual structure. *J. Mol. Biol.* 259:805–818.

Zhang, J., X. Peng, A. Jonas, and J. Jonas. 1995. NMR study of the cold, heat, and pressure unfolding of ribonuclease A. *Biochemistry.* 34:8631–8641.

Interactive Intermediates Are Formed during the Urea Unfolding of Rhodanese*

Paul M. Horowitz‡ and Michael Butler

From the Department of Biochemistry, University of Texas Health Science Center at San Antonio, San Antonio, Texas 78284-7760

Structural transitions have been studied on the pathway for urea denaturation of rhodanese. Unlike guanidinium hydrochloride, urea gives no visible precipitation. Increasing urea concentrations cause a transition in which the enzyme activity is completely lost by 4.5 M urea, and there is a shift of the intrinsic fluorescence maximum from 335 nm for the native enzyme to 350 nm. There is a maximum exposure of organized hydrophobic surfaces at 4.5 M urea as reported by the fluorescence of 1,1'-bi(4-anilino)naphthalene-5,5'-disulfonic acid. Above 4.5 M urea, this probe reports the progressive loss of organized hydrophobic surfaces. The polarization of the intrinsic fluorescence falls with increasing urea concentrations in a complex transition showing that rhodanese flexibility increases in at least two phases. Rhodanese becomes increasingly susceptible to digestion by subtilisin between 3.5 and 4.5 M urea, giving rise to large fragments. At urea concentrations >5 M, rhodanese is completely digested. There is a small increase in the rate of sulfhydryl accessibility between 3.5 and 4.5 M urea, but there is a large increase in the sulfhydryl accessibility above 4.5 M urea. Dimethyl suberimidate cross-linking shows the presence of associated species in 3–5 M urea, but there are few cross-linkable species at lower or higher urea concentrations. These results are consistent with a model in which urea unfolding of rhodanese is associated with the initial production of a species having organized regions of structure with exposed hydrophobic surfaces separated by flexible elements.

Refolding of the denatured enzyme rhodanese (thiosulfate sulfurtransferase; EC 2.8.1.1) is difficult because of competition from aggregation and because of sulfhydryl oxidation (1). When denaturation was attempted using guanidinium HCl, almost all of the rhodanese precipitated from solution (2). Successful refolding of rhodanese can be achieved under conditions that include the use of assistants such as detergents (3, 4), liposomes (5), or proteins called chaperonins (6) to limit aggregation, together with reducing agents and the substrate thiosulfate. Folding with detergents revealed intermediates that had the properties of molten globules, but it was

not clear whether the detection of the intermediates required the presence of detergents (7). This led to the general question: which aspects of the denaturation are properties of the protein, and which parts depend on the interaction of the protein with the particular assistant used in renaturation? Thus, the specific question arose as to whether one could detect intermediate states of rhodanese in the absence of detergents, lipids, or chaperonins? An opportunity appeared recently to approach this question when it was demonstrated that reversible folding was possible for rhodanese without using assistants (8). Rhodanese denaturation during urea unfolding was shown to follow a reversible path, and in this process, there was no precipitation, indicating that aggregated states, at least those of the size formed in guanidinium HCl, were not present in urea.

In the present paper, we have studied the urea unfolding of rhodanese in the absence of detergents, chaperonins, or liposomes under conditions that have been shown previously to produce an unfolding transition that approximated the reversible pathway (8). Under these conditions, it is demonstrated here that the major transition leading to enzyme inactivation is not associated with total unfolding of the polypeptide chain; instead, it produces a state with a considerable degree of structure and a maximum exposure of organized hydrophobic surfaces. Apparently, it is this type of structure that must be protected by interactions with accessory substances for the successful high yield reactivation of rhodanese after denaturation.

EXPERIMENTAL PROCEDURES

Reagents and Proteins—All the reagents used were of analytical grade. Bovine liver rhodanese (9) and recombinant rhodanese (10) were prepared as described previously and stored at −70 °C as a crystalline suspension in 1.8 M ammonium sulfate. Rhodanese concentration was determined using a value of $A^{0.1\%}_{280\ nm} = 1.75$ (11) and a molecular mass of 33 kDa (12).

Rhodanese Assay—Rhodanese activity was measured by a colorimetric method based on the absorbance at 460 nm of the complex formed between ferric ion and the reaction product thiocyanate (12).

Rhodanese Denaturation—Rhodanese was typically denatured in 50 mM Tris, pH 7.6, at a protein concentration of 10 μg/ml. The buffer contained 200 mM 2-mercaptoethanol and 50 mM thiosulfate, which were shown previously to be necessary to prevent oxidative damage (13). Samples were denatured at each urea concentration for at least 3 h before measurements were made. Typically, rhodanese assays used 10 μl of enzyme solution for 10 min, and time courses of product formation were used to detect nonlinearities in the progress curves.

Fluorescence Measurements—Fluorescence measurements were made on an SLM 500C fluorometer (SLM Instruments, Urbana, IL). Intrinsic fluorescence emission spectra were measured at various urea concentrations in solutions containing 50 mM Tris-HCl, pH 7.8, at a protein concentration of 50 μg/ml at 23 °C, unless indicated otherwise. Excitation was at 280 nm (band pass, 5 nm) and the emission was either monitored at 335 nm or recorded as a spectrum from 300

‡ To whom correspondence should be addressed: Dept. of Biochemistry, University of Texas Health Science Center, 7703 Floyd Curl Dr., San Antonio, TX 78284-7760. Tel.: 512-567-3737; Fax: 512-567-2490.

to 400 nm (band pass, 7.5 nm). The temperature was controlled by circulating water through the cell holder. Solutions were equilibrated for 20 min before addition of the enzyme. For solutions containing 10 μM bis-ANS[1], 1,1'-bi(4-anilino)naphthalene-5,5'-disulfonic acid, the excitation wavelength was 395 nm, and the emission was either monitored at 482 nm or recorded as a spectrum from 480 to 600 nm. Individual samples were used for the bis-ANS measurements. As a control for the ability of urea to disrupt interactions between bis-ANS and hydrophobic surfaces, the complex of 10 μM bis-ANS with 0.9% γ-cyclodextrin was prepared and titrated with urea under the same conditions as used for the protein. Measurements of the polarization of the intrinsic fluorescence were made with excitation at 300 nm and emission at 345 nm. For each sample the determined value was the average of 10 measurements. The readings were stable for 24 h. Polarization readings were corrected for any instrumental artifacts as described by the manufacturer.

Sodium Dodecyl Sulfate-Polyacrylamide Gel Electrophoresis—SDS-PAGE was performed using the formulations of Laemmli (14). Gels contained 11% acrylamide in the resolving gel and 4% acrylamide in the stacking gel. Samples from the cross-linking experiments were analyzed by SDS-gel electrophoresis using 9% acrylamide in the resolving gels, and they were stained with 0.05% Coomassie Brilliant Blue R-250.

Proteolysis by Subtilisin—Samples of rhodanese at 200 μg/ml were digested with 1% subtilisin (w/w). Reaction was carried out for 30 min, stopped by the addition of phenylmethylsulfonyl fluoride at 100 μg/ml, and incubated for 10 min. Samples were prepared for SDS-PAGE; which was run in a 1.5-mm thick minigel format using an 11% resolving gel. Gels were stained with Coomassie Brilliant Blue R-250.

Cross-linking Experiments—Dimethyl suberimidate (DMS) cross-linking was performed using rhodanese at 300 μg/ml in 15 mM Tris-HCl, pH 7.6. Rhodanese was denatured for 2.5 h in different urea concentrations, and after the urea incubation, DMS was added at 300 μg/ml. After incubation for 2 h, the pH was lowered to 6.8 with MES, 2-(N-morpholino)ethanesulfonic acid, in order to increase the hydrolysis of DMS. Samples were incubated further and then were prepared for SDS-PAGE. Stained gels were imaged using a video camera system.

Measurements of Sulfhydryl Reactivity—Rate constants for reaction of rhodanese with DTNB, 5,5'-dithiobis-(2-nitrobenzoic acid), were determined as functions of the urea concentration. Sulfhydryl titers were measured using 250 μg/ml rhodanese with no thiosulfate or 2-mercaptoethanol because of their interference with the assay. These assays were performed in 100 mM Tris-HCl, pH 7.6, with a final concentration of 1 mM for DTNB. DTNB was quantified using an E_{412} of 12,500 M^{-1} cm^2. The A_{412} versus time was acquired, and a first order plot of the data was used to derive rate constants.

RESULTS

Urea-induced Inactivation of Rhodanese Is Correlated with a Transition in Its Intrinsic Fluorescence—Fig. 1 shows the enzymatic activity (*open circles*) and the wavelength of the intrinsic fluorescence maximum (*closed circles*) for rhodanese as functions of increasing urea concentration. The activity falls in a transition that occurs between approximately 3 and 4.5 M urea with 50% inactivation at about 3.7 M urea. The intrinsic fluorescence shifts from approximately 335 nm, characteristic of the native protein, to about 351 nm that is characteristic of the denatured protein. The transition in fluorescence correlates with that observed in the activity. The activity beyond 4.5 M urea appears to give about 10–12% of the initial activity, because there is some reactivation during the assay. This reactivation has been previously demonstrated (1). There was no appearance of visible turbidity associated with the activity loss as has been reported for denaturation with guanidinium HCl.

Increased Hydrophobic Exposure Is Associated with Urea-

---

[1] The abbreviations used are: BME, 2-mercaptoethanol; bis-ANS, 1,1'-bi(4-anilino)naphthalene-5,5'-disulfonic acid; DMS, dimethyl suberimidate; DTNB, 5,5'-dithiobis-(2-nitrobenzoic acid); MES, 2-(N-morpholino)ethanesulfonic acid; PAGE, polyacrylamide gel electrophoresis.
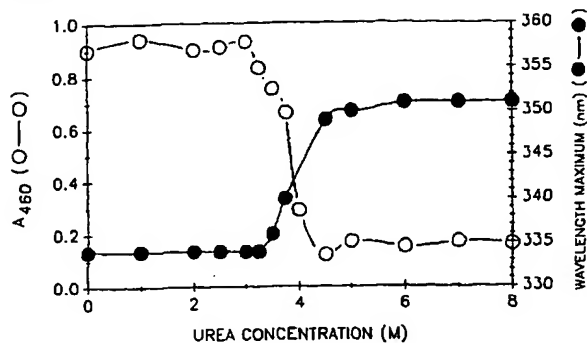

FIG. 1. **Urea concentration dependence of rhodanese activity and wavelength maximum of intrinsic protein fluorescence.** Rhodanese activity (mm) is expressed as the absorbance at 460 nm in the standard assay. Fluorescence wavelength maxima were obtained from spectra excited at 280 nm and scanned from 300 to 400 nm. Rhodanese concentration was 10 μg/ml. All samples were prepared at the indicated urea concentrations in 50 mM Tris-HCl, pH 7.6, containing 200 mM 2-mercaptoethanol and 50 mM thiosulfate. Rhodanese was denatured at the indicated urea concentrations for 3 h, and all experiments were performed at 23 °C.
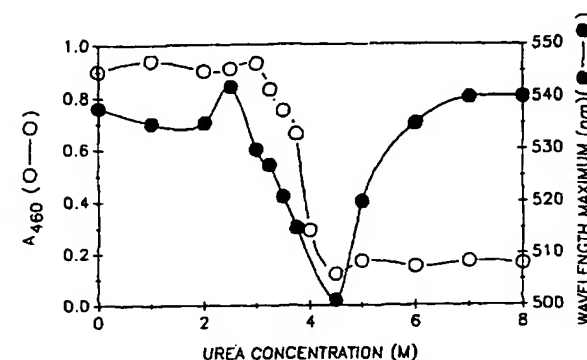

FIG. 2. **Wavelength maximum for bis-ANS binding to rhodanese as a function of the urea concentration.** Bis-ANS wavelength maxima (11) were determined from individual fluorescence spectra measured with excitation at 395 nm and scanned from 480 to 600 nm. The samples contained 10 μM bis-ANS. All other conditions were the same as for Fig. 1. For comparison, the activity of rhodanese is shown as a function of urea concentration (mm).

induced Inactivation—The wavelength maximum for the fluorescent probe bis-ANS was used to monitor the exposure of hydrophobic surfaces (15). Fig. 2 shows that, as the urea concentration is increased from 0 to 4.5 M urea, the fluorescence of bis-ANS shifts to shorter wavelengths in a transition that follows the loss in activity. The wavelength maximum reaches its lowest value, 500 nm, at the point where the activity has fallen to a minimum. As the concentration of urea is increased further, the fluorescence wavelength maximum shifts back toward the red, and it reaches 540 nm at 8 M urea. Thus, the maximum hydrophobic exposure in rhodanese occurs at 4.5 M urea, a concentration giving minimum activity. As the urea concentration is increased beyond 4.5 M, there is a continual decrease in hydrophobic exposure. This apparently indicates that rhodanese is not fully unfolded at 4.5 M urea, and the transition that is being monitored by both the intrinsic fluorescence and the enzyme activity does not represent a transition between the native and the fully unfolded protein.

Fig. 3 shows that the intensity for the bis-ANS fluorescence changes in a complex transition (Fig. 3, *closed triangles*). As
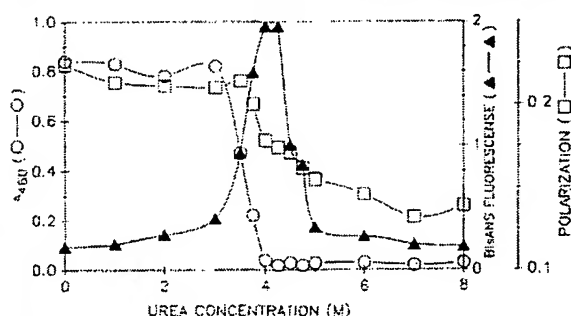
FIG. 3. Urea concentration dependence of bis-ANS fluorescence intensity and the polarization of the intrinsic protein fluorescence shown together with the enzyme activity. Rhodanese was prepared in individual samples at 40 μg/ml, and separate samples were used for polarization and bis-ANS fluorescence. Intrinsic polarization was measured with excitation at 300 nm, and emission was monitored at 345 nm. Readings were stable for 24 h. All other conditions were the same as noted in the legend to Fig. 2.

the urea concentration increases, the changes in the fluorescence intensities are inversely related to the shifts of the bis-ANS wavelength maxima shown in Fig. 2. This correspondence between the wavelength maximum and the fluorescence intensity is expected for a system in which the hydrophobicity of the site is changing. It is generally expected that increased hydrophobic exposure, resulting from an increase in the number of sites each with the same hydrophobicity, would lead to more of an increase in the intensity rather than significantly shifting the wavelength maximum of the bis-ANS fluorescence (16, 17).

The decrease in bis-ANS fluorescence with increasing urea concentration above 4.5 M could be due either to a shift of the binding equilibrium due to increased bis-ANS solubility and/or to a disruption of organized hydrophobic surfaces on rhodanese as the protein denatured. A control with γ-cyclodextrin was used to address the issue. The γ-cyclodextrin enhanced the fluorescence of bis-ANS, presumably as a result of binding to the hydrophobic cavity in the center of the cyclodextrin ring. Increasing urea concentrations, over the range used in the titration of the protein, did not cause any significant fall of the bis-ANS fluorescence (data not shown), so there was no significant shift of the binding equilibrium between bis-ANS and the γ-cyclodextrin. Thus, it is likely that the decrease of bis-ANS fluorescence at the higher urea concentrations in the protein titration is due to a loss of the rhodanese structure, and it is not primarily due to interference with interactions between rhodanese and bis-ANS. This distinction is necessary, because, as a protein is unfolded by chemical denaturants, it is expected that hydrophobic residues become more exposed to the solvent. However, the feature that is important for the maximum binding of bis-ANS is not simply having individual exposed residues, but having those residues be part of an organized hydrophobic surface. Additionally, since the protein unfolds because denaturants can disrupt hydrophobic interactions, it is not expected that hydrophobic probes would bind as tightly, and the γ-cyclodextrin control was a potential way of sorting out these differences. The bis-ANS intensity, as noted above, reflects the same features observed in the bis-ANS wavelength maximum shift shown in Fig. 2. There is a gentle rise in intensity to 3 M urea and then there is a steep rise that follows the loss of activity. The maximum of the fluorescence intensity occurs in the region of the maximum loss of activity. The steeply falling intensity beyond 4.5 M urea indicates the loss of organized hydrophobic surfaces. The maximum in the bis-

ANS intensity due to competing effects is in the same region as the maximum shift in the wavelength maximum. The activity profile is shown for comparison (*open circles*), and the activities are lower at the higher urea concentrations in this figure compared with Fig. 1, because these experiments are done at higher protein concentration, which requires a shorter incubation in the assay and, therefore, less opportunity for recovery in the assay (1).

Polarization of the Intrinsic Fluorescence of Rhodanese Reveals a Complex Transition during the Loosening of Protein Structure—Polarization of the intrinsic fluorescence was measured for rhodanese during the unfolding transition (*open squares*, Fig. 3). The polarization fell in a complex transition during the urea perturbation. The transition appears not to be a smooth two-state transition, and it looks as if there are at least two transitions. Part of the polarization loss occurs in the region of the activity loss, between approximately 3.75 and 4.50 M urea. In fact, the activity may fall at somewhat lower urea concentrations than the polarization change. There is a more gradual change in the polarization as the urea concentration is raised further, and the lowest polarization is observed at approximately 7 M urea.

Proteolysis by Subtilisin Reflects Urea-induced Transitions—Fig. 4 shows that rhodanese is quite resistant to digestion by subtilisin when equilibrated between 0 and 3 M urea. The protein becomes increasingly susceptible to digestion in a transition between 3 and 5 M urea. The protein is very susceptible to proteolysis at 5 and 6 M urea. Between 3.5 and 4.5 M urea, digestion produces discrete high molecular weight fragments as opposed to the behavior at and above 5 M urea where digestion produces only small fragments. Subtilisin was chosen because of its broad specificity, so that proteolytic patterns reflect exposure of the structure rather than the specificity of the protease. These data indicate that rhodanese behaves, at concentrations of urea that give minimum activity and maximum hydrophobic exposure, as if there are elements of organized structure separated by proteolytically susceptible regions.

Rhodanese Sulfhydryl Accessibility Reflects Urea-induced Structural Changes—The four sulfhydryl groups of rhodanese are all reduced in the native state, and these sulfhydryl groups are very resistant to reaction with DTNB when the protein is fully folded (18). Fig. 5 shows rate constants for the reaction of DTNB with rhodanese as a function of the urea concentration. The sulfhydryl groups of rhodanese react slowly with

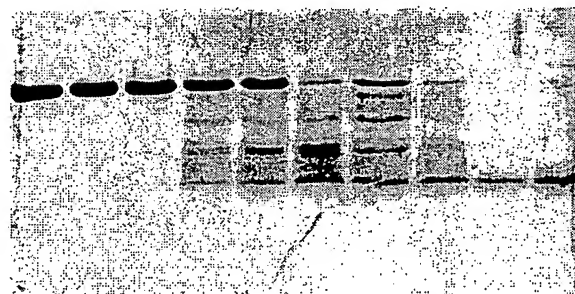| 0	2.5	3	3.5	3.75	4	4.25	4.5	5	6

FIG. 4. The lability of rhodanese to proteolysis by subtilisin as a function of the urea concentration. Rhodanese at 200 μg/ml was equilibrated at various urea concentrations and then was digested with 1% subtilisin for 30 min before being stopped by phenylmethylsulfonyl fluoride. The lanes on the SDS gel shown here correspond to increasing urea concentrations. From the *left* they are 0, 2.5, 3, 3.5, 3.75, 4, 4.25, 4.5, 5, and 6 M urea, respectively.
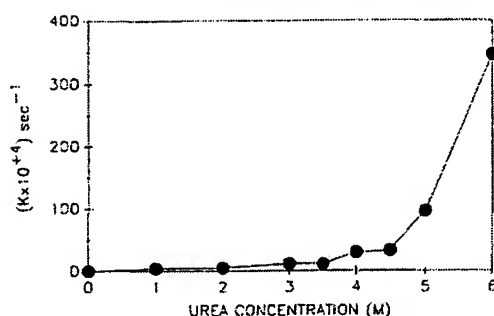
FIG. 5. **Urea concentration dependence of the reaction of rhodanese sulfhydryl groups with DTNB.** Rate constants for the reaction of DTNB with rhodanese as a function of the urea concentration were measured as described under "Experimental Procedures." Sulfhydryl titers were determined with rhodanese at 250 μg/ml in the absence of thiosulfate or 2-mercaptoethanol. Samples were prepared in 100 mM Tris-HCl, pH 7.6, with a final DTNB concentration of 1 mM.

FIG. 6. **Urea concentration dependence of the dimethyl suberimidate cross-linking of rhodanese.** Rhodanese was present at 300 μg/ml in 15 mM Tris-HCl, pH 7.5, denatured at various concentrations of urea for 2.5 h, and treated with dimethyl suberimidate as indicated under "Experimental Procedures." The lanes on the SDS gel shown here correspond to the following urea concentrations, from the *left*, 1, 2, 3, 4, 5, 6, and 7 M urea, respectively.

DTNB up to 3.5 M urea. Beyond this urea concentration, a transition begins that leads to increasingly rapid reaction. At 4 M urea, where the activity is zero, and the first phase of the polarization drop is completed, there is still no large change in the rate of reaction of the sulfhydryl groups. Sulfhydryl accessibility does not increase substantially until the region of 5 M urea, where rhodanese becomes completely susceptible to protease and where bis-ANS binding has substantially decreased. It is interesting that, at 5 M urea, the bis-ANS intensity is almost at its minimum, whereas the shift in the wavelength maximum of the bis-ANS that is bound has not quite shifted to its maximum extent, which may indicate that some hydrophobic surfaces are still present, although they are only weakly able to bind bis-ANS. If this is the case, then there are still organized hydrophobic surfaces while the sulfhydryl titer has increased substantially. Thus, there are several identifiable stages in the denaturation profile of rhodanese.

Dimethyl Suberimidate Cross-linking Reveals Urea-induced Protein Association—The strong exposure of hydrophobic surfaces at 4 M urea introduces the possibility that association of interactive intermediates was occurring even though these associated species were not large enough to cause significant scattering of visible light as was observed in the guanidinium HCl unfolding. Fig. 6 shows the results of DMS cross-linking of rhodanese that had been equilibrated at various urea concentrations. With increasing urea concentration, those concentrations giving evidence of incompletely denatured rhodanese give rise to a small amount of associated species. For example, there are no associated species observed from 1 to 3 M urea. At 4 and 5 M urea, there is clear formation of cross-linked species that correspond in molecular weight to dimers and trimers. At 6 M urea, there is a diminished amount of cross-linking, and at 7 M urea, there is virtually no cross-linking observed.

DISCUSSION

The structural transition leading to inactivation is not associated with complete unfolding of rhodanese. Urea-induced unfolding apparently occurs in at least two stages, and the first stage is associated with loss of activity and a sufficient opening of the rhodanese structure to give what appear to be exposed tryptophan residues. However, the structure that is so produced still has (a) restricted mobility of those same tryptophan residues, (b) large regions of exposed hydrophobic
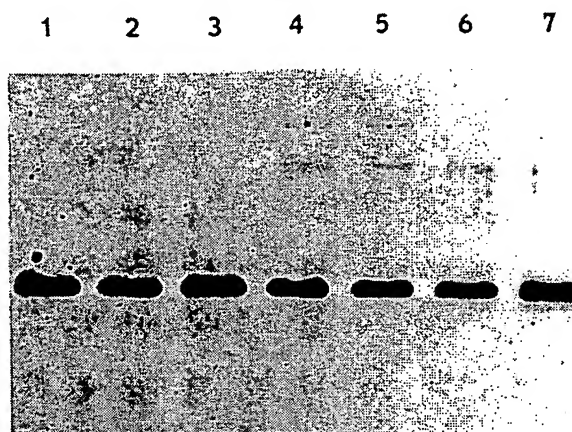
surface, and (c) enough retained structure so that the exposure of proteolytic cleavage sites leads to the formation of discrete large fragments, rather than complete proteolysis. In addition, even though the sulfhydryl groups in rhodanese are all reduced in the native structure, there is still significant restriction to the access of the reagent DTNB up to 4.5 M urea. This description is similar to the properties described for the molten globule states that many proteins, including rhodanese, adopt in the course of reversible unfolding (7, 19, 20).

The concentration of urea that leads to complete loss of activity (4–4.5 M) gives a protein that is apparently not denatured to the random coil, but instead it forms sticky species that can associate, but they do not form large enough aggregates to give visible light scattering as would be seen in guanidinium HCl denaturation.

The results demonstrated here are consistent with Model I.
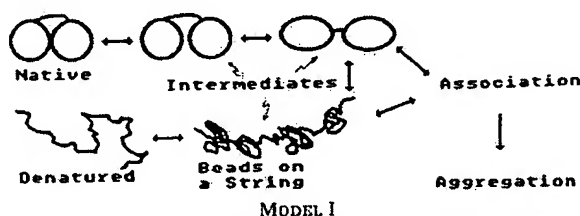
MODEL I

In this model, native enzyme, when perturbed by increasing urea concentrations, initially forms intermediates that, while compact, contain exposed hydrophobic surfaces. As the urea concentration is increased, there are further increases in the opening of the structure. This structural opening may be related to a partial separation of the two domains into which the single polypeptide chain is folded. As the urea concentration is increased further, structures that perhaps can be best envisioned as beads on a string form to give the kind of structure that can give rise to the pattern observed in the subtilisin digestion. Finally, in the region of 6 M urea, the protein completely unfolds, finally, to give a structure that would be more like the random coil normally pictured for a denatured protein. Circular dichroism measurements are consistent with a random coil conformation of rhodanese at 6 M

urea (7, 21). This model would be in keeping with the multiple intermediates that have been observed in the binding of rhodanese to the chaperonin cpn60 and by the results that indicate that the interaction with cpn60 involves more than one part of the rhodanese structure (22).[2] These results would also be in keeping with findings from liposome disruption studies that suggest that more than one portion of the rhodanese structure is important for interactions with liposomes (24). The formation of these types of potentially interactive intermediates may be the reason that efficient refolding requires assistants such as detergents or liposomes or the chaperonin protein cpn60.

There are some common elements that are present after any perturbation of the rhodanese structure. For example, perturbation by both urea and guanidinium HCl have the common characteristic that intermediates are formed with sticky surfaces that can be diverted to associated species. Even in the absence of significant light scattering, there can be significant association that can short-circuit refolding. This last is important to emphasize, because many recent folding studies using rhodanese and similar proteins focus on the ability of chaperonins and assistants to influence light scattering after dilution of the protein from denaturants (6, 15, 23). Thus, it is possible to suggest a common model that can be used to understand irreversible denaturation, unassisted folding, chaperonin-assisted folding, detergent-assisted refolding, and liposome-assisted refolding that we observed previously with rhodanese. In this common model, as shown above, rhodanese can adopt partially folded intermediate states with strongly exposed interactive surfaces that can lead to small associated species which can give rise to large aggre-

[2] J. Mendoza and P. M. Horowitz, submitted for publication.

gates. This aggregation would give states that are kinetically prevented from folding quickly, and the folding could become so slow that it appears irreversible. By stabilizing these intermediates, they can be protected from interactions, and folding would be favored. Thus, in keeping with numerous previous studies on protein folding, it is likely that the control of folding intermediates can control the fates of proteins.

REFERENCES

1. Horowitz, P. M., and Simon, D. (1986) *J. Biol. Chem.* **261**, 13887–13891
2. Horowitz, P. M., and Criscimagna, N. L. (1986) *J. Biol. Chem.* **261**, 15652–15658
3. Tandon, S., and Horowitz, P. M. (1987) *J. Biol. Chem.* **261**, 15615–15618
4. Tandon, S., and Horowitz, P. M. (1987) *J. Biol. Chem.* **262**, 4486–4491
5. Zardeneta, G., and Horowitz, P. M. (1992) *J. Biol. Chem.* **267**, 5811–5816
6. Mendoza, J. A., Rogers, E., Lorimer, G. H., and Horowitz, P. M. (1991) *J. Biol. Chem.* **266**, 13044–13049
7. Horowitz, P. M., and Criscimagna, N. L. (1990) *J. Biol. Chem.* **265**, 2576–2583
8. Mendoza, J. A., Rogers, E., Lorimer, G. H., and Horowitz, P. M. (1991) *J. Biol. Chem.* **266**, 13587–13591
9. Horowitz, P. M. (1978) *Anal. Biochem.* **86**, 751–753
10. Miller, D. M., Kurzban, G. P., Mendoza, J. A., Chirgwin, J. M., Hardies, S. C., and Horowitz, P. M. (1992) *Biochim. Biophys. Acta,* **1121**, 286–292
11. Sorbo, B. H. (1953) *Acta Chem. Scand.* **7**, 1129–1136
12. Ploegman, J. H., Drent, G. H., Kalk, K. H., Hol, W. G. J., Heinrikson, R. L., Keim, P., Weng, L., and Russell, J. (1978) *Nature* **273**, 1245–1249
13. Tandon, S., and Horowitz, P. M. (1989) *J. Biol. Chem.* **264**, 9859–9866
14. Laemmli, U. K. (1970) *Nature* **227**, 680–685
15. Rosen, C. G., and Weber, G. (1969) *Biochemistry* **8**, 3915–3920
16. McClure, W. O., and Edelman, G. M. (1966) *Biochemistry* **5**, 1908–1919
17. Turner, D. C., and Brand, L. (1968) *Biochemistry* **7**, 3381–3390
18. Pensa, B., Costa, M., Pecci, L., Cannella, and Cavallini, D. (1977) *Biochim. Biophys. Acta* **484**, 368–374
19. Dolgikh, D. A., Abaturov, L. V., Bolotina, I. A., Brazhnikov, E. V., Bushuev, V. N., Bychkova, V. E., Gilmanshin, R. I., Lebvedev, Y. O., Semisotnov, G. V., Tiktopulo, E. I., and Ptitsyn, O. B. (1985) *Eur. Biophys. J.* **13**, 109–121
20. Kuwajima, K. (1989) *Proteins Struct. Funct. Genet.* **6**, 87–103
21. Chow, S. F., and Horowitz, P. M. (1986) *J. Biol. Chem.* **261**, 7264–7269
22. Mendoza, J. A., Lorimer, G. H., and Horowitz, P. M. (1992) *J. Biol. Chem.* **267**, 17631–17634
23. Langer, T., Lu, C., Echols, H., Flanagan, J., Hayer, M. K., and Hartl, F.-U. (1992) *Nature* **356**, 683–689
24. Zardeneta, G., and Horowitz, P. M. (1993) *Eur. J. Biochem.*, in press

EXHIBIT A

Hydrostatic Pressure Rescues Native Protein from Aggregates

Debora Foguel[†], Clifford R. Robinson[#,¶], Pedro Caetano de Sousa Jr.[†],

Jerson L. Silva[†], and Anne Skaja Robinson[*,¶]

[*] corresponding author:

e-mail: skaja@che.udel.edu; PH (302) 831-0557; FAX (302) 831-6262

Present address: Department of Chemical Engineering, University of Delaware,

Newark, DE 19716

[¶] Department of Biology, MIT, Cambridge, MA 02139

[†] Departamento de Bioquímica Médica, Instituto de Ciências Biomédicas, Universidade Federal do

Rio de Janeiro, 21941-590 Rio de Janeiro, RJ, Brazil

[#] Present address: 3-Dimensional Pharmaceuticals, 665 Stockton Drive, Exton, PA 19341

Summary

Misfolding and misassembly of proteins are major problems in the biotechnology industry, in biochemical research, and in human disease. Here we describe a novel approach for reversing aggregation and increasing refolding by application of hydrostatic pressure. Using P22 tailspike protein as a model system, intermediates along the aggregation pathway were identified and quantitated by size-exclusion HPLC. Tailspike aggregates were subjected to hydrostatic pressures of 2.4 kbar (35,000 PSI). This treatment dissociated the tailspike aggregates and resulted in increased formation of native trimers once pressure was released. Tailspike trimers refolded at these pressures were fully active for formation of infectious viral particles. This technique facilitates conversion of aggregates to native proteins without addition of chaotropic agents, changes in buffer, or large scale dilution of reagents required for traditional refolding methods. Our results also indicate that one or more intermediates at the junction between the folding and aggregation pathways is pressure sensitive. This finding supports the hypothesis that specific determinants of recognition exist for protein aggregation, and that these determinants are similar to those involved in folding to the native state. An increased understanding of this specificity should lead to improved refolding methods.

Introduction

Protein aggregation and misfolding play major roles in protein production in the biotechnology industry, in limiting the biochemical study of proteins, and in the onset of pathogenesis in human disease. The native, correctly-folded state is necessary for a protein's biological function and recognition by other molecules; misfolding and misassembly lead to significant loss of biological activity. Because the mechanism that drives aggregation is poorly understood it represents a challenge to industrial, academic, and medical research scientists.

Improved methods to reverse and inhibit aggregation are needed. During production, the need to refold proteins from large aggregates, or inclusion bodies, often requires denaturation by harsh chaotropic reagents such as guanidine chloride or urea, and reducing agents (Cleland, 1993). Removal of the denaturant may then require large dilution and therefore large working volumes; low refolding yields are common due to loss of protein during refolding and concentration (De Bernardez-Clark and Georgiou, 1991).

Misfolding has also been identified as the causative agent in a number of human diseases including cystic fibrosis, prion spongiform encephalopathies such as Creutzfeldt-Jacob, Alzheimer's disease and other amyloid diseases (Bychkova and Ptitsyn, 1995; Thomas, Qu *et al.*, 1995). A better understanding of the interactions which lead to aggregation will enhance our ability to design inhibitors and therapeutics for aggregation-driven diseases.

The tailspike protein of P22 bacteriophage is an excellent model system for aggregation because the structure is known, the folding and aggregation pathways are well characterized, and aggregation of tailspike chains occurs by specific interactions. The tailspike protein is a homotrimer of 666 residues per monomer chain (Sauer, Krovatin *et al.*, 1982). Figure 1A shows the X-ray crystal structure of residues 108-666, which indicates that tailspike is a member of the β-coil family (Steinbacher, Seckler *et al.*, 1994). The main body of each subunit of the trimer, residues 143 through 535, is a long β-coil made of thirteen complete turns (Steinbacher, Seckler *et al.*, 1994). The three chains then twist around each other to form three intertwined β-sheets comprising residues 536 to 619, where each sheet contains β-strands from all three subunits. The

1

native tailspike trimer is thermostable (t_m = 88 °C), and resistant to SDS and proteolysis. No covalent linkages exist in the native state of tailspike, and it is thought that the intertwined β-sheet plays a major role in stabilizing the tailspike trimer.

Tailspike protein is both a structural and functional component of the P22 bacteriophage. Tailspike binds to the O-antigen on the outer membrane lipopolysaccharide of *Salmonella* species and facilitates infection through hydrolysis of the α(1-3) glycosidic linkages (Iwashita and Kanegasaki, 1976). This activity can be assayed for *in vitro* by incubating purified tailspike with tail-free viral heads, and measuring the "tailing" level by the formation of infectious particles (Berget and Poteete, 1980). The "tailing" ability serves as a functional assay for folded protein, while formation of native-like tertiary structure can be monitored by changes in fluorescence.

A number of intermediates along the *in vivo* and *in vitro* folding and aggregation pathways for P22 tailspike have been identified through native and denaturing gel electrophoresis (Figure 1B) (Goldenberg, Berget *et al.*, 1982; Goldenberg and King, 1982; Haase-Pettingell and King, 1988; Seckler, Fuchs *et al.*, 1989; Fuchs, Seiderer *et al.*, 1991; Speed, Wang *et al.*, 1995; Robinson and King, 1997). Folding intermediates of tailspike are thermolabile, and aggregate under physiological conditions in the host (Goldenberg, Smith *et al.*, 1983; Haase-Pettingell and King, 1988). A late trimeric intermediate named "protrimer" lacks the SDS resistance and thermal stability of the native proteins (Goldenberg, Berget *et al.*, 1982; Goldenberg and King, 1982). Although early folding intermediates are susceptible to aggregation, the propensity to aggregate is diminished once protrimer is formed. The presence of transient disulfide bonds in the protrimer intermediate along the folding pathway of tailspike may help promote folding and chain association (Robinson and King, 1997).

Aggregation of tailspike *in vitro* is not limited to sequential addition of monomers. Association can occur between subunit assemblies of any size — dimers can associate with monomers, dimers, trimers, tetramers, etc. (Speed, Wang *et al.*, 1995). Aggregation does not occur by covalent association of the chains, as the addition of SDS in the absence of reducing agents dissociates aggregates into monomeric subunits (Speed, Wang *et al.*, 1995; Robinson and

2

King, 1997). In general, aggregation involves specific interactions between chains, since mixing of denatured tailspike protein with other aggregation-competent proteins (P22 coat protein, carbonic anhydrase) does not yield mixed aggregate species (Speed, Wang *et al.*, 1996). *In vitro*, the extent of aggregation is dependent on both the protein and urea concentrations present in the refolding buffer (A.S. Robinson, S. Betts and J.A. King, unpublished results).

Hydrostatic pressure is an efficient tool to dissociate oligomeric proteins and other macromolecular complexes without denaturing the secondary and tertiary structure of the subunits (Robinson and Sligar, 1995; Silva, Foguel *et al.*, 1996). Elevated hydrostatic pressure favors the state of lowest total volume — for most macromolecular assemblages this is the dissociated state (Silva and Weber, 1993). Quaternary structures of oligomeric protein assemblies usually dissociate to monomeric subunits between 1-3 kbar, but secondary and tertiary structures of proteins typically do not denature until pressures above 5 kbar at room temperature (Silva and Weber, 1993; Robinson and Sligar, 1995). Hydrostatic pressure has also proved to be a very powerful method to produce partially folded protein chains under equilibrium conditions (Silva, Silveira *et al.*, 1992; Silva, Foguel *et al.*, 1996; Foguel, Silva *et al.*, 1998).

What is the effect of hydrostatic pressure on protein aggregates? It was recently shown that aggregation of rhodonase proceeds more slowly at 2 kBar than at ambient pressure, and that a combination of hydrostatic pressure and 4 M urea can disrupt small rhodonase aggregation intermediates until pressure is released (Gorovits and Horowitz, 1998). We sought to determine whether hydrostatic pressure alone would increase or decrease the extent of aggregation. Many believe that protein aggregates, particularly those formed as inclusion bodies *in vivo*, are simply jumbled arrays of essentially unfolded chains (De Bernardez-Clark and Georgiou, 1991; Gorovits and Horowitz, 1998). If this model is accurate, then since hydrostatic pressure favors denatured, dissociated states, it would be expected to increase the extent of aggregation. However, it has been proposed that aggregates are formed from specifically associated chains that closely resemble the native state (Betts, Haase-Pettingell *et al.*, 1997; Speed, Morshead *et al.*, 1997). If this is true, we reasoned that pressure should dissociate oligomeric aggregated species while preserving secondary

3

and tertiary structure, allowing accurate protein-protein recognition and formation of native quaternary structure. Aggregates dissociated by pressure would thus be competent for refolding to produce native active proteins when returned to ambient pressure.

To investigate this phenomenon we subjected tailspike protein aggregation intermediates to hydrostatic pressure. Here we demonstrate that hydrostatic pressure can reverse aggregation and enhance formation of active native protein.

Materials and Methods

Tailspike protein production

Tailspike protein was produced by infecting *Salmonella typhimurium* strain 7136 with phage P22 (Winston, Botstein *et al.*, 1979). Purification and ^{14}C metabolic labeling for radioactive protein was performed essentially as described previously (Robinson and King, 1997). Tailspike appeared as a single band on both Coomasie and silver stained SDS gels. The tailspike protein was stored as an ammonium sulfate precipitate at 4°C, then dialyzed against Tris buffer, pH 7.0, 1 mM EDTA just prior to use.

In vitro aggregation reactions

Native tailspike protein was denatured for approximately 60 min. in 7 M urea, Tris-Cl, pH 3. The aggregation reaction was initiated by rapid dilution (12.5-fold) with 50 mM Tris-HCl (1 mM EDTA) pH 7.6 to a final protein concentration of 100 μg/mL protein at 20 °C and 0.6 M urea. To monitor the extent of aggregation, 50 μl aliquots of the sample were taken at various time points and rapidly transferred to tubes containing 25 μl 3x sample buffer (0.015M Tris, pH 6.8, 0.12 M Glycine, 50% glycerol, bromophenol blue), preincubated to 0°C in an ice-water bath. These aliquots were then analyzed by electrophoresis. For the HPLC analysis, 100 μl aliquots were removed, placed in an ice-water bath, and promptly injected into the HPLC.

4

Gel Electrophoresis

Nondenaturing polyacrylamide gel electrophoresis was performed using a discontinuous buffer system (Davis, 1964; Ornstein, 1964). The resolving gel contained 0.37 M Tris buffer, pH 8.0, with 3.8 mM TEMED, 3.0 mM ammonium persulfate, and 7.5% acrylamide. The stacking gel contained 0.07 M Tris buffer, pH 6.7, with 4.3% acrylamide, 7.5 mM TEMED, and 2.5 mM ammonium persulfate. The gels were run at constant current (10 mA/gel) for ~4 h at 4 °C and then silver-stained.

High Performance Liquid Chromatography:

High performance liquid chromatography (HPLC) was carried out in a Shimadsu system using a prepacked TSK3000 column. The system was equilibrated with 25 mM Tris-Acetate buffer in the presence of 0.5 M urea, pH 7.0, at a flow rate of 1.0 mL/min. Urea (0.5 M) was included to decrease the propensity of partially folded proteins to stick to the column matrix. Sample elution was monitored by absorption at 280 nm and tryptophan emission at 340 nm (excitation at 280 nm). The column and buffer temperature were maintained at 0°C.

Fluorescence Spectroscopy

Fluorescence spectra were recorded using an Hitachi F4500 Spectrofluorometer. All measurements were made at 25°C, in a buffer containing 50 mM sodium phosphate (pH 7.0) and 1 mM EDTA. For all tailspike samples (native, ambient aggregated, and pressure-treated aggregates) the protein concentration was 4 μg/mL. The excitation wavelength was 280 nm, and emission spectra were recorded from 300-400 nm. Relative differences in the spectra were determined by determining total peak area as well as the center of mass (average energy of emission).

Enzymatic "Tailing" Assay

Tail-free heads were prepared from *Salmonella* cells infected with P22 carrying an amber mutation in the tailspike gene as described previously (Berget and Poteete, 1980). Tailspike protein samples were diluted serially 1:3 into M9 media (Sambrook, Fritsch *et al.*, 1989)

5

supplemented with 2 mM MgSO4, to yield a final volume of 100 μl. 100 μl aliquots containing 10^9 tail-free heads were then added. Absorption was allowed to proceed until completion (~4 hours) at room temperature. The reaction mixture was then diluted serially 1:100, and 0.1 and 0.5 mLs of each dilution was added to two parallel tubes containing 2 mL of top agar (Sambrook, Fritsch *et al.*, 1989) and approximately 2×10^8 cells/mL of plating bacteria (*Salmonella* strain 7136) (Israel, Anderson *et al.*, 1967). This mixture was rapidly mixed and plated onto LB plates and incubated at 37°C to develop plaques. Plaques were counted for dilutions that resulted in 50-400 plaques per plate. A control sample containing only tail-free heads was used to measure background phage present; controls containing only tailspike protein were used to determine residual phage in tailspike preps; and a sample of only plating bacteria was used to control for cross-contamination during plating.

Results and Discussion

Aggregation Reactions can be monitored by HPLC

In the P22 tailspike system, folding and aggregation intermediates have been separated and visualized using native gel electrophoresis (Goldenberg, Berget *et al.*, 1982; Speed, Wang *et al.*, 1995; Robinson and King, 1997). A time course for aggregation can be visualized and quantitated with native gel electrophoresis by using ^{14}C-labeled tailspike (Figure 2A). Early time points (2 min., 5 min.) show monomer, dimer, and higher order aggregate species. Later time points (30 min., 2 hr.) show formation of some native trimer; however, higher order aggregation intermediates are the predominant species under the conditions of this experiment.

In order to identify and quantitate aggregation intermediates rapidly, we developed an HPLC assay using size exclusion HPLC (TSK3000 column, Supelco). The column and buffer were kept at 4°C in all of the experiments described here in order to avoid additional association of tailspike chains inside the column during the run.

Using purified tailspike, we monitored the elution profiles of the native trimeric and the denatured monomeric species by absorption at 280 nm and by fluorescence emission at 340 nm.

The monomer and trimer both resolved as single peaks (data not shown). The trimer eluted as a uniform peak around 6.7 minutes, and the monomer eluted at 7.6 minutes.

To determine whether HPLC could be used as a probe for aggregation intermediates, tailspike was denatured, then rapidly diluted into refolding buffer. After the onset of the aggregation aliquots were removed at designated times and injected in the HPLC (Figure 2B). Three distinct peaks elute at 5.0, 6.6, and 7.5 minutes after injection and a broad shoulder appears at 5.2 to 6.0 min. Peaks were collected and analyzed by native gel electrophoresis, which enabled us to identify the peaks as follows: 5.0 minutes, large aggregates; 6.6 minutes, trimer; 7.5 minutes, monomer (data not shown). Monomer and trimer eluted at the same times as purified tailspike samples, confirming the reproducibility of the technique for samples under refolding conditions. The broad shoulder that decreases with time is comprised mainly of intermediate sized aggregates (smaller than those eluting at 5 min.), which are not clearly resolved on this HPLC column.

Increasing reaction times lead to an increase in the size of peaks of aggregated species (eluting at 5.0 min.) and a concomitant decrease in the size of the monomer peak (7.5 min.) (Figure 2B). Similar results are obtained when native gel electrophoresis is used to monitor the time course of aggregation. In both cases, the amount of trimer changes very little with increasing reaction time, presumably because the conditions favor aggregation so strongly.

Quantitation of peak area from HPLC, and radioactive counts per band in native gel electrophoresis shows that both methods yield similar levels of monomer, trimer and aggregate (Figure 2C). Small differences between the aggregate peak and the monomer formed under native PAGE vs. HPLC are likely due to the small buffer variations, such as the inclusion of 1 M Urea in the HPLC. Since HPLC is substantially faster than native gel electrophoresis (1 hr. vs. 5 hr.) and less labor intensive, it is well suited to measure the extent of aggregation on-line during refolding reactions. This capability represents an enormous advantage for those interested in monitoring and controlling protein aggregation in biotechnology, research, and industrial applications.

Hydrostatic pressure inhibits and reverses tailspike aggregation

To test the effect of hydrostatic pressure upon aggregation, samples of native tailspike were denatured, then transferred to refolding buffer under conditions which favor aggregation (t = 26°C, [Pt] = 1.4 μM chains). These samples were termed "ambient aggregated tailspike." An identical set of samples were denatured, transferred to refolding buffer under aggregation conditions, then subjected to 35,000 PSI (2.4 kbar) for 90 minutes after 3.25 hours of aggregation at atmospheric conditions. These samples were termed "pressure-treated tailspike". For each sample, the extent of refolding and aggregation was analyzed by HPLC (Figure 3A).

Treatment with 35,000 PSI (2.4 kbar) hydrostatic pressure markedly increases the yield of native trimer, while substantially decreasing the extent of aggregation. Figure 3B shows the distribution of tailspike monomers, trimers, and aggregates for pressure-treated tailspike samples and for the ambient aggregated tailspike sample. In the absence of pressure under these conditions, aggregation is favored: over 40% of the chains are in an aggregated form, with only 22% monomer and 37% trimer after 3.25 hours. In samples incubated at 35,000 PSI for 90 minutes, the fraction of trimer and monomer are increased by 25% and 38% respectively, and the extent of aggregation is decreased by more than 50%.

Tailspike trimers from pressure treatment have native-like structure and activity

We sought to determine whether tailspike trimers recovered native-like structural and functional properties in pressure-treated aggregates. We compared the intrinsic fluorescence spectra of native, pressure-treated, and ambient aggregated tailspike. Tailspike aggregation is accompanied by a large decrease in fluorescence intensity compared to native tailspike trimers. Pressure treatment of tailspike aggregates produced a 25% increase in fluorescence intensity which exactly corresponded to the 25% increase in SDS-resistant trimer in these samples. This result is consistent with the idea that tailspike trimers in this sample have fluorescence properties similar to native trimers. Pressure-treated and native tailspike trimers also have essentially identical native-gel electrophoretic mobility, and size-exclusion HPLC elution times, indicating that their

hydrodynamic volume and hydrophobic surface areas are similar (Figure 3). Moreover, the pressure-treated tailspike recovers the SDS resistance that is characteristic of native tailspike trimers. Incompletely folded tailspike species, including the protrimer, are sensitive to SDS. These observations strongly suggest that trimers recovered by pressure treatment have native-like tertiary and secondary structure.

To assess whether tailspike trimers produced by pressure-treating aggregates recovered wild-type function, tailspike samples were subjected to a "tailing" assay to determine ability to complement tail-less P22 viral heads and produce infectious viral particles. Samples of native tailspike, ambient aggregated and pressure-treated aggregates were diluted and incubated with tail-less heads as described in Experimental Protocol. Tailspike trimers produced by pressure treatment of aggregates are essentially fully active, and form viral plaques as efficiently as native tailspike trimers (data not shown). These results confirm that refolding under pressure produces tailspike trimers with essentially native structural and functional characteristics.

Implications

We have shown that hydrostatic pressure can be used to reverse protein aggregation in the absence of urea or other chemical additives. After pressure is released, dissociated aggregates refold to form biologically active protein with native characteristics. This process substantially increases the level of refolded protein. Pressure therefore appears to be an efficient tool for combating aggregation in a variety of research and industrial settings. It enables rapid refolding to active native proteins without buffer changes or dilution. Pressure application is cost effective in industrial applications, easy to scale up, and straightforward to tune to achieve optimal refolding for each protein.

Several applications of pressure in biotechnological processes have been recently developed. The use of high pressure in food technology has rapidly increased (Heremans, 1997). Food pasteurized by hydrostatic pressure is being marketed worldwide (Shigehisa, Ohmori et al., 1991; Tauscher, 1995). The ability of pressure to inactivate viruses has been evaluated with a

view toward two potential applications, vaccine development and virus sterilization (Silva, Luan *et al.*, 1992; Jurkiewicz, Villas-Boas *et al.*, 1995; Pontes, Fornells *et al.*, 1997). Our knowledge about the specificity of aggregation will open new avenues of research in this area.

We have not yet determined which are responsible for the reversal of aggregation by hydrostatic pressure. The folding pathway of tailspike is complicated — multiple species are involved in the various reactions, including a number of oligomeric intermediates (Figure 1B). It is likely that each of these reactions is differently sensitive to pressure. In fact, application of 15,000 psi of hydrostatic pressures enhances aggregation yields, and the timing of application is also critical (unpublished observations). These observations indicate that pressure probably acts at one or more junctions between folding and aggregation.

Our findings also indicate that protein aggregations share some crucial features with native protein associations, and the molecular determinants of specificity may be similar in the two kinds of reactions. Reversal of protein aggregation by hydrostatic pressure may be analogous to pressure dissociation of oligomeric proteins. The chains that are dissociated by pressure are competent for rapid productive folding, suggesting that secondary and tertiary structures are retained. The pressure-sensitive interfaces of aggregates are likely to be well-packed and solvent-excluded, supporting the idea that aggregation involves specific protein-protein interactions. Thus, in addition to providing a valuable method for combating aggregation, this study emphasizes the importance of further characterization of the nature of protein aggregates.

Acknowledgments

References

Berget, P. B. and Poteete, A. R. 1980. Structure and functions of the bacteriophage P22 tail protein. Journal of Virology 34(1): 234-243.

Betts, S., Haase-Pettingell, C. and King, J. 1997. Mutational Effects on Inclusion Body Formation. Adv. Prot. Chem. 50: 243-264.

Bychkova, V. E. and Ptitsyn, O. B. 1995. Folding intermediates are involved in genetic diseases? FEBS Letters 359: 6-8.

Cleland, J. L. 1993. Impact of protein folding on biotechnology. 1-21. In: J. L. Cleland (eds). Protein folding: *In vivo* and *in vitro*. American Chemical Society, Washington, D.C.

Davis, B. J. 1964. Disk Electrophoresis - II. Methods and Application to Human Serum Proteins. Ann. N Y Acad. Sci. 121: 404-427.

De Bernardez-Clark, E. and Georgiou, G. 1991. Inclusion bodies and recovery of proteins from the aggregated state. 1-20. In: G. Georgiou and E. De Bernardez-Clark (eds). Protein refolding. American Chemical Society, Washington, D.C.

Foguel, D., Silva, J. L. and Prat-Gay, G. 1998. Characterization of a partially folded monomer of the DNA-binding domain of human Papillomavirus E2 obtained at high pressure. Journal of Biological Chemistry 273: 9050-9057.

Fuchs, A., Seiderer, C. and Seckler, R. 1991. *In vitro* folding pathway of phage P22 tailspike protein. Biochemistry 30: 6598-6604.

Goldenberg, D., Berget, P. and King, J. 1982. Maturation of the tailspike endorhamnosidase of *Salmonella* phage P22. J. Biol. Chem 257: 7864-7871.

Goldenberg, D. and King, J. 1982. Trimeric intermediate in the *in vivo* folding and subunit assembly of the tail spike endorhamnosidase of bacteriophage P22. Proceedings of the National Academy of Sciences, USA **79**: 3403-3407.

Goldenberg, D. P., Smith, D. H. and King, J. 1983. Genetic analysis of the folding pathway for the tail spike protein of phage P22. Proc Natl Acad Sci U S A **80**(23): 7060-7064.

Gorovits, B. M. and Horowitz, P. M. 1998. High hydrostatic pressure can reverse aggregation of protein folding intermediates and facilitate acquisition of native structure. Biochemistry **37**: 6132-6135.

Haase-Pettingell, C. A. and King, J. 1988. Formation of aggregates from a thermolabile *in vivo* folding intermediate in P22 tailspike maturation: A model for inclusion body formation. J Biol Chem **263**(10): 4977-4983.

Heremans, K. 1997. High Pressure Research in the Biosciences and Biotechnology. Leuven University Press, Leuven.

Israel, J. V., Anderson, T. F. and Levine, M. 1967. *In vitro* morphogenesis of phage P22 from heads and base-plate parts. Proceedings of the National Academy of Sciences, USA **57**: 284-291.

Iwashita, S. and Kanegasaki, S. 1976. Enzymic and molecular properties of base-plate parts of bacteriophage P22. European Journal of Biochemistry **65**: 87-94.

Jurkiewicz, E., Villas-Boas, M., *et al.* 1995. Inactivation of simian immunodeficiency virus by hydrostatic pressure. Proc Natl Acad Sci U S A **92**(15): 6935-7.

Ornstein, L. 1964. Disc Electrophoresis - I. Background and Theory. Ann. N Y Acad. Sci. **121**: 321-349.

Pontes, L., Fornells, L. A., *et al.* 1997. Pressure inactivation of animal viruses: Potential

biotechnological applications. 91-94. In: K. Heremans (eds). High Pressure Research in

the Biosciences and Biotechnology. Leuven University Press, Leuven.

Robinson, A. S. and King, J. 1997. Disulphide-bonded intermediate on the folding and assembly

pathway of a non-disulphide bonded protein. Nature Structural Biology 4(6): 450-455.

Robinson, C. R. and Sligar, S. G. 1995. Hydrostatic and osmotic pressure as tools to study

macromolecular recognition. Methods Enzymol 259: 395-427.

Sambrook, J., Fritsch, E. F. and Maniatis, T. 1989. Molecular Cloning, A Laboratory Manual.

Cold Spring Harbor Laboratory Press, New York.

Sauer, R. T., Krovatin, W., Poteete, A. R. and Berget, P. B. 1982. Phage P22 tail protein: Gene

and amino acid sequence. Biochemistry 21: 5811-5815.

Seckler, R., Fuchs, A., King, J. and Jaenicke, R. 1989. Reconstitution of the thermostable

trimeric phage P22 tailspike protein from denatured chains *in vitro*. J. Biol. Chem.

264(20): 11750-11753.

Shigehisa, T., Ohmori, T., Saito, A., Taji, S. and Hayashi, R. 1991. Effects of high hydrostatic

pressure on characteristics of pork slurries and inactivation of microorganisms associated

with meat and meat products. Int J Food Microbiol 12(2-3): 207-15.

Silva, J. L., Foguel, D., Da Poian, A. T. and Prevelige, P. E. 1996. The use of hydrostatic

pressure as a tool to study viruses and other macromolecular assemblages. Curr Opin

Struct Biol 6(2): 166-75.

Silva, J. L., Luan, P., Glaser, M., Voss, E. W. and Weber, G. 1992. Effects of hydrostatic

pressure on a membrane-enveloped virus: High immunogenicity of the pressure-

inactivated virus. J. Virol. 66: 2111-2117.

Silva, J. L., Silveira, C. F., Correa, A. and Pontes, L. 1992. Dissociation of a native dimer to a molten globule monomer. Effects of pressure and dilution on the associaton equilbrium constant of Arc repressor. Journal of Molecular Biology **223**: 545-555.

Silva, J. L. and Weber, G. 1993. Pressure stability of proteins. Annu. Rev. Phys. Chem. **44**: 89-113.

Speed, M. A., Morshead, T., Wang, D. I. and King, J. 1997. Conformation of P22 tailspike folding and aggregation intermediates probed by monoclonal antibodies. Protein Sci **6**(1): 99-108.

Speed, M. A., Wang, D. I. C. and King, J. 1995. Multimeric intermediates in the pathway to the aggregated inclusion body state for P22 tailspike polypeptide chains. Protein Science **4**(5): 900-908.

Speed, M. A., Wang, D. I. C. and King, J. 1996. Specific aggregation of partially folded polypeptide chains: The molecular basis of inclusion body composition. Nature Biotechnology **14**: 1283-1287.

Steinbacher, S., Seckler, R., *et al.* 1994. Crystal structure of P22 tailspike protein: Interdigitated subunits in a thermostable trimer. Science **265**: 383-386.

Tauscher, B. 1995. Pasteurization of food by hydrostatic high pressure: chemical aspects. Z Lebensm Unters Forsch **200**(1): 3-13.

Thomas, P. J., Qu, B. H. and Pedersen, P. L. 1995. Defective protein folding as a basis of human disease. Trends Biochem. Sci. **20**(11): 456-459.

Winston, R., Botstein, D. and Miller, J. 1979. Characterization of amber and ochre suppressors in *Salmonella typhimurium*. J. Bacteriology **137**: 433-439.

Figure Legends

Figure 1. Structure and folding/aggregation pathway of P22 tailspike.

A) Structure of P22 tailspike (108-666) (Steinbacher, Seckler *et al.*, 1994). B) Schematic diagram of the folding pathway for P22 tailspike. Intermediates along both pathways can be identified and quantitated by non-denaturing polyacrylamide gel electrophoresis (Goldenberg, Berget *et al.*, 1982; Goldenberg, Smith *et al.*, 1983; Speed, Wang *et al.*, 1995; Robinson and King, 1997). I_M, monomeric folding intermediate; I_M^*, monomeric aggregation intermediate; I_D, dimeric folding intermediate; I_D^*, dimeric aggregation intermediate.

Figure 2. Tailspike aggregation intermediates can be identified and quantitated by size-exclusion HPLC. A) Native gel electrophoresis of ^{14}C-tailspike aggregation intermediates. Tailspike was denatured and refolded as described in Experimental Protocol. At the times indicated, aliquots were removed and added to native sample buffer and placed on wet ice. Intermediates were visualized by native gel electrophoresis followed by exposure of the dried gel to phosphor screens and image analysis (Molecular Dynamics). B) Size-exclusion HPLC separates tailspike aggregation intermediates. Tailspike was denatured and refolded as described in Experimental Protocol. At the times indicated, 100 µl aliquots were removed and injected into a TSK 3000 column. Peaks were detected by adsorbance at 280 nm. Intermediates were identified by comparison to standards, and by collection of the peaks and visualization by native gel electrophoresis followed by silver staining. Sample times: 5 min. - - - ; 30 min. ——; 120 min. —— -. C) Quantitation of aggregation intermediates. Values for HPLC peaks (solid bars) and electrophoretic bands (shaded bars) were determined as described in Experimental Protocol. Error bars reflect variation in total intensity from sample to sample for both HPLC and native PAGE experiments.

Figure 3. Pressure reverses tailspike aggregation.

Native tailspike was denatured and refolded under aggregation conditions as described in Experimental Protocol. After 3.5 hours at room temperature, aggregates were either left untreated (ambient) or subjected to pressures of 35,000 psi for 90 minutes (pressure-treated). A) Size-exclusion HPLC traces. Peaks were detected by adsorbance at 280 nm. Samples: Ambient - - -; Pressure-treated ——. B) Quantitation of HPLC traces. Values for the Ambient samples (solid bars) and Pressure-treated (shaded bars) were determined as described in Experimental Protocol. Error bars reflect variation in total intensity from sample to sample for HPLC experiments.
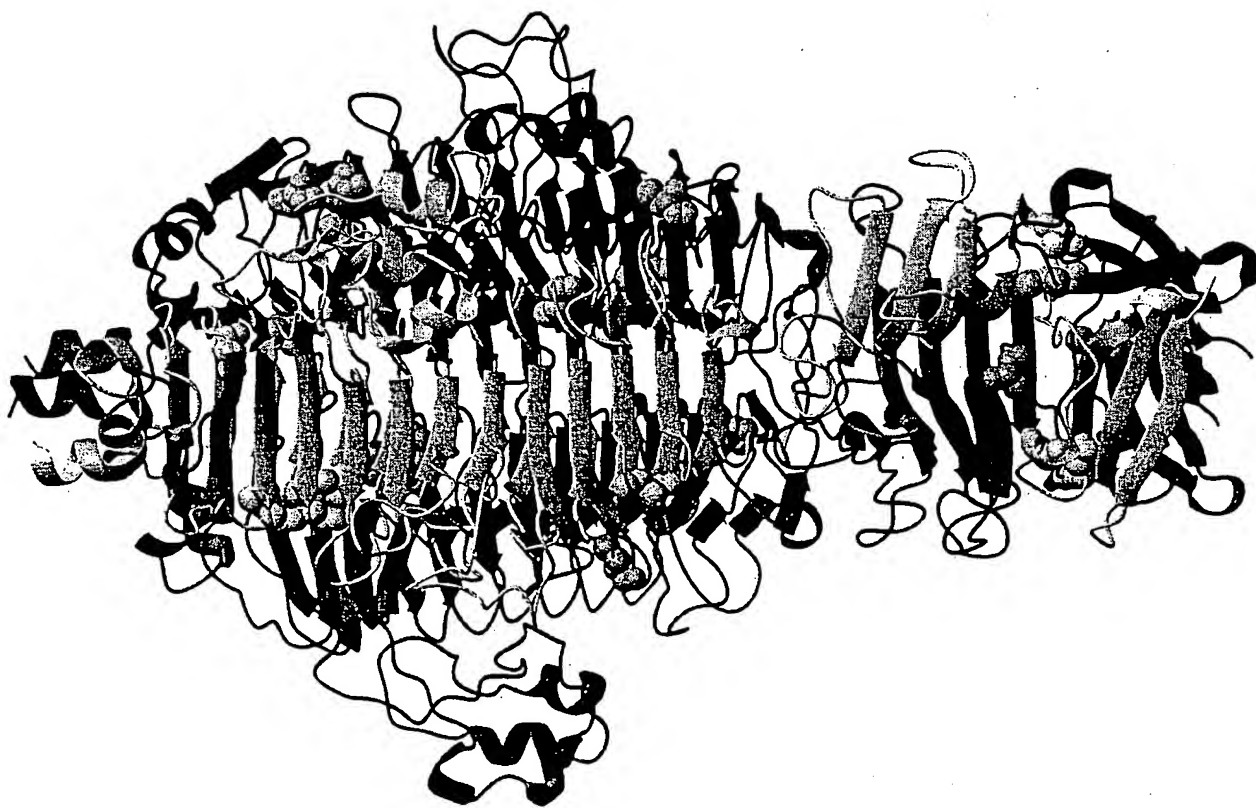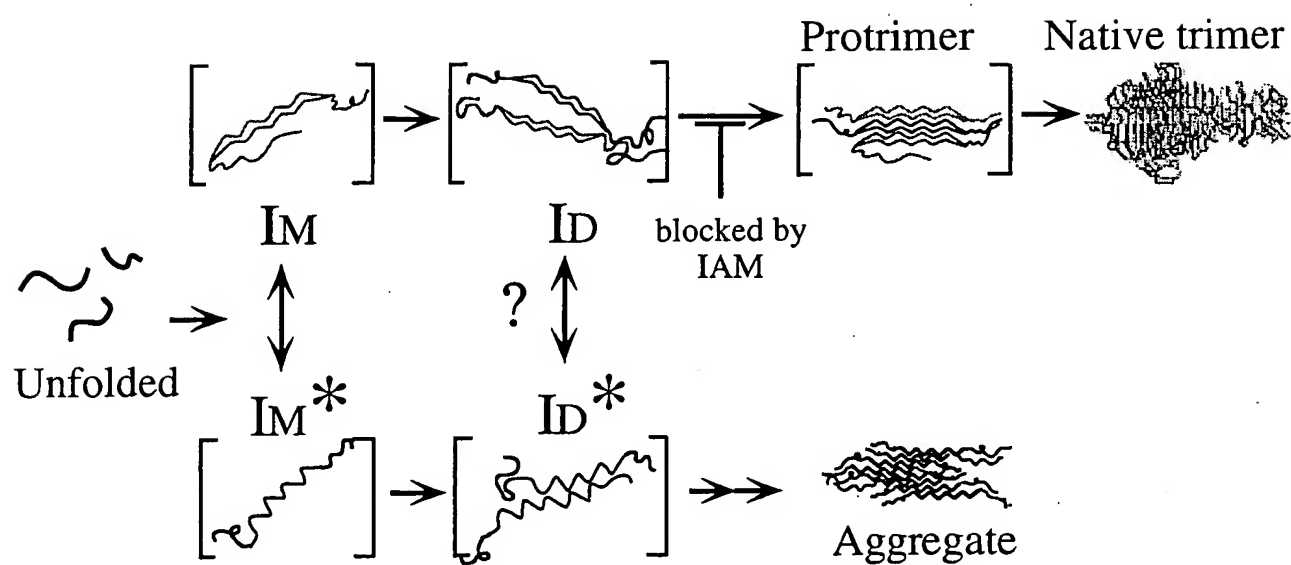
Protrimer   Native trimer

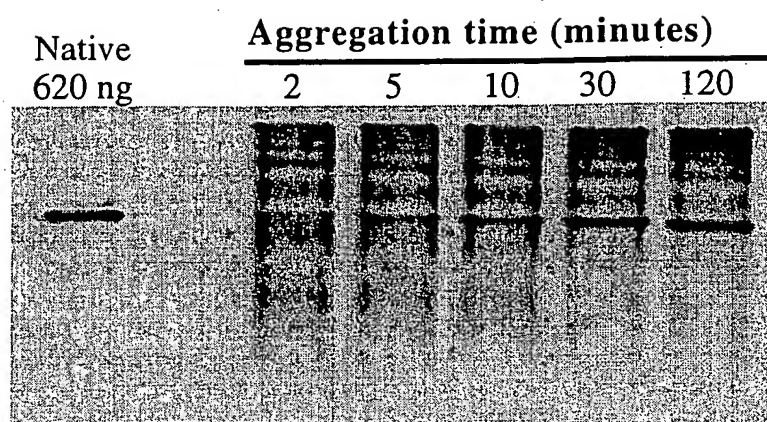IM   ID   blocked by
                    IAM

Unfolded   ?

IM*   ID*

Aggregate

18

Figure 2A

Native
620 ng

Aggregation time (minutes)
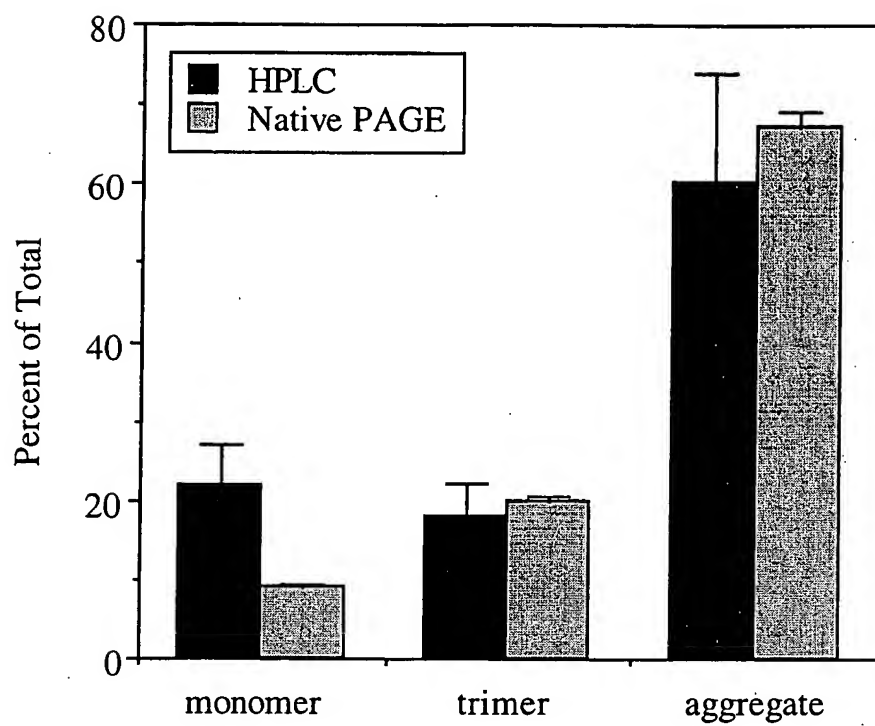
2   5   10   30   120

20
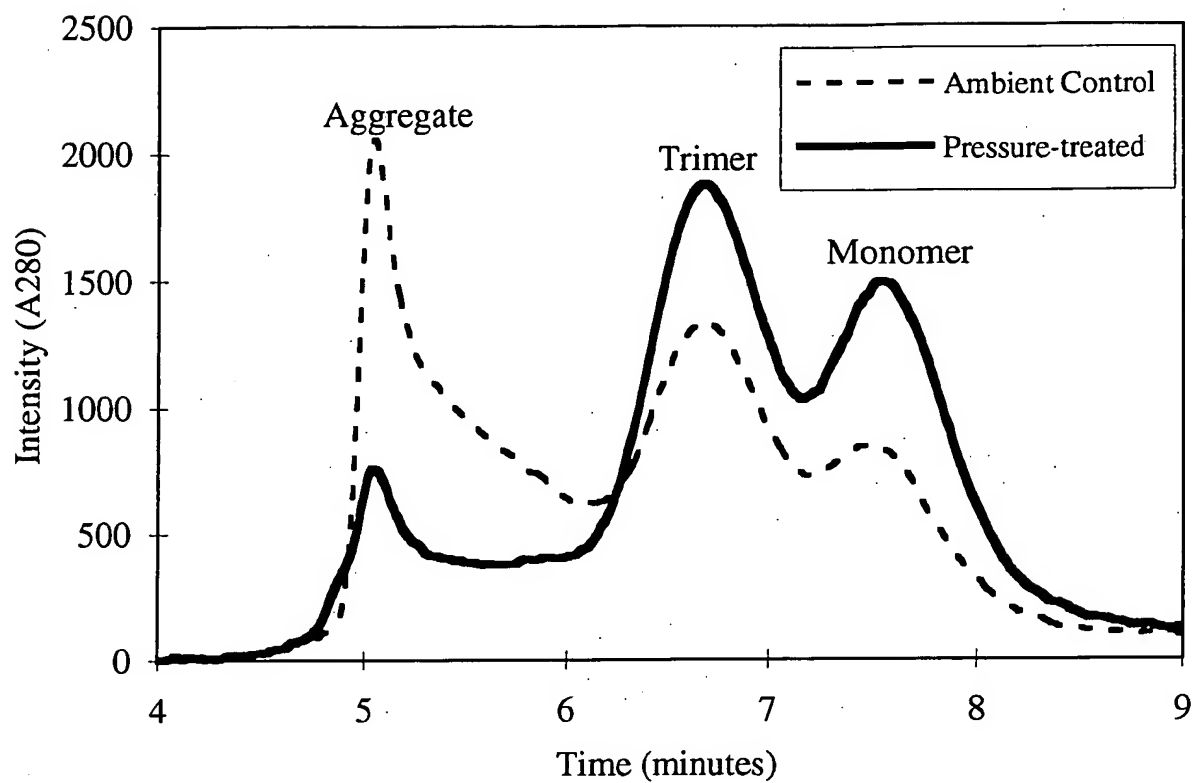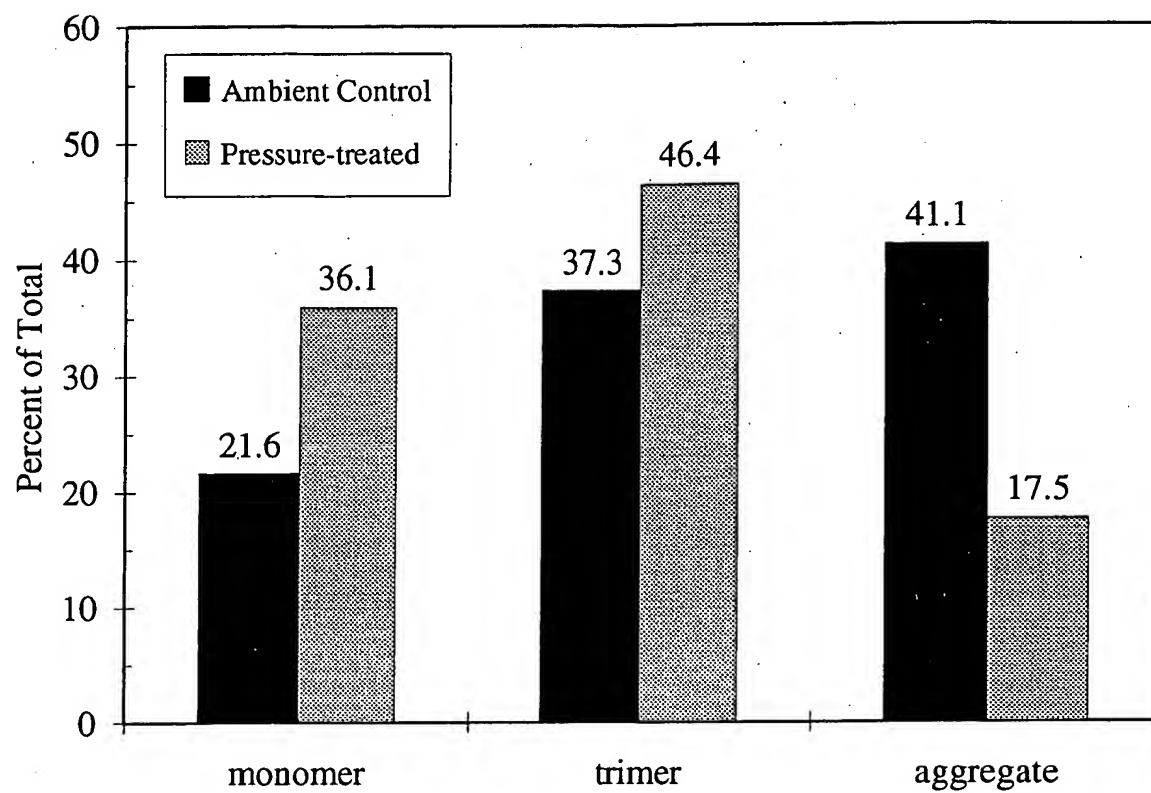
FEE SUMMARY SHEET

Petition for Extension of Time Under 37 CFR 1.136(a) (PTO SB-22)

Date: October 30, 2006   Filing Date: September 26, 2003
Time: 3:53 PM   Application No: 10/673,000
Docket: 00131-00350-US   Total Fee: $ 60.00

Code	Amount	37 CFR	Fee Description	Listed on
2251	60.00	1.17(a)(1)	Extension for response within first month	Petition for Extension of Time Under 37 CFR 1.136(a) (PTO SB-22)

Biotechnology
——— and ———
Bioengineering

Editor-in-Chief: Douglas S. Clark
Department of Chemical Engineering
University of California
Berkeley, CA 94720-9989

Phone: (510) 642-8063; Fax: (510) 643-0302
E-mail: alan@cchem.berkeley.edu

June 24, 1998

FAX TRANSMISSION

Professor Anna Robinson
University of Delaware
Department of Chemical Engineering
Newark DE 19716
U. S. A.
Fax: **302-831-6262**

Pages including this one: 1

Dear Professor Robinson:

We have received your manuscript entitled "Hydrostatic pressure rescues native protein from aggregates" and have assigned to it the serial number **BB-98-264**. Please refer to this serial number in any future correspondence. Your manuscript will be treated as a *paper*.

Professor Clark, the senior editor of the journal, will also act as handling editor. Please feel free to call on this office directly if you have any questions or if we can be of any assistance. Our contact information is:

> The University of California at Berkeley
> Department of Chemical Engineering
> 110-C Gilman Hall
> Berkeley, CA 94720-1462
> Phone: 510-642-8063 Fax: 510-643-0302
> e-mail: Alan@Cchem.Berkeley.edu

My only request is that you confirm receipt of this fax.

1 review

→ 2 reviews still pending

→ Publication w/ revision.
Revise

Sincerely yours,

Alan Haley
Editorial Assistant

Docket No.: 00131-00350-US

EXHIBIT B

FEE SUMMARY SHEET

Petition for Extension of Time Under 37 CFR 1.136(a) (PTO SB-22)

Date: October 30, 2006   Filing Date: September 26, 2003
Time: 3:53 PM   Application No: 10/673,000
Docket: 00131-00350-US   Total Fee: $ 60.00

Code	Amount	37 CFR	Fee Description	Listed on
2251	60.00	1.17(a)(1)	Extension for response within first month	Petition for Extension of Time Under 37 CFR 1.136(a) (PTO SB-22)

Hydrostatic Pressure Rescues Native Protein from Aggregates

Docket No.: 00131-00350-US

Exhibit C

Debora Foguel,[1] Clifford R. Robinson,[2*] Pedro Caetano de Sousa, Jr.,[1] Jerson L. Silva,[1] Anne Skaja Robinson[2,3]

[1]Departamento de Bioquímica Médica, Instituto de Ciências Biomédicas, Universidade Federal do Rio de Janeiro, Rio de Janeiro, RJ, Brazil
[2]Department of Biology, Massachusetts Institute of Technology, Cambridge, Massachussetts, USA
[3]Department of Chemical Engineering, University of Delaware, Newark, Delaware, USA

Abstract: Misfolding and misassembly of proteins are major problems in the biotechnology industry, in biochemical research, and in human disease. Here we describe a novel approach for reversing aggregation and increasing refolding by application of hydrostatic pressure. Using P22 tailspike protein as a model system, intermediates along the aggregation pathway were identified and quantitated by size-exclusion high-performance liquid chromatography (HPLC). Tailspike aggregates were subjected to hydrostatic pressures of 2.4 kbar (35,000 psi). This treatment dissociated the tailspike aggregates and resulted in increased formation of native trimers once pressure was released. Tailspike trimers refolded at these pressures were fully active for formation of infectious viral particles. This technique can facilitate conversion of aggregates to native proteins without addition of chaotropic agents, changes in buffer, or large-scale dilution of reagents required for traditional refolding methods. Our results also indicate that one or more intermediates at the junction between the folding and aggregation pathways is pressure sensitive. This finding supports the hypothesis that specific determinants of recognition exist for protein aggregation, and that these determinants are similar to those involved in folding to the native state. An increased understanding of this specificity should lead to improved refolding methods. © 1999 John Wiley & Sons, Inc. *Biotechnol Bioeng* 63: 552–558, 1999.
Keywords: protein folding; protein aggregation; inclusion body; hydrostatic pressure; size-exclusion HPLC; p22 tailspike

INTRODUCTION

Protein aggregation and misfolding play major roles in protein production in the biotechnology industry, in limiting the biochemical study of proteins, and in the onset of pathogenesis in human disease. The native, correctly folded state is necessary for a protein's biological function and recognition by other molecules; misfolding and misassembly lead to significant loss of biological activity. Because the mechanism that drives aggregation is poorly understood it represents a challenge to industrial, academic, and medical research scientists.

Improved methods to reverse and inhibit aggregation are needed. During production, the need to refold proteins from large aggregates, or inclusion bodies, often requires denaturation by harsh chaotropic reagents such as guanidine chloride or urea, and reducing agents (Cleland, 1993). Removal of the denaturant may then require large dilution and therefore large working volumes; low refolding yields are common due to the loss of protein during refolding and subsequent concentration (De Bernardez-Clark and Georgiou, 1991).

Misfolding has also been identified as the causative agent in a number of human diseases including cystic fibrosis, prion spongiform encephalopathies such as Creutzfeldt-Jacob's disease, Alzheimer's disease, and other amyloid diseases (Bychkova and Ptitsyn, 1995; Thomas et al., 1995). A better understanding of the interactions that lead to aggregation will enhance our ability to design inhibitors and therapeutics for aggregation-driven diseases.

The tailspike protein of P22 bacteriophage is an excellent model system for aggregation because the structure is known, the folding and aggregation pathways are well characterized, and aggregation of tailspike chains occurs by specific interactions. The tailspike protein is a homotrimer of 666 residues per monomer chain (Sauer et al., 1982). Figure 1A shows the X-ray crystal structure of residues 108–666, which indicates that tailspike is a member of the β-coil family (Steinbacher et al., 1994). The main body of each subunit of the trimer, residues 143–535, is a long β-coil made of 13 complete turns (Steinbacher et al., 1994). The three chains then twist around each other to form three intertwined β-sheets comprising residues 536–619 (the "tail" region), where each sheet contains β-strands from all three subunits. The native tailspike trimer is thermostable

Exhibit D

Exhibit E

— Same as unf ts lot diluted
5µl into 45µl Acidurea
before loading
✻ Cooled column 50µl

15:18:46

CLASS-CR10 SYS=1 Ch=1 REPORT.NO=1 DATA=UNF3TS.D01
Sample   : unf3ts
ID   : hex8mu40dil
Dilution Factor: 40
Type   : Unknown
Operator : anne

*** Chromatogram ***
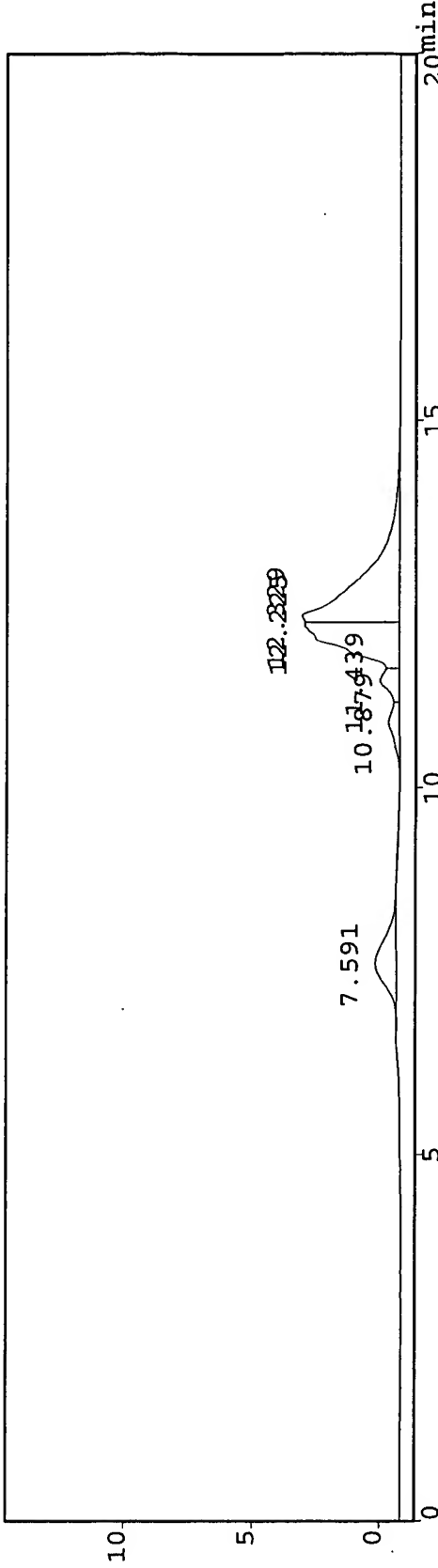
*** Peak Report ***

PKNO	TIME	AREA	HEIGHT	MK	IDNO	CONC	NAME
1	7.591	35662	829			12.2069	
2	10.879	12266	421	V		4.1985	
3	11.439	14891	778	V		5.0971	
4	12.225	91788	3745	V		31.4184	
5	12.329	137540	3832	V		47.0791	
		292146	9605			100.0000	
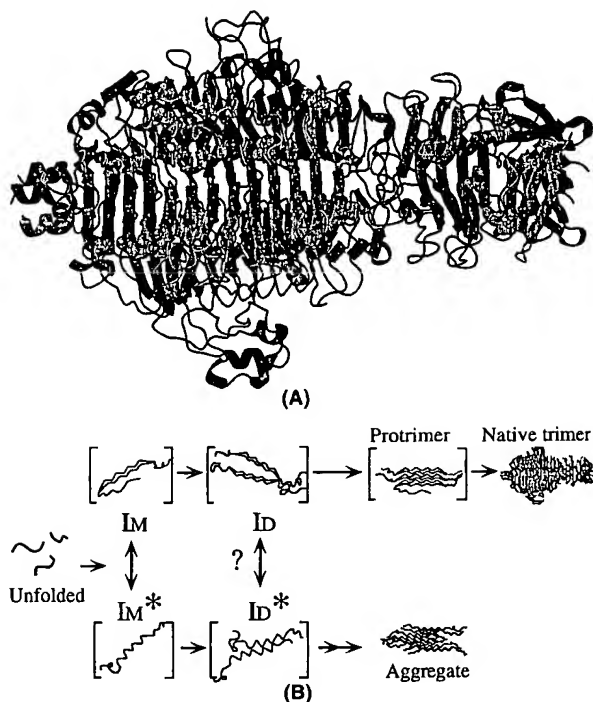
1 - 1/2

Figure 1. Structure and folding/aggregation pathway of P22 tailspike. (A) Structure of P22 tailspike (residues 108–666) (Steinbacher et al., 1994). Subunits shown in black, dark gray, or light gray. (B) Schematic diagram of the folding pathway for P22 tailspike. Intermediates along both pathways can be identified and quantitated by nondenaturing polyacrylamide gel electrophoresis (Goldenberg et al., 1982, 1983; Robinson and King, 1997; Speed et al., 1995). I_M, monomeric folding intermediate; I_M^*, monomeric aggregation intermediate; I_D, dimeric folding intermediate; I_D^*, dimeric aggregation intermediate.

(t_m = 88°C), and resistant to SDS and proteolysis. No covalent linkages exist in the native state of tailspike, and it is thought that the intertwined β-sheet plays a major role in stabilizing the tailspike trimer.

Tailspike protein is both a structural and functional component of the P22 bacteriophage. Tailspike binds to the O-antigen on the outer membrane lipopolysaccharide of *Salmonella* species and facilitates infection through hydrolysis of the α(1–3)-glycosidic linkages (Iwashita and Kanegasaki, 1976). This activity can be assayed for in vitro by incubating purified tailspike with tail-free viral heads, and measuring the "tailing" level by the formation of infectious particles (Berget and Poteete, 1980). The "tailing" ability serves as a functional assay for folded protein, whereas formation of native-like tertiary structure can be monitored by changes in SDS resistance and intrinsic fluorescence.

A number of intermediates along the in vivo and in vitro folding and aggregation pathways for P22 tailspike have been identified through native and denaturing gel electrophoresis (Fig. 1B) (Fuchs et al., 1991; Goldenberg et al., 1982; Goldenberg and King, 1982; Haase-Pettingell and King, 1988; Robinson and King, 1997; Seckler et al., 1989; Speed et al., 1995). Folding intermediates of tailspike are thermolabile, and aggregate under physiological conditions

in the host (Goldenberg et al., 1983; Haase-Pettingell and King, 1988). A late trimeric intermediate, "protrimer," lacks the SDS resistance and thermal stability of the native proteins (Goldenberg et al., 1982; Goldenberg and King, 1982). Although early folding intermediates are susceptible to aggregation, the propensity to aggregate is diminished once protrimer is formed. The presence of transient disulfide bonds in the protrimer intermediate may help promote folding and chain association of tailspike protein (Robinson and King, 1997).

Aggregation of tailspike in vitro is not limited to sequential addition of monomers. Association can occur between subunit assemblies of any size—dimers can associate with monomers, dimers, trimers, tetramers, etc. (Speed et al., 1995). Aggregation does not occur by covalent association of the chains, as the addition of SDS in the absence of reducing agents dissociates aggregates into monomeric subunits (Robinson and King, 1997; Speed et al., 1995). In general, aggregation involves specific interactions between chains, since mixing of denatured tailspike protein with other aggregation-competent proteins (P22 coat protein, carbonic anhydrase) does not yield mixed aggregate species (Speed et al., 1996). In vitro the extent of aggregation is dependent on both the protein and urea concentrations present in the refolding buffer (Robinson et al., unpublished results).

Hydrostatic pressure is an efficient tool to dissociate oligomeric proteins and other macromolecular complexes without denaturing the secondary and tertiary structure of the subunits (Robinson and Sligar, 1995; Silva et al., 1996). Elevated hydrostatic pressure favors the state of lowest total volume—for most macromolecular assemblages this is the dissociated state (Silva and Weber, 1993). Quaternary structures of oligomeric protein assemblies usually dissociate to monomeric subunits between 1 and 3 kbar, but secondary and tertiary structures of proteins typically do not denature until pressures above 5 kbar at room temperature (Robinson and Sligar, 1995; Silva and Weber, 1993). Hydrostatic pressure has also proved to be a very powerful method to produce partially folded protein chains under equilibrium conditions (Foguel et al., 1998; Silva et al., 1996; Silva et al., 1992b).

What is the effect of hydrostatic pressure on protein aggregates? It was recently shown that aggregation of rhodonase proceeds more slowly at 2 kbar than at ambient pressure, and that a combination of hydrostatic pressure and 4 M urea can disrupt small rhodonase aggregation intermediates until pressure is released (Gorovits and Horowitz, 1998). We sought to determine whether hydrostatic pressure alone would increase or decrease the extent of aggregation. Many believe that protein aggregates, particularly those formed as inclusion bodies in vivo are simply jumbled arrays of essentially unfolded chains (Gorovits and Horowitz, 1998). If this model is accurate, then because hydrostatic pressure favors denatured, dissociated states, it would be expected to increase the extent of aggregation. However, it has been proposed that aggregates are formed from specifi-

cally associated chains that closely resemble the native state (Betts et al., 1997; Speed et al., 1997). If this is true, we reasoned that pressure should dissociate oligomeric aggregated species while preserving secondary and tertiary structure, allowing accurate protein–protein recognition and formation of native quaternary structure. Aggregates dissociated by pressure would thus be competent for refolding to native active proteins when returned to ambient pressure.

To investigate this phenomenon we subjected tailspike protein aggregation intermediates to hydrostatic pressure. Here, we demonstrate that hydrostatic pressure can reverse aggregation and enhance formation of active native protein once pressure is released.

MATERIALS AND METHODS

Tailspike Protein Production

Tailspike protein was produced by infecting *Salmonella typhimurium* strain 7136 with phage P22 (Winston et al., 1979). Purification and ^{14}C metabolic labeling for radioactive protein was performed essentially as described previously (Robinson and King, 1997). Tailspike appeared as a single band on both Coomasie- and silver-stained SDS gels. The tailspike protein was stored as an ammonium sulfate precipitate at 4°C, then dialyzed against 50 mM Tris-HCl (pH 7.0) and 1 mM EDTA just prior to use.

In Vitro Aggregation Reactions

Native tailspike protein was denatured for approximately 60 min in 7 M urea, 50 mM Tris-HCl (pH 3). The aggregation reaction was initiated by rapid dilution (12.5-fold) with 50 mM Tris-HCl (1 mM EDTA) at pH 7.6 to a final protein concentration of 100 μg/mL protein at 20°C and 0.6 M urea. To monitor the extent of aggregation, 50-μL aliquots of the sample were taken at various time points and rapidly transferred to tubes containing 25 μL of 3× sample buffer (15 mM Tris-HCl [pH 6.8], 120 mM glycine, 50% glycerol, bromophenol blue), preincubated to 0°C in an ice-water bath. These aliquots were then analyzed by electrophoresis. For HPLC analysis, 100-μL aliquots were removed, placed in an ice-water bath, and promptly injected into the HPLC.

Gel Electrophoresis

Nondenaturing polyacrylamide gel electrophoresis was performed using a discontinuous buffer system (Davis, 1964; Ornstein, 1964). The resolving gel contained 0.37 M Tris-HCl (pH 8.0) with 3.8 mM TEMED, 3.0 mM ammonium persulfate, and 7.5% acrylamide. The stacking gel contained 70 mM Tris-HCl (pH 6.7) with 4.3% acrylamide, 7.5 mM TEMED, and 2.5 mM ammonium persulfate. The gels were run at constant current (10 mA/gel) for ~4 h at 4°C and then silver-stained. Quantitation of protein in different intermediates was determined by phosphorimaging of dried gels. In the native gels, the amount of aggregated protein was determined by adding the intensities of all aggregation intermediates in the resolving gel and large aggregates, which accumulated at the top of the stacking gel.

High-Performance Liquid Chromatography

High performance liquid chromatography (HPLC) was carried out in a Shimadsu system using a prepacked TSK3000 column. No precolumn was used in order to decrease the possibility of filtering out large, but soluble, aggregates. The system was equilibrated with 25 mM Tris-acetate (pH 7.0) in the presence of 0.5 M urea at a flow rate of 1.0 mL/min. Urea was included to decrease the propensity of partially folded proteins to stick to the column matrix. Sample elution was monitored by absorption at 280 nm and tryptophan emission at 340 nm (excitation at 280 nm). The column and buffer temperature were maintained at 0°C.

Fluorescence Spectroscopy

Fluorescence spectra were recorded using an Hitachi F4500 Spectrofluorometer. All measurements were made at 25°C, in a buffer containing 50 mM sodium phosphate (pH 7.0) and 1 mM EDTA. For all tailspike samples (native, ambient aggregated, and pressure-treated aggregates) the protein concentration was 4 μg/mL. The excitation wavelength was 280 nm, and emission spectra were recorded from 300 to 400 nm. Relative differences in the spectra were determined by determining total peak area as well as the center of mass (average energy of emission).

Enzymatic "Tailing" Assay

Tail-free heads were prepared from *Salmonella* cells infected with P22 carrying an amber mutation in the tailspike gene as described previously (Berget and Poteete, 1980). Tailspike protein samples were diluted serially 1:3 into M9 media (Sambrook et al., 1989) supplemented with 2 mM MgSO$_4$, to yield a final volume of 100 μL. Then 100-μL aliquots containing 10^9 tail-free heads were added. Adsorption was allowed to proceed until completion (~4 h) at room temperature. The reaction mixture was then diluted serially 1:100, and 0.1 mL and 0.5 mL of each dilution were added to two parallel tubes containing 2 mL of top agar (Sambrook et al., 1989) and approximately 2 × 10^8 cells/mL of plating bacteria (*Salmonella* strain 7136) (Israel et al., 1967). This mixture was rapidly mixed and plated onto LB plates and incubated at 37°C to develop plaques. Plaques were counted for dilutions that resulted in 50 to 400 plaques per plate. A control sample containing only tail-free heads was used to measure background phage present; controls containing only tailspike protein were used to determine residual phage in tailspike preps; and a sample of plating bacteria only was used to control for cross-contamination during plating.

RESULTS AND DISCUSSION

Aggregation Reactions Can Be Monitored by HPLC

In the P22 tailspike system, folding and aggregation intermediates have been separated and visualized using native

gel electrophoresis (Goldenberg et al., 1982; Robinson and King, 1997; Speed et al., 1995). King and colleagues assigned aggregation oligomerization states to native gel mobilities using Ferguson analysis (Speed et al., 1995). A time course for aggregation can be visualized and quantitated with native gel electrophoresis by using ^{14}C-labeled tailspike (Fig. 2A). Early timepoints (2 min, 5 min) show monomer, dimer, and higher order aggregate species. Later timepoints (30 min, 2 h) show formation of some native trimer; however, higher order aggregation intermediates are the predominant species under the conditions of this experiment.
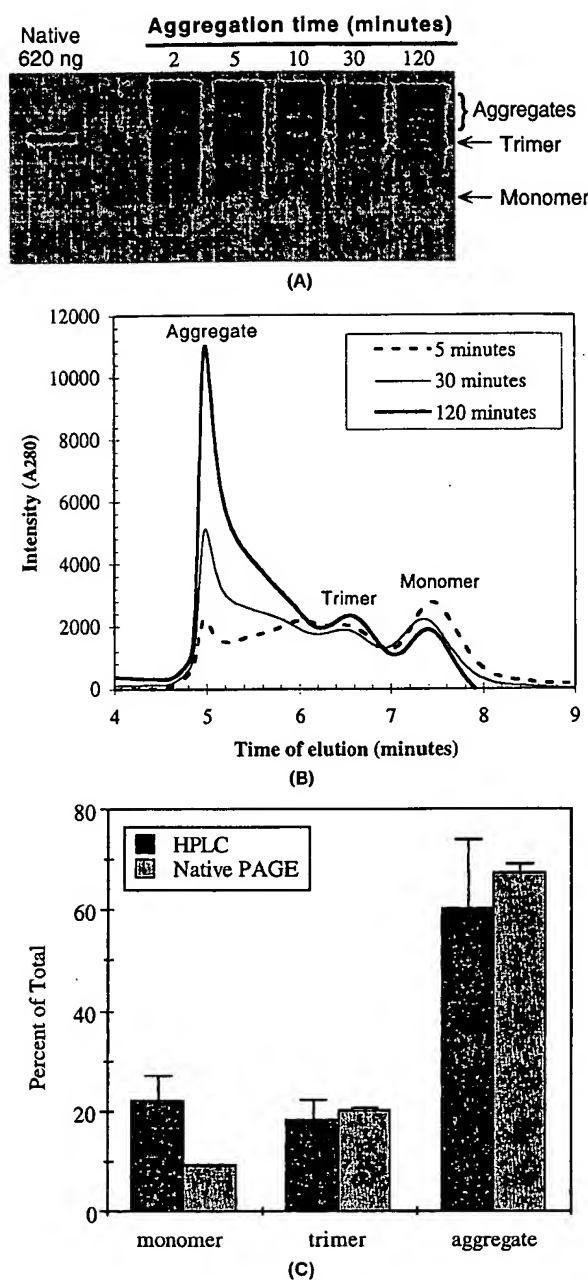
To identify and quantitate aggregation intermediates rapidly, we developed an HPLC assay using size-exclusion HPLC (TSK3000 column, Supelco). The column and buffer were kept at 0°C in all of the experiments described here to avoid additional association of tailspike chains inside the column during the run.

Using purified tailspike, we monitored the elution profiles of the native trimer and the denatured monomers by absorption at 280 nm and by fluorescence emission at 340 nm. The monomer and trimer both resolved as single peaks (data not shown). The trimer eluted as a uniform peak at 6.7 min, and the monomer eluted at 7.6 min.

To determine whether HPLC could be used as a probe for aggregation intermediates, tailspike was denatured, then rapidly diluted into refolding buffer. After the onset of aggregation, aliquots were removed at designated times and injected in the HPLC (Fig. 2B). Three distinct peaks eluted at 5.0, 6.6, and 7.5 min after injection and a broad shoulder appeared at 5.2 to 6.0 min. Peaks were collected and analyzed by native gel electrophoresis, which enabled us to identify the peaks as follows: 5.0 min, large aggregates; 6.6 min, trimer; 7.5 min, monomer (data not shown). Monomer and trimer eluted at the same times as purified tailspike samples, confirming the reproducibility of the technique for samples under refolding conditions. The broad shoulder that decreased with time was comprised mainly of intermediate-sized aggregates (smaller than those eluting at 5 min), which are not clearly resolved on this HPLC column.

Increasing reaction times led to an increase in the size of peaks of aggregated species (eluting at 5.0 min) and a concomitant decrease in the size of the monomer peak (7.5 min) (Fig. 2B). Similar results were obtained when native gel electrophoresis was used to monitor the time course of aggregation. In both cases, the amount of trimer changed very little with increasing reaction time, presumably because the conditions favored aggregation so strongly.

Quantitation of peak area from HPLC, and radioactive counts per band in native gel electrophoresis showed that both methods yielded similar levels of monomer, trimer, and aggregate (Fig. 2C). Small differences between the aggregate peak and the monomer formed under native PAGE vs. HPLC were likely due to the small buffer variations, such as the inclusion of 0.5 M urea in the HPLC. Because HPLC is substantially faster than native gel electrophoresis (1 h vs. 5 h) and less labor intensive, it is well suited to

(A)

(B)

(C)

Figure 2. Tailspike aggregation intermediates can be identified and quantitated by size-exclusion HPLC. (A) Native gel electrophoresis of ^{14}C-tailspike aggregation intermediates. Tailspike was denatured and refolded as described in text. At the times indicated, aliquots were removed and added to native sample buffer and placed on wet ice. Intermediates were visualized by native gel electrophoresis followed by exposure of the dried gel to phosphor screens and image analysis (Molecular Dynamics). (B) Size-exclusion HPLC separates tailspike aggregation intermediates. Tailspike was denatured and refolded as described in text. At the times indicated, 100-μL aliquots were removed and injected into a TSK 3000 column. Peaks were detected by adsorbance at 280 nm. Intermediates were identified by comparison to standards, and by collection of the peaks and visualization by native gel electrophoresis followed by silver staining. Sample times: 5 min (dashed line); 30 min (solid line); 120 min (bold line). (C) Quantitation of aggregation intermediates. Values for HPLC peaks (solid bars) and electrophoretic bands (shaded bars) were determined as described in text. Error bars reflect variation in total intensity from sample to sample for both HPLC and native PAGE experiments.

measure the extent of aggregation on-line during refolding reactions. This capability represents an enormous advantage for those interested in monitoring and controlling protein aggregation in biotechnology, research, and industrial applications.

Hydrostatic Pressure Inhibits and Reverses Tailspike Aggregation

To test the effect of hydrostatic pressure upon aggregation, samples of native tailspike were denatured, then transferred to refolding buffer under conditions which favor aggregation ($t = 26°C$, [Pt] = 1.4 μM chains). These samples were termed "ambient aggregated tailspike." An identical set of samples were denatured, transferred to refolding buffer under aggregation conditions, then subjected to 2.4 kbar for 90 min after 3.25 h of aggregation at atmospheric conditions. These samples were termed "pressure-treated tailspike." For each sample, the extent of refolding and aggregation was analyzed by HPLC (Fig. 3A).

Treatment with 2.4-kbar hydrostatic pressure markedly increased the yield of native trimer, while substantially decreasing the extent of aggregation. Figure 3B shows the distribution of tailspike monomers, trimers, and aggregates for pressure-treated tailspike samples and for the ambient aggregated tailspike sample. In the absence of pressure under these conditions, aggregation was favored: over 40% of the chains were in an aggregated form, with only 22% monomer and 37% trimer after 3.25 h. In samples incubated at 2.4-kbar for 90 min, the fractions of trimer and monomer were increased by 25% and 38%, respectively, and the extent of aggregation was decreased by more than 50%.

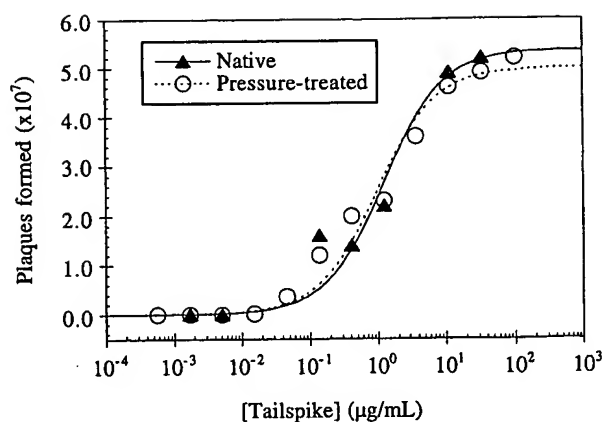## Tailspike Trimers from Pressure Treatment Have Native-Like Structure and Activity

We sought to determine whether tailspike trimers formed from pressure-treated aggregate recovered native-like structural and functional properties. We compared the intrinsic fluorescence spectra of native, pressure-treated, and ambient aggregated tailspike. Tailspike aggregation is accompanied by a large decrease in fluorescence intensity compared with native tailspike trimers. Pressure treatment of tailspike aggregates produced a 25% increase in fluorescence intensity, which corresponded exactly to the 25% increase in SDS-resistant trimer in these samples relative to ambient aggregated tailspike. This result is consistent with the idea that tailspike trimers in this sample had fluorescence properties similar to native trimers. Pressure-treated and native tailspike trimers also had essentially identical native-gel electrophoretic mobility and size-exclusion HPLC elution times, indicating that their hydrodynamic volume and hydrophobic surface areas are similar (Fig. 3). Moreover, the pressure-treated tailspike recovered the SDS resistance characteristic of native tailspike trimers. Incompletely folded tailspike species, including the protrimer, were sen-
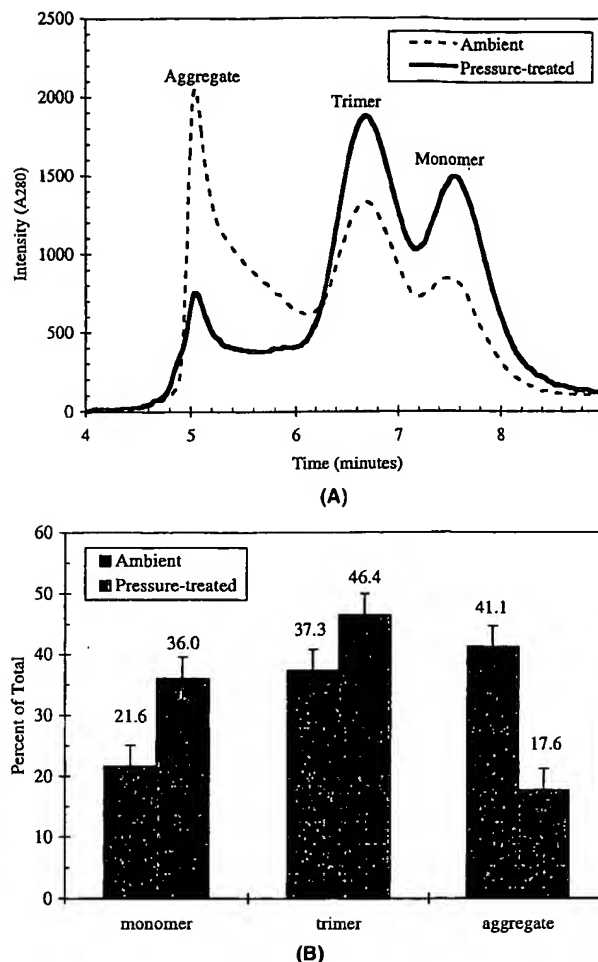
Figure 3. Pressure reverses tailspike aggregation. Native tailspike was denatured and refolded under aggregation conditions as described in text. After 3.5 h at room temperature, aggregates were either left untreated (ambient) or subjected to pressures of 2.4 kbar for 90 min (pressure-treated). (A) Size-exclusion HPLC traces. Peaks were detected by absorbance at 280 nm. Samples: ambient (dashed line); pressure-treated (solid line). (B) Quantitation of HPLC traces. Values for the ambient samples (solid bars) and pressure-treated (shaded bars) were determined as described in text. Error bars reflect variation in total intensity from sample to sample for HPLC experiments.

sitive to SDS. These observations strongly suggest that trimers produced by pressure treatment have native-like secondary and tertiary structure.

To assess whether tailspike trimers produced by pressure-treating aggregates recovered wild-type function, tailspike samples were subjected to a "tailing" assay to determine ability to complement tail-free P22 viral heads and produce infectious viral particles. Samples of native tailspike and pressure-treated aggregates were diluted and incubated with tail-free heads as described earlier. Tailspike trimers produced by pressure treatment of aggregates were essentially fully active, and formed viral plaques efficiently (Fig. 4). These results confirm that refolding under pressure produces tailspike trimers with essentially native structural and functional characteristics.

Figure 4. Pressure-treated tailspike trimers recover native activity. Native tailspike was denatured and refolded under aggregation conditions as described in text. After 3 h at room temperature, aggregates were subjected to pressures of 2.4 kbar for 90 min (pressure-treated). Activity of tailspike trimers was determined by a "tailing" assay, as described in text (Berget and Poteete, 1980). Plaque formation is the result of lysis of *Salmonella* cells by active P22 virus formed from tailspike protein bound to purified tail-free viral heads. Pressure-treated (open circles) tailspike was compared with native (solid triangles) tailspike trimers that were not subjected to denaturation or pressure treatment.

IMPLICATIONS

We have shown that hydrostatic pressure can be used to reverse protein aggregation in the absence of urea or other chemical additives. After pressure is released, dissociated aggregates refold to form biologically active protein with native characteristics. This process substantially increases the level of refolded protein. Pressure therefore could act as an efficient tool for combating aggregation in a variety of research and industrial settings. Although in our experiments we diluted denatured protein into buffer to create aggregates, there should be no need to change buffers or dilute protein in order to apply pressure to aggregates and produce native proteins. Pressure application is cost effective in industrial applications, easy to scale up, and straightforward to tune to achieve optimal refolding for each protein.

Several applications of pressure in biotechnological processes have been developed. The use of high pressure in food technology has increased rapidly (Heremans, 1997). Food pasteurized by hydrostatic pressure is being marketed worldwide (Shigehisa et al., 1991; Tauscher, 1995). The ability of pressure to inactivate viruses has been evaluated with a view toward two potential applications, vaccine development and virus sterilization (Jurkiewicz et al., 1995; Pontes et al., 1997; Silva et al., 1992a). Understanding the specificity of aggregation will open new avenues of research in this area.

We have not yet determined what is responsible for the reversal of aggregation by hydrostatic pressure. The folding pathway of tailspike is complicated—multiple species are involved in the various reactions, including a number of

oligomeric intermediates (Fig. 1B). It is likely that each of these reactions is differently sensitive to pressure. Formation of the native protein requires precise alignment and interdigitation of the β-strands in both the "body" and "tail" sections (Fig. 1A). Slight errors in alignment or interdigitation can easily be envisioned to result in off-pathway aggregation precursors. An investigation of mutant tailspike proteins that alter the partitioning of the intermediates should help determine the affected pathways.

Reversal of protein aggregation by hydrostatic pressure may be analogous to pressure dissociation of oligomeric proteins. The chains that are dissociated by pressure are competent for rapid productive folding, perhaps because the secondary and tertiary structure is preserved. The pressure-sensitive interfaces of aggregates are likely to be well-packed and solvent-excluded, supporting the idea that aggregation involves specific protein–protein interactions. However, the molecular details of how aggregates differ from native protein structures await further structural and mutagenesis studies.

Aggregation can occur by many distinct mechanisms (De Bernardez Clark, 1998). One such mechanism is formation of intermolecular disulfide bonds (e.g., Stoyan et al., 1993). Currently, refolding of proteins that have aggregated by incorrect disulfide bonding has been achieved by addition of oxidants or redox buffers (Builder et al., 1997; De Bernardez-Clark and Georgiou, 1991; Rudolph and Lilie, 1996). However, in many cases, other mechanisms predominate. For example, the aggregation events that result in Alzheimer's disease and prion diseases such as Creutzfeldt–Jacob's disease and bovine spongiform encephalopathy are believed to occur by noncovalent association of β-strands (Bychkova and Ptitsyn, 1995; Jarrett et al., 1993; Thomas 1992, 1995). Aggregation of tailspike protein is also believed to result from specific association of partially folded chains, possibly by misalignment of the β-strands (Speed et al., 1996). Because noncovalent interactions are susceptible to hydrostatic pressure we believe our approach is well-suited to combat this class of specific protein aggregation.

How do the effects of hydrostatic pressure compare with refolding by other methods? The range of refolding yields varies considerably for different proteins. Refolding of low-density lipoprotein receptor from *E. coli* was optimized at 10% (Simmons et al., 1997). Similar results were seen with hen egg white lysozyme (Maachupalli-Reddy et al., 1997). A monomeric protein, α-glucosidase, was refolded at high concentrations on a immobilized matrix to improve yields 10% to 30% (Stempfer et al., 1996). In our study, application of hydrostatic pressure increased tailspike refolding by 30% compared with control reactions.

One advantage of hydrostatic pressure is that it obviates the need to denature and refold. Moreover, it allows refolding at higher protein concentrations, a crucial parameter in the assembly of oligomeric proteins (De Bernardez Clark, 1998). We are in the process of optimizing pressure treatment to improve both native protein yields and activity for tailspike. We are also determining the ability to refold ag-

gregates from inclusion bodies formed in *E. coli*. Further studies on additional proteins will demonstrate whether this technique is widely applicable.

References

Berget PB, Poteete AR. 1980. Structure and functions of the bacteriophage P22 tail protein. J Virol 34:234–243.

Betts S, Haase-Pettingell C, King J. 1997. Mutational effects on inclusion body formation. Adv Prot Chem 50:243–264.

Builder S, Hart R, Lester P, Reifsnyder D. 1997. Refolding of misfolded insulin-like growth factor-1. US Patent 5663304.

Bychkova VE, Ptitsyn OB. 1995. Folding intermediates are involved in genetic diseases? FEBS Letters 359:6–8.

Cleland JL. 1993. Impact of protein folding on biotechnology. In: Protein folding: In vivo and in vitro. Cleland JL, editor. vol. 526. ACS Symposium Series, Washington, DC: American Chemical Society. p 1–21.

Davis BJ. 1964. Disk electrophoresis—II. Methods and application to human serum proteins. Ann NY Acad Sci 121:404–427.

De Bernardez Clark E. 1998. Refolding of recombinant proteins. Curr Opin Biotechnol 9:157–163.

De Bernardez-Clark E, Georgiou G. 1991. Inclusion bodies and recovery of proteins from the aggregated state. In: Protein Refolding. Georgiou G, De Bernardez-Clark E, editors. vol. 470. ACS Symposium Series, Washington, DC: American Chemical Society. p 1–20.

Foguel D, Silva JL, Prat-Gay G. 1998. Characterization of a partially folded monomer of the DNA-binding domain of human *Papillomavirus* E2 obtained at high pressure. J Biol Chem 273:9050–9057.

Fuchs A, Seiderer C, Seckler R. 1991. *In vitro* folding pathway of phage P22 tailspike protein. Biochemistry 30:6598–6604.

Goldenberg D, Berget P, King J. 1982. Maturation of the tailspike endorhamnosidase of *Salmonella* phage P22. J Biol Chem 257:7864–7871.

Goldenberg D, King J. 1982. Trimeric intermediate in the *in vivo* folding and subunit assembly of the tail spike endorhamnosidase of bacteriophage P22. Proc Natl Acad Sci USA 79:3403–3407.

Goldenberg DP, Smith DH, King J. 1983. Genetic analysis of the folding pathway for the tail spike protein of phage P22. Proc Natl Acad Sci USA 80:7060–7064.

Gorovits BM, Horowitz PM. 1998. High hydrostatic pressure can reverse aggregation of protein folding intermediates and facilitate acquisition of native structure. Biochemistry 37:6132–6135.

Haase-Pettingell CA, King J. 1988. Formation of aggregates from a thermolabile *in vivo* folding intermediate in P22 tailspike maturation: A model for inclusion body formation. J Biol Chem 263:4977–4983.

Heremans K. 1997. High pressure research in the biosciences and biotechnology. Leuven: Leuven University Press.

Israel JV, Anderson, TF, Levine M. 1967. *In vitro* morphogenesis of phage P22 from heads and base-plate parts. Proc Natl Acad Sci USA 57:284–291.

Iwashita S, Kanegasaki S. 1976. Enzymic and molecular properties of base-plate parts of bacteriophage P22. Eur J Biochem 65:87–94.

Jarrett JT, Berger EP, Lansbury PT Jr. 1993. The C-terminus of the beta protein is critical in amyloidogenesis. Ann NY Acad Sci 695:144–148.

Jurkiewicz E, Villas-Boas M, Silva JL, Weber G, Hunsmann G, Clegg RM. 1995. Inactivation of simian immunodeficiency virus by hydrostatic pressure. Proc Natl Acad Sci USA 92:6935–6937.

Maachupalli-Reddy J, Kelley BD, De Bernardez Clark E. 1997. Effect of inclusion body contaminants on the oxidative renaturation of hen egg white lysozyme. Biotechnol Progr 13:144–150.

Ornstein L. 1964. Disc electrophoresis—I. Background and theory. Ann NY Acad Sci 121:321–349.

Pontes L, Fornells LA, Giongo V, Araujo JRV, Sepulveda A, Villas-Boas M, Bonafe CFS, Silva JL. 1997. Pressure inactivation of animal viruses: Potential biotechnological applications. In: High-pressure research in the biosciences and biotechnology. Heremans K, editor. Leuven: Leuven University Press. p 91–94.

Robinson AS, King J. 1997. Disulphide-bonded intermediate on the folding and assembly pathway of a non-disulphide bonded protein. Nature Struct Biol 4:450–455.

Robinson CR, Sligar SG. 1995. Hydrostatic and osmotic pressure as tools to study macromolecular recognition. Meth Enzymol 259:395–427.

Rudolph R, Lilie H. 1996. In vitro folding of inclusion body proteins. FASEB J 10:49–56.

Sambrook J, Fritsch EF, Maniatis T. 1989. Molecular cloning, a laboratory manual. Cold Spring Harbor, NY: Cold Spring Harbor Laboratory Press.

Sauer RT, Krovatin W, Poteete AR, Berget PB. 1982. Phage P22 tail protein: Gene and amino acid sequence. Biochemistry 21:5811–5815.

Seckler R, Fuchs A, King J, Jaenicke R. 1989. Reconstitution of the thermostable trimeric phage P22 tailspike protein from denatured chains *in vitro*. J Biol Chem 264:11750–11753.

Shigehisa T, Ohmori T, Saito A, Taji S, Hayashi R. 1991. Effects of high hydrostatic pressure on characteristics of pork slurries and inactivation of microorganisms associated with meat and meat products. Int J Food Microbiol 12:207–215.

Silva JL, Foguel D, Da Poian AT, Prevelige PE. 1996. The use of hydrostatic pressure as a tool to study viruses and other macromolecular assemblages. Curr Opin Struct Biol 6:166–175.

Silva JL, Luan P, Glaser M, Voss EW, Weber G. 1992a. Effects of hydrostatic pressure on a membrane-enveloped virus: High immunogenicity of the pressure-inactivated virus. J Virol 66:2111–2117.

Silva JL, Silveira CF, Correa A, Pontes L. 1992b. Dissociation of a native dimer to a molten globule monomer. Effects of pressure and dilution on the association equilibrium constant of Arc repressor. J Molec Biol 223:545–555.

Silva JL, Weber G. 1993. Pressure stability of proteins. Annu Rev Phys Chem 44:89–113.

Simmons T, Newhouse YM, Arnold KS, Innerarity TL, Weisgraber KH. 1997. Human low density lipoprotein receptor fragment. Successful refolding of a functionally active ligand-binding domain produced in *Escherichia coli*. J Biol Chem 272:25531–25536.

Speed MA, Morshead T, Wang DI, King J. 1997. Conformation of P22 tailspike folding and aggregation intermediates probed by monoclonal antibodies. Prot Sci 6:99–108.

Speed MA, Wang DIC, King J. 1995. Multimeric intermediates in the pathway to the aggregated inclusion body state for P22 tailspike polypeptide chains. Prot Sci 4:900–908.

Speed MA, Wang DIC, King J. 1996. Specific aggregation of partially folded polypeptide chains: The molecular basis of inclusion body composition. Nature Biotechnol 14:1283–1287.

Steinbacher S, Seckler R, Miller S, Steipe B, Huber R, Reinemer P. 1994. Crystal structure of P22 tailspike protein: Interdigitated subunits in a thermostable trimer. Science 265:383–386.

Stempfer G, Holl-Neugebauer B, Rudolph R. 1996. Improved refolding of an immobilized fusion protein. Nature Biotechnol 14:329–334.

Stoyan T, Michaelis U, Schooltink H, Van Dam M, Rudolph R, Heinrich PC, Rose-John S. 1993. Recombinant soluble human interleukin-6 receptor. Expression in *Escherichia coli*, renaturation and purification. Eur J Biochem 216:239–245.

Tauscher B. 1995. Pasteurization of food by hydrostatic high pressure: Chemical aspects. Z Lebensm Unters Forsch 200:3–13.

Thomas PJ, Ko YH, Pedersen PL. 1992. Altered protein folding may be the molecular basis of most cases of cystic fibrosis. FEBS Lett 312:7–9.

Thomas PJ, Qu BH, Pedersen PL. 1995. Defective protein folding as a basis of human disease. Trends Biochem Sci 20:456–459.

Winston R, Botstein D, Miller J. 1979. Characterization of amber and ochre suppressors in *Salmonella typhimurium*. J Bacteriol 137:433–439.

Docket No.: 00131-00350-US

Exhibit F

OIPE IAP89
NOV 0 2 2006
PATENT & TRADEMARK OFFICE

TSK 3000 cooled
40 µl injection
Aggregation 100 µg/ml
5' - control

13:46:28

CLASS-CR10 SYS=1 Ch=1 REPORT.NO=1   DATA=15AGC5A.D01
Sample   : 15agc5
ID   : tailspike
Dilution Factor: 1
Type   : Unknown
Operator   : anne

BM V em EGTA. Pool 2. 90 µl

*** Chromatogram ***

*** Peak Report ***
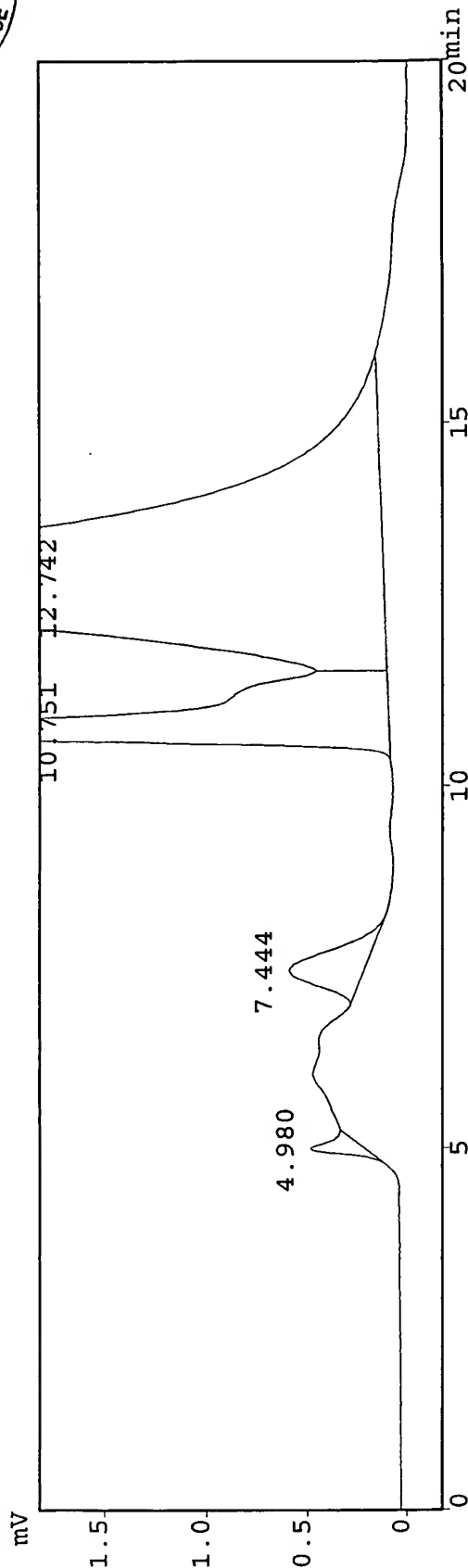
PKNO	TIME	AREA	HEIGHT	MK	IDNO	CONC	NAME
1	4.980	3144	273			0.7154	
2	7.444	12092	371			2.7519	
3	10.751	92081	3806			20.9558	
4	12.742	332089	3527	V		75.5768	
		439406	7977			100.0000	

1 - 1/1

TSK-3000
40μl injection

Aggregation control (
(100μg/mc)

30' control

CLASS-CR10 SYS=1 Ch=1 REPORT.NO=9   DATA=15AGC30A.D01
Sample   : 15agc30   15:24:14
ID   : tailspike
Dilution Factor: 1
Type   : Unknown
Operator   : anne

BM V em EGTA. Pool 2. 90 μl

*** Chromatogram ***

*** Peak Report ***

PKNO	TIME	AREA	HEIGHT	MK	IDNO	CONC	NAME
1	4.990	26179	916			9.7213	
2	7.351	8318	262			3.0889	
3	10.759	31097	1322			11.5474	
4	11.338	15792	844	V		5.8643	
5	11.921	10198	739	V		3.7871	
6	12.883	177710	1591	V		65.9911	
		269293	5674			100.0000	

9 - 1/1

Docket No.: 00131-00350-US

Exhibit H

TSK 3000 cooled
SD μl injection
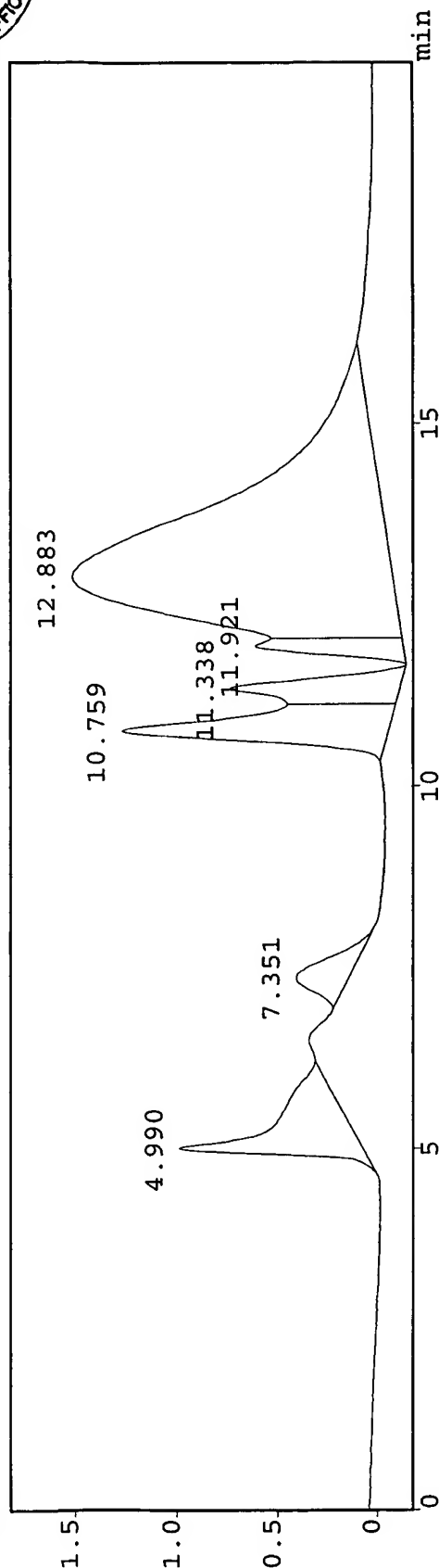Aggregation (100 μg/ml)
3hr — control

CLASS-CR10 SYS=1 Ch=1 REPORT.NO=5 DATA=15AGCINA.D01 17:53:24
Sample   : 15agcinf
ID   : tailspike
Dilution Factor: 1
Type   : Unknown
Operator : anne

BM V em EGTA. Pool 2. 90 μl

*** Chromatogram ***

*** Peak Report ***

PKNO	TIME	AREA	HEIGHT	MK	IDNO	CONC	NAME
1	4.990	74079	2161			18.7482	
2	6.562	19032	491	V		4.8167	
3	7.393	16718	437	V		4.2310	
4	10.758	45016	2064	V		11.3926	
5	11.376	21608	934	V		5.4687	
6	11.929	11101	903	V		2.8093	
7	12.698	207574	2177	V		52.5334	
		395128	9166			100.0000	

5 - 1/2

Aggregation ∞ (before pressure ∞)

CONTROL

OIPE IAP89
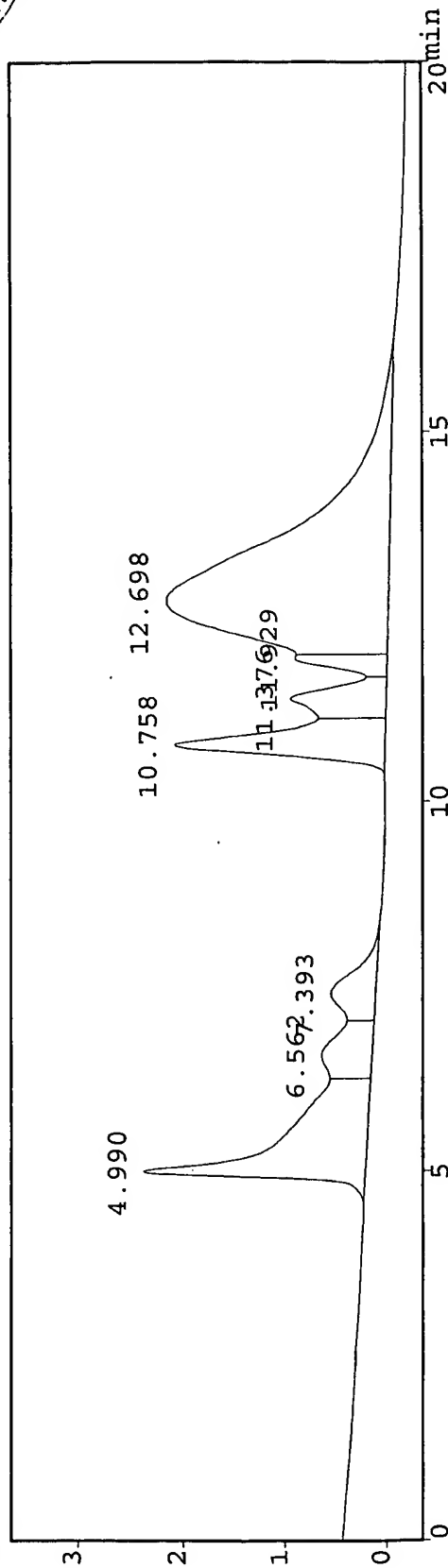NOV 0 2 2006
PATENT & TRADEMARK OFFICE

CLASS-CR10 SYS=1 Ch=1 REPORT.NO=3   DATA=19AGINA.D01   18:36:12
Sample   : 19agin
ID   : lamagit3
Dilution Factor: 1
Type   : Unknown
Operator   : anne

BM V em EGTA. Pool 2. 90 μl

*** Chromatogram ***

*** Peak Report ***

PKNO	TIME	AREA	HEIGHT	MK	IDNO	CONC	NAME
1	5.063	23663	666			5.0368	
2	6.703	20717	440	V		4.4097	
3	7.479	10421	277	V		2.2182	
4	10.909	155143	7601			33.0237	
5	11.482	11616	847	V		2.4727	
6	12.113	12407	997			2.6409	
7	12.948	235827	2167	V		50.1980	

469794   12994   100.0000

3 - 1/4

Exhibit J

"no sample stayed in the bench co aggregation and was pured for 90' (35,000 psc).

```
CLASS-CR10 SYS=1  Ch=1  REPORT.NO=5   DATA=19AGINPA.D01
Sample          : 19aginp                        20:06:32
ID              : 1amagit3
Dilution Factor: 1
Type            : Unknown
Operator        : anne

BM V em EGTA. Pool 2. 90 μl

*** Chromatogram ***
```
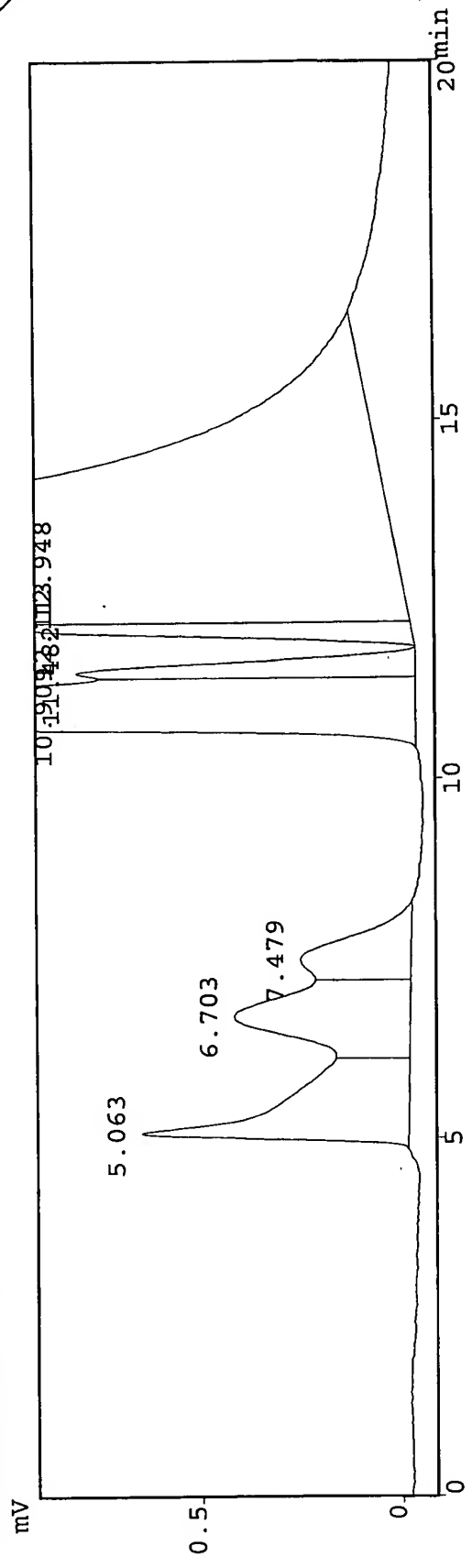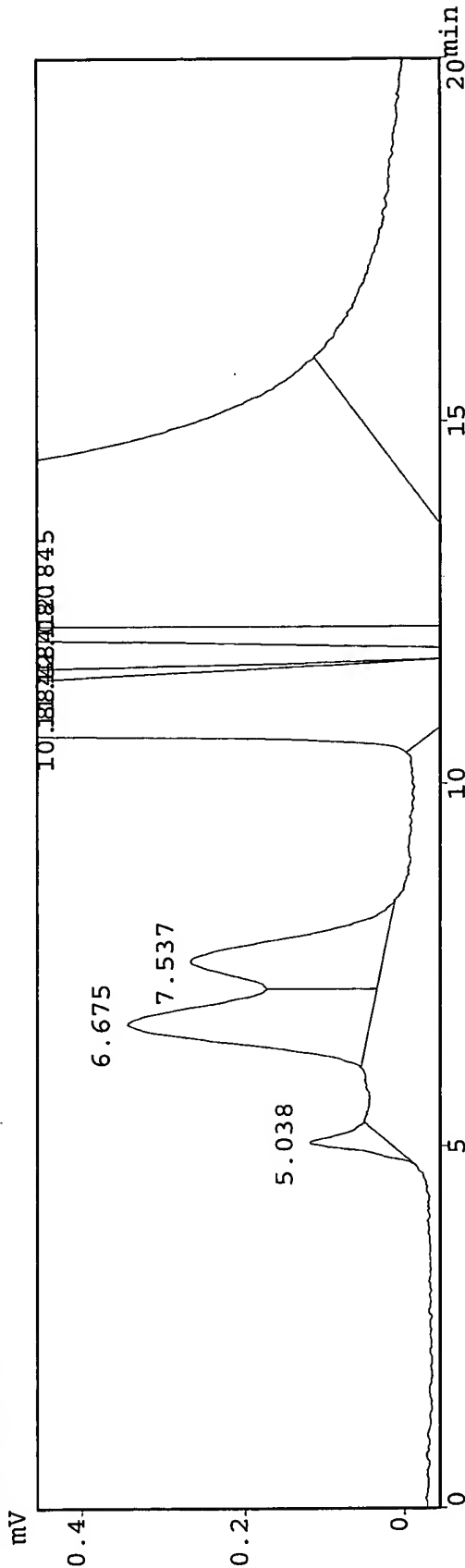


```
*** Peak Report ***
PKNO   TIME      AREA   HEIGHT  MK  IDNO       CONC      NAME
1     5.038      1492     100                0.3918
2     6.675     11665     300                3.0639
3     7.537      9328     239    V           2.4499
4    10.884    143532    6981    S          37.6994
5    11.484      3448     297    T           0.9055
6    12.080     15045    1220                3.9517
7    12.845    196218    1910    V          51.5379
-------------------------------------------------------------
          380726   11048                   100.0000

                                          5 - 1/4
```

Experiment	Testing assay of Presenilin					Date ▮▮▮▮	
Cells			Plate				

Phage		T°C	D	Vml	N	Titer	Comments
P100	100 ug/ml 1		10^6	0.5	26	5.2 E7	1:90 :15
▲	33.3 2		10^6	0.5	24	4.9 E7	5.5
	11.1 3		10^6	0.5	23	4.6 E7	5.5
	3.7 4		10^4	0.1	367	3.6 E7	5.5 4.1
	1.2 5		10^4	0.1	233	2.3 E7	5.5 4.11
	0.41 6		10^4	0.1	205	2.0 E7	4.1 4.15
	0.13 7		10^4	0.5	512	1.E7	4.5
	0.045 8		10^4	0.5	186	3.7 E6	4.5 2.1
	0.0152 9		10^2	0.1	164	1.6 E5	2.5
	5.08-3 10		10^2	0.1	52	5E 4	2.1 2.5
	1.69-3 11		10^2	0.1	37	3.7 E4	2.5
	5.64-4 12		10^2	0.5	95	1.9 E4	2.5
	1.88-4 13		10^2	0.5	158	3. E5	2.5
	6.27-5 14		10^2	0.5	122	2.4 E5	2.5
A 100	1		10^2	0.5	?	$10^?$	5.1
△	2				145 S		6. 5.1
	3				145 S		
	4				145 S		4.11
	5				145 -		4.3 4.5
	6				145 S		4.1 4.15
	7				0		4.5
	8				145 S		4.5
	9				4×307	2.5 E5	
	10				358	7.1 E4	
	11				99	200 E4	
	12				48	9.4 E3	
	13		10^2	0.5	21	4.2 E3	
	14		10^2	0.5	20	4 E3	

Docket No.: 00131-00350-US

Exhibit K

Titlespike 1 ont tetralotive tal sp

Experiment								Date ▓▓▓▓▓	
Determine if mesure treated renal									TOR 500
Cells 7155		Plate							
Phage		T°C	D	Vml	N		Titer		Comments
WT Natve 1	1		10^6	0.5	13		2.6 E7		5.15
2			10^6	0.5	22		4.4 E7		5.5
3			10^6	0.5	11		2.2 E7		5.5 4.1
4			10^6	0.5	11		2.2 E7		5.5 4.1
5			10^4	0.1	147		1.4 E7		4.1 5.5
6			10^4	0.1	68		1.6 E7		4.1 5.5
7			10^4	0.5	204		4.08 E7		4.1 5.5
8			10^4	0.5	44		8.8 E6		4.5 2.1
9			10^2	0.1	129		1.3 E5		2.1
10		37°C	10^2	0.5	471		9.4 E4		2.1

ce7
cn7
4

Exhibit L

$17^6 3 - 12$